MECHANICAL AND TRIBOLOGICAL BEHAVIOR OF NANOFILLER REINFORCED POLYMER NANOCOMPOSITE

A THESIS SUBMITTED IN PARTIAL FULFILMENT OF THE REQUIREMENTS FOR THE DEGREE OF

Doctor of Philosophy
in
Mechanical Engineering

By

GUJJALA RAGHAVENDRA

Department of Mechanical Engineering
National Institute of Technology
Rourkela - 769008

December-2014

MECHANICAL AND TRIBOLOGICAL BEHAVIOR OF NANOFILLER REINFORCED POLYMER NANOCOMPOSITE

A THESIS SUBMITTED IN PARTIAL FULFILMENT OF THE REQUIREMENTS FOR THE DEGREE OF

Doctor of Philosophy
in
Mechanical Engineering

By

GUJJALA RAGHAVENDRA

Under the Guidance of

PROF. S. K. ACHARYA
Dept. of Mechanical Engineering

PROF. S. K. PAL
Dept. of Ceramic Engineering

Department of Mechanical Engineering
National Institute of Technology
Rourkela – 769008

December-2014

Dedicated to

My Grand Mother

Late Chandramma

TABLE OF CONTENTS

Chapter-3 Nano fabrication and Characterization

Chapter-4 Mechanical properties of Jute-glass fiber hybrid composite with micro and nano filler

Chapter-5 Solid particle erosion studies of jute-glass fiber reinforced epoxy hybrid composite

DEPARTMENT OF MECHANICAL ENGINEERING
NATIONAL INSTITUTE OF TECHNOLOGY,
ROURKELA, ODISHA,
INDIA-769008

CERTIFICATE

This is to certify that the thesis entitled "**Mechanical and Tribological Behavior of Nano filler Reinforced Polymer Nanocomposite"** submitted to the National Institute of Technology, Rourkela by **Gujjala Raghavendra**, Roll No. **511-ME-112** for the award of the Degree of Doctor of Philosophy in Mechanical Engineering is a record of bonafide research work carried out by him under our supervision and guidance. The results presented in this thesis has not been, to the best of our knowledge, submitted to any other University or Institute for the award of any degree or diploma.

The thesis, in our opinion, has reached the standards fulfilling the requirement for the award of the degree of **Doctor of Philosophy** in accordance with regulations of the Institute.

Dr. S. K. ACHARYA
Professor
Dept. of Mechanical Engineering
National Institute of Technology
Rourkela – 769008

Dr. S. K. PAL
Assistant professor
Dept. of Ceramic Engineering
National Institute of Technology
Rourkela – 769008

ACKNOWLEDGEMENT

I would like to express my special appreciation and thanks to my advisors **Dr. S.K. Acharya,** Professor, Dept. of Mechanical Engineering and **Dr. S.K. Pal,** Assistant Professor, Dept. of Ceramic Engineering, NIT, Rourkela for suggesting the topic of my thesis and their ready and able guidance throughout the course of my work.

I express my sincere thanks to Director NIT Rourkela **Prof Sunil Kumar Sarangi** and **Prof S.S. Mohapatra,** Head of the Department of Mechanical Engineering for providing all academic and administrative help during the course of my work.

The guidance, review and critical suggestion of the Doctoral scrutiny Committee (DSC) during various presentations and review meeting comprising of **Prof. K.P. Maity**, **Prof. R.K. Behera**. **Prof. S.C. Mishra** and **Prof. S. Sarkar** are acknowledged. I also express my thanks to **Prof. S. K. Pratihar** of Ceramic Engineering Department for his help during my experimental work in the laboratory.

I am thankful to the director of NIT Warangal and Head of the mechanical Department for giving me moral and administrative support as and when I required. I am thankful to all the staff members of the department of Mechanical Engineering and to all my well-wishers for their inspiration and help.

This work is also the outcome of the blessing guidance and support of my father **Mr. Honnurappa**, my mother **Mrs. Lakshmi Devi** and my brother **G Siva sankar.** This work could have been a distant dream if I did not get the moral encouragement and help from my wife **Mrs. Shakuntala Ojha**. This thesis is the outcome of the sincere prayers and dedicated support of my family.

Finally I wish to acknowledge the support given to me by all the PhD and M-tech Scholars of Tribology Laboratory during the course of my work. My special thanks go to **Mr. Ramu Inala, Mr. Kiran Gurrala and Dhananjay M** for their unconditional help to see this work in this form.

Date: (Gujjala Raghavendra)

ABSTRACT

Increasing demand for special materials lead to new inventions, one of the most promising inventions is the concept of composites. We always will strive to understand and modify the world around us and the stuff of which it is made. A new era is opened when the thorough understanding of a particular material and combining the valuable properties of the different materials are taken together to optimize the individual properties.

Nowadays, engineering material at the atomic and molecular levels are creating a revolution in the fields of materials and processing. Nanoscale particles are presently considered to be high potential filler material for improving the properties of the existing material. Due to the nano technology the polymer composites are become more attractive. As surely as polymer composites changed the face of industry twenty-five years ago, polymer nanocomposites will usher in a new era in materials development.

Natural materials are one of the prominent and cost effective options for alternating the synthetic fibers reinforced composites. The availability of the natural material and ease of manufacturing attracts the researchers to try the locally available inexpensive fibers and to study their feasibility in reinforcing in to polymers. Accordingly extensive studies on preparation and properties of polymer matrix composite (PMC) replacing the synthetic fiber with natural fiber like Jute, Sisal, Pineapple, Bamboo and Kenaf were carried out. These plant fibers have many advantages over glass fiber or carbon fiber like renewable, environmental friendly, low cost, lightweight, high specific mechanical performance.

There are many potential natural resources, which India has in abundance. Most of it comes from the forest and agriculture. Jute is an annual plant in the genus corchorus. The major types grown are generally known as white jute and tossa jute. Jute, grown mainly in India and Bangladesh, is harvested at 2 to 3 months of growth, at which time it is 3-5 meters tall. Jute is most common agro-fibers having high tensile modulus and low elongation at break. If the low density of this fiber is taken in to consideration, then its specific stiffness and strength are comparable to the respective quantities of glass fibers. Jute contains about 61-71% cellulose, 13-20% hemicellulose, and 12-13% lignin. The fiber has a high aspect ratio, high strength to weight

ratio, is low in energy conversion, and has good insulation properties. The jute fiber composites can be very cost-effective material especially for building and construction industry, packing, automobile and railway coach interiors and storage devices.

The main disadvantage of natural fibers is their hydophilicity nature. The presence of these micropores in the fibers cell wall is responsible for this defect. This gives rise to manufacturing defects in composites, such as interfacial failure and air pockets. Hence the strength of the natural fiber composite is less. The term hybridization very broad and encompasses a very wide range of materials which plays an important role for compensation the drawbacks of the one material with combining the potential material.

Recently Micro or nanoparticle reinforced polymer has drawn interest of many researchers due to its versatile applications. Micro or nanofiller in polymer matrix can improve the end use performance of the composite in many different ways. Reinforcing of inorganic particulate fillers into polymer matrix has been proved to be an effectual way of improving the tribological and mechanical properties of the matrix. It should be noticed that a very few literature is available related to micro or nanofiller addition to hybrid composites. Addition of high surface area fillers to the hybrid composites definitely exhibits variation in the mechanical properties. The concept of combining the micro and nano composites as matrix material with the fiber reinforcement is a new three-phase composite reinforcement.

Fly ash which is an industrial waste popularly recognized as an environmental pollutant has many potential ceramic materials such as Al_2O_3, SiO_2 etc. Because of the environmental problems presented by the fly ash, considerable research has been under taken on the subject worldwide. Its utilization as a low cost adsorbent for the removal of organic compounds, light weight aggregate, road sub-baser, construction material, mine and pit filler etc. has already been established. However, very little is reported on its potential as nano material filler in polymer composites. Alumina is one such ceramic material which has recently been recognized as potential filler in many applications starting from cosmetic, packaging materials to aerospace applications. Alumina especially has a high melting point, high strength, corrosion resistance, chemical stability, low thermal conductivity and good electrical insulation properties. As a type

of important structural ceramic material, alumina has applications in absorbent, catalyst, carrier and reinforcement of ceramic composites.

Therefore the present research work has been under taken with an objective to produce nano-fly ash and alumina nano particles in the laboratory by utilizing the method of high energy ball milling and by auto combustion process. It is also planned to use these nanofillers as reinforcing material in polymer composite. The low modulus of glass fiber composites has limited their use in applications where buckling stability or high natural frequency is the criteria. It is also known that natural fibres composite possess much lower mechanical strength properties than synthetic fibre reinforced composite. Hence the use of natural fibre alone in polymer composite is inadequate in satisfactorily tackling all the technical needs of a fibre reinforced composite. It is reported that if natural fibre is hybridised with a synthetic fibre in the same matrix the properties of natural fibre could be improved by taking the advantage of both the fibres.

In this work an attempt has also been made to prepare woven jute–glass fiber hybrid composite. Efforts are made to study the effect of hybridization of glass and layering sequence effect on tensile strength, flexural strength, tensile modulus and flexural modulus of the composite with both micro and nanofillers. Experiment is also carried out to study the erosive wear behavior of the composite developed incorporating both nano and micro fly-ash and alumina particles in the composite. Effect of different parameters like impingement angle and velocity on the erosive wear behavior of hybrid composite has also been studied and reported in the thesis. The test results indicates that there is increase in both tensile and flexural and as well as the modulus for micro and nano filled composites. The trend observed in the strength are hybrid<micro filler<nano filler. The solid particle erosion test clearly indicates that the hybrid composite behavior changes form semi brittle to pure brittle due to filler addition. It is also clearly observed that the fiber breakage and chipping of fiber is reduced due to micro and nano filler addition. Improved mechanical properties are observed for the hybrid composite GJGJ in flexural and GJJG in tensile with 4wt.% nano alumina filler composites, whereas the better tribological properties are observed for the natural fiber composites JJJJ with 4wt.% nano alumina.

List of Figures

LIST OF TABLES

Chapter 1

Introduction

1.1 BACK GROUND

Materials and material development are fundamental to our very culture. We even ascribed major historical periods of our society to materials such as the Stone age, Bronze age, Iron age, Steel age (industrial revolution), silicon age and silica age (telecom revolution). This reflects how important materials are to us. We have and always will strive to understand and modify the world around us and the stuff of which it is made. The next societal frontiers will be opened not through understanding a particular material, but rather by understanding and optimizing the relative contributions afforded by material combinations.

The nanoscale, and associated excitement surrounding nanoscience and technology (NST) affords unique opportunities to create revolutionary material combinations. These new materials will enable the circumvention of classic material performance trade-offs by accessing new properties and exploiting unique synergism between materials that only occur when the length-scale of morphology and the fundamental physics associated with a property coincides, i.e. on the nanoscale. The confluence of fundamental understanding of materials at this scale and the realization of fabrication and processing techniques that provides simultaneous structural control on the nano, as well as micro and macro, length scales is the core of the exciting area of nanoengineered materials. Examples of such material technologies are rapidly increasing, impacting many diverse areas of the commercial and military arena.

One of the ways nanoscience has advanced the state-of-the art has been to enhance and improve the properties of existing conventional classes of materials. Polymer composites, for example, have been a mainstay of high-performance aircraft for over a quarter century, offering a multitude of desirable (and tailorable) properties, such as high strength and stiffness, and dimensional and thermal stability. With the advent and application of nanotechnology, polymer composites could become even more attractive. As surely as polymer composites changed the face of industry twenty five years ago, polymer nanocomposites will usher in a new era in materials development.

1.2 “NANOCOMPOSITE” CONCEPT

Nanocomposites are materials that are created by introducing nanoparticulates into a microscopic sample material. This is part of the growing field of nanotechnology. The

nanomaterials tend to drastically add to the electrical and thermal conductivity as well as to the mechanical strength properties of the original material. In general, the nano substances used are carbon nanotubes, nanoparticles and they are dispersed into the other composite materials during processing. The percentage by weight of the nanomaterials introduced is able to remain very low (on the order of 0.5% to 5%) due to the incredibly high surface area to volume ratio of the particles. Much research is going in to developing more efficient combinations of materials and to impart multifunctionalities to the nanocomposites.

A nanocomposite is the hybrid material consisting of a polymer matrix reinforced with a fiber, platelet, or particle having one dimension on the nanometer (nm) scale (10^{-9} m). Nanocomposites can be classified in the following way: (i) reinforcements having all three dimensions at the nanometer level, e.g., spherical silica; (ii) elongated structures with two dimensions at the nanometer level, e.g., carbon nanotubes and cellulose whiskers; (iii) sheet like structures having only one dimension on the nanometer scale, e.g., layered silicates (clay, mica, etc.).

The preparation of nanocomposites is a scientific and technical challenge. In many systems, the chemical nature of the filler is less important than the particle size and shape, the surface morphology, and the extent of distribution within the polymer matrix. The layered silicate nanocomposites have attracted attention due to their inexpensive and abundant availability, high aspect ratio, and excellent barrier properties.

1.3 POLYMER NANOCOMPOSITES

The term “polymer nanocomposite” broadly describes any number of multicomponent systems, where the primary component is the polymer and the filler material has at least one dimension below 100nm [1].Polymer nanocomposites are generally lightweight, require low filler loading, are often easy to process, and provide property enhancements extending orders of magnitude beyond those realized with traditional composites.

1.4 POLYMER MATRICES

The word polymer derived from the Greek word, “Poli” means “many” and “meros” means “parts”. The name itself suggests that this material has high molecular weight. This material has different processing methods which in turn has versatility in properties. This

versatility in properties of polymer makes them attractive matrix material for many applications.

A very large number of polymeric materials, both thermosetting and thermoplastic, are used as matrix materials for the composites. Some of the major advantages and limitations of resin matrices are shown in Table 1.1.

Generally speaking, the resinous binders (polymer matrices) are selected on the basis of adhesive strength, fatigue resistance, heat resistance, chemical and moisture resistance etc. The resin must have mechanical strength commensurate with that of the reinforcement. It must be easy to use in the fabrication process selected and also stand up to the service conditions. Apart from these properties, the resin matrix must be capable of wetting and penetrating into the bundles of fibers which provide the reinforcement, replacing the dead air spaces therein and offering those physical characteristics capable of enhancing the performance of fibers.

Table 1.1 Advantages and limitations of polymeric matrix materials

Advantages	**Limitations**
Low densities	Low transverse strength
Good corrosion resistance	Low operational temperature limits
Low thermal conductivities	
Low electrical conductivities	
Translucence	
Aesthetic Color effects	

1.5 FILLER

The term filler is very broad and encompasses a very wide range of materials which plays an important role for the improvement in performance of polymers and their composites. Filler materials are used to reduce the material cost, to improve the mechanical properties to some extent and in some cases to improve process ability. Besides, it also increases properties like abrasion resistance, hardness and reduces shrinkages. Therefore a judicious selection of matrix and the reinforcing phase can lead to a composite with combination of strength and modulus comparable or even better than conventional metallic

materials. The physical and mechanical properties can further be modified by addition of a solid filler phase to the matrix body during the composite preparation.

1.5.1 Conventional Fillers

Particulate fillers have played a vital role in the development of commercial uses for polymers. The primary filler types utilized may be classified as either natural or synthetic fillers. Naturally occurring fillers are generally a pure, crystalline mineral. Common natural filler is calcium carbonate, $CaCO_3$ which has been used in polyvinyl chloride, polypropylene, elastomers, and unsaturated polyesters. Other filler materials include micron sized clay particulates such as kaolinite and metakaolin. These materials have been used to impart electrical resistivity to polyvinyl chloride for cable insulation applications. Crystalline silicas and calcium sulphate are additional commonly employed, natural fillers. Synthetic fillers are prepared by chemical processes, with carbon black being among the most well-known. Carbon black has been widely used for rubber reinforcement. Synthetic silica is another example of synthetically prepared filler. Silica particulates have found wide application in silicone elastomers [2].

Originally, fillers were primarily considered cheap diluents. However, their ability to beneficially modify polymer properties was quickly realized. Some of the main reasons for using particulate fillers include: cost reduction, improved processing, thermal conductivity, controlled thermal expansion, flame retardancy and improved mechanical properties. Evidently no single filler has provided all of these benefits. Ideally filler improves some properties without negatively affecting others. The magnitude of the property change observed is not only a function of the filler composition but is strongly influenced by particle size, shape, and surface chemistry [2].Particle size, shape, and ability to bond with the polymer matrix are all important factors in determining filler performance.

1.5.2 Conventional and Nano Fillers

In nanocomposites, at least one dimension of the dispersed particles is in the nanometer range. One can distinguish three types of nanocomposites, depending on how many dimensions of the dispersed particles are in the nanometer range. When the three dimensions are in the order of nanometers, we are dealing with isodimensional nanoparticles (or simply nanoparticles). Carbon black, silica, aluminum oxide, titanium dioxide, zinc oxide,

silicon carbide, polyhedral oligomeric sislesquioxanes (POSS) are examples for nanoparticle fillers. When two dimensions are in the nanometer scale and the third is larger, forming an elongated structure, we speak about nanotubes or whiskers or nanofibers. Examples are Carbon nanotubes, carbon nanofibers, cellulose whiskers. The third type of nanocomposites is characterized by only one dimension in the nanometer range.

In this case the filler is present in the form of sheets of one to a few nanometer thick to hundreds to thousands nanometers long. This family of composites can be gathered under the name of nano platelet based nanocomposites. Layered silicates, layered graphite flakes and layered double hydroxides are examples for layered nano fillers. Figure 1.1 shows all three types of nanofillers.

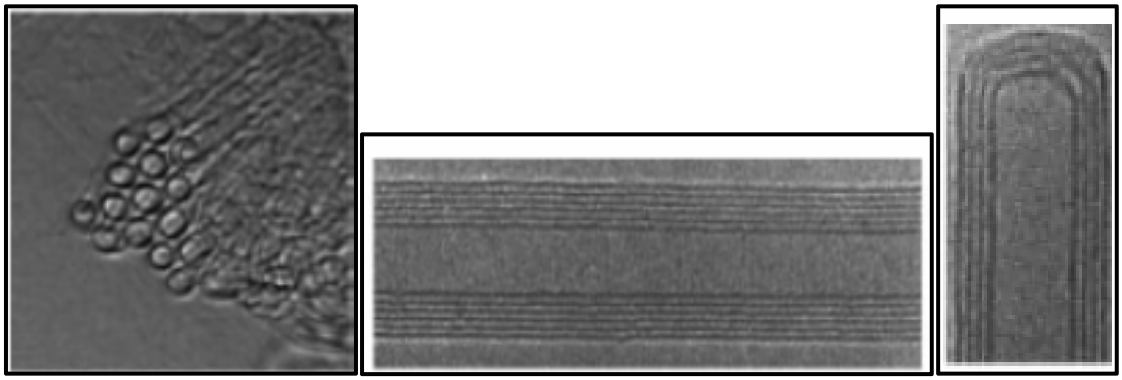

(a) Multi walled carbon nano tube

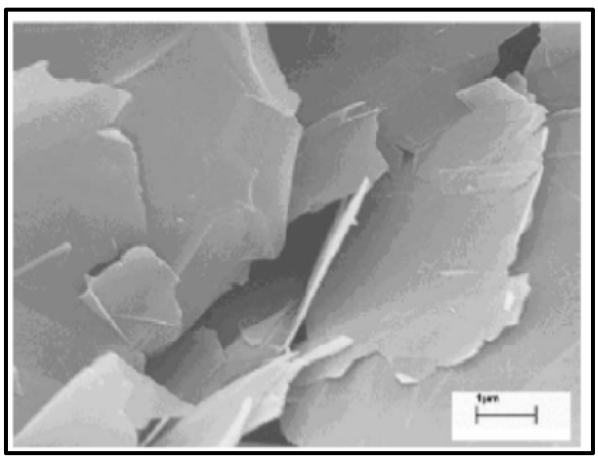

(b) Graphite flakes

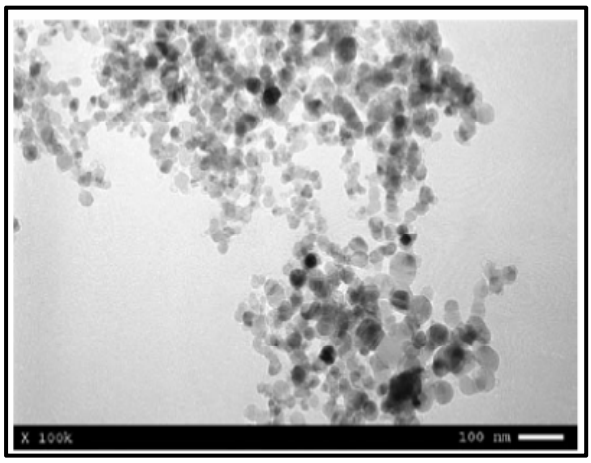

(c) Silica nanoparticles

Figure 1.1 Different types of multifunctional fillers (a) Nano particle type (b) Nano tube or nanofiber type (c) Nano platelet type [3]

A morphological characteristic that is of fundamental importance in the understanding of the structure property relationship of nanocomposites is the surface area/volume ratio of the nano reinforcement materials. Particulate composites reinforced with micron sized particles of various materials are perhaps the most widely utilized composites in today's structures. Particles are typically added to enhance the matrix elastic modulus and yield strength. By scaling the particle size down to the nanometer scale, it has been shown that novel material properties can be obtained [3].

The filler particle size determines the "inner" or specific surface area which is the potential contact area between filler material and surrounding binder matrix. Since nanomaterials tend to agglomeration may already occur in agglomerated states, the resulting surface area is largely affected by the degree of exfoliation and dispersion. Fully exfoliated and perfectly dispersed nanofiller will have the greatest effect on the physical properties. A comparison between different particles sizes is shown in Figure1.2.

The specific surface area is increased100fold when going from 10µm to 100nmwhile keeping the theoretical volume or the filling level constant.

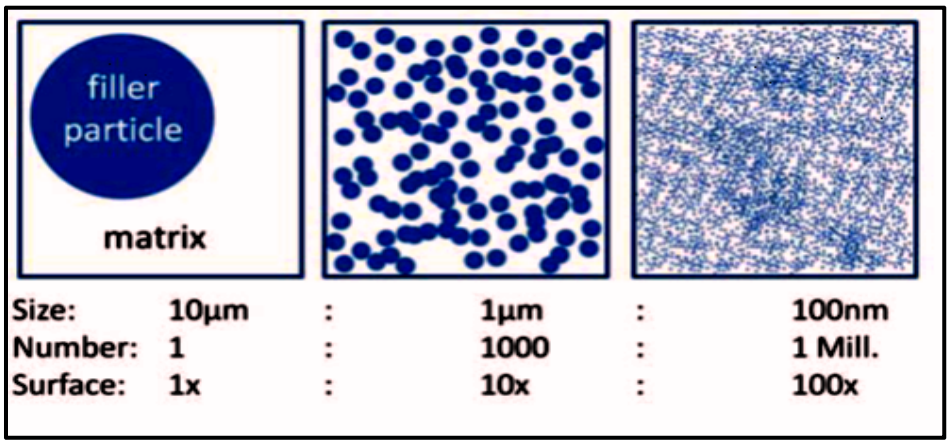

Figure 1.2 Different filler particle sizes at the same filling level. Going from 10µm to 100nm: a million times more particles exhibit a 100-fold increased inner surface area [4]

The infusion of nanoparticles into polymeric and other matrices results in nanocomposites materials with enhanced multifunctional characteristics. Nanocomposites are fundamentally new materials or hybrids in which at least one of the components has dimensions in the nanometer scale. The presence of nanoscale components gives nanocomposites intrinsically new properties and characteristics that are not present in

conventional composites or the pure components. The structure property relationship of nanocomposites is very much influenced by surface area/volume ratio of the nano inclusions.

The change in particle diameter, layer thickness, or fibrous material diameter from micrometer to nanometer, changes the surface area/volume ratio by three orders in magnitude. At this scale, there is often distinct size dependence of the material properties. With the increase in interfacial area, the properties of the composite become dominated by the properties of the interface or interphase. Figure 1.3shows the Schematic comparisons of 'macrocomposite' fibers in an amorphous matrix to that of a 'nanocomposite' at the same volume fraction of nanoclay filler

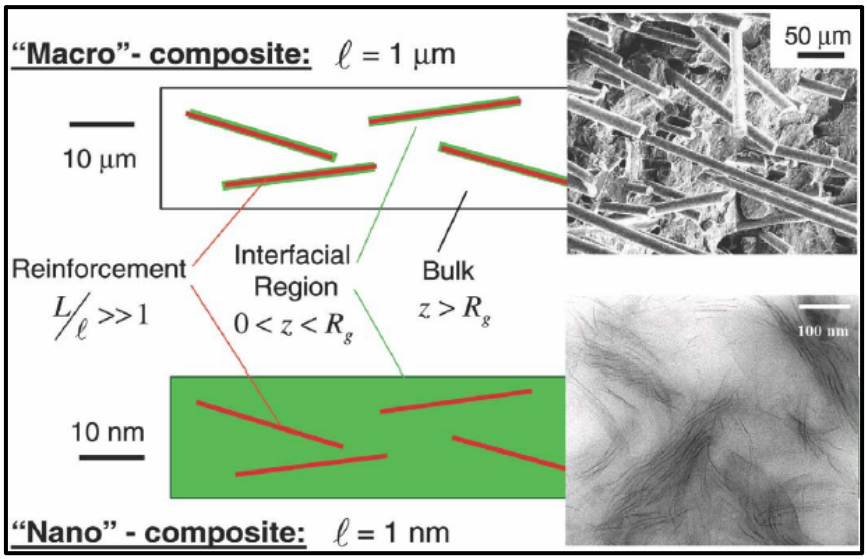

Figure 1.3 Schematic comparisons of 'macrocomposite' fibers in an amorphous matrix to that of a 'nanocomposite' at the same volume fraction of nanoclay filler

Recognizing these benefits, many researchers stated using various fillers in the polymer composites. The filler addition in to polymer leads to great improvement of their properties increases the demand on the filers. New nano filers have got great demand and start increasing in number such as nanoclays, carbon nanotubes, nanooxides, POSS, etc.

More recently new development has shown that much smaller fillers for example, nano sized particles, can lead to special effects which cannot be reached so easily with conventional/traditional fillers. However often the optimum effects for reducing both, coefficient of friction and the wear rate can only are achieved if nano fillers are used with combination with some of traditional tribo fillers [5].

1.6 NATURAL FIBER AS REINFORCING MATERIAL

Now-a-days, research and engineering interest have been shifting from traditional synthetic fiber composite to lignocellulosic natural fiber composite due to their advantages like high strength to weight ratio, non-carcinogenic and bio-degradability [6-9]. Besides the availability of natural fibers and easy of manufacturing have tempted researchers to try locally available inexpensive fiber and to study their feasibility of reinforcement purpose and to what extent they satisfy the required specifications of good reinforced polymer composite for different applications. With low cost and high specific mechanical properties, natural fiber represents a good renewable and biodegradable alternative to the most common synthetic reinforcement, i.e. glass fiber.

The term “natural fiber” covers a broad range of vegetable, animal and mineral fibers. However in the composite industry, it is usually refers to wood fiber and agro based bast, leaf, seed, and stem fibers. These fibers often contribute greatly to the structural performance of plant and, when used in plastic composites, can provide significant reinforcement.

Despite the interest and environmental appeal of natural fibers, their use is limited to non-bearing applications due to their lower strength compared with synthetic fiber reinforced polymer composite. The stiffness and strength shortcomings of bio composites can be overcome by structural configurations and better arrangement in a sense of placing the fibers in specific locations for highest strength performance. Accordingly extensive studies on preparation and properties of polymer matrix composite (PMC) replacing the synthetic fiber with natural fiber like Jute, Sisal, Pineapple, Bamboo and Kenaf were carried out [10-14]. These plant fibers have many advantages over glass fiber or carbon fiber like renewable, environmental friendly, low cost, lightweight, high specific mechanical performance.

Increased technical innovation, identification of new applications, continuing political and environmental pressure and government investments in new methods for fiber harvesting and processing are leading to projections of continued growth in the use of natural fibers in composites, use of 150,000 tonnes biocomposites (using 80,000 tonnes of wood and natural fibres) in the automotive sector in 2012 could expand to over 600,000 tonnes of biocomposites in 2020, using 150,000 tonnes of wood and natural fibres each along with some recycled cotton[15]. The easy availability of natural fibers and manufacturing have motivated researchers worldwide recently to try locally available inexpensive fibers and to

study their feasibility of reinforcement purposes and to what extent they satisfy the required specifications of good reinforced polymer composite for tribological applications [16].

There are many natural resources which India has in abundance. Most of it comes from the forest and agriculture. However in most cases residues from traditional crops such as rice husk or sugarcane bagasse or from the usual processing operations of timber industries do not meet the requisites of being long fibers. This biomass left over are abundant, and their use as a particulate reinforcement in resin matrix composite is strongly considered as a future possibility.

1.6.1 Jute fiber composite

Jute is an annual plant in the genus corchorus. The major types grown are generally known as white jute and tossa jute. Jute, grown mainly in India and Bangladesh, is harvested at 2 to 3 months of growth, at which time it is 3-5 meters tall. Jute has a pithy cover, known as jute stick and the blast fibers grow lengthwise around this core. Jute blast fiber is separated from the pith in a process known as retting. Retting is accomplished by placing cut jute stalks in ponds for several weeks. Microbial action in the pond softens the jute fiber and weakens the bonds between the individual fiber and the pith. The fiber stands are then manually stripped from the jute stick and hung on tracks to dry. Very long fiber stands can be obtained this way. If treated with various oils or conditioners to increase flexibility, the retted jute fiber stands are suitable for manufacturing of textiles.

Jute is multicelled in structure (Figure 1.4). The cell wall of a fiber is made up of a number of layers: the so-called primary wall (the first layer deposited during cell development) and the secondary wall (S), which again is made up of the three layers (S_1, S_2 and S_3**).** As in all lignocelluloses fibers, these layers mainly contain cellulose, hemicelluloses and lignin in varying amounts. The individual fibers are bonded together by a lignin-rich region known as the middle lamella. Cellulose attains highest concentration in the S_2 layer (about 50%) and lignin is most concentrated in the middle lamella (about 90%) which, in principle, is free of cellulose.

The S_2 layer is usually by far the thickest layer and dominates the properties of the fibers. Cellulose, a primary component of the fiber, is a linear condensation polymer

consisting of D-anhydro-glucopyranose units joined together by ß-1, 4-glucosidic bonds. The long chains of cellulose are linked together in bundles called micro-fibrils (Figure 1.5).

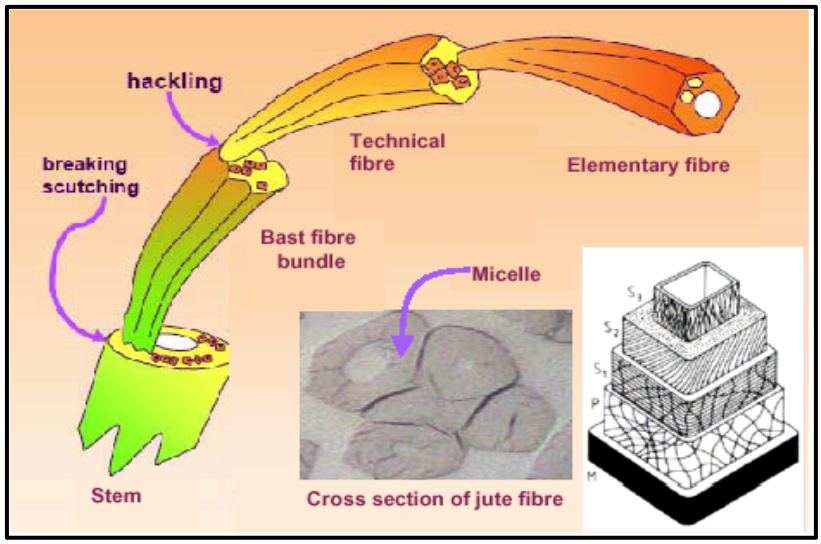

Figure 1.4 Scheme of jute fiber structure

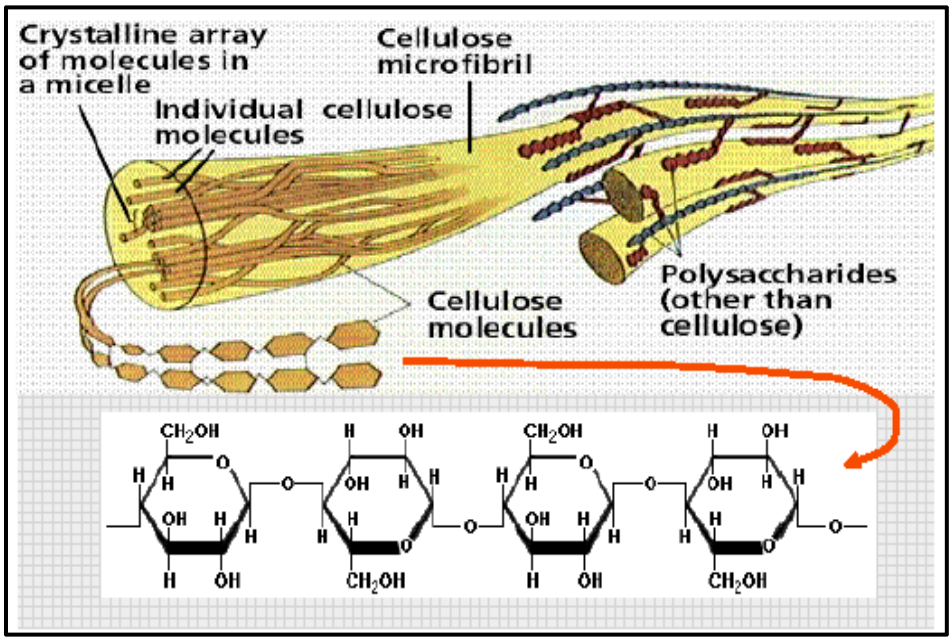

Figure 1.5 Structure of cellulose as it occurs in a plant cell wall

Hemicelluloses are also found in all plant fibers. Hemicelluloses are polysaccharides bonded together in relatively short, branching chains. They are intimately associated with the cellulose microfibrils, embedding the cellulose in a matrix. Hemicelluloses are very hydrophilic and have lower molecular masses than both cellulose and lignin. The degree of

polymerization (DP) is about 50 – 200. The two main types of hemicelluloses are xylans and glucomannans.

The structure of the jute fiber is influenced by climatic conditions, age and the fermentation process, which influence also the chemical composition [17]. A typical composition of the jute fiber is shown in Table 1.2.

Table 1.2 A typical composition of jute fiber

Substances	Weight percent (%)
Cellulose	61-71.5
Hemicelluloses	13.6-20.40
Pectin	0.2
Lignin	12-13
Moisture content	5-12.6
wax	0.5

There is a greater awareness of the need for materials with an expanding population and jute based composite provide an opportunity to fill this growing need for materials within a cost effective and acceptable environmental framework. Our history using jute in textile applications has limited our expectations of performance, which, ultimately, limits our ability to accept for improved jute-based composite materials. This is interesting as we have accepted completely new material such as material alloys, ceramics, and plastics that have limitations in their performance. But we tend to overlook any deficiencies they may have because our expectations of these materials are higher than those we have for jute-based composites. May be it is because we think we know everything there is about jute because it is very old familiar fiber used by common people for low cost markets.

Jute fiber is a not a low value resource with poor properties and it can be used in a great many value added products. Using jute fiber for composite has many advantages. Jute is renewable versatile nonabrasive, porous, hydroscopic, visco elastic, biodegradable, combustible, computable and reactive.

The fiber has a high aspect ratio, high strength to weight ratio, is low in energy conversion, and has good insulation properties. The jute fiber composites can be very cost-effective material especially for building & construction industry (panels, false ceilings, partition boards etc.), packing, automobile & railway coach interiors and storage devices.

1.6.2 Glass fibers

Glass fiber is a generic name like carbon fiber or steel. A variety of different chemical compositions is commercially available. Common glass fibers are silica based (50-60% SiO_2) and contains a host of other oxides of calcium boron, sodium, aluminum, and iron. Table 1.3 gives the composition of some common used glass fibers .The designation 'E' stands for electrical because E-glass is a good electrical insulator in addition to having good strength and a reasonable Young's Modulus. 'C' stands for corrosion because C-glass has a better resistance to chemical corrosion; 'S' stands for high silica content that makes S-glass withstand higher temperature than other glasses. It should be pointed out that most of the continuous glass fiber produced is of the E-glass type but, notwithstanding the designation E, electrical use of E-glass fiber are only small fraction of the total market**.**

Table 1.3 Approximate chemical composition of some glass fibers (wt.%)

Composition	**E-glass**	**C-glass**	**S-glass**
SiO_2	55.2	65.0	65.0
Al_2O_3	8.0	4	25.0
CaO	18.7	14.0	-
MgO	4.6	3.0	10
Na_2O	0.3	8.5	0.3
K_2O	0.2	-	-
B_2O_3	7.3	5.0	-

1.6.3 Limitation of glass fiber

Glass fiber reinforced composites suffer from three important limitations:

1. Comparatively low modulus of elasticity (the specific modulus of unidirectional fiber glass composites being of same order as aluminum, titanium, magnesium and steel).
2. Low interlaminar shear strength in relation to tensile strength.
3. Low compressive properties in relation to tensile properties (the comparison allowable for unidirectional layup being less than one half of tensile strength).

The low modulus of glass-reinforced composites has limited their usefulness in applications where buckling stability or high natural frequency is criteria. Both shear and compressive deficiencies have restricted performance in bending.

1.7 NEED FOR FLY-ASH AND ALUMINA AS FILLER MATERIAL

Since resins are very expensive, it will not be cost effective to fill up the voids in a composite matrix purely with resins. Fillers are added to the resin matrix for controlling material cost and improving its mechanical and chemical properties. Some composites that are rich in resins can be subject to high shrinkage and creep and low tensile strength. Although these properties may be undesirable for structural applications, there may be a place for their use.

Fillers are particles which added to material (plastics, composite material, and concrete) to lower the amount of more expensive matrix material or to enhance some properties of the mixture material. These filler also help to increase properties like mechanical, thermal properties, optical, electrical and fire-retardant properties. These filler are relatively high price even after giving numerous advantages. This problem can be addressed to by exploring the possibility of using some cheaper filler materials such as industrial wastes and slag. Rapid industrial development over the last decade has led to the generation of large amounts of solid waste in the form of ash, mud or slag, which has now come to a stage of environmental threat and needs disposal and/or utilization. Most of these wastes are buried in landfills, which is costly and environmentally unsatisfactory. Therefore, it is essential to see new options to recycle theses residues. It is evident from the characteristics of some of these wastes, generated from different processes, that they have good potential for recycling and for utilization in developing various value-added products.

In the past two decades, ceramic filled polymer composites have emerged as a subject of extensive research, but due to the high cost of conventional fillers it has become important to explore the potential use of cheap materials like minerals ores and industrial wastes like fly ash and red mud for utilization in preparing particles reinforced polymer composites.

1.7.1 Fly-Ash and Alumina

Fly ash is such an industrial waste, the potential of which as a filler material in polymers needs to be explored. It is generated during the combustion of coal for energy production and is an industrial by-product which is recognized as an environmental pollutant. Because of the environmental problems presented by the fly ash, considerable research has been under taken on the subject worldwide [18]. With rapid industrialization, it is but natural

that the power generation will keep increasing in future. About 70% of total power generation in India is through thermal power plants where sub-bituminous coal and/or lignite are burnt in huge amount and consequently there is an estimated generation of about 130 million tons of fly ash per annum as the major solid waste [19]. The research and development carried out in India for utilization of fly ash in making building materials has proved that fly ash can be successfully used for production of bricks, cement and other building materials. Indigenous technologies for construction of building materials utilizing fly ash are available and are being practiced in a few industries. However, large scale utilization is yet to takeoff. Even if the full potential of fly ash utilization through production of fly ash bricks and blocks is explored, the quantity, the quantity of fly ash produced by the thermal power plants is so huge that major portion of it will still remain unutilized. Hence, there is a need to evolve strategies and plans for safe and environmentally sound method of its disposal.

This disposal and utilization of fly ash will continue to be an important area of global concern due to dependence of countries like India on coal based power generation. Although fly ash management has been considerable improvement over the past few years, still its utilization level is very low. Some areas of fly ash utilization wherein technology projects have been completed or are under way include mine filling, road construction, embankments, hydraulic structures, manufacturing of bricks, blocks and tiles etc. Due to increasing environmental threat and growing magnitude of the problem it has become imperative to manage fly ash. It is true that from the same time from coal utilization perspective, fly ash is a resource yet to be fully utilized. This is why the producers of thermal electricity keep looking for ways to exploit fly ash.

Fly ash consists of fine, powdery particles predominantly spherical in shape either solid or hollow and mostly glassy (amorphous). It is generally grey in color, abrasive, mostly alkaline and refractory in nature. Its utilization as a low cost adsorbent for the removal of organic compounds, light weight aggregate, road sub-baser, construction material, mine and pit filler etc. has already been established [18]. However, very little is reported on its potential as nano material filler in polymer composites.

Alumina is one such ceramic material which has recently been recognized as potential filler in many applications starting from cosmetic, packaging materials to aerospace applications.

Visualizing the increase rate of generation of fly-ash as a waste material, though it has got lot of metal values its potential use for manufacturing value added products has not been addressed so far in a large scale. The present research work has been under taken to fabricate nano fly ash and alumina nano particles in the laboratory by utilizing the method of high energy ball milling and by auto combustion process. It is also planned to use these nano fillers as reinforcing material in polymer composite. The low modulus of glass-reinforced composites has limited their usefulness in applications where buckling stability or high natural frequency is criteria. Both shear and compressive deficiencies have restricted performance in bending. In this present investigation an attempt has also been made to prepare woven jute-glass fiber hybrid composite. Efforts are also made to study the effect of hybridization of glass and layering sequence on tensile strength, flexural strength, tensile modulus and flexural modulus of the composite with both micro and nano fillers. Experiment was also carried out to study the erosive wear behavior of the composite developed. In addition the incorporation of both nano fly-ash and alumina nano particles effects on the erosive wear behavior of hybrid composite has also been studied and reported in the thesis.

In the second chapter detail discussion of properties and structure of natural fibers, hybrid composites, nanocomposites and a literature review designed to provide a summary of the work related to present investigation are presented.

In the third chapter detail discussion on the fabrication and characterization of the fly ash, alumina nanoparticles and also characterization of jute fiber material have been presented.

In the fourth chapter mechanical characterization of Jute/glass fiber Hybrid composite with micro and nano filler has been studied.

In the fifth chapter the solid particle wear response of Jute/glass fiber hybrid composite with different layering sequence has been studied.

Sixth chapter discusses solid particle erosion wear behavior of the jute/glass-epoxy hybrid composite filled with fly ash/ alumina particulate fillers (both nano and microfiller).

In the seventh chapter conclusions have been drawn from the above studies mentioning scope for the future work.

Chapter 2

Literature Survey

2.1 INTRODUCTION

The literature survey is carried out as a part of the thesis work to have an overview of the production processes, properties and tribological behavior of polymer composite. Composite structures have shown universally a savings of at least 20% over metal counterparts and a lower operational and maintenance cost [20]. As the data on the service life of composite structures is becoming available, it can be safely said that they are durable, maintain dimensional integrity, resist fatigue loading and are easily maintainable and repairable. Composites will continue to find new applications, but the large scale growth in the market place for these materials will require less costly processing methods and the prospect of recycling [21] will have to be solved [22].

Composites materials have emerged as a major class of structural elements and are either used or being considered as substitutions for metals/traditional material in aerospace, automotive and other industries. The outstanding features of fiber reinforced polymer composites (FRPs) are their high specific stiffness, high specific strength and controlled anisotropy, which make them very attractive structural materials. Other advantages of composites are light weight, good corrosion resistance, impact resistance, fatigue strength and flexibility in design capabilities. A unique feature of composites is that the characteristics of the finished product can be tailored to a specific engineering requirement by a careful selection of matrix and reinforcement type. FRP composite materials consist of two or more chemically distinct constituents have a distinct interface separating them. It has a unique combination of properties that are noticeably different from the constituent properties.

Generally, a discontinuous phase (reinforcement) is embedded into a continuous phase (matrix). Polymer based composite materials (PMC) or FRP constitutes a major category of composites materials with a wide range of applications. They offer very attractive properties, which can be tailored to the specific requirements by careful selection the fiber, matrix, fiber configuration (short, long, strength, woven, braided, laminated, etc.) and fiber surface treatment. PMCs exhibit desirable physical and chemical properties that include lightweight coupled with

high stiffness and strength along the direction of the reinforcing fiber, dimensional stability, temperature and chemical resistance and relatively easy processing.

The role of matrix in a fiber-reinforced composite is to

(a) Transfer stresses between the fibers

(b) Provide a barrier against an adverse environment

(c) Protect the surface of fibers from mechanical abrasion

2.2 MATERIAL SELECTION

Many materials when they are in fibrous form exhibit very good strength properties but to achieve these properties the fiber should be bonded by a suitable matrix. The matrix isolates the fibers from one another in order to prevent abrasion and formation of new surface flaws and acts as a bridge to hold the fibers in place. A good matrix should possess ability to deform easily under applied load, transfer the load on to the fibers and evenly distribute stress concentration.

A study of the nature of bonding forces in laminates [23] indicates that upon initial loading there is a tendency for the adhesive bond between them accounts for the high strength properties of the laminates.

The polymer matrix binds the fibers together so as to transfer the load to and between them and protect them from environments and handling. Polymer or resin systems used to manufacture advanced Polymer Matrix Composites (PMCs) are of two basic types, thermosets and thermoplastics (including bio-derived ones).

2.2.1 Thermosets

Much of the early work used thermosetting resins as matrix material for composite production. Products like tufnol which is made from cotton fibers and epoxy resin, have been available for some time, having good stiffness and strength [24]. In the last few years there has been renewed interest in these products for use in automotive applications [25]. To achieve reinforcing effects in composites it is necessary to have good adhesion between the fibres and

resins. Epoxy and phenolic thermosetting resins are known to be able to form covalent cross-links with plant cell walls via -OH groups [26]. Composite manufacture can be achieved using low viscosity epoxy and phenolic resins that cure at room temperature. In addition epoxy resin does not produce volatile products during curing which is most desirable in production of void free composites. Therefore, although epoxy resins are relatively more expensive than polyester, they have potential for the development of high added value plant fiber composites, where long fibers at a high content are required.

The functional group in epoxy resins is called the oxirane, a three-membered strained ring containing oxygen. Epoxy resins, depending on their backbone structure, may be low or high viscosity liquids or solids. In low viscosity resin, it is possible to achieve a good wetting of fibres by the resin without using high temperature or pressure. The impregnation of fibers with high viscosity resins is done by using high temperature and pressure.

A wide range of starting materials can be used for the preparation of epoxy resins thereby providing a variety of resins with controllable high performance characteristics. These resins generally are prepared by reacting to a polyfunctional amine or phenol with epichlorohydrin in the presence of a strong base. The commercially available diglycidyl ether of bisphenol-A (DGEBA) Figure-2.1 is characterized by epoxy equivalent weight, which can be determined either by titration or quantitative infrared spectroscopy. The presence of glycidyl units in these resins enhances the process ability but reduces thermal resistance.

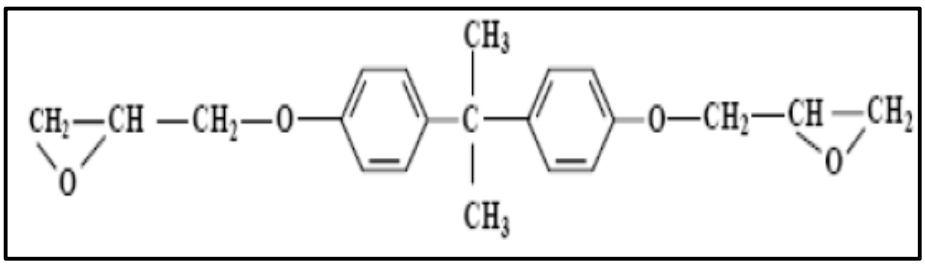

Figure 2.1 Chemical structure of DGEBA

The most widely used curing agents for epoxy resins are primary and secondary amines. The overall reaction rate of an amine with an epoxide is influenced by the steric hindrance and the electron withdrawing or electron donating groups present in the amine [27].

During curing, epoxy resins can undergo three basic reactions: Epoxy groups are rearranged and form direct linkages between themselves.

1. Aromatic and aliphatic -OHs link up to the epoxy groups.
2. Cross-linking takes place with the curing agent through various radical groups.

The advantages of epoxy resins are low polymerization shrinkages unlike polyesters during cure, good mechanical strength, excellent resistance to chemicals and solvents, and excellent adhesion to fibers. The epoxy molecule also contains two ring groups at its center, which are able to absorb both mechanical and thermal stresses better than linear groups, giving epoxy resin very good stiffness, toughness and heat resistance.

The primary disadvantages of the epoxy resins are that they require long curing times and, in general, their mold release characteristics are poor. The epoxy resins are characterized by their high adhesive strengths. This property is attributed to the polarity of aliphatic -OH groups and ether groups that exist in both the initial resin and cured system. The polarity associated with these groups promotes electromagnetic bonding forces between epoxy molecules and the polar fibers.

2.2.2 Bio-derived Thermoplastic Matrices

Cellulose fibers (e.g. hemp, flax, jute) are widely used with conventional thermoplastic polymers (e.g. PolyPropylene (PP), polyether (PE)) as reinforcement in composite production to improve mechanical properties. In fact, the history of composites from renewable resources is far longer than conventional polymers. The study and utilization of natural polymers is an ancient science. Typical examples, such as paper, silk, skin, and bone arts, can easily be found in museum around the world. In the biblical Book of Exodus, Moses's mother built the ark from rushes, pitch and slime- a kind of fiber reinforced composite, according to the current classification of material. During the opium war more than 1000 years ago, the Chinese built their castles to defend against invaders using a kind of mineral particle reinforced composite made from gluten rice, sugar, calcium carbonate and sand [28].

However, the availability of petroleum at a lower cost and the bio-chemical inertness of petroleum based products have proven disastrous for the market of natural polymers. It is only about last two decades when the significance of eco-friendly materials has been realized. Now polymers from renewable resources have started drawing an increasing amount of attention. The two main reasons for that are environmental concerns [29], and the realization that the petroleum resources are limited.

Generally, polymers from renewable resources can be classified into three groups: (1) natural polymers such as starch, protein, and cellulose. (2) Synthetic polymers from natural monomers, such as Polylactic acid (PLA) and (3) polymers from microbial fermentation, such as polyhydroxy butyrate (PHB). Like numerous other petroleum based polymers, many properties of polymers from renewable resources can be improved through composite production [28].

The development of synthetic polymers like PLA using monomers from natural resources has been a driving force for the development of biodegradable polymers from renewable resources. Therefore, in today's world PLA is the most promising among bio-derivable polymers [28]. PLA can be processed (e.g. compression molding, pultrusion, extrusion and injection moulding) like petroleum based polyolefins and its mechanical property is better than the widely used polymer PP [30]. On degradation PLA does not emit any carbon dioxide to the environment like other biodegradable materials from renewable resources. The degradation occurs by hydrolysis to lactic acid, which is metabolized by micro-organisms to water and carbon dioxide. If PLA is comprised together with other biomass, the biodegradation occurs within a couple of weeks and the material can fully disappear within a month [31]. Chemically, it is linear aliphatic polyester of lactic acid which can be obtained by fermentation of renewable agricultural materials like corn, sugarcane and sugar beets. Lactic acid is converted to a cyclic lactide dimer which is then polymerized to PLA through a ring opening reaction.

The major applications of PLA products are in household wastes as plastic bags, barriers for sanitary products and diapers, planting, and disposable cups and plates. However, a number of authors reported the possibilities of developing fully bio-degradable composite products by using biodegradable polymers as matrix and natural fibers as reinforcements [32, 33]. Keller et al. [34] reported that PLA should produce fiber reinforced composites with high mechanical

properties for light weight construction materials. Oksman et al. [30] observed that PLA had good potential as a polymer matrix in flax fiber reinforcement for composites production. They reported that the composite strength produced with PLA/flax was about 50% better than that of PP/flax composites. Due to the increasing commercial interest for natural fiber reinforced polymer composites for use in automotive applications and building constructions as well as demands for environmentally friendly materials, the development of fully biodegradable composites for many applications could be an interesting area of research.

2.2.3 Reinforcement

Reinforcement increases the strength, stiffness and the temperature resistance capacity and lowers the density of PMC. In order to achieve these properties the selection depends on the type of reinforcement, its method of production and chemical compatibility with the matrix and the following aspects must be considered while selecting the reinforcement material.

- Size – diameter and aspect ratio
- Shape – Chopped fiber, whisker, spherical or irregular particulate, flake, etc:
- Surface morphology – smooth or corrugated and rough:
- Poly – or single crystal
- Structural defects – voids, occluded material, second phase
- Surface chemistry
- Impurities
- Inherent properties – strength, modulus and density.

2.2.4 Reinforcement Materials

Particles used for reinforcing include ceramics and glasses such as small mineral particles, metal particles such as aluminum and amorphous materials, including polymers and carbon black. Particles are used to increase the modules of the matrix and to decrease the ductility of the matrix. Particles are also used to reduce the cost of the composites. Reinforcements and matrices can be common, inexpensive materials and are easily processed.

Some of the useful properties of ceramics and glasses include high melting temperature, low density, high strength, stiffness, wear resistance, and corrosion resistance. Many ceramics are good electrical and thermal insulators. Some ceramics have special properties; some ceramics are magnetic materials; some are piezoelectric materials; and a few special ceramics are even superconductors at very low temperatures. Ceramics and glasses have one major drawback: they are brittle. An example of particle reinforced composites is an automobile tire, which has carbon black particles in a matrix of poly-isobutylene elastomeric polymer.

Polymer composite materials have generated wide interest in various engineering fields, particularly in aerospace applications. Research is underway worldwide to develop newer composites with varied combinations of fibers and fillers so as to make them useable under different operational conditions.

2.3 FABRICATION METHODS OF PMCs

There are two general divisions of composites manufacturing processes: **open molding** and **closed molding.** With open molding, the gel coat and laminate are exposed to the atmosphere during the fabrication process. In closed molding, the composite is processed in a two-part mold set, or within a vacuum bag. There are a variety of processing methods within the open and closed molding categories:

(a) Open Molding Method:

1. Hand Lay-Up,
2. Spray-Up,
3. Filament Winding.

(b) Closed Molding Method:

1. Compression molding,
2. Pultrusion,
3. Vacuum Bag Molding,
4. Vacuum Infusion Processing,
5. Resin Transfer Molding (RTM).

2.3.1 Open Molding Method

Open molding process is saturating fiber reinforcement with resin, using manual rollout techniques to consolidate the laminate and removing the entrapped air. A major factor in this operation is the transfer of resin from a drum or storage tanks to the mold. The means used to transport the resin, in many cases, characterizes the specific process method.

(a) Hand Lay-Up

Hand lay-up is an open molding method suitable for making a wide variety of composites products including: boats, tanks bath ware, housings, truck/auto components, architectural products and many other products ranging from very small to very large. Production volume per mold is low; however, it is feasible to produce substantial production quantities using multiple molds. Simple, single-cavity molds of fiberglass composites construction are generally used. Molds can range from very small to very large and are low cost in the spectrum of soft composites molds.

Gel coat is first applied to the mold using a spray gun for a high-quality surface. When the gel coat has cured sufficiently, roll stock fiberglass reinforcement is manually placed on the mold. The lamination resin is applied by pouring, brushing, spraying, or using a paint roller. FRP rollers, paint rollers, or squeegees are used to consolidate the laminate, thoroughly wetting the reinforcement, and removing entrapped air. Subsequent layers of fiberglass reinforcement are added to build laminate thickness (Figure 2.2).

Simplest method offering low-cost tooling, simple processing and wide range of part sizes are the major advantages of this process. Design changes are readily made. There is a minimum investment in equipment. With skilled operators, good production rates consistent quality is obtainable.

(b) Spray Lay-Up

Spray-up or chopping is similar to hand lay-up in its suitability for making boats, tanks, transportation components and tub/shower units in a large variety of shapes and sizes. A chopped

laminate has good conformability and is sometimes faster than hand lay-up in molding complex shapes. In the spray-up process the operator controls thickness and consistency, therefore the process is more operator dependent than hand lay-up. Although production volume per mold is low, it is feasible to produce substantial production quantities using multiple molds. As with hand lay-up, gel coat is first applied to the mold prior to spray-up of the substrate laminate.

Continuous strand glass roving and catalyzed resin are fed through a chopper gun, which deposits the resin-saturated "chop" on the mold as shown in Figure 2.3. The laminate is then rolled to thoroughly saturate the glass strands and compact the chop. Additional layers of chop laminate are added as required for thickness.

(c) Filament Winding

Filament winding is an automated open molding process that uses a rotating mandrel as the mold. The male mold configuration produces a finished inner surface and a laminated rough surface on the outside diameter of the product. Filament winding results in a high degree of fiber loading, which provides high tensile strengths in the manufacture of hollow, generally cylindrical products such as chemical and fuel storage tanks, pipes, stacks, pressure vessels, and rocket motor cases. Mandrels of suitable size and shape, made of steel or aluminum form the inner surface of the hollow part. Some mandrels are collapsible to facilitate part removal.

Figure 2.4 shows the schematic picture of a typical filament winding process. Continuous strand roving is fed through a resin bath and would onto a rotating mandrel. The roving feed runs on a trolley that traverses the length of the mandrel. The filament is laid down in a predetermined geometric pattern to provide maximum strength in the directions required. When sufficient layers have been applied, the laminate is cured on the mandrel. The molded part is then stripped from the mandrel. Equipment is available for filament winding on a continuous basis with two axes winding for pressure cylinders. This process makes high strength-to-weight ratio laminates and provides a high degree of control over uniformity and fiber orientation.

The filament winding process can be used to make structures, which are highly engineered and meet strict tolerances. Because filament winding is automated, the labor factor for filament winding is lower than other open molding processes.

2.3.2 Closed Molding Method

(a) Compression Molding

Compression molding is a high-volume, high-pressure method suitable for molding complex, fiberglass-reinforced plastic parts on a rapid cycle time. There are several types of compression molding including: sheet molding compound (SMC) which are, bulk molding compound (BMC), thick molding compound (TMC), and wet lay-up compression molding. Compression molding tooling consists of heated metal molds mounted in large presses. Tooling is usually machined steel or cast alloy molds that can be in either single or multiple-cavity configurations. Steel molds are hardened and sometimes chrome plated for enhanced durability. The molds are heated using steam, hot oil, or electricity. Side cores, provisions for inserts, and other refinements are often employed. Mold materials include cast of forged steel, cast iron, and cast aluminum.

The mold set is mounted in a hydraulic or mechanical molding press. The molds are heated to 2500 to 4000°F. A weight charge of molding compound is placed in the open mold as shown in Figure 2.5. The two halves of the mold are closed and pressure is applied. Depending on thickness, size, and shape of the part, curing cycles range from less than a minute to about five minutes. The mold is opened and the finished part is removed. Typical parts include: automobile components, appliance housings and structural components, furniture, electrical components, and business machine housings and parts.

Compression molding produces fast molding cycles and high part uniformity. The process can be automated. Good part design flexibility and features such as inserts, ribs, bosses, and attachments can be molded in. Good surface finishes are obtainable, contributing to lower part finishing cost. Subsequent trimming and machining operations are minimized in compression molding.

(b) Pultrusion

Pultrusion is a continuous process for the manufacture of products having a constant cross section, such as rod stock, structural shapes, beams channels, pipe, tubing, fishing rods, and

golf club shafts. Pultrusion produces profiles with extremely high fiber loading, thus pultruded products have high structural properties. Hardened steel dies are machined and include a perform area to do the initial shaping of the resin- saturated roving. The dies include heating which can be electric or hot oil. The latest pultrusion technology uses direct injection dies, in which the resin is introduced inside the die, rather than through an external resin bath, which may be called as partial RTM.

Continuous strand fiberglass roving, mat, cloth, or surfacing veil is impregnated in a resin bath, then pulled (pultrusion) through a steel die, by a powerful tractor mechanism (Figure 2.6). The steel die consolidates the saturated reinforcement, sets the shape of the stock, and controls the fiber/resin ratio. The die is heated to rapidly cure the resin. Many creels (balls) of roving are positioned on a rack, and a complex series of tensioning devices and roving guides direct the roving into the die.

The process is a continuous operation that can be readily automated. It is adaptable to both simple and complex cross-sectional shapes. Very high strengths are possible due to the fiber loading and labor costs are low.

c) Vacuum Bag Molding

The mechanical properties of open-mold laminates can be improved with vacuum bagging. By reducing the pressure inside the vacuum bag, external atmospheric pressure exerts force on the bag. The pressure on the laminate removes entrapped air, excess resin and compact the laminate. Vacuum bagging can be used with wet lay laminates and prepreg advanced composites. In wet lay-up bagging the reinforcement is saturated using hand lay-up, then the vacuum bag is mounted on the mold and used to compact the laminate and remove air voids. In the case of prepreg advanced composites molding, the prepreg material is laid up on the mold, the vacuum bag is mounted and the mold is heated or the mold is placed in an autoclave that applies both heat and external pressure, adding to the force of atmospheric pressure. The prepreg-vacuum bag-autoclave method is most often used to create advanced composites used in aircraft and military products. Molds are similar to those used for conventional open-mold processes.

In the simplest form of vacuum bagging, a flexible film (PVA, Nylon, Mylar, or Polyethylene) is placed over the wet lay-up, the edges sealed, and a vacuum drawn. A more advanced form of vacuum bagging places a release film over the laminate, followed by a bleeder ply of fiberglass cloth, non-woven nylon, polyester cloth, or other material that absorbs excess resin from the laminate. Figure 2.7 shows the schematic picture of vacuum bag molding process. A breather ply of a non-woven fabric is placed over the bleeder ply, and the vacuum bag is mounted over the entire assembly. Pulling a vacuum from within the bag uses atmospheric pressure to eliminate voids and force excess resin from the laminate. The addition of pressure further results in high fiber concentration and provides better adhesion between layers of sandwich construction. When laying non-contoured sheets of PVC foam or balsa into a female mold, vacuum bagging is the technique of choice to ensure proper secondary bonding of the core to the outer laminate.

Vacuum bag processing can produce laminates with a uniform degree of consolidation, while at the same time removing entrapped air, thus reducing the finished void content. Structures fabricated with traditional hand lay-up techniques can become resin rich and vacuum bagging can eliminate the problem. Additionally, complete fiber wet-out can be accomplished if the process is done correctly. Improved core-bonding is also possible with vacuum bag processing.

(d) Vacuum Infusion Processing

Vacuum infusion is a variation of vacuum bagging where the resin is introduced into the mold after the vacuum has pulled the bag down and compact the laminate. The method is defined as having lower than atmospheric pressure in the mold cavity. The reinforcement and core material are laid-up dry in the mold. This is done by hand and provides the opportunity to precisely position the reinforcement. When the resin is pulled into the mold the laminate is already compacted; therefore, there is no room for excess resin. Very high resin to glass ratio are possible with vacuum infusion and the mechanical properties of the laminate are superior. Vacuum infusion is suitable to mold very large structures and is considered a low volume molding process. Molds are similar to those used for conventional open-mold processes.

The mold may be gel coated in the tradition fashion. After the gel coat cures, the dry reinforcement is positioned in the mold. This includes all the plies of the laminate and core material if required. A perforated release film is placed over the dry reinforcement. Next a flow media consisting of a course mesh or a "crinkle" ply is positioned, and perforated tubing is positioned as a manifold to distribute resin across the laminate. The vacuum bag is then positioned and sealed at the mold perimeter. A tube is connected between the vacuum, bag and the resin container. A vacuum is plied to consolidate the laminate and the resin is pulled into the mold (Figure 2.8).

Vacuum infusion can produce laminates with a uniform degree of consolidation, producing high strength, lightweight structures. This process uses the same low cost tooling as open molding and requires minimal equipment. Very large structures can be fabricated using this method. Vacuum infusion offers a substantial emissions reduction compared to either open molding or wet lay-up vacuum bagging.

(e) Resin Transfer Molding

Resin transfer molding is an intermediate volume molding process for producing composites. The RTM process is to inject resin under pressure into a mold cavity. Vacuum assist can be used to enhance resin flow in the mold cavity. RTM can use a wide variety of tooling, ranging from low cost composite molds to temperature controlled metal tooling. RTM can utilize either "hard" or "soft" tooling, depending upon the expected duration of the run. Soft tooling would be either polyester or epoxy molds, while hard tooling may consist of cast machined aluminum, electroformed nickel shell, or machined steel molds. RTM can take advantage of the broadest range of tooling.

Figure 2.9 shows the picture of resin transfer molding process of polyester resin with peroxide catalyst. The mold set is gel coated conventionally, if required. The reinforcement (and core material) is positioned in the mold and the mold is closed and clamped. The resin is injected under pressure, using mix/meter injection equipment, and the part is cured in the mold. The reinforcement can be either performs or pattern cut roll stock material. Performs are reinforcement that is pre-formed in a separate process and can be quickly positioned in the mold.

RTM can be done at room temperature; however, heated molds are required to achieve fast cycle times and product consistency.

This closed molding process produces parts with two finished surfaces. By laying up reinforcement material dry inside the mold, any combination of materials and orientation can be used, including 3-D reinforcements. Part thickness is determined by the tool cavity.

2.4 NATURAL FIBER REINFORCED POLYMER COMPOSITES

Natural fiber reinforced polymer composites are hybrid with their properties, with characteristics of both natural fibers and polymers. In the beginning of the 20th century wood- or cotton fiber reinforced phenol- or melamine formaldehyde resins were fabricated and used in electrical applications for their non-conductive and heat-resistant properties. Incorporation of natural fibers in to polymer is now a standard technology to improve the mechanical properties of polymer. Mechanical properties like tensile strength and young's modulus are enhanced in the end products (composites) as the fibers in the composites determine the tensile strength and young's modulus of the materials [35].

One of the largest areas of recent growth in natural fiber plastic composites in worldwide is the automotive industry, where natural fibers are advantageously used as a result of their low density and increasing environmental pressures. Natural fibers composites found application where load bearing capacity and dimensional stability under moist and high thermal conditions are of second order importance. For example, flax fiber reinforced polyolefin are extensively used today in the automotive industry, but the fiber acts mainly as filler material in non-structural interior panels [36]. Natural fiber composites used for structural purposes do exist, but then usually with synthetic thermo-set matrices which of course limit the environmental benefits [37, 38].

Plant fibers, such as hemp, flax and wood, have large potential as reinforcement in structural materials due to the high aspect ratio and high specific strength- and stiffness of the fibers [17, 39-41]. Apart from good specific mechanical properties and positive environmental impact, other benefits from using natural fibers worth mentioning are low cost, friendly

processing, low tool wear, no skin irritation and good thermal and acoustic insulating properties [41].

A complete biodegradable system may be obtained if the matrix material also comes from a renewable resource. Examples of such materials are lignophenolics, starch and PLA. Some of these systems show encouraging results. For example Oksman et al. [30] have reported that flax fiber composites with PLA matrix can compete with and even outperform flax/polypropylene composites in terms of mechanical properties. In a recent study [42] it was found that composites of poly-L-Lactide Acid (PLLA) reinforced by flax fibers can show specific tensile modulus equivalent to that of glass/polyester short fiber composites. The specific strength of flax/PLLA composites was lower than that of glass/polyester, but higher than that of flax/polyester.

The limited use of natural fiber composites is also connected with some other major disadvantages still associated with these materials. The fibers generally show low ability to adhere to common non-polar matrix materials for efficient stress transfer. Furthermore, the fibers inherent hydrophilic nature makes them susceptible to water uptake in moist conditions. Natural fiber composites tend to swell considerably with water uptake and as a consequence mechanical properties, such as stiffness and strength, are negatively influenced. However, the natural fiber is not inert. The fiber-matrix adhesion may be improved and the fiber swelling reduced by means of chemical, enzymatic or mechanical modifications [17].

There are many application of natural fiber composite in everyday life. For example, jute is a common reinforcement for composites in India. Jute fibers with polyester resins are used in buildings, elevators, pipes, and panels [43]. Natural fiber composites can also be very cost effective material for application in building and construction areas (e.g. walls, ceiling, partition, window and door frames), storage devices (e.g. bio-gas container, post boxes, etc.), furniture (e.g. chair, table, tools, etc.), electronic devices (outer casting of mobile phones), automobile and railway coach interior parts (inner fenders and bumpers), toys and other miscellaneous applications (helmets, suitcases).

During the last few years, a series of works have been done to replace the conventional synthetic fiber with natural fiber composites [44–50]. For instant, hemp, sisal, jute, cotton, flax

and broom are the most commonly fibers used to reinforce polymers like polypropylene [51], polystyrene [52], and epoxy resins [26]. In addition, fibers like sisal, jute, coir, oil palm, bamboo, bagasse, wheat and flax straw, waste silk and banana [45, 46, 51–61] have proved to be good and effective reinforcement in the thermoset and thermoplastic matrices. Nevertheless, certain aspects of natural fiber reinforced composite behavior still poorly understood such as their visco-elastic, visco-plastic or time-dependent behavior due to creep and fatigue loadings [62], interfacial adhesion [63, 64], and tribological properties. Little information concerning the tribological performance of natural fiber reinforced composite material [55–59, 64] has been available in the literatures. In this context, long plant fibers, like hemp, flax [66, 67], bagasse [23] and bamboo [58, 59] have considerable potential in the manufacture of composite materials for tribo applications.

Among these fibers, Jute is the one of the most common argo-fibers which has high tensile modulus and low elongation at break. If the low density ($1.4gm/cm^3$) of this fiber is taken into consideration, then its specific stiffness and strength are comparable to those of glass fiber [65-67]. There are many reports about the use of jute as reinforcing fibers for thermosets [68, 69].

A.K Rana and Jayachandran [70] given a comparison of the jute fiber as a reinforcing material compared to glass fiber and conclude that this natural fiber possesses some draw backs and needs chemical modification for improvement in properties.

Shima et al. [71] tried to evaluate the mechanical properties of jute fibers by subjecting them to different types of surface treatment. Their results show the increase in strength for short fiber and decrease in strength for long fiber after subjecting them to different treatment.

Ray, Sarkar et al. [72] studied the thermal behavior of vinyl ester resin matrix composite reinforced with jute fibers treated for 2, 4, 6, and 8hr with 5% NaOH. They report that the modulus of jute fibers improved by 12, 68 and 79% after 4, 6 and 8hrs of treatment, respectively. The tenacity of fibers improved by 46% after 6 and 8hrs treatments and the percent breaking strain is reduced by 23% after 8h treatment.

Mishra et al. [73] studied on improve the mechanical performance of jute composite by using unidirectional oriented jute silvers as the reinforcements and general purpose polyester resin as the matrix. The primary objective of their work to develop surface modification through the bleaching process in an economical way unlike the conventional grafting and surface coating used by previous workers. Composites having 60 wt.% of jute fiber yielded the best results. The flexural storage modulus was found to be 12.3GPa at 30°C and to decrease slowly with temperature. The major finding in this work is the attainment of high mechanical properties of composite specimens with 60 wt.% fiber loading. On a weight and cost basis, bleached jute fibers were found to be better reinforcements than other fibers with usual surface modification by coating or grafting processes.

Giridhar and Rao [74] made a comparative study in which raw jute fiber has been incorporated in a polyester resin matrix to form uniaxial reinforced composite containing up to 60 volume percent fiber. The tensile strength and young's modulus work of fracture determined by charpy impact and inter- laminar shear strength have been measured as a function of fiber volume fraction.

Ray et al. [75] studied the effect of 5% NaOH treatment for short duration on jute reinforcing fiber material to vinylester resin. Their reports showed improved mechanical properties. The Flexural strength improved by 20% and modulus by 23%.

Mitra et al. [76] tried to improve the fiber matrix bonding by treating the surface of the jute fibers with pre-condensate like phenol formaldehyde, and melamine formaldehyde and cashew nut shell formaldehyde before impregnating with the PF resin for composite fabrication.

Md. Rezaur Rahman et al. [77] while studying the strength behavior of jute fiber found that young's modulus, flexural modulus and hardness of the composites increases with increase in the fiber loading and also showed that 30% jute fiber reinforcement had the optimum set of mechanical properties.

K. Sabeel Ahmeda and S. Vijayarangan [78] studied the Effect of stacking sequence on tensile, flexural and interlaminar shear properties of woven jute-glass fabric reinforced isothalic

polyester composites and reported that incorporation of glass in jute fiber composites enhances the properties of resulting hybrid composites and the Layering sequence (altering the position of glass plies) significantly affects the flexural and interlaminar shear strength.

Recently C. Santulli and A.P. Caruso [79] studied the comparison between two composite architectures namely a hemp/epoxy random mat and a jute/epoxy plain weave laminate, both with 45±2% volume fraction and their work reported that manufacturing a hybrid laminate, using jute/epoxy plain woven and hemp/epoxy random mat, most preferably the latter (inherently stronger) as skins and the former as core, would be able to reduce the scattering in impact resistance values and lead to a better predictability of its impact behavior.

P. Kanakasabai, et al. [80] studied the effect of fabric treatment and filler content on jute polymer composites and their result found that fabric treatment significant improve mechanical property of composite and the filler (calcium carbonate up to 40%) no significant improve the mechanical property or say decrease the mechanical property of composite and so that, we can use filler 10% for reducing the moisture absorption of the composite.

S.K. Acharya et al. [81] processed a composite using fly ash, jute with epoxy and investigate its weathering behavior on mechanical properties such as flexural strength. Their reports state that three layered jute composite shows maximum stress value with 15% fly ash reinforcement.

Thi-Thu-Loan Doan et al. [82] treated the surface of jute fiber with alkaline to enhance the interfacial interaction between jute natural fibers and experimented single fiber pull-out tests combined with SEM and AFM characterization of the fracture surfaces were used to identify the interfacial strengths and to reveal the mechanisms of failure and an epoxy matrix**.**

As explained earlier nano sized particles, can lead to special effects which cannot be reached so easily with conventional/traditional fillers [83]. Accordingly lot of research has been carried out in recent past with nano filler. Table 2.1 shows the list of research work carried out with nano fillers.

Table 2.1 List of researchers worked on nanofiller composites

Researcher	Year	Reinforcement	Matrix type	Studies	Ref
Li-xin Zhao et al.	2006	nano-Al_2O_3	Polyamide 6	Tribological properties	84
Y. Wang et al.	2006	nano Al_2O_3	Xylan 1810/D1864	micro-hardness test, single-pass scratch test, abrasive wear test	85
L. Chang et al.	2006	short carbon fibre, graphite, PTFE and nano-TiO_2	Epoxy	Tribological properties	86
Jin-Chein Lin et al.	2006	Na-montmorillonite and titanium dioxide	Polyester epoxy	Mechanical behavior	87
S. Kumar et al.	2007	carbon nanofiber	Polyetherimide	mechanical, morphological and electrical properties	88
D.K. Kolluri et al.	2007	graphite	Phenolic	tribo-performance	89
Zhenyu Jiang et al.	2008	short carbon fibers and sub-micro TiO_2 particles	Polyphenylene sulfide	Friction and wear behavior	90
G. Zhang et al.	2008	nano-SiO_2	Polyetheretherketone	Tensile and tribological behavior	91
Feng-hua Su et al.	2008	Nanometer ZnO	Phenolic	Friction and wear behavior	92
Hui-juan Zhang et al.	2009	Sb_2O_3 and melaminecyanurate	Phenolic resin	Tribological behavior	93
Qing Bing Guo et al.	2009	nano-SiO_2/ short carbon	Epoxy	Sliding wear performance	94
Hao-Jie Song et al.	2010	nano-ZnO	Polyurethane	Tribological behavior	95
A. Mirmohseni	2010	poly(acrylonitrile-co-butadiene-co-styrene) (ABS), clay (layered nano-filler) and nano-TiO_2	Epoxy	Impact and tensile strength	96

Yanhong Yan	2011	nano-Al_2O_3, nano-copper, nano-SiO2 and nano-TiO_2,	Polytetrafluroethylene	Mechanical properties	97
Mohit Sharma	2011	Carbon fabric	Polyethersulphone	Sliding wear performance	98
Yijun Shi	2011	micrometer and nanometer TiO_2	Polytetrafluoroethylene/Polyimide	Tribological behavior	99
R.V. Kurahatti	2011	nano-zirconia (nano-ZrO_2)	Bismleimide (BMI)	friction and dry sliding wear behavior	100
Guo-ming Lin	2012	carbon fibers (CFs) and nano-ZrO_2	Polyetheretherketone	Mechanical and wear properties	101
B. Ben Difallah	2012	graphite powder	Acrylonitrile Butadiene Styrene	Mechanical and tribological	102
Boon-Peng Chang	2013	micro-andnano-ZnO	Polyethylene	Abrasive test	103
S.R. Chauhan	2013	cenosphere	Vinylester	Friction and wear properties	104
Zheng-zhi Wang	2013	silica	Epoxy	Wear properties	105
P.V. Antunes	2014	SiC	Polyester	Mechanical and wear behaviors	106

After reviewing the existing literature available on hybrid composite with both micro and nano fillers it is clear that the interfacial bond between the reinforcing fiber and the resin matrix is an important element to realize the mechanical properties of the composite. It is also found that mechanical properties of natural fiber composite are much lower than those of synthetic fiber composite. Another disadvantage of jute fiber which makes it less attractive is the poor resistance to moisture absorption. Hence use of jute fiber alone in polymer matrix is inadequate in satisfactorily tackling all the technical needs of a fiber reinforced composite. In addition, to obtain the desired properties from composite system reinforcement and fillers both micro and nano are added for polymer materials.

Thus the priority of this work is twofold.

(1) To develop a polymer matrix hybrid composite with jute and glass fiber as reinforcement material. To improve the mechanical strength of the hybrid composite particulate filler both micro and nano are added to the composite. Fillers like fly ash and alumina (both micro and nano) are added to the fibers. These fillers are cheap and non-toxic and can be obtained from renewable resources and are easily recyclable. The mechanical properties like tensile, flexural stresses and modulus with and without fillers are evaluated and reported.

(2) The potential of the developed hybrid composite for tribological application (solid particle erosion test) with and without fillers have also been carried out and reported in this thesis.

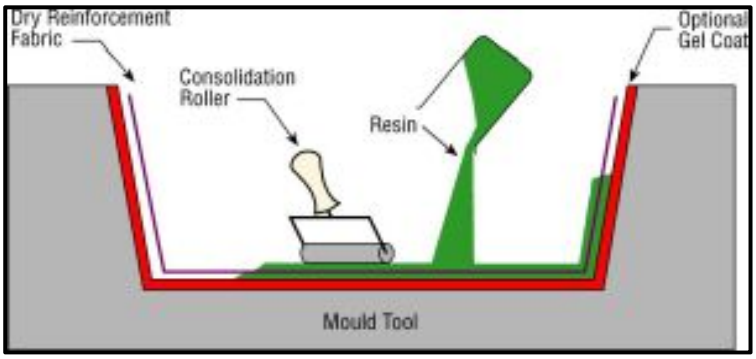

Figure 2.2 Hand Lay-Up Technique

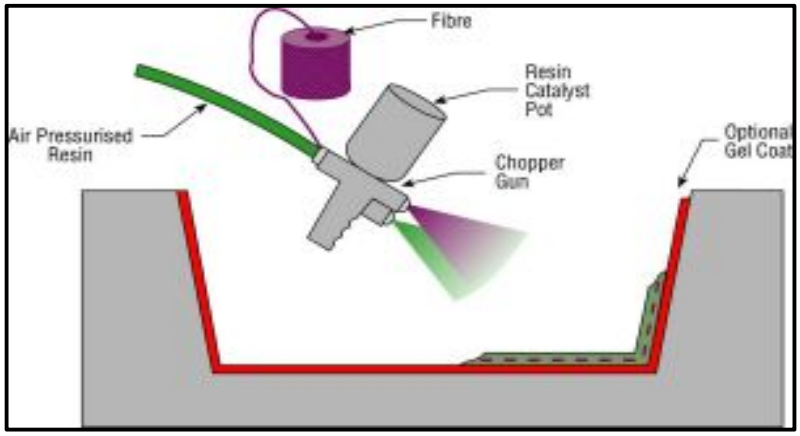

Figure 2.3 Spray up Technique

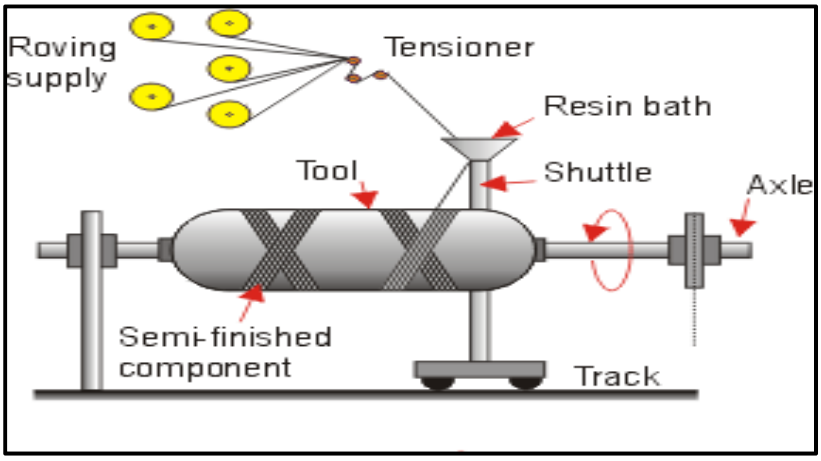

Figure 2.4 Filament Winding Process

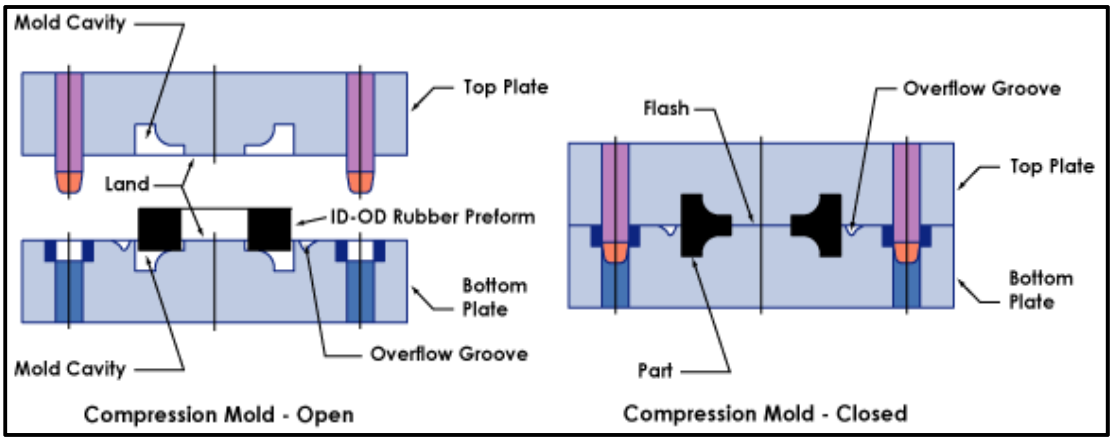

Figure 2.5 Compression Molding Technique

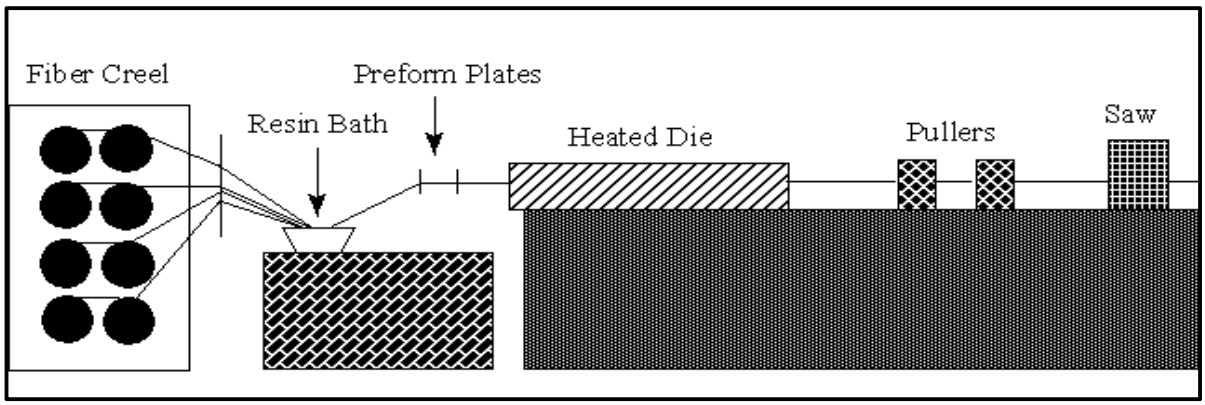

Figure 2.6 Pultrusion Process

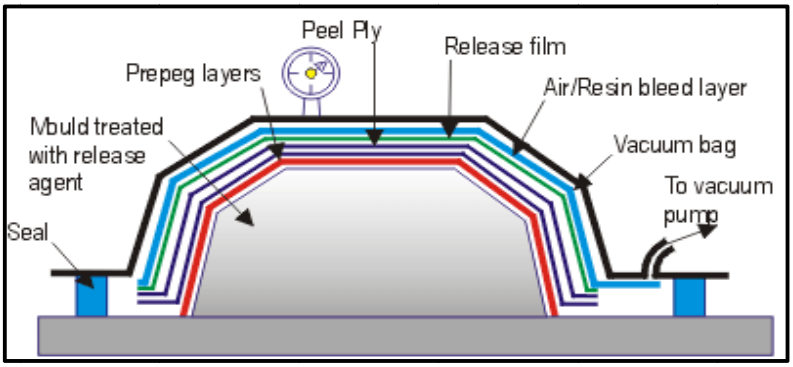

Figure 2.7 Vacuum Bag Molding

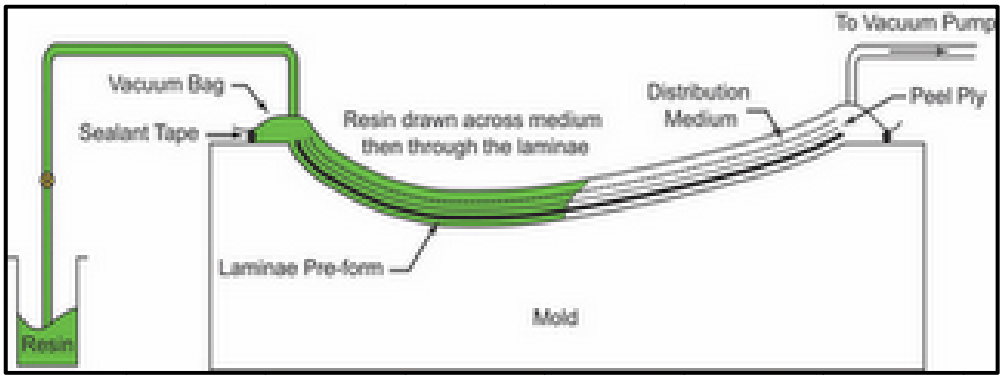

Figure 2.8 Vacuum Infusion Process

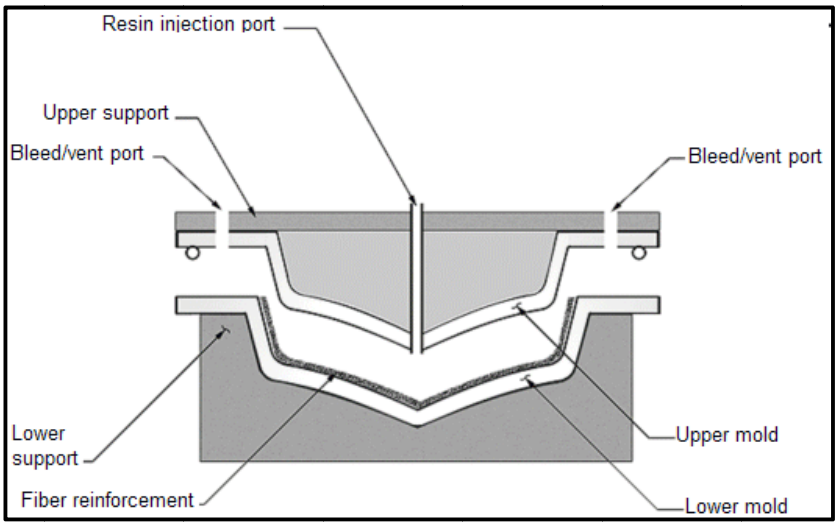

Figure 2.9 Resin Transfer Molding

Chapter 3

Nano Fabrication and Characterization

3.1 INTRODUCTION

The prefix “nano” has found in last decade an ever-increasing application to different fields of the science and engineering. Nanoscience, nanotechnology, nanomaterials or nanochemistry are only a few of the new nano-containing terms that occur frequently in scientific reports, in popular books as well as in newspapers, electronic media and that have become familiar to a wide range of people.

The Science and Engineering of Nanomaterials is proving to be one of the most attractive and promising fields for technological development in this century. Nanomaterial is defined as the materials with the microstructure having at least one dimension in nanometer range. It has appeal of miniaturization; also it imparts enhanced mechanical, electronic, magnetic, optical and chemical properties to a level that cannot be achieved by conventional materials. In the scientific literature several terms related to Nanoscience can be found, of which it is worth highlighting nanoparticles, nanocrystals, nanofibers, nanotubes and nanocomposites. In fact, all these are related to nanostructure materials, which have well defined structural features.

Nano particles have been extremely interesting subject in modern materials science over the past decades due to their enormous technological important. Nanoparticles often have unexpected visible properties because they are small enough to scatter visible light rather than absorb it. The interesting and sometimes unexpected properties of nanoparticles are therefore largely due to the large surface area of the material, which dominates the contributions made by the small bulk of the material.

The term nanoparticle is a combined name for both nanospheres and nanocapsules. Nanospheres are solid core spherical particulates which are nanometric in size. Nanocapsules are systems in which the drug is confined to a cavity surrounded by a unique polymer membrane.

Ceramics are inorganic, crystalline, nonmetallic solids made by the heating and subsequent cooling of the material. The nanoparticles made up of inorganic (ceramic) compounds silica, (inorganic/metal) Titania and alumina. Exist in size less than 50nm, which helps them in evading deeper parts of the body.

3.1.1 Structure of nanoparticles

Nanostructured materials as a subject of nanotechnology are low dimensional materials comprising of building units of a submicron or nanoscale size at least in one direction and exhibiting size effects. The structure of the nanomaterials can be classified as zero-dimensional, one-dimensional, two-dimensional and three-dimensional. Zero-dimensional nanostructures are such as uniform particles arrays (quantum dots), heterogeneous particles arrays, core–shell quantum dots, onions, hollow spheres and nanolenses. One-dimensional nanostructures are such as whiskers, fibers (or fibrils), nanowires, nanorods, nanotubes, nanobelts, nanoribbons, and hierarchical nanostructures.

Two-dimensional nanostructures have two dimensions outside of the nanometric size range. Two-dimensional nanostructures are such as junctions (continuous islands), branched structures, nanoprisms, nanoplates, nanosheets, nanowalls, and nanodisks. Three-dimensional nanostructures have recently attracted intensive research interests because the nanostructures have higher surface area and supply enough absorption sites for all involved molecules in a small space. Three-dimensional nanostructures are such as nanoballs (dendrite structures), nanocoils, nanocones, nanopillers and nanoflowers.

3.2 NANOPARTICLE SYNTHESIS

The methods of synthesis of nanoparticles are well known for a long time as compared to the other nanomaterials. For the synthesis of nanoparticles, the processing conditions need to be controlled in such a manner that the resulting nanoparticles have the following characteristics:

1. Identical size of all particles
2. Identical shape
3. Identical chemical composition and crystal structure and
4. Individually dispersed with no agglomeration

There are three main approaches to the synthesis of nanomaterials and the fabrication of nanostructures; via top-down, bottom-up and hybrid approach.

3.2.1 Top down approach

Top down approach involves the breaking down of the bulk material into nano sized structures or particles. These techniques are an extension of those that have been used for producing micron- sized particles.

Attrition or milling is a typical top down method in preparing nanoparticles, whereas chemical precipitation involving the building up of the atom or molecular constituents is a typical bottom up method.

3.2.1.1 High energy ball milling method (Mechanical alloying method)

This is a top-down approach for nanomaterial synthesis. This method has been used for the generation of magnetic, metallic and catalytic nanoparticles. Ball milling and subsequent annealing is a simple method for the large production of various nanopowders. In these process elemental blends, pre alloyed powders and ceramics are milled to achieve alloying at the atomic level. A ball mill, a type of grinder, is a cylindrical device used in grinding (or mixing) materials like ores, chemicals, ceramic raw materials and paints. Ball mills rotate around a horizontal axis, partially filled with the material to be ground plus the grinding medium. Different materials are used as media, including ceramic balls, and stainless steel balls. An internal cascading effect reduces the material to a fine powder.

3.2.2 Bottom-up approach

The alternative approach, which has the potential of creating less waste and hence the more economical, is the ‘bottom-up’. Bottom-up approach refers to the buildup of a material from the bottom: atom-by-atom, molecule-by-molecule, or cluster-by-cluster (e.g. growth of a crystal). This approach plays a very important role in preparing nanomaterials having very small size where the top-down process cannot deal with the very tiny objects.

Relevant techniques can be further grouped into two categories thermodynamic equilibrium approach and kinetic approach.

In the thermodynamic equilibrium approach, synthesis process consists of (1) generation of super saturation, (2) nucleation, and (3) subsequent growth.

In the kinetic approach, formation of nanoparticles is achieved by either limiting the amount of precursors available for the growth (e.g., molecular beam epitaxy), or confining the process in a limited space (e.g., aerosol synthesis and micelle synthesis).

Different methods of bottom-up approaches are:

3.2.2.1 Gas (vapor) phase synthetic methods

These processes are typically conducted in vacuum under elevated temperatures, i.e., via pyrolysis or chemical vapor deposition shown in Figure 3.1.

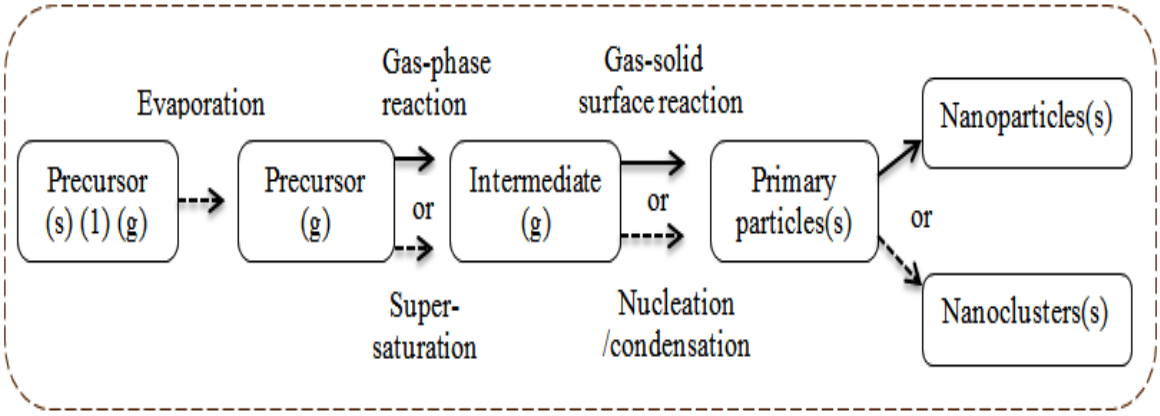

Figure 3.1 Gas (vapor) phase synthetic method

3.2.2.2 Pyrolysis (Spray pyrolysis) system

Spray pyrolysis is the aerosol process that atomizes a solution and heats the droplets to produce solid particles. The solid particles are then collected via, for instance, electric field precipitator. The advantages of vapor phase pyrolysis include it being a simple process, cost effective, a continuous operation with high yield.

3.2.2.3 Liquid phase synthesis methods

The liquid phase fabrication entails a wet chemistry route shown in Figure 3.2.

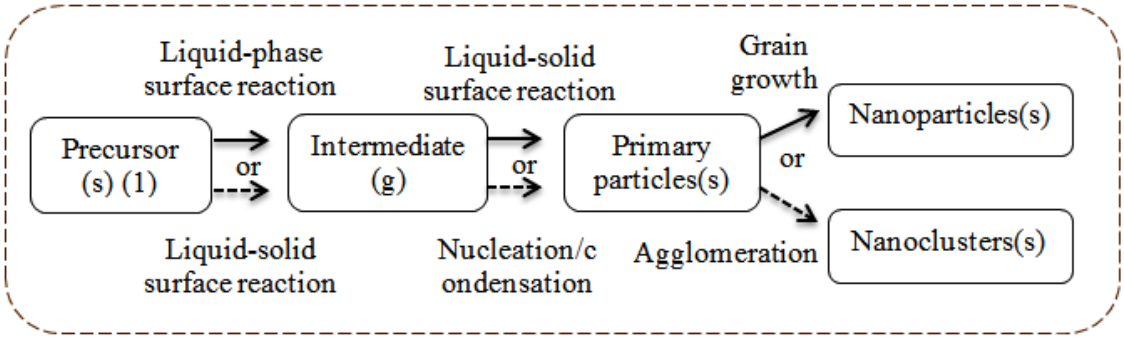

Figure 3.2 Liquid phase fabrication

3.2.2.4 Solvothermal methods

Solvothermal synthesis of nanoparticles provides precise control over the size, shape distribution, and crystallinity the crystallization process. The reaction process is conducted above the boiling point of the solvent and internal autogeneous pressure, and involves a hot solvent within an autoclave (sealed vessel). The process is called hydrothermal synthesis when the solvent is water.

3.2.2.5 Sol-gel methods

Sol-gel processing is a wet chemical synthesis approach which entails first the creation of a sol (solid particles in solution), which is followed by the formation of a gel. This method is carried out in solution. Through this method tailoring of certain desired structural characteristic such as compositional homogeneity, grain size, particle morphology and porosity can be achieved. A wide range of pure and mixed oxides can be produced through this process. In a typical sol-gel method, a colloidal suspension or a sol is formed from hydrolysis and polymerization reactions of precursors, which are usually inorganic metal salts or metal organic compounds such as metal oxide.

3.2.2.6 Synthesis in structure media

The microemulsion system consists of an oil phase, a surfactant phase and an aqueous phase. Microemulsions are transparent solutions consisting of small droplets of an immiscible phase (non-polar or polar) dispersed in a continuous phase. Surfactants are added to lower the

interfacial tension between the immiscible dispersed and continuous phases to stabilize the droplets. Microemulsions may consist of oil-in-water or water-in-oil, depending on the concentration of the different components. By varying the concentration of the dispersed phase and the surfactant, it is possible to tailor the size of the droplets in the range 1–100 nm, approximately.

3.2.2.7 Co-precipitation method

Co-precipitation synthesis involves dissolution of compound salt precursor in aqueous media and subsequent precipitation from the solution by pH adjustment. The co-precipitation technique is a useful method for the preparation of ceramics and metal oxide powders. Apart from its simplicity, atomic mixing of the constituents by chemical co precipitation yields a final product of near-perfect stoichiometry without high-temperature treatment.

3.2.3 Hybrid approach

An approach where top-down and bottom-up techniques are employed is known as a hybrid approach. Lithography is an example in which the growth of thin film is a bottom-up method whereas itching is a top-down method. However, nanolithography and nanomanipulation is commonly a bottom up approach.

3.3 AUTO COMBUSTION SYNTHESIS

One such approach is “combustion synthesis” also known as self-propagating high temperature synthesis (SHS) and fire or furnaceless synthesis. It is also known as auto combustion is an important technique widely used for the synthesis of a variety of oxides for different applications. The process makes use of highly exothermic redox chemical reaction between metals and nonmetals, the metathetical (exchange) reaction between reactive compounds or reactions involves redox compounds/mixtures.

The combustion method has been successfully used in the preparation of a large number of technologically useful oxide (refractory oxides, magnetic, dielectric, semiconducting,

insulators, catalysts sensors, phosphores etc.) and nonoxide (carbides, borides, silicides, nitrides etc.) materials.

3.3.1 Advantages of Auto combustion synthesis

Among the several alternative, combustion synthesis is a useful technique for synthesis of high purity nano materials. Because the advantages of auto-combustion route over other mentioned synthesis routes are low processing cost, energy efficiency and high production rate. This method is a simple method for oxides synthesis and has been used to produce homogeneous, crystalline nanopowders but its success depends on the correct understanding of the influence of the synthesis process parameters. This technique has been tremendous interest in the combustion synthesis of materials because it is simple, fast, energetically economic and yields high purity products compared to the conventional routes used to prepare these materials.

Among the various auto combustion synthetic Sol–gel auto combustion process offers a molecular-level mixing of the precursors, which is capable of improving chemical homogeneity of the resulting powders to a significant extent. However, since this method makes use of the exothermicity of redox reaction, agglomeration commonly exists in the ceramic powders synthesized by sol–gel combustion method.

3.3.2 Advantages of sol gel auto combustion synthesis

Sol gel auto-combustion synthesis are achieving

1. Good chemical homogeneity (mixing of captions of desired composition at molecular level)
2. High product purity and crystallinity
3. Fine and Narrow particle size distribution
4. Easy to control stoichiometry
5. Dopants can be easily introduced into the final product
6. Simple equipment and preparation process
7. Low processing time
8. Low external energy consumption (process initiates at low temperatures) and multiple steps are not involved.

3.4 IMPORTANCE OF ALUMINA AND FLY ASH NANOMATERIALS

3.4.1 Alumina (Al_2O_3)

Alumina has many appealing properties which makes the material interesting for applications in many different areas is shown in Figure 3.3. Alumina especially has a high melting point, high strength, corrosion resistance, chemical stability, low thermal conductivity and good electrical insulation properties. As a type of important structural ceramic material, alumina has applications in absorbent, catalyst, carrier and reinforcement of ceramic composites. Alumina exists in a number of crystalline phases (polymorphs), three of the most important being α, γ and θ. The α-alumina structure is thermodynamically stable at all temperatures up to its melting point at 2051°C, but the metastable phases (e.g., γ and θ) still appear frequently in alumina growth studies. The structures of aluminium oxide are of two types, hexagonal and octahedral. Hexagonal sites are the corner atoms in the cell while the octahedral sites are present between two layers of vertical stacking. The oxygen present in octahedral sites permits strong bonding and therefore, gives rise to the characteristics properties of alumina. Among one-dimensional nanostructures, nanofibers show broad application and properties. So, alumina nanofiber has a large number of applications including high-temperature insulation [107], catalyst support in high temperature reactions [108,109], fire protection and as reinforcement for resins [110,111], metal and ceramic.

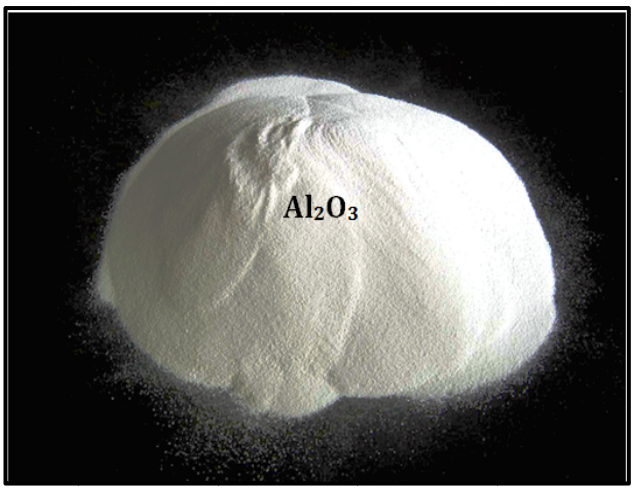

Figure 3.3 Picture of Alumina powder

3.4.1.1 Different routes of nano alumina synthesis

Nano alumina particles have been synthesized by various techniques such as: sol gel, agarose, flame spray pyrolysis, control precipitation, hydrothermal and combustion synthesis [112, 113]. Among these techniques, combustion synthesis is particularly an easy, safe and rapid production process and the main advantages are energy and time savings. Among the various auto combustion methods sol gel auto combustion synthesis (also called low temperature self-combustion, auto ignition or self-propagation, as well as gel thermal decomposition) is a novel method that uses a unique combination of the chemical sol-gel process and combustion.

3.4.2 Fly ash

Fly ash is a fine, glassy/amorphous powder recovered from of burning coal during the production of electricity. These micron-sized earth elements consist primarily of silica, alumina and iron. When mixed with lime and water the fly ash forms a cementitious compound with properties very similar to that of Portland cement. Because of this similarity, fly ash can be used to replace a portion of cement in the concrete, providing some distinct quality advantages. The concrete is denser resulting in a tighter, smoother surface with less bleeding. An import ant engineering property that is necessary for using fly ash in many geotechnical applications is its strength. The compressive strength characteristics of fine ash are higher than those of coarser ash specimen. Also most of the shear strength of the fly ash specimen is due to internal friction. The fly ash as a reinforcing material has many application in mechanical [114-116] and tribological [117-119] fields.

3.5 APPLICATION OF NANOMATERIALS

Nanotechnology is moving into the centre of world-wide public attention because of its broad range of applications which could dramatically impact both the scientific community and the commerce market place. A complete list of the potential applications of nanomaterials is too vast and diverse. Few of these applications are described briefly as follows.

1. Chemical applications
    a. Catalysis
    b. Paints, pigments and coating

2. Optical and electronic applications
3. Magnetic applications
4. Metal and ceramics applications
5. Biological applications
6. Environmental application
    a. Adsorptive removal of metal ions
    b. Adsorptive removal of organic dyes

3.6NANO FABRICATION AND CHARACTERIZATION

3.6.1 Nano Alumina synthesis

The nano alumina powder was synthesized by auto combustion method using Aluminium nitrate (Al $(NO_3)_3.9H_2O$), Citric acid and Glycine are used as fuel. At first the prerequisite amount of Aluminium nitrate was dissolved in the 200 ml distilled water. The citric acid and glycine was then gradually added two different Al $(NO_3)_3.9H_2O$ solutions. The solution was then stirred using a magnetic stirrer at 50°C for 2 to 3hrs to obtain a gel like mass and the gel is allowed heat up on the hot plate until combustion took place. The combustion process converted the sieved mass into ash like material.

The obtained ash was then fired in a closed furnace at different temperatures between (800, 900 and 1000°C) to get the pure alumina. The schematic diagram of the auto combustion process is given in the Figure-3.4 and the flow diagram 3.5 shows the process of nano alumina preparation.

For optimizing the particle size of alumina different percentage of Glycine and Citric acid was used with Aluminium nitrate (Al $(NO_3)_3.9H_2O$). The compositions are given in Table 3.1 and 3.2.

Table 3.1 Different moles of Glycine with Aluminium nitrate

Aluminium nitrate (Al $(NO_3)_3.9H_2O$)	**Glycine**
1 mole	0.5 mole
1 mole	1 mole
1 mole	1.5 mole

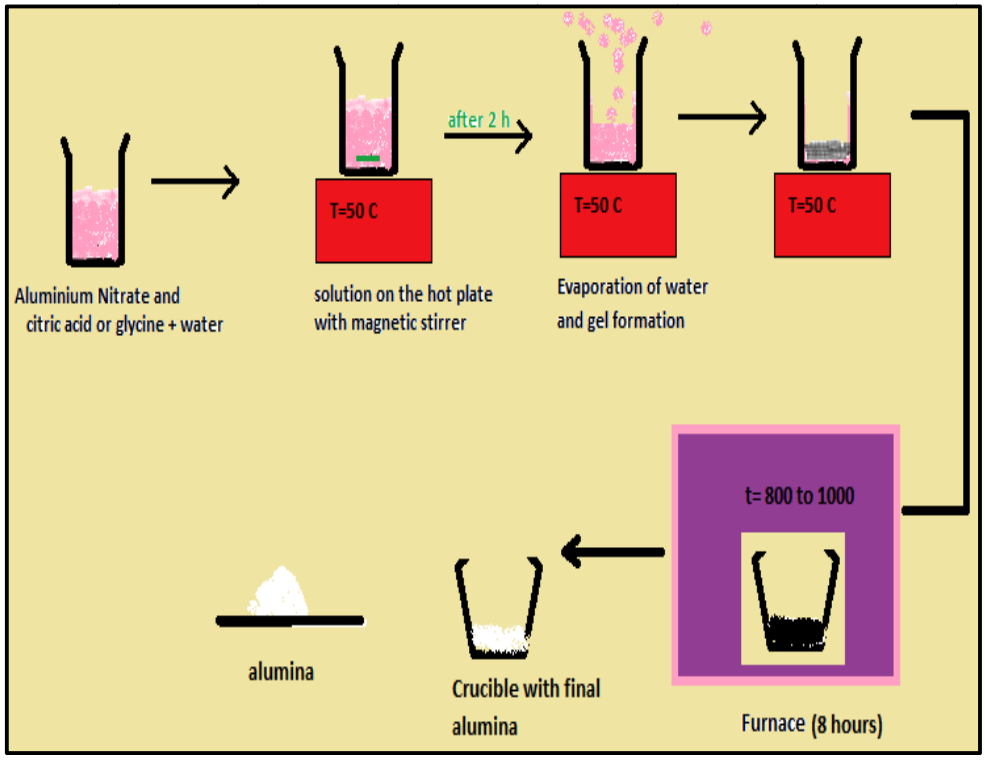

Figure 3.4 Schematic diagram of the auto combustion [120, 121]

Table 3.2 Different moles of Citric acid with Aluminium nitrate

Aluminium nitrate ($Al(NO_3)_3.9H_2O$)	**Citric acid**
1 mole	0.5 mole
1 mole	1 mole
1 mole	1.5 mole
1 mole	2 mole
1 mole	2.5 mole
1 mole	3 mole

In the preliminary testing we had chosen the three different concentrations (in moles) of glycine and citric acid. After calcination the BET results shows that the greater surface area has been obtained for the citric acid fuel. So to optimize the size of the nano we had chosen the three more mole fraction for citric acid.

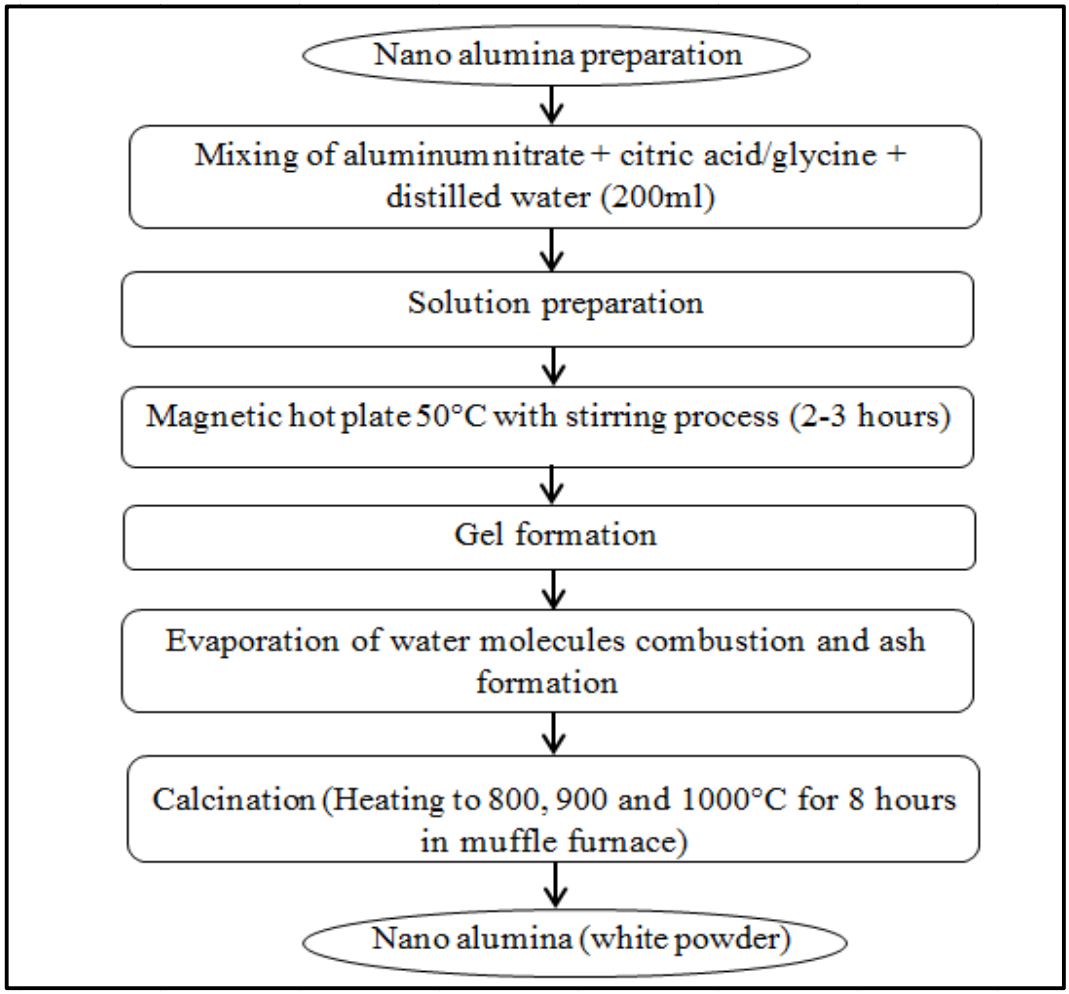

Figure 3.5 Flow diagram of alumina nano preparation [122]

3.6.2 Nano Fly ash synthesis

Fly Ash particles were also used for this study as filler materials. The fly ash was collected from Rourkela Steel Plant of SAIL (Steel Authority of India Limited), Rourkela, India. As obtained fly ash samples were fired in a furnace at 1000ºC to burn out the unfired material. From the fired fly ash powder one kilogram powder is taken and sieved to different mesh sizes ranging from 1 to 420µm. the obtained particle size fraction are shown in Table 3.3.

The Figure 3.6 shows the particle analysis of the fly ash which having less than 200 µm. From the Figure it is observed that the size range of the particles is very wide ranging from 0.1µm to 150 µm. Based on the result it is concluded that some of the particles are in 100 nano range in fresh fly ash.

Table 3.3 Cumulative particle size [123]

Sample No.	Size range -- micron	Size range + micron	Weight Grams approx.	Weight %
1	420	212	50	6%
2	211	150	78	9%
3	**149**	**104**	**550**	**70%**
4	103	0	183	15%

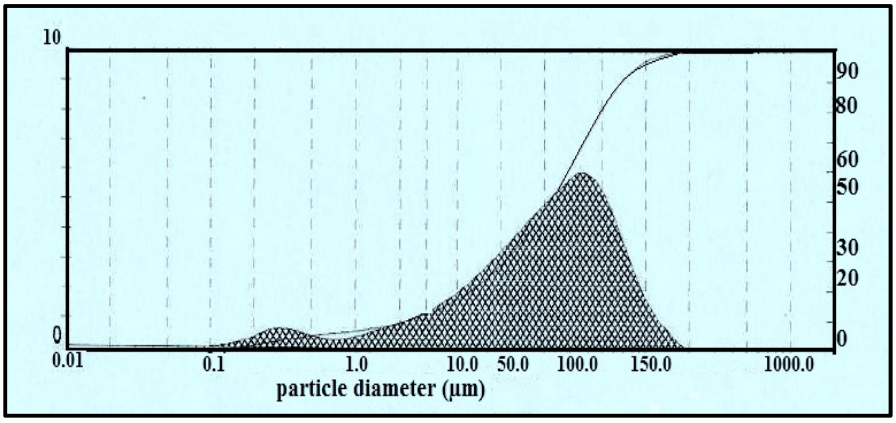

Figure 3.6 Particle size of fresh fly ash

3.6.2.1 Fly ash composition

The chemical compositions of the fly ash are shown in Table 3.4. It consists of SiO_2, Al_2O_3, Fe_2O_3, TiO_2, CaO, MgO, Na_2O and K_2O.

Table 3.4 Chemical composition of fly ash [123]

SiO_2	Al_2O_3	Fe_2O_3	TiO_2	CaO	MgO	Na_2O	K_2O	Loss on ignition
48.32	31.2	8.23	2.56	1	2.1	1.2	1.35	3.5

3.6.3 Production of nanostructure fly ash by planetary ball milling

The particle size of fly ash from micro to nanorange was reduced by using a planetary ball mill in a Tungsten Carbide coated stainless steel bowl with a tungsten carbide and zirconia

balls of 10 mm and 5 mm diameter. The total duration of milling was 6 hours with an interval of 30 min. The rotation speed of the planet carrier is 400 rpm. The ball mill is loaded with ball to powder weight ratio (BPR) of 10:1. Toluene was used as process controlling agent to avoid oxidation and excessive cold welding of powders to vials and balls. The milled powder is taken out and kept in the drier at 120°C to remove the toluene. The flow diagram of the nano fly ash fabrication is shown in Figure 3.7.

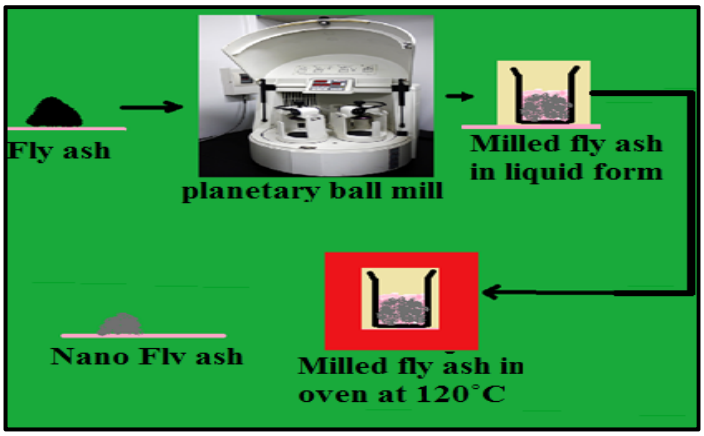

Figure 3.7 Flow diagram of nano fly ash preparation

3.6.4 Surface Area Analysis (BET) and Average particle diameter

The specific surface area of the particles is the summation of the areas of the exposed surfaces of the particles per unit mass. There is an inverse relationship between particle size and surface area. Nitrogen adsorption can be used to measure the specific surface area of a powder [124,125]. The method of Brunauer, Emmett, and Teller (BET) is commonly used to determine the total surface area.

The average particle size can be estimated by assuming all the particles to have the same spherical shape and size. The average particle diameter, D, is given by:

$$BET = \frac{6}{(S_f \times \rho)} \tag{3.1}$$

Where 'S_f' is specific surface area in m^2/g and 'ρ' is the theoretical density in g/cm^3 [126].

3.6.5 X-ray diffraction studies

X-ray diffraction studies have been widely used in particle research to characterize their critical features such as crystal structure, crystallite size, and strain. The X-ray diffraction patterns of the samples were recorded on a Siemens D-500 diffractometer using Ni-filtered CuKα radiation. X-pert software was used to investigate the structural changes and phase transformations of the material. Sample preparation of XRD is done as per the standard practice. The samples were scanned in the range from 10° to 90° of 2θ with a scan rate of 2 degrees per minute using Bragg-Brantano configuration.

3.6.6 Proximate analysis of Jute fiber

The proximate analysis of jute fibber has been done under the ASTM standards E-871, E-1755, E-872; for moisture, ash and volatile matter respectively. In addition to this, fixed carbon content was calculated by using the equation 3.2

$$\%FC = 100 - (\%ASH + \%VM + \%M) \tag{3.2}$$

where %FC, %Ash, %M and %VM respectively indicates the weight percentage of fixed carbon, ash, moisture and volatile matter of the jute fiber.

Table 3.5 Proximate analysis of jute fiber

Sample	Jute fiber
Fixed carbon	27.28
Moisture	6.09
Ash	1.29
Volatile	65.34

3.6.7 Ultimate analysis of Jute fiber

The Ultimate Analysis of jute fibre was carried out in a CHNS Analyser (CHN-932) or Elementary Analyser. The Ultimate Analysis of a sample determines the elemental compositions (Carbon (C), Hydrogen (H), Nitrogen (N) and Sulphur (S) contents) of the sample. In the

ultimate analysis carbon and hydrogen are integrally analysed in accordance with ASTM E 777; the measurement of sulphur contain follows ASTM E 775; and the measurement of nitrogen content follows ASTM E 778. The oxygen content of jute fibre is a calculated value and is the difference between 100% and the sum of the C, H, N, S and ash.

Table 3.6 Ultimate analysis of jute fiber

Sample	Jute fiber
C	52.13
H	4.13
N	0.10
S	0.88
O	41.47

3.6.8 Chemical composition of Jute fiber

The jute fibers were subjected to Soxhlet extraction with ethanol/toluene (1:2, v/v) for 12h, to remove extractives. Moisture content was calculated based on oven dry weight of the sample. The composition (extractive, a-cellulose, hemicelluloses, lignin, and ash contents) of the fibers was analyzed according to Technical Association of Pulp and Paper Industry (TAPPI) standards. The holocellulose content (a-cellulose + hemicelluloses) of the fibers was determined by treating the fibers with a $NaClO_3$ and NaOH mixture solution. The a-cellulose content of the fibers was then determined by further treating holocellulose with 17.5% NaOH to remove the hemicelluloses. The difference between the values of holocellulose and a-cellulose gives the hemicellulose content of the fibers. The lignin content of the fibers was found by treating them with a sulfuric acid solution based on TAPPI standard T222 om-83.

Table 3.7 Chemical composition of Jute fiber

Sample	Jute fiber
Cellulose (%)	39.54
Holocellulose (%)	65.6
Lignin (%)	29.86

3.6.9 Thermogravimetric analysis of jute-epoxy composite (TGA)

In this work, the decomposition behavior of the raw jute and epoxy polymer were analyzed in an Al_2O_3 crucible at heating rate 5^oCmin^{-1}. Temperature was raised from room temperature 30 to 650°C in the presence of nitrogen atmosphere with a flow rate of nitrogen at 30 ml/min. For each experiment 10 mg mass of sample was taken. The apparatus provides for the continuous measurement of sample weight as a function of temperature (TGA).

3.6.10 FTIR Spectra of Jute fiber

FTIR spectra of the jute fiber are recorded using an IR-Prestige-21spectrometer. A total of 100 scans were taken from 400-4000cm^{-1} with a resolution of 2cm^{-1} for each sample. The samples were chopped into small particles using scissors and ground to a fine powder. This powder is pelletized by pellitizer and studies the FTIR spectra under standard conditions. The functional groups of the natural fiber can be identified by the FTIR spectrum graph which confirms the cellulose lignin and hemicellulose.

3.6.11 Experimental density of sample

The density of materials in terms of weight fraction is found out from the following equations 3.3.

$$S_m = \frac{w_o}{(w_o)+(w_a - w_b)} \tag{3.3}$$

Where 'S_m' represents specific gravity of the material, 'w_o' represents the weight of the sample; 'w_a' represents the weight of the bottle + kerosene, 'w_b' represents the weight of the bottle + kerosene + sample.

$$\text{Density} = S_m * \text{Density of kerosine} \tag{3.4}$$

3.8 RESULTS AND ANALYSIS

The density, surface area and average particle size of the alumina particles are shown in Table 3.8. It is clearly observed that as the citric acid mole fraction increases the density, and particles size decreases up to 2 moles and starts increasing again whereas the surface area is increasing. When alumina which was prepared with glycine as a fuel material the densities are less but the particle size and the surface area is more when compared with the other alumina particles prepared with citric acid.

Table 3.8 Density, Surface area and Average particle size of different Samples

Sample	**Density(gm/cm^3)**	**Surface area by BET, m^2/g**	**Average particle size**
0.5 mole citric acid	1.86	36.2	105
1.0 mole citric acid	1.56	39.59	88
1.5 mole citric acid	1.37	58.8	74
2 mole citric acid	**1.35**	**74.73**	**59**
2.5 mole citric acid	1.45	52.36	79
3 mole citric acid	1.68	22.57	158
0.5 mole Glycine	0.9	24.65	270
1.0 mole Glycine	0.93	29.4	219
1.5 mole Glycine	0.90	10.46	637

3.8.1 X-ray diffraction studies

3.8.1.1 Alumina

The XRD pattern of alumina prepared with glycine and citric acid heat treated at different temperatures(800,900 and 1000°C) are shown in 3.8(a-d). Form the Figures it is clearly observed that the alumina prepared with citric acid of 2 moles gives 90% alpha alumina and partial beta alumina when heat treated at 800°C. It has been observed that, heat treatment at 900°C gives 100% pure alpha alumina. From the Figures it has been observed that the alumina prepared with the glycine as fuel from auto combustion technique, gives pure beta alumina at

900°C, however heat treatment at higher temperature, 1000°C gives 90% alpha alumina and partial beta alumina.

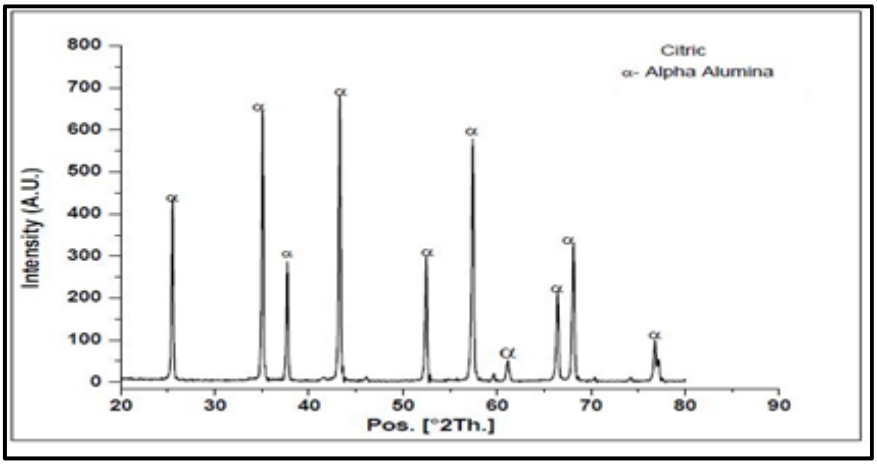

Figure 3.8(a) 2 mole Citric acid 900°C

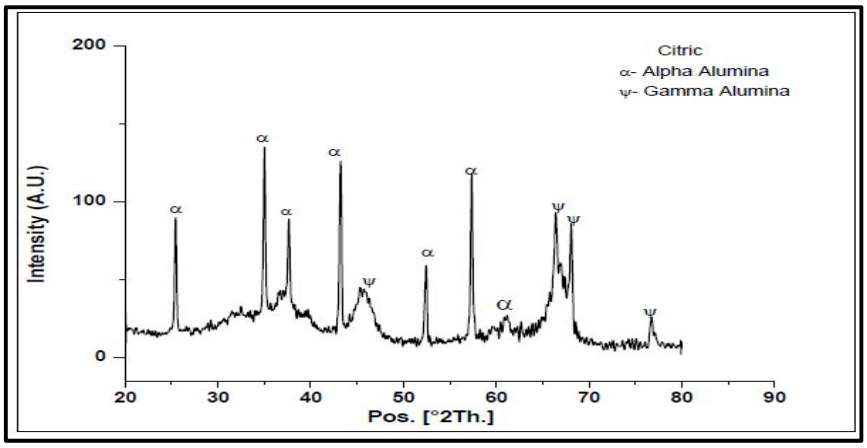

Figure 3.8(b) 2 moles of Citric acid 800°C

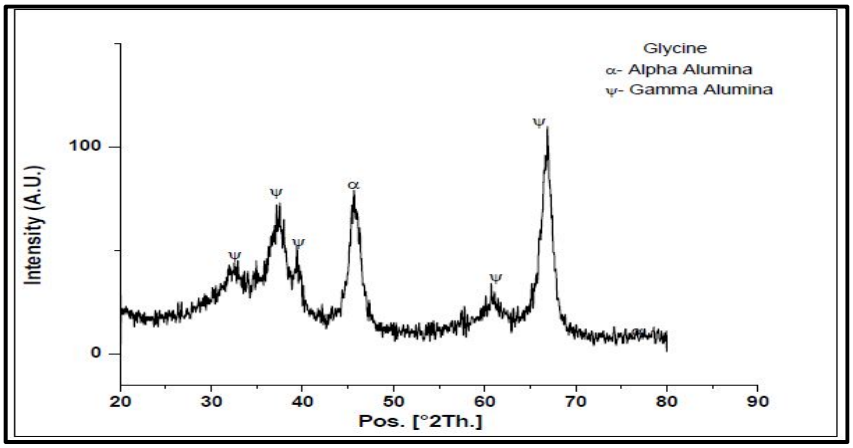

Figure 3.8(c) 1 moles of Glycine 900°C

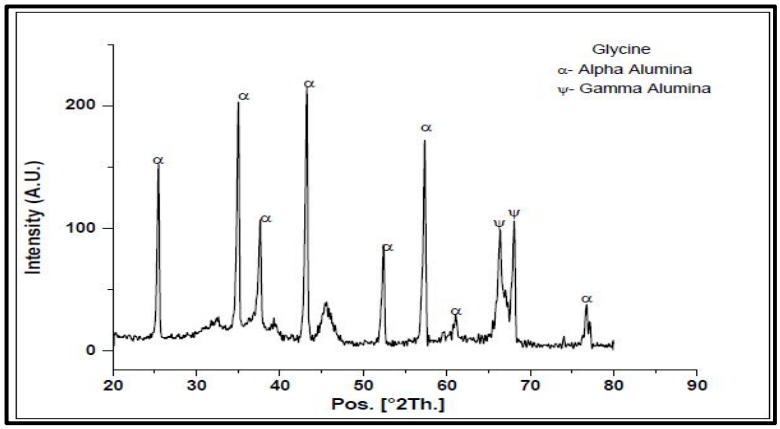

Figure 3.8(d) 1moles of Glycine 1000°C

Figure 3.8 XRD studies of nano alumina prepared by (a) 2 mole Citric acid 900°C, (b) 2 moles of Citric acid 800°C (c) 1 moles of Glycine 900°C and (d) 1moles of Glycine 1000°C

3.8.1.2 Fly ash

The Figure 3.9 shows, X-Ray pattern of the fly ash before and after planetary ball milling. From the Figure, it is clearly observed that the intensity of the peaks got reduced and the increased peak broadening also took place.

The average particle diameter was determined from the full width at half maximum (FWHM) of the X-ray diffraction peak using Scherrer's equation 3.5.

$$D = \frac{K\lambda}{B\cos\theta} \qquad (3.5)$$

Where 'D' is the particle diameter, 'k' is the X-Ray wavelength, 'B' is the FWHM of the diffraction peak, 'h' is the diffraction angle and 'K' is the Scherrer's constant of the order of unity for usual crystals.

Generally fly ash exhibited lower degree of crystallinity it consists of Quartz (silica) mullite (alumina silicate), hematite and calcium oxide. The figure displays the variation in crystallite size with the time of planetary ball milling. The major crystalline domains presented in the fly ash are Quartz (silica) mullite (alumina silicate) and hematite. A steady decrease in the crystallite size is observed. The high energy milling decreases the crystallinity of the fly ash, thus

increasing the amorphous domains in it. The same type of results was also reported by the Thomas Paul et al. [127]. The variation in crystalline phases in the obtained fly ash and milled fly ash were studied by XRD analysis. The percentage crystallinity of fly ash was reduced and also the particle size is decreased.

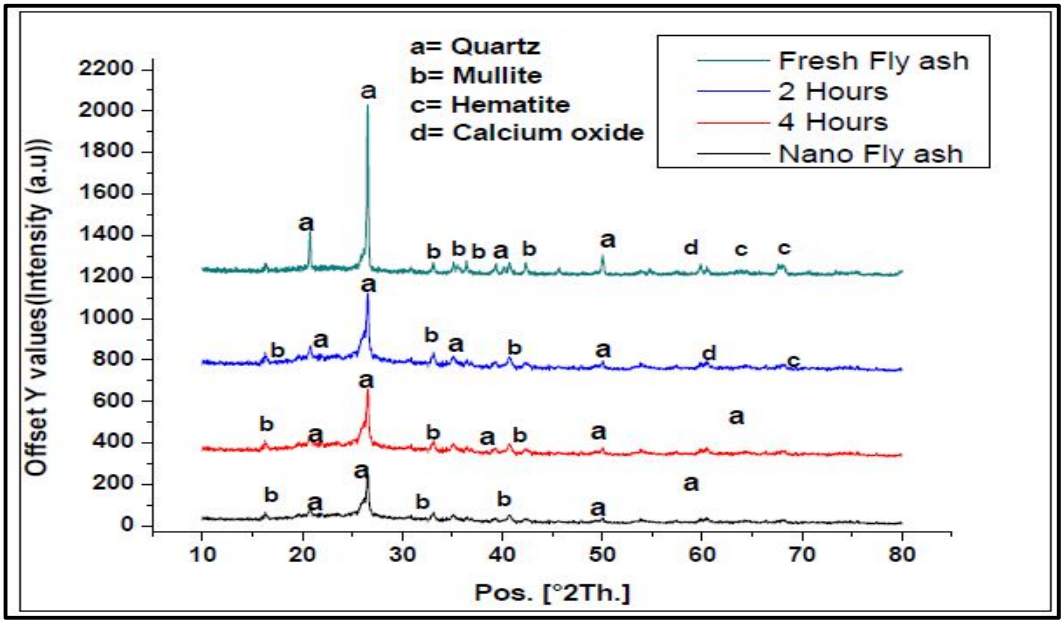

Figure 3.9 XRD of fly ash with different hours of time [123]

Figure 3.10 shows typical XRD pattern of raw jute. It presents two peaks, which are well defined in literature. The major diffraction peaks appears at 17.50º and 22.50º, respectively. According to several researchers [128, 129] these two peaks situated at 16.30º and 22.50º can be attributed to cellulose I and to cellulose IV, both of which exhibit a monoclinic structure [128-130].

The estimation of the crystallinity index CI has been calculated using the following equation [131].

$$CI = \frac{H_{22.5} - H_{17.5}}{H_{22.5}} \qquad (3.6)$$

Where $H_{22.5}$ is the height of the peak at 22.5º it results from both amorphous and crystalline fraction contributions. $H_{17.5}$ is the diffracted intensity at 17.5º, which is attributed to

the amorphous fraction [132, 133] the calculated crystalline index (CI) is 70%. This value is higher than that of Wrighitia tinctoria seed fibers (49.2%) and ramie (58%) [133], but close to that of sisal (71%) [132] and smaller than that of flax (80%) and hemp (88%) [134].The phases of these peaks revealed that this particle may have composition of hemicelluloses, cellulose, and lignin which are in crystalline in nature as also observed by Kumar et al [135] and Anuradha Jabasingh [136].

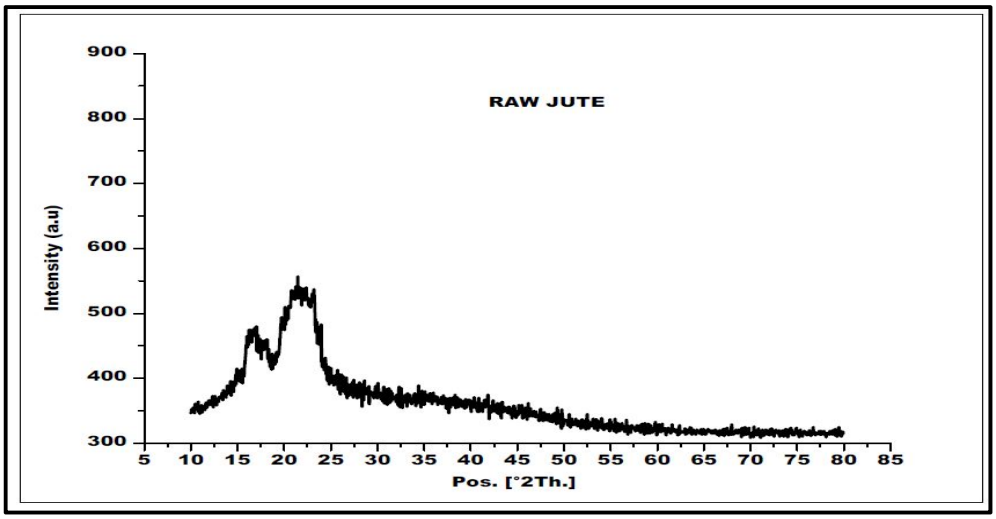

Figure 3.10 XRD pattern of the raw jute

3.8.2 EDX analysis

3.8.2.1 EDX analysis of Jute fiber

Energy dispersive X-ray diffraction (EDX) was used for elemental analysis of jute fiber for the compositional accuracy of five different samples which used in the present work. The EDX spectrum (as shown in Figure 3.11) showed the peaks for carbon, oxygen, silicon and alumina. The main components of Jute fiber are carbon 45 to 65% and oxygen 41 to 54% silicon 5 to 8% and alumina 3 to 6% remaining are sulfate groups to some extent. Similar type of results was also reported by the Senthil kumaar et al. [137] in his elemental and proximate analysis of the jute fibers.

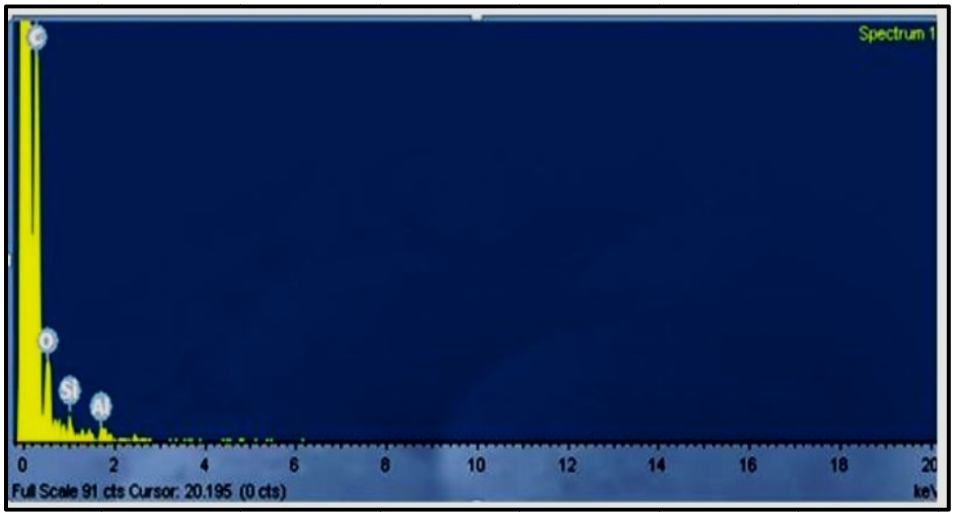

Figure 3.11 EDX of the jute fiber [138]

3.8.3 BET analysis of fly ash

Figure 3.12(a) and 3.12(b) show the BET analysis of the fresh and ball milled fly ash. Surface area of the as obtained fly ash and the ball milled fly ash are 0.31 and 24.65 m^2/g, respectively. Due to the planetary high-energy ball, milling the surface area of fresh fly ash increased to great extent as the particle size decreases. The average particle size based on the surface area is 11 micron for as obtained fly ash and 148 nano meters to the ball milled fly ash after six hours.

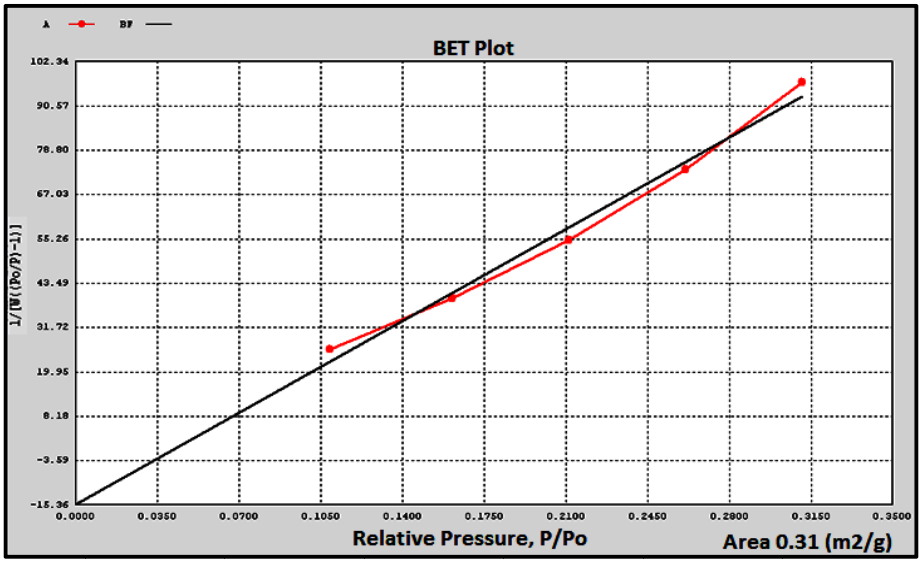

3.12(a) Fresh Fly ash

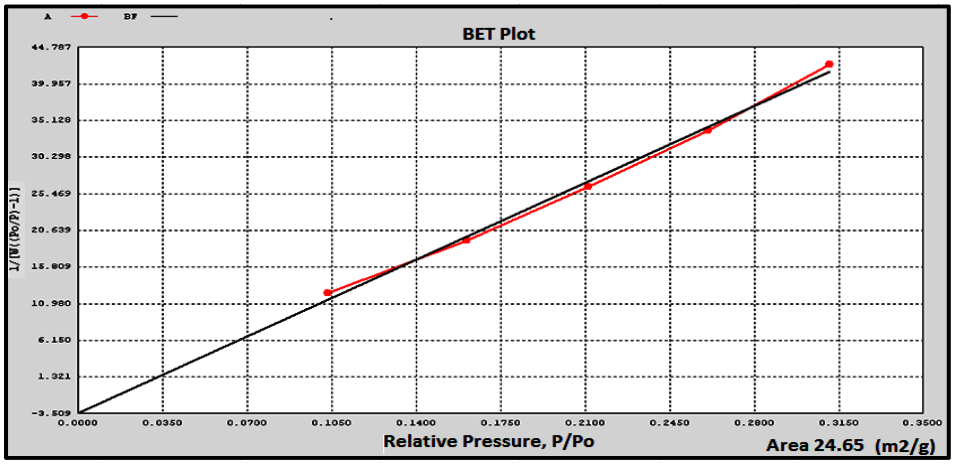

3.12(b) Milled Fly ash

Figure 3.12 BET of (a) obtained fly ash (b) milled fly ash

3.8.4 FTIR analysis of jute fiber

Figure 3.13 represents The FTIR spectra of raw jute fibers it is observed the presence broad absorbance peak at 3200–3600 cm^{-1} range representing O–H stretching of hydrogen bond network [139]. The bands which found 3270 cm-1(3100 cm-1 in Figure 3.13) and at 710 cm^{-1} (730 cm^{-1} in Figure 3.13) attributed to cellulose [131, 140]. The bands at 1740 cm^{-1} (1690 in Figure 3.13) and at 1510 cm^{-1} (1540 in Figure 3.13) are attributed to lignin [131].

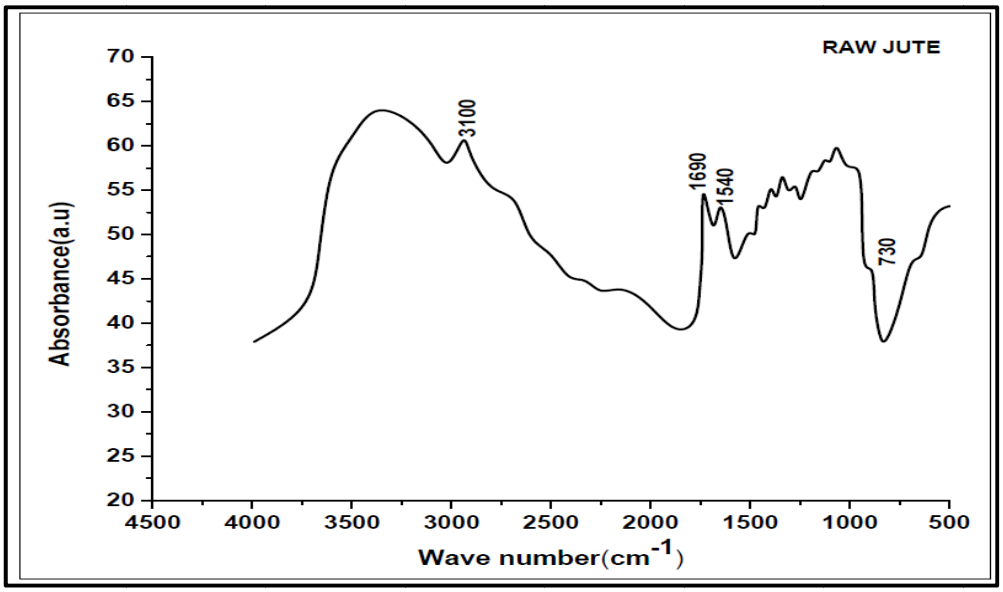

Figure 3.13 FTIR analysis of jute fiber

3.8.5 TGA analysis (Thermogravimetric analysis) of Jute fiber

Thermal analysis is the concept that purely reflects the decomposition reactions that occur at the molecular level of the materials with variation in temperature. Figure 3.1 shows the TGA curve of jute fiber and neat epoxy. The TGA curve for the jute fiber is less when compared with the neat epoxy matrix, indicating the lesser thermal stabilities of the jute fiber. From Figure it is clear that for jute fiber initial decrease in weight loss completed below 100°C is due to the moisture loss from the biomass material at this temperature.

Next step is the thermal degradation of biomass. In thermal degradation, firstly at 155-169°C lignin is the first component which decomposes followed by decomposition of hemicellulose which starts from 230-307°C. After Hemicelluloses decomposition in the final step major weight loss occurred within the temperature range of 323–392°C as a consequence of the cellulose decomposition.

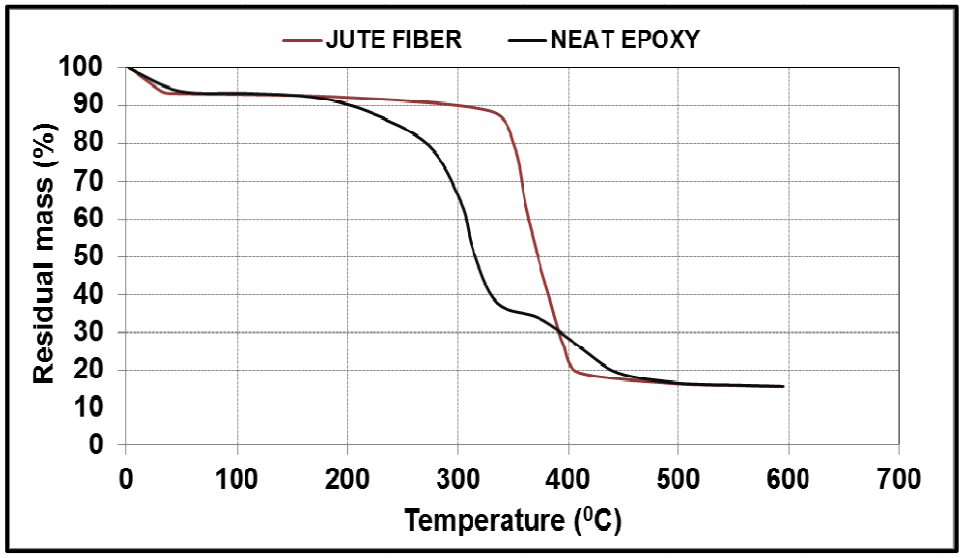

Figure 3.14 TGA of the jute and epoxy

The same types of thermal behavior were reported by Nunn et al. [141]. They reported that the decomposition of cellulose and lignin took place at a wide temperature range of 200-400°C and 150-750°C, respectively. Furthermore the rate of decomposition was slow. Zeriouh et al. [142] reported that the decomposition of hemicellulose, cellulose and lignin occurred at temperature ranges of 180–240°, 230–310°, and 300–400°C, respectively. Researchers already reported that lignin is the first component which decomposes at low temperature (160-170°C).

In case of epoxy material the initial decrease in weight loss was completed by 120^{o}C is due to the moisture loss from the material. It is clearly observed that the epoxy is stable up to 335°C. From the existence literature [143, 144] it has been found that due to addition of thermoplastic into the epoxy, there increase in the thermal resistance to high temperature. The thermal stability of jute epoxy composites also increase due to addition of jute fiber, which has high content of cellulose, hemicelluloses and lignin.

3.8.6 SEM Analysis

3.8.6.1 SEM analysis of micro and nano Alumina

Morphological features of the micro alumina and nano alumina were studied using a Secondary Electron Imaging mode of scanning electron microscopy (SEM). Figure 3.15 (a) ,(b) and 3.16 (c) show the micrographs of micro alumina and nano alumina prepared using citric acid and glycine. These Figures estimate the micro alumina particle size in the range of 20-70 µm whereas the nano alumina fabricated by one mole of glycine as a fuel material has range of 200-600 nm and those nano alumina which was prepared with 2 moles of citric acid are in the range of 40-120 nm.

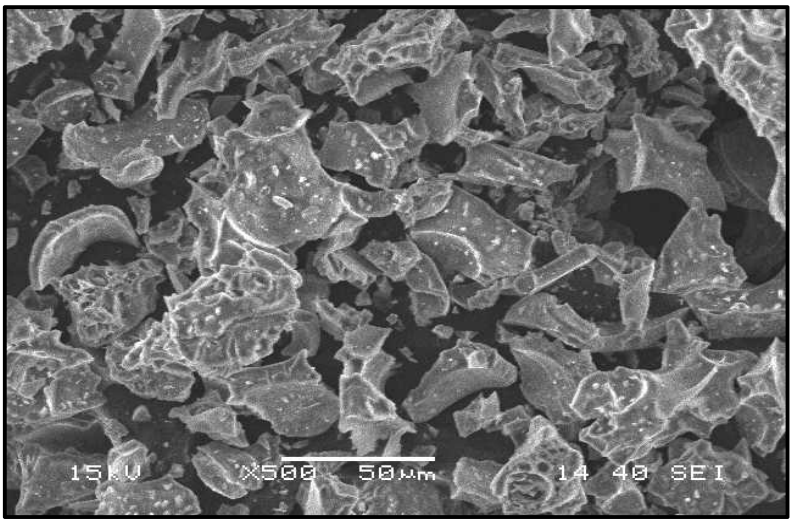

(a) Micro alumina

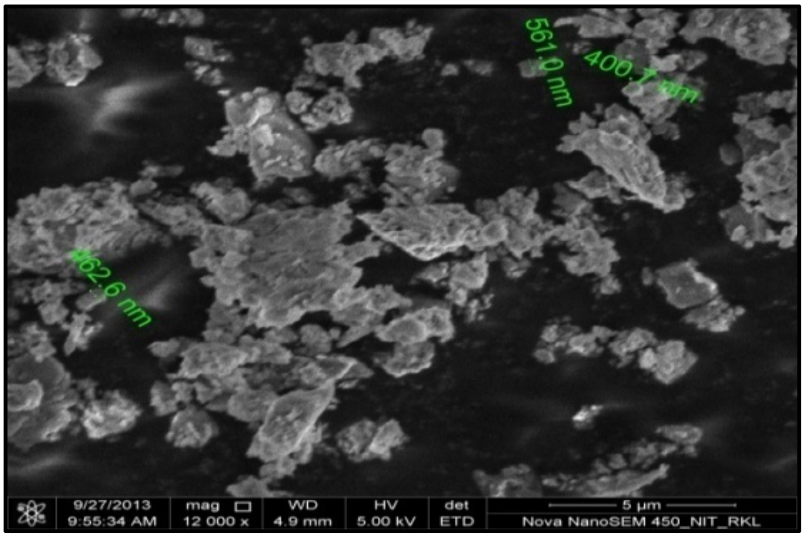

(b) Alumina (glycine)

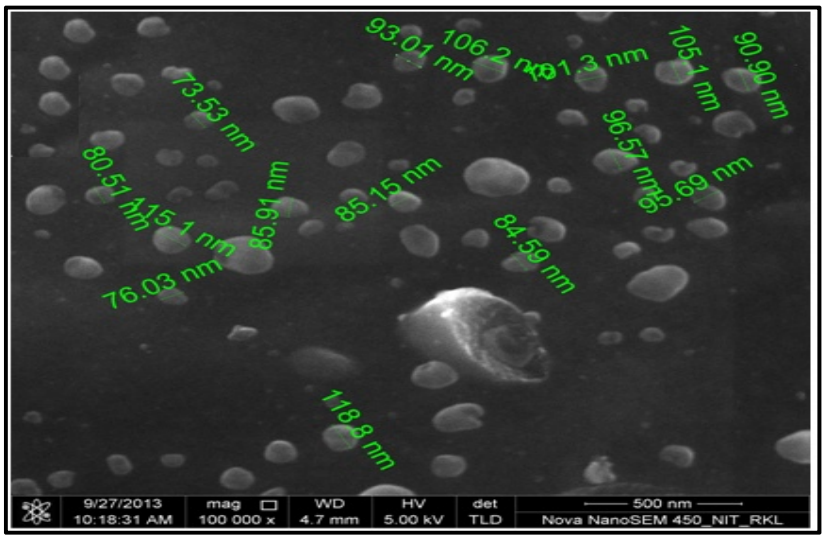

(c) Alumina (Citric acid)

Figure 3.15 SEM micrographs of the (a) micro alumina (b) nano alumina (glycine) (c) nano alumina (Citric acid)

3.8.6.2 SEM analysis of micro and nano Fly ash

Morphological structures of the as obtained and planetary ball milled fly ash were also studied using secondary electron imaging mode of scanning electron microscopy (SEM) (JEOL jsm-6480lv). Figure 3.16(a-d) shows the SEM image of micro fly ash and nano fly ash. From the

Figure 3.17(a and b) it is evident that majority of the fly ash particles in between 140-20µm. From the Figure 3.17(c and d) it has been observed that the large fly ash particle has been destroyed and crushed by intense impacts of the balls; hence the decreases in particle size are observed in this Figure.

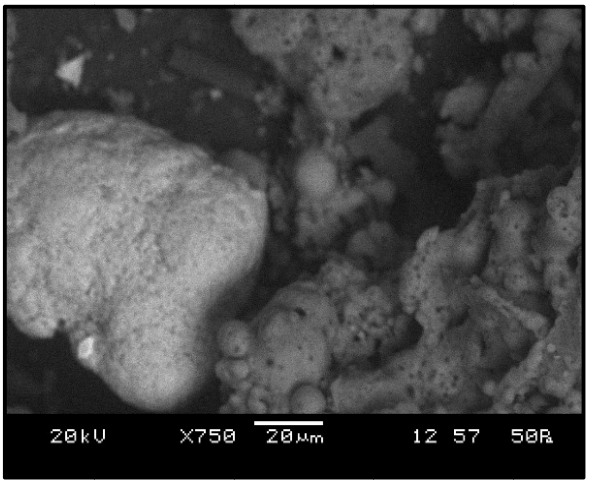

(a)

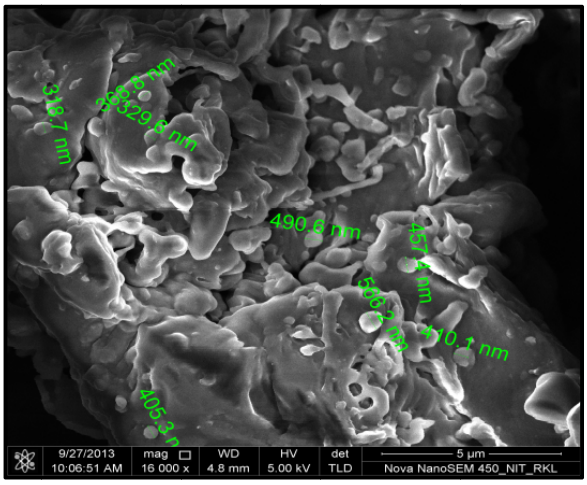

(b)

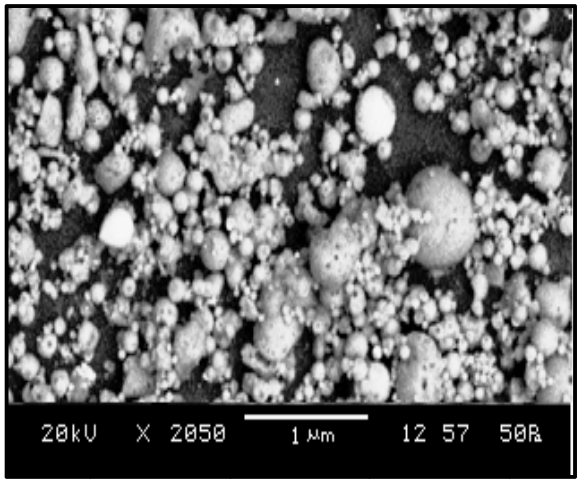

(c)

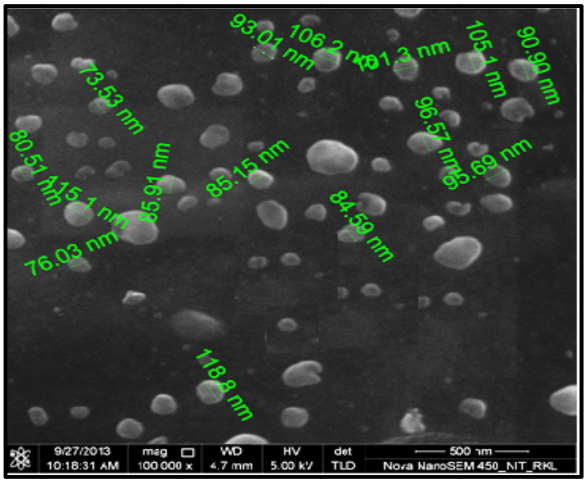

(d)

Figure 3.16 SEM of the (a, b) fresh micro fly ash. (c, d) nano fly ash after 6 hours ball milling

3.9 CONCLUSION

In nano Alumina preparation citric acid (as fuel) gives best optimum results when compared with the glycine. The XRD, SEM, BET and EDX characterization techniques confirmed the formation of pure nanosized alumina powder. Alumina nano particles with surface area 74.73 m^2/g have been synthesized by the sol-gel auto combustion method. XRD analysis of the alumina calcined at 900°C confirms the formation of pure α-alumina phase. The size diminution of obtained fly ash from micro range to nano range has been achieved by planetary ball milling in the period of 6 hours. The surface area of the obtained fly ash increase from 0.31 to 24.65 m^2/g, this indicates the nano range. SEM images of micro and nano suggests that the large flake like material demolished to small nano particles by high energy planetary ball mill. The FTIR analysis of the jute fiber confirms that the jute material has O-H groups which positively can make bond with the polymer material like epoxy.

Chapter 4

Mechanical Properties of Jute-Glass Fiber Hybrid Composite with Micro and Nano Filler

4.1 INTRODUCTION

The polymers have replaced many of the conventional metals/materials in various applications over the past few decades. This is owing to the advantages of polymers over conventional materials such as ease of processing, productivity, cost reduction etc. Research is underway worldwide to develop newer composites with varied combinations of fibers and fillers so as to make them useable under different operational conditions. In most of these applications, the properties of polymers are modified using fillers and fibers to suit the high strength/high modulus requirements. A notable advance in the polymer industry has been the use of fiber and particulate fillers as reinforcements in polymer matrix. Particulate fillers are of considerable interest, not only from an economic viewpoint, but as modifiers especially the physical properties of the polymer. It is well documented in the literature that majority fillers have a positive influence on mechanical properties.

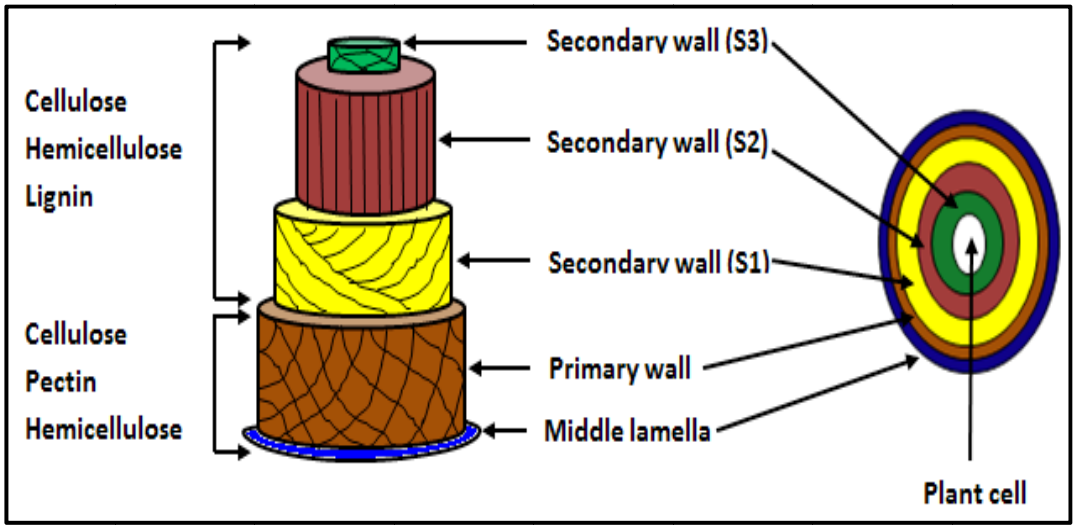

Figure 4.1 Cell wall structure of natural fiber

The cell wall structure of natural fibers (Figure 4.1) contains many micropores. Also, some of the lignin and hemicellulose of natural fibers are usually removed during chemical treatments or pulping, which created additional micropores [145]. The presence of these micropores in the cell wall could cause manufacturing defects in composites, such as interfacial

failure and air pockets. In order to reduce the air pocket defect, one can incorporate a vacuum assist system in the natural fiber polymer composite (NPC) processing to reduce the air bubble to some extent. Another efficient method is to introduce nano-particles into the micropores of the fiber cell wall structure through an impregnation process to fill those voids. Compatibility between the hydrophilic natural fibers and the hydrophobic polyolefins has been a major issue for the NPC [146, 147]. Lee et al. [148] indicated that the deposited nano-scale particles on the natural fiber surface may serve as heterogeneous nucleation sites to initiate the crystalline orientation of the molten polymer matrix. These results suggested that nanoparticles might control the heterogeneous nucleation of a semi crystalline polymer on the natural fiber surface. The natural fiber itself cannot initiate nuclei due to extremely unbalanced free energy between the cellulosic fibers and molten polyolefin matrices [148-150]. Therefore, the nanoparticle impregnation could not only fill the micro-pores of the fiber cell wall structure minimizing the air bubble defects of the NPC, but also introduce nanoparticles onto the fiber surfaces serving as attraction force manipulators to polymer matrixes to improve the compatibility at the fiber and polymer interfaces.

Hard particulate fillers consisting of ceramic or metal particles and fiber fillers made of glass are being used these days to dramatically improve the properties of composite materials, even up to three orders of magnitude [151]. Various kinds of polymers and polymer matrix composites reinforced with metal particles have a wide range of industrial applications such as heaters, electrodes [152], composites with thermal durability at high temperature [153] etc. These engineering composites are desired due to their low density, high corrosion resistance, ease of fabrication and low cost [154-156]. Similarly, ceramic filled polymer composites have been the subject of extensive research in last two decades. The inclusion of inorganic fillers into polymers for commercial applications is primarily aimed at the cost reduction and stiffness improvement [157,158]. Along with fiber-reinforced composites, the composites made with particulate fillers have been found to perform well in many real operational conditions. When silica particles are added into a polymer matrix to form a composite, they play an important role in improving electrical, mechanical and thermal properties of the composites [159,160]. Currently, particle size is being reduced rapidly and many studies have focused on how single-particle size affects mechanical properties [161-168]. The shape, size, volume fraction, and

specific surface area of such added particles have been found to affect mechanical properties of the composites greatly. In this regard, Yamamoto et al. [169] reported that the structure and shape of silica particle have significant effects on the mechanical properties such as fatigue resistance, tensile and fracture properties. Nakamura et al. [170,171] discussed the effects of size and shape of silica particle on the strength and fracture toughness based on particle matrix adhesion and also found an increase of the flexural and tensile strength as specific surface area of particles increased.

In the literature, many works devoted to the mechanical properties of natural fibers from micro to nano scales are available. In these, the effects of reinforcement of matrix (thermoplastic starch) by using cellulose whiskers, commercial regenerated cellulose fibers are also proposed. A number of investigations have been conducted on several types of natural fibers such as kenaf, hemp, flax, bamboo, and jute to study the effect of these fibers on the mechanical properties of composite materials [172,173]. Mansur and Aziz [174] studied bamboo-mesh reinforced cement composites, and found that this reinforcing material could enhance the ductility and toughness of the cement matrix, and increase significantly its tensile, flexural, and impact strengths. A pulp fiber reinforced thermoplastic composite was investigated and found to have a combination of stiffness increased by a factor of 5.2 and strength increased by a factor of 2.3 relative to the virgin polymer [175,176]. Information on the usage of banana fibers in reinforcing polymers is limited in the literature. In dynamic mechanical analysis Pothan et al. [56] have investigated banana fiber reinforced polyester composites and found that the optimum content of banana fiber is 40%. Mechanical properties of banana–fiber–cement composites were investigated physically and mechanically by Corbiere-Nicollier et al. [177]. It was reported that craft pulped banana fiber composite has good flexural strength. In addition, short banana fiber reinforced polyester composite was studied by Pothan et al. [61]; the study concentrated on the effect of fiber length and fiber content. The maximum tensile strength was observed at 30 mm fiber length while maximum impact strength was observed at 40 mm fiber length. Incorporation of 40% untreated fibers provides a 20% increase in the tensile strength and a 34% increase in impact strength. Joseph et al. [45] tested banana fiber and glass fiber with varying fiber length and fiber content as well. Luo and Netravali [178] studied the tensile and flexural properties of the green composites with different pineapple fiber content and compared with the virgin resin. Sisal fiber

is fairly coarse and inflexible. It has good strength, durability, ability to stretch, affinity for certain dye stuffs, and resistance to deterioration in seawater. Sisal ropes and twines are widely used for marine, agricultural, shipping, and general industrial use. Belmeres et al. [179] found that sisal, henequen, and palm fiber have very similar physical, chemical, and tensile properties. Cazaurang et al. [180] carried out a systematic study on the properties of henequen fiber and pointed out that these fibers have mechanical properties suitable for reinforcing thermoplastic resins. Ahmed et al. [181] carried out research work on filament wound cotton fiber reinforced for reinforcing high-density polyethylene (HDPE) resin. Khalid et al. [182] also studied the use of cotton fiber reinforced epoxy composites along with glass fiber reinforced polymers. Fuad et al. [183] investigated the new type wood based filler derived from oil palm wood flour (OPWF) for bio-based thermoplastics composites by thermo-gravimetric analysis and the results are very promising. Schneider and Karmaker [184] developed composites using jute and Kenaf fiber and polypropylene resins and they reported that jute fibre provides better mechanical properties than Kenaf fibre. Sreekala et al. [185] performed one of the pioneering studies on the mechanical performance of treated oil palm fiber-reinforced composites. They studied the tensile stress stain behavior of composites having 40% by weight fiber loading. Isocyanante, silane, acrylated, latex coated and peroxide-treated composite withstood tensile stress to higher strain level.Isocyanate treated, silane treated, acrylated, acetylated and latex coated composites showed yielding and high extensibility. Tensile modulus of the composites at 2% elongation showed slight enhancement upon mercerization and permanganate treatment. The elongation at break of the composites with chemically modified fiber was attributed to the changes in the chemical structure and bondability of the fiber. Alkali treated (5%) sisal-polyester biocomposites showed about 22% increase in tensile strength [186]. Ichazo et al. [187] found that by adding silane treated wood flour to PP produced a sustained increase in the tensile modulus and tensile strength of the composite. Joseph and Thomas [188] studied the effect of chemical treatment on the tensile and dynamic mechanical properties of short sisal fiber reinforced low density polyethylene composites. It was observed that the CTDIC (cardanol derivative of toluene diisocyanate) treatment reduced the hydrophilic nature of the sisal fiber and enhanced the tensile properties of the sisal-LDPE composites. They found that peroxide and permanganate treated fiber-reinforced composites showed an enhancement in tensile properties. They concluded that

with a suitable fiber surface treatment, the mechanical properties and dimensional stability of sisal-LDPE composites could be improved.

There are some researches about the influence of the filler and its size over the mechanical and physical properties of wood-flour reinforced thermoplastics [189,190] it has been observed that the elongation at break and the impact strength of the composites decrease with the addition of filler independently of its size. The behavior of the tensile modulus and the tensile strength seems to depend on the shape of the particles. This behavior can improve with the load as the aspect ratio does so. There are several reports available in the literature which discuss the of different types of natural fibers composites and their mechanical behavior, very limited work has been done on study of mechanical behavior of hybridization of natural fiber and synthetic fiber reinforced polymer composites.

Pavithran et al. [191] evaluated the enhancement in the properties of coir-polyester composites by incorporating glass as intimate mix with coir. Mohan and Kishore [192] reported that jute provided a reasonable core material in jute-glass hybrid laminates. They evaluated flexural properties and compressive properties of the jute-glass reinforced epoxy laminates fabricated by filament winding technique using flat mandrel. Four different hybrid combinations were studied with different glass fiber volume fractions and the results were compared with jute reinforced plastic. They found substantial increase in flexural and compressive properties with hybridization.

Pavithran et al. [193] determined the work of fracture by impact testing on sisal–glass hybrid composites with two arrangements, one with sisal shell and glass core and the other with glass shell and sisal core. They showed that the sisal shell laminate had the higher work of fracture compared with glass shell hybrid laminates of equivalent volume fraction of sisal and glass fibers. Mishra et al. [194] studied the effect of glass fiber addition on tensile and flexural strength and izode impact strength of pine apple leaf fiber (PALF) and sisal fiber reinforced polyester composites. K. John et al. [195-197] have studied the unsaturated polyester based sisal glass composites with 5% and 8% volume fraction and found a considerable enhancement in impact, compression flexural and tensile properties.

In this chapter, effect of hybridization of glass and layering sequence effect on tensile and flexural properties of woven jute-glass fiber hybrid composites is studied. The effect of both micro and nano filler on mechanical properties of glass-jute hybrid composite with different stacking sequences have also been studied and reported in this chapter.

4.2 MATERIALS AND METHODS

4.2.1 Raw materials used

Raw materials used in this experimental work are listed below:

1. Jute fiber
2. E-glass fiber
3. Epoxy resin
4. Hardener
5. Alumina (Micro and Nano particles)
6. Fly ash (Micro and Nano particles)

4.2.1.1 Jute fiber

As explained earlier natural vegetable fibers have attracted worldwide attention as a potential reinforcement for composite because of their easy availability as a renewable resource, easy process ability, low density, light weight, nonabrasive, low cost and above all for their bio friendly characteristics. The jute fiber shown in Figure 4.2, used for the present investigation is an important bast fiber and comprises bundled of ultimate cells, each containing spirally oriented micro fibrils bound together. The main component of jute fiber is cellulose which leads to higher stiffness. Other components of jute fiber are hemi-cellulose, lignin, pectin, waxy and water soluble substances. In the present work, bi-directional jute fibers have been used for experimentation.

Figure 4.2 Woven Jute fiber mat

4.2.1.2 E-glass fiber

Glass is the most common fiber used in polymer matrix composites is shown in Figure 4.3. Its advantage includes its high strength, low cost, high chemical resistance, and good insulating properties. In the present investigation E-glass fiber 360 roving supplied by saint Gobian ltd, was used. The fibers were cut to sizes 150×60 mm from the long sheet.

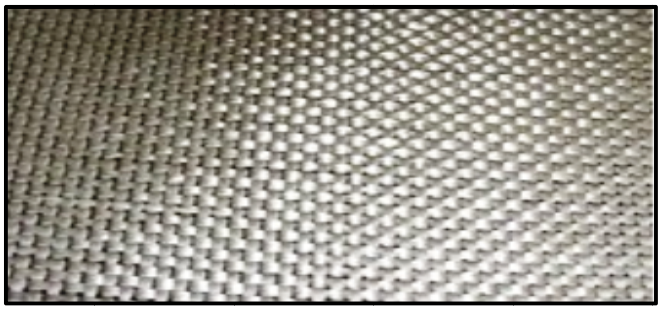

Figure 4.3E-Glass fiber mat

4.2.1.3 Epoxy resin and Hardener

Epoxy resins are relatively low molecular weight pre-polymers capable of being processed under a variety of conditions. Two important advantages of these over unsaturated polyester resins are: first, they can be partially cured and stored in that state, and second they exhibit low shrinkage during cure. However, the viscosity of conventional epoxy resins is higher and they are more expensive compared to polyester resins. The cured resins have high chemical, corrosion resistance, good mechanical and thermal properties, outstanding adhesion to a variety of substrates, and good electrical properties. Approximately 45% of the total amount of epoxy resins produced is used in protective coatings while the remaining is used in structural

applications such as laminates and composites, tooling, molding, casting, construction, adhesives, etc.

The type of epoxy resin used in the present investigation is Araldite LY-556 which chemically belongs to epoxide family. Epoxy resins are characterized by the presence of a three-membered ring containing two carbons and an oxygen (epoxy group or epoxide or oxirane ring). Epoxy is the first liquid reaction product of bisphenol-A with excess of epichlorohydrin and this resin is known as Diglycidyl-Ether of Bisphenol-A (DGEBA). DGEBA is used extensively in industry due to its high fluidity, processing ease, and good physical properties of the cured of resin. The hardener with IUPAC name NNO-bis (2amino ethyl ethane-1,2diamin) has been used with the epoxy designated as HY 951. This has a viscosity of 10-20 MPa at 25ºC.Both the epoxy and hardener were supplied by Ciba-Geigy of India Ltd.

4.2.2 Preparation of composites

Hybrid laminates of jute and glass composite were prepared by the hand layup technique with different stacking sequence. A wooden mold of (150x60x5) $mm^3$was used for composite fabrication. For quick and easy removal of the composite a mold release sheet is placed on the top and bottom of the wooden mold. The mold release spray is also applied to the inner surface of the mold wall to facilitate easy removal of the composite specimen. A calculated amount of epoxy resin and hardener (ratio of 10:1 by weight) was thoroughly mixed with a mechanical stirrer. After 5 min stirring, some mixture was poured into the mold uniformly and jute fiber mat was placed then the required amount of epoxy resin was poured over it. The process was continued for 4 layers of jute mat and for each time, a roller was used to roll over the fiber in order to remove the air bubbles from it. Figure 4.4 (a-d) illustrates the mold used to construct the composite and photograph of the composite slab with specimens cut for flexural and tensile test.

Hybrid FRP composite plate preparation also been done in the same way, but the placing of fibers was done alternately one over the other, i.e. one layer of woven pure jute fiber mat followed by E-Glass fiber mat is shown in Figure 4.5.

Hybrid FRP composite with micro and nano filler addition also been done in the similar manner. In first set, the micro-Al_2O_3 or fly ash (5, 10 and 15 wt.%) is used as a filler material and

mixed in the epoxy resin before the jute/glass fiber is reinforced in the matrix. In second set, nano-Al_2O_3or fly ash (2, 4 and 6 wt.%) is used as a filler material and mixed with the epoxy resin before the jute/glass fiber is reinforced in the matrix is shown in Figure 4.6.

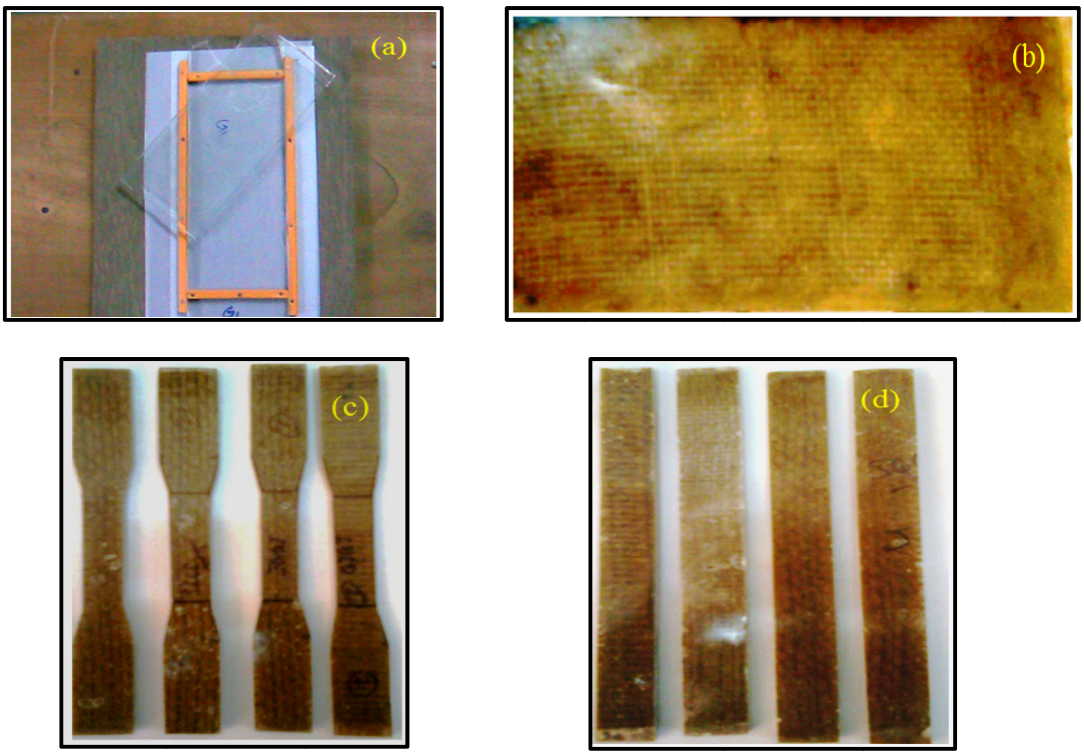

Figure 4.4(a) Photograph of composite slab (b) Mold used for composite preparation (c) Specimen for Tensile test and (d) Flexural test

After the required thickness and volume fraction were obtained, the composite plates were allowed to dry at room temperature for 24h. Then, the FRP composite plates were removed from the mold and the laminate was cut into required size of mechanical and tribological tests by the diamond cutter. Five groups of laminate composite samples with total four plies were manufactured by a varying stacking sequence of jute and glass fabrics as presented in Table 4.1. Care was taken to keep the thickness of the samples to 5 mm as far as possible. In the present case the composites prepared were consists of 23±wt.% fiber. The total fiber volume fraction is calculated using equation.

$$\frac{(W_j/\rho_j)+(W_g/\rho_g)+(W_f/\rho_f)}{(W_j/\rho_j)+(W_g/\rho_g)+(W_r/\rho_r)+(W_f/\rho_f)} \quad (4.1)$$

Where 'W_j', 'W_g' and 'W_f' are the known weights of the jute, glass, resin and filler respectively and 'ρ_j', 'ρ_g' and 'ρ_f' are the densities of jute, glass, resin and filler respectively. The density of epoxy resin, jute and glass fiber is found to be 1.0974 g/cm^3, 1.42 g/cm^3 and 2.55 g/cm^3 respectively.

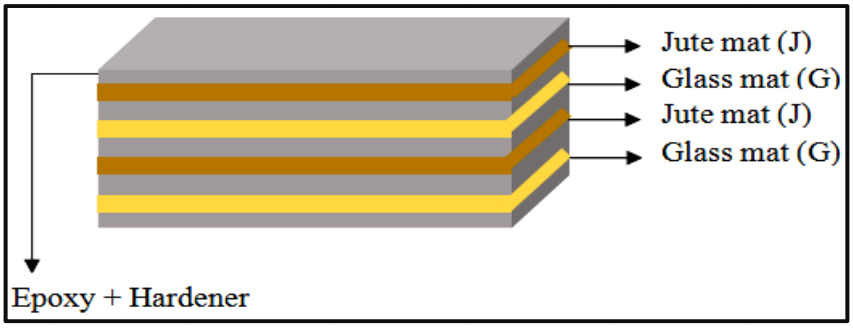

Figure 4.5 Schematic view of the hybrid composite

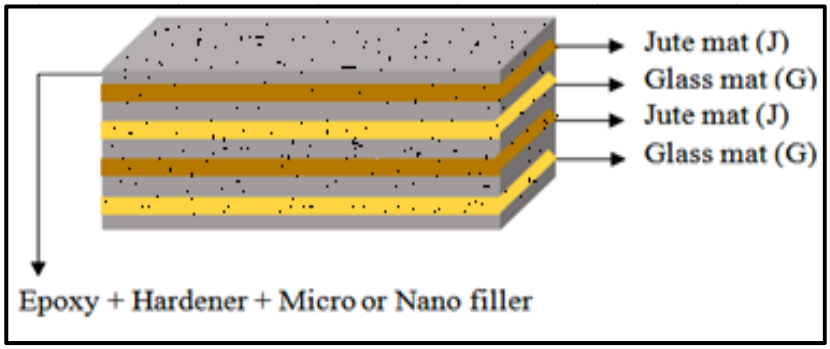

Figure 4.6 Schematic view of the hybrid nano composite

Table 4.1 weight percentage of fiber and matrix

Symbol	**Stacking sequence**	**wt.% of Fibers**		**Fiber weight fraction (%) in composites**	**Fiber volume fraction (%) in composites**	**Epoxy weight fraction (%) in composites**
		Jute	Glass			
L1	GGGG	00	100	26	16.6	74
L2	JJJJ	100	00	20	18.5	80
L3	GJGJ	50	50	23	17.5	77
L4	JGGJ	50	50	23	17.5	77
L5	GJJG	50	50	23	17.5	77
J-Jute ply, G-Glass ply						

4.3 CHARACTERIZATION OF THE COMPOSITES

4.3.1 Density and void fraction

In terms of weight fraction the theoretical density of the composite materials can be calculated using Agarwal and Broutman [126] equation.

$$\rho_{ct} = \frac{1}{\left(W_f / \rho_f\right) + \left(W_m / \rho_m\right)} \tag{4.2}$$

where 'W' and 'ρ' represent the weight fraction and density respectively. The suffix '*f*', '*m*' and '*ct*' stand for the fiber, matrix and theoretical density of composite materials, respectively.

According to present study the composite consists of matrix, fiber and particulate filler. Hence the modified form of above expression for the density of the composite can be written as .

$$\rho_{ct} = \frac{1}{\left(W_m / \rho_m\right) + \left(W_f / \rho_f\right) + \left(W_p / \rho_p\right)} \tag{4.3}$$

The details of the Actual density (Experimental density) are same as explained in chapter 3 art 3.7.

The volume fraction of voids (V_v) in the composite is calculated by using equation.

$$V_v = \frac{\rho_{ct} - \rho_{ca}}{\rho_{ct}} \tag{4.4}$$

where 'ρ' represents the density of the composite. The suffix '*ct*' and '*ca*' stand for the theoretical and experimental density of the composite materials.

For the present investigation the theoretical density, actual density and the void fraction so obtained for hybrid composite and composite with different wt. % of micro and nano fillers are presented in Table 4.2 to 4.6.

Table 4.2 Density and Void content of hybrid composites

Composite composition	Theoretical density (g/cm^3)	Experimental density (g/cm^3)	Voids fraction (%)
Epoxy	1.200	1.193	0.583
Epoxy + 26 wt.% GGGG	1.381	1.371	0.724
Epoxy + 20 wt.% JJJJ	1.209	1.196	1.075
Epoxy + 23 wt.% GJGJ	1.256	1.245	0.876
Epoxy + 23 wt.% GJJG	1.256	1.244	0.955
Epoxy + 23 wt.% JGGJ	1.256	1.243	1.035
G-Glass fiber, J-Jute fiber			

Table 4.3 Density and Void content of micro alumina filler hybrid composites

Composite composition	Theoretical density (g/cm^3)	Experimental density (g/cm^3)	Voids fraction (%)
Epoxy + 20 wt.% JJJJ+5 wt.% Alumina	1.247	1.222	2.005
Epoxy + 23 wt.% GJGJ+5 wt.% Alumina	1.297	1.273	1.850
Epoxy + 23 wt.% GJJG+5 wt.% Alumina	1.297	1.272	1.928
Epoxy + 23 wt.% JGGJ+5 wt.% Alumina	1.297	1.271	2.005
Epoxy + 20 wt.% JJJJ+10 wt.% Alumina	1.289	1.226	4.888
Epoxy + 23 wt.% GJGJ+10 wt.% Alumina	1.342	1.302	2.981
Epoxy + 23 wt.% GJJG+10 wt.% Alumina	1.342	1.299	3.204
Epoxy + 23 wt.% JGGJ+10 wt.% Alumina	1.342	1.293	3.651
Epoxy + 20 wt.% JJJJ+15 wt.% Alumina	1.332	1.250	6.156
Epoxy + 23 wt.% GJGJ+15 wt.% Alumina	1.389	1.332	4.104
Epoxy + 23 wt.% GJJG+15 wt.% Alumina	1.389	1.322	4.824
Epoxy + 23 wt.% JGGJ+15 wt.% Alumina	1.389	1.312	5.544
G-Glass fiber, J-Jute fiber			

Table 4.4 Density and Void content of nano alumina filler hybrid composites

Composite composition	Theoretical density (g/cm^3)	Experimental density (g/cm^3)	Voids fraction (%)
Epoxy + 20 wt.% JJJJ+2 wt.% Alumina	1.224	1.219	0.408
Epoxy + 23 wt.% GJGJ+2 wt.% Alumina	1.272	1.268	0.314
Epoxy + 23 wt.% GJJG+2 wt.% Alumina	1.272	1.267	0.393
Epoxy + 23 wt.% JGGJ+2 wt.% Alumina	1.272	1.265	0.550
Epoxy + 20 wt.% JJJJ+4 wt.% Alumina	1.240	1.212	2.258
Epoxy + 23 wt.% GJGJ+4 wt.% Alumina	1.289	1.271	1.396
Epoxy + 23 wt.% GJJG+4 wt.% Alumina	1.289	1.270	1.474
Epoxy + 23 wt.% JGGJ+4 wt.% Alumina	1.289	1.269	1.552
Epoxy + 20 wt.% JJJJ+6 wt.% Alumina	1.255	1.201	4.303
Epoxy + 23 wt.% GJGJ+6 wt.% Alumina	1.306	1.281	1.914
Epoxy + 23 wt.% GJJG+6 wt.% Alumina	1.306	1.269	2.833
Epoxy + 23 wt.% JGGJ+6 wt.% Alumina	1.306	1.262	3.369
G-Glass fiber, J-Jute fiber			

Table 4.5 Density and void content of micro fly ash filler hybrid composites

Composite composition	Theoretical density (g/cm^3)	Experimental density (g/cm^3)	Voids fraction (%)
Epoxy + 20 wt.% JJJJ+5 wt.% Fly ash	1.214	1.184	2.443
Epoxy + 23 wt.% GJGJ+5 wt.% Fly ash	1.261	1.231	2.323
Epoxy + 23 wt.% GJJG+5 wt.% Fly ash	1.261	1.234	2.121
Epoxy + 23 wt.% JGGJ+5 wt.% Fly ash	1.261	1.232	2.285
Epoxy + 20 wt.% JJJJ+10 wt.% Fly ash	1.218	1.153	5.391
Epoxy + 23 wt.% GJGJ+10 wt.% Fly ash	1.266	1.225	3.220
Epoxy + 23 wt.% GJJG+10 wt.% Fly ash	1.266	1.224	3.286
Epoxy + 23 wt.% JGGJ+10 wt.% Fly ash	1.266	1.218	3.759
Epoxy + 20 wt.% JJJJ+15 wt.% Fly ash	1.223	1.138	6.955
Epoxy + 23 wt.% GJGJ+15 wt.% Fly ash	1.271	1.213	4.592
Epoxy + 23 wt.% GJJG+15 wt.% Fly ash	1.271	1.206	5.147
Epoxy + 23 wt.% JGGJ+15 wt.% Fly ash	1.271	1.192	6.180
G-Glass fiber, J-Jute fiber			

Table 4.6 Density and void content of nano fly ash filler hybrid composites

Composite composition	Theoretical density (g/cm^3)	Experimental density (g/cm^3)	Voids fraction (%)
Epoxy + 20 wt.% JJJJ+2 wt.% Fly ash	1.211	1.200	0.928
Epoxy + 23 wt.% GJGJ+2 wt.% Fly ash	1.258	1.247	0.812
Epoxy + 23 wt.% GJJG+2 wt.% Fly ash	1.258	1.249	0.667
Epoxy + 23 wt.% JGGJ+2 wt.% Fly ash	1.258	1.248	0.737
Epoxy + 20 wt.% JJJJ+4 wt.% Fly ash	1.213	1.181	2.581
Epoxy + 23 wt.% GJGJ+4 wt.% Fly ash	1.260	1.238	1.715
Epoxy + 23 wt.% GJJG+4 wt.% Fly ash	1.260	1.235	1.933
Epoxy + 23 wt.% JGGJ+4 wt.% Fly ash	1.260	1.223	2.924
Epoxy + 20 wt.% JJJJ+6 wt.% Fly ash	1.215	1.156	4.816
Epoxy + 23 wt.% GJGJ+6 wt.% Fly ash	1.262	1.218	3.497
Epoxy + 23 wt.% GJJG+6 wt.% Fly ash	1.262	1.216	3.647
Epoxy + 23 wt.% JGGJ+6 wt.% Fly ash	1.262	1.218	3.476
G-Glass fiber, J-Jute fiber			

4.3.2 Tensile Strength

The tension test is generally performed on flat specimens. The most commonly used specimen geometries are the dog-bone specimen (Figure 4.7) and straight-sided specimen with end tabs. The standard test method as per ASTM D 3039-76 has been used and the length of the test specimen used is 125 mm. The tensile test is performed in universal testing machine INSTRON H10KS. The tests were performed with a cross head speed of 10mm/min. For each test composite of five samples were tested and average value was taken for analysis. Figure 4.8(a, b) shows the machine used for the test and the sample in loading condition. The results obtained from the tests are presented in Table 4.7. Few tested samples are shown in Figure 4.8(c).

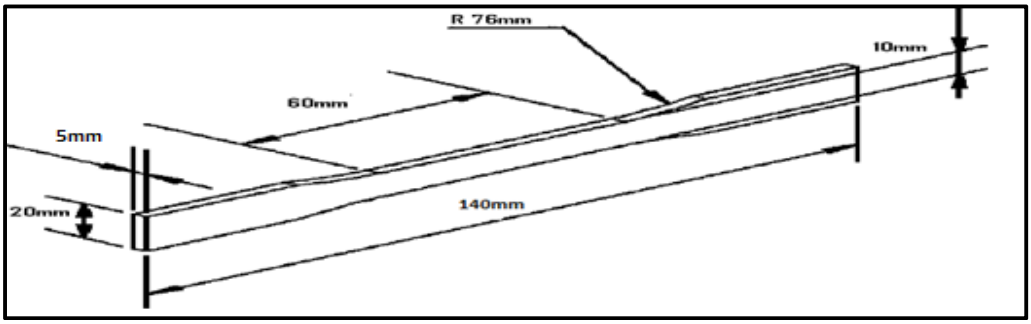

Figure 4.7 Tensile specimen

(a) **(b)** **(c)**

Figure 4.8Photograph of (a) INSTRON H10KS testing machine (b) Sample in loading condition (c) Tested samples

Table 4.7 Mechanical properties of pure, hybrid and micro, nano filler composites

Composite samples	Tensile Strength (MPa)	Flexural Strength (MPa)	Tensile Modulus (GPa)	Flexural Modulus (GPa)
Epoxy	21.2	41.2	0.69	0.73
GGGG	116.22	184.82	6.92	6.96
JJJJ	51.94	72.18	1.97	3.42
JJJJ+5 wt.% micro Fly ash	57.32	79.02	2.13	3.61
JJJJ+10 wt.% micro Fly ash	69.61	91.70	3.90	4.10
JJJJ+15 wt.% micro Fly ash	63.25	115.76	3.41	4.93
JJJJ+2 wt.% nano Fly ash	63.23	91.23	2.33	3.75

JJJJ+4 wt.% nano Fly ash	81.23	124.23	4.23	4.40
JJJJ+6 wt.% nano Fly ash	76.81	119.93	3.92	5.12
JJJJ+5 wt.% micro Alumina	59.32	82.02	2.23	3.82
JJJJ+10 wt.% micro Alumina	75.61	94.70	3.95	4.39
JJJJ+15 wt.% micro Alumina	67.25	116.76	3.62	5.12
JJJJ+2 wt.% nano Alumina	66.23	94.23	2.45	4.19
JJJJ+4 wt.% nano Alumina	89.23	129.23	4.65	4.53
JJJJ+6 wt.% nano Alumina	83.81	123.93	4.12	5.39
GJJG	86.57	133.06	4.83	6.40
GJJG +5 wt.% micro Fly ash	93.88	145.39	5.36	6.40
GJJG +10 wt.% micro Fly ash	106.91	149.91	5.69	5.62
GJJG +15 wt.% micro Fly ash	100.43	136.43	5.15	5.34
GJJG +2 wt.% nano Fly ash	96.28	152.23	5.90	6.50
GJJG +4 wt.% nano Fly ash	115.35	176.30	6.50	6.86
GJJG +6 wt.% nano Fly ash	111.58	162.39	6.24	6.55
GJJG +5 wt.% micro Alumina	103.88	153.39	5.46	6.57
GJJG +10 wt.% micro Alumina	114.91	166.91	5.85	6.32
GJJG +15 wt.% micro Alumina	108.43	146.43	5.23	5.67
GJJG +2 wt.% nano Alumina	109.28	166.23	6.12	6.63
GJJG +4 wt.% nano Alumina	125.35	182.30	6.90	6.92
GJJG +6 wt.% nano Alumina	119.58	176.39	6.48	6.60
JGGJ	73.47	87.00	2.67	4.64
JGGJ +5 wt.% micro Fly ash	79.69	109.69	3.05	5.78
JGGJ +10 wt.% micro Fly ash	87.38	135.38	3.95	5.99
JGGJ +15 wt.% micro Fly ash	82.27	128.27	3.68	5.27
JGGJ +2 wt.% nano Fly ash	85.23	125.20	3.75	5.80
JGGJ +4 wt.% nano Fly ash	93.78	149.60	4.36	6.20
JGGJ +6 wt.% nano Fly ash	89.25	144.80	4.26	5.92
JGGJ +5 wt.% micro Alumina	86.69	119.69	3.25	5.84
JGGJ +10 wt.% micro Alumina	93.38	147.38	4.15	6.21
JGGJ +15 wt.% micro Alumina	87.27	139.27	3.95	5.32
JGGJ +2 wt.% nano Alumina	94.23	129.20	4.13	5.99
JGGJ +4 wt.% nano Alumina	106.78	156.60	4.69	6.32
JGGJ +6 wt.% nano Alumina	98.25	151.80	4.38	6.17
GJGJ	78.35	165.90	3.07	6.55

GJGJ +5 wt.% micro Fly ash	83.75	171.47	3.23	6.69
GJGJ +10 wt.% micro Fly ash	95.09	159.09	4.19	6.29
GJGJ +15 wt.% micro Fly ash	86.88	145.88	3.92	5.83
GJGJ +2 wt.% nano Fly ash	92.56	182.23	3.82	6.71
GJGJ +4 wt.% nano Fly ash	106.28	194.30	4.56	7.02
GJGJ +6 wt.% nano Fly ash	90.35	185.65	4.33	6.52
GJGJ +5 wt.% micro Alumina	95.75	175.47	3.13	6.71
GJGJ +10 wt.% micro Alumina	103.09	182.09	4.28	6.36
GJGJ +15 wt.% micro Alumina	93.88	165.88	4.03	5.96
GJGJ +2 wt.% nano Alumina	99.56	193.23	4.23	6.80
GJGJ +4 wt.% nano Alumina	116.28	209.30	4.86	7.10
GJGJ +6 wt.% nano Alumina	109.35	199.65	4.49	6.65

4.3.3 Flexural Strength

Flexural test was conducted on UTM 201 machine in accordance with ASTM D2344-84. Specimens of 150 mm length and 20 mm wide were cut and were loaded in three point bending with a recommended span to depth ratio of 16:1 as shown Figure 4.9 (a) and Figure 4.9 (b) shows the sample in loading condition. The test was conducted on the same machine used for tensile testing using a load cell of 10 kN at 2 mm/min rate of loading. The flexural stress in a three point bending test is found out by using following equation. The results obtained from the tests is presented in Table 4.7

$$\sigma_{max} = \frac{(3P_{max}L)}{(bh^2)} \tag{4.5}$$

Where 'P_{max}' is the maximum load at failure (N), 'L' is the span (mm), 'b' and 'h' is the width and thickness of the specimen (mm), respectively. The flexural modulus is calculated from the slope of the initial portion of the load-deflection curve which is found out by using by using following equation.

$$E = \frac{(mL^3)}{(4bh^3)} \tag{4.6}$$

Where m is the initial slope of the load deflection curve for each stacking sequence, five specimens are tested and average result is obtained. The fractured specimens of flexural is shown in Figure 4.9(c)

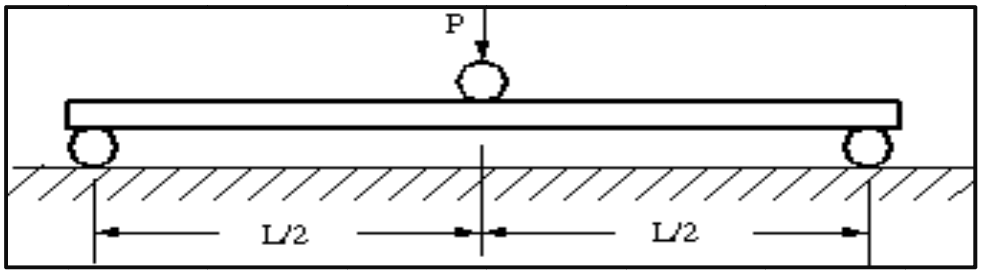

(a) Flexural specimen

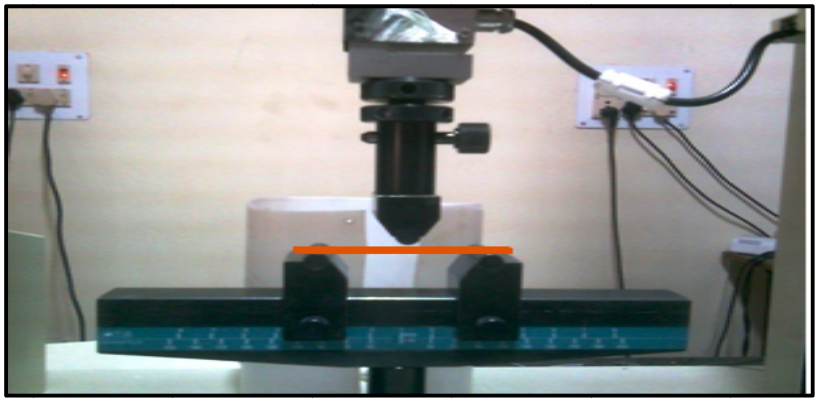

(b) Sample in loading position

(c) Fractured samples

Figure 4.9 Photograph of (a) Flexural specimen (b) sample in loading position (c) fractured samples

4.4 RESULTS AND DISCUSSION

4.4.1 Effect of alumina Filler Content on Void Fraction

To define the properties of the composites one of the most important property is density. In composites, density generally depends upon the relative proportion of the matrix and the reinforcing materials [198].The results for the void content in the hybrid composites for different stacking sequences varies with the position of jute fiber and glass fiber layer and their values are shown in Table 4.2.

It is seen from the Table 4.3 and 4.4 that the void fraction of the composites increases with increasing the concentration of filler in hybrid composites. The composite with the 15 wt.% alumina fillers showed the maximum void content. This might have happened due to improper mixing of higher weight fraction of fillers with the matrix.

With the nano filler addition the void content of the composites with the 2 wt. % nano filler addition shows least percentage of void fraction. This might have happened due to high surface area to volume ratio of the nano filler. Similar type of results was observed by the Hamidi et al. [199] in the fabrication of nanoclay/E-glass/Epoxy composites.

It is also found that with 4 and 6 wt. % filler content the void content increases. This might have happened due to particle agglomeration during mixing because of higher filler content. This type of agglomeration formation in higher filler loading was also observed by Deyu Kong et al. [200] during fabrication of nano-silica cement pastes.

4.4.2 Effect of fly ash filler content on void fraction

The results of the void content for micro and nano fly ash filler hybrid composites shows similar type of trend as observed in alumina fillers composites is shown in Table 4.5 and Table 4.6. However it is found that the percentage of void contain is more in the fly ash filler composites. This might be the result of different shapes and sizes of the fly ash particles material.

4.4.3 Hybrid Composites

4.4.3.1 Effect of tensile strength on hybrid composite

The variation tensile strength of unreinforced epoxy resin, jute fibers, glass fibers and also for various laminate stacking sequences of jute–glass fiber epoxy composites is shown in Figure 4.10.It is observed that the tensile strength of unreinforced epoxy resin is 21.03 MPa. When only laminates of jute and glass fibers are reinforced with epoxy, it is found to be 142 and 442% greater than the neat epoxy resin. Wambua et al. [201] quoted in their research article that jute fiber has 1.8% elongation of failure whereas glass fiber has 3%. When comparing the tensile strength of the jute fiber epoxy composite with glass fiber epoxy composites, it gives about 55% strength of glass fiber composites. It is also observed that an increase in the tensile strength of 51, 41, and 66% is for 50:50 jute–glass fiber-reinforced hybrid laminate (GJGJ, JGGJ and GJJG) composites when compared to that of only jute laminate (JJJJ) composite. There is an increase in the tensile strength of the composites observed with the incorporation of glass fibers in composite to jute composite. The glass fiber strength is in the range of 1950-2050 MPa where as the jute fiber strength is 331-414 MPa which is almost six times less than glass fiber. Naturally strength of GGGG composites remains higher even after hybridized with jute fiber. Micro mechanics principle has been used during manufacturing of composite.

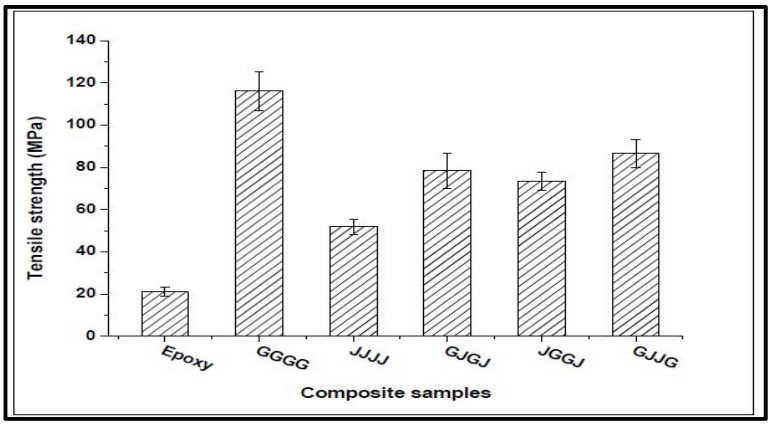

Figure 4.10 Tensile strength of jute–glass fiber epoxy composite

4.4.3.2 Effect of Flexural strength on hybrid composite

The variation flexural strength of unreinforced epoxy resin, jute fibers, glass fibers and also for various laminate stacking sequences of jute–glass fiber epoxy composites is shown in Figure 4.11. Due to the incorporation of glass and jute fibers into the epoxy resin, the strength of

the composites increases to a great extent. The flexural strength of the unreinforced epoxy resin is found to be 42.23 MPa whereas the flexural strength of laminate (only jute and glass fiber) reinforced composites is found to be 72.18 MPa and 184.82 MPa, which is greater than that of the neat epoxy resin. The jute fiber, gives 61% strength more of the glass fiber composites. The maximum flexural load that the neat epoxy withstands is up to 110 N but after incorporation of 24 wt.% of glass fiber, the load with stand resistance increase to 440 N. It is also found that in hybrid composites, GJGJ gives about 165.90 MPa of strength as compared glass fiber–epoxy composites. The same type of behavior is also observed by Gowda et al. [202] while they worked with treated jute fiber composite.

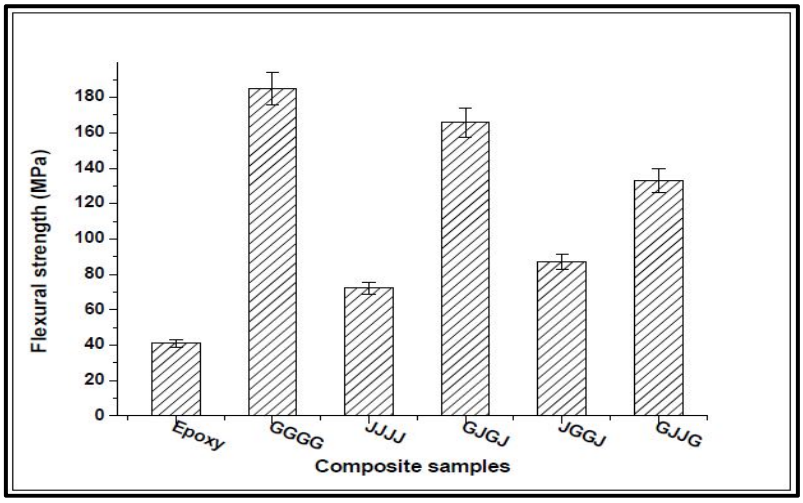

Figure 4.11 Flexural strength of jute-glass fiber epoxy composite

4.4.3.3 Effect of tensile and flexural modulus on hybrid composite

The variation tensile modulus and flexural modulus of unreinforced epoxy resin, jute fibers, glass fibers and also for various laminate stacking sequences of jute-glass fiber epoxy composites is shown in Figure 4.12 and 4.13. The modulus of the neat epoxy increases due to fiber incorporation. It is observed that the tensile and flexural modulus of unreinforced epoxy resin is found to be 0.69 GPa and 0.73 GPa. The higher module was recorded for the conventional glass fiber composites in both cases. The tensile and flexural modulus of the jute fiber composites is 30% and 50% of the glass fiber modulus. There is a similar observation found in Wambua et al. [201]. There is also a similar observation seen in case of flexural modulus of the laminated composites as seen in flexural strength of the laminated composites.

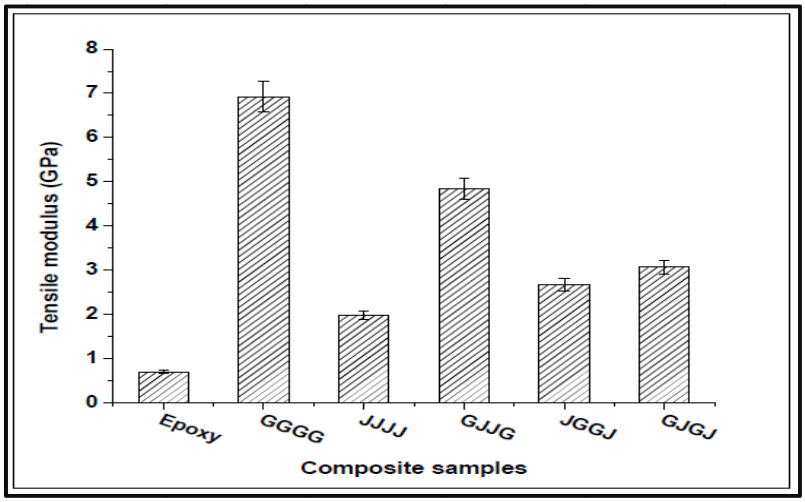

Figure 4.12 Effect of stacking sequence on tensile modulus of jute-glass fiber epoxy composite

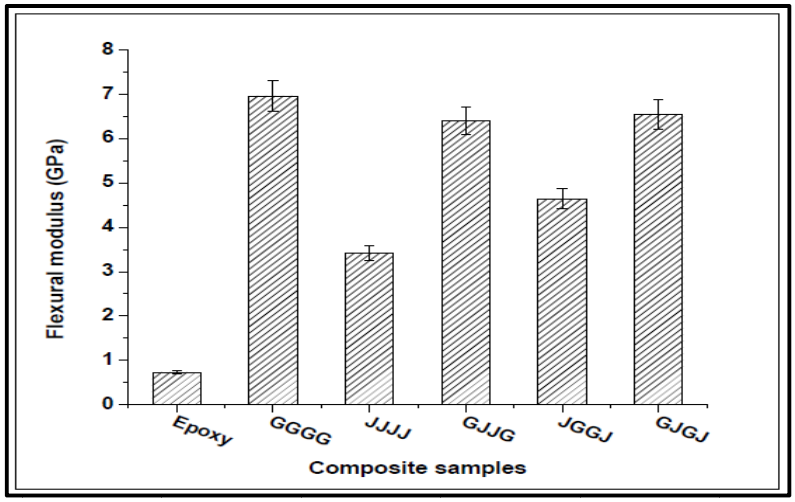

Figure 4.13 Effect of stacking sequence on flexural modulus of jute-glass fiber epoxy composite

4.4.4 Micro Filler Hybrid Composites

4.4.4.1 Fly ash micro filler

4.4.4.1.1 Effect of micro fly ash on tensile strength

Figure 4.14 shows the effect of micro fly ash addition on the tensile strength of hybrid composite as well as pure glass and jute composite. Different weight percentages of (5, 10 and 15 wt.%) of fly ash filler are added to the hybrid composites. The effect of filler addition on different stacking sequences of glass and jute fiber on the tensile and flexural properties is tested as per ASTM standard. For comparison purpose composite with only glass and jute fiber with

filler are also tested. It is clearly observed from the plot that a noticeable increase in strength up to 5 wt.% filler addition in hybrid and pure jute composites is achieved also beyond 5 wt.% the strength increases an all the composites up to 10 wt.% but strength variation ins not so high compared from 0 wt.% to 5 wt.% filler addition. Further addition of filler (15 wt.%) the strength in all the composites decreases. This might have happened due to improper bonding of the fly ash particle with the matrix material.

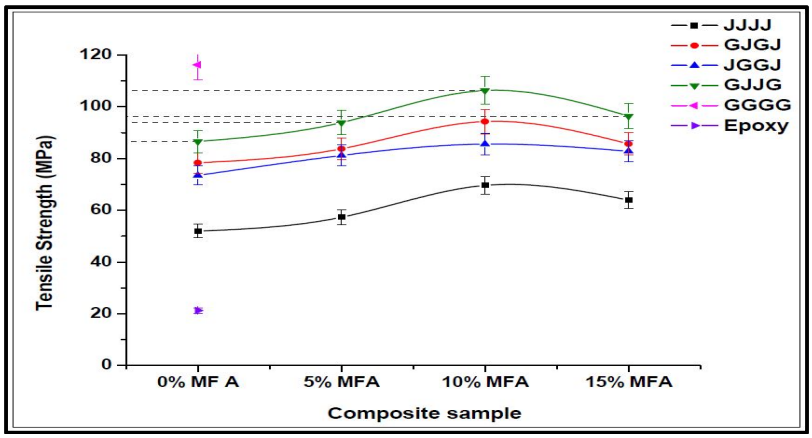

Figure 4.14 Effect of micro fly ash on tensile strength of hybrid composites

4.4.4.1.2 Effect of micro fly ash on flexural strength

Figure 4.15 shows the effect of micro fly ash filler in hybrid composites as well as pure jute composites. From the figure it is clearly observed that even after hybridization and filler addition none of the composites crosses the strength of the glass fiber. It is also seen from the plot that for all composite sequences expects GJGJ the flexural properties decreases beyond 5 wt.%. The increases in flexural strength up to 10 wt.% for the sequence GJGJ is observed beyond which it decreases. This increase in flexural strength can be compared with pure glass fiber composite.

Even after hybridization and filler addition none of the composites crosses the strength of the glass fibers. Among all the composites tested, GJJG composite with 10 wt.% fly ash filler addition shows the best comparative result with the pure conventional (glass) fiber composites.

It can be conclude here that by addition of two layers of Jute (natural) fiber and inclusion of particulate filler for the present case 10wt% of fly ash micro filler both tensile and flexural

strength are comparable to purely glass fiber composite. Our aim was to reduce the use of glass fiber which is costly and non-biodegradable. Our objective was fulfilled to certain extent

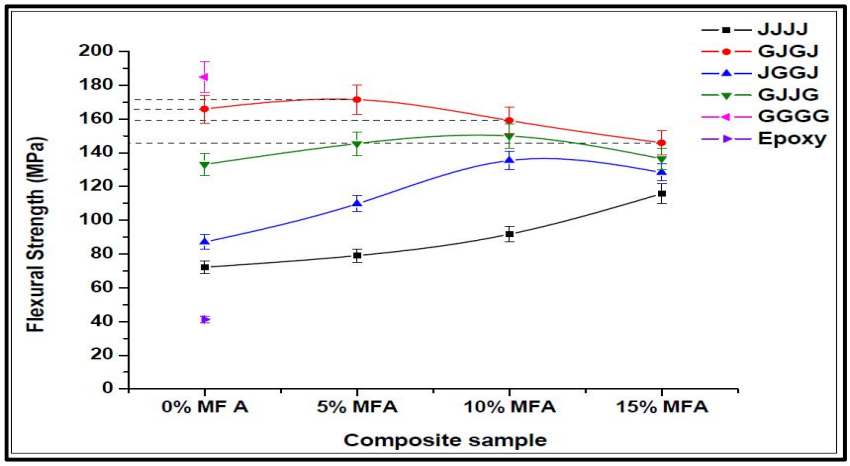

Figure 4.15 Effect of micro fly ash on flexural strength of hybrid composites

4.4.4.1.3 Effect of micro fly ash on tensile and flexural modulus

The deviation of tensile modulus and flexural modulus for different laminate stacking sequences of jute and glass along with and without the fly ash filler addition are shown in Figure 4.16 and 4.17. The flexural modulus of the neat epoxy resin is found to be 0.73 MPa. A similar observation as in case of flexural strength is also noticed for the modulus of the composites. But the modulus of the GJJG along with fly ash filler addition reaches almost equal to the glass fiber composites. There is no significant variation found for the tensile modulus of the composite with fly ash filler addition.

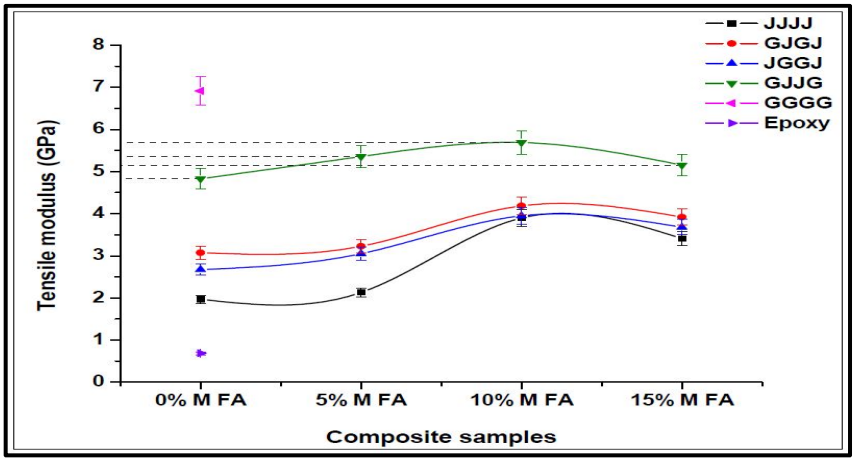

Figure 4.16 Effect of micro fly ash on tensile modulus of hybrid composites

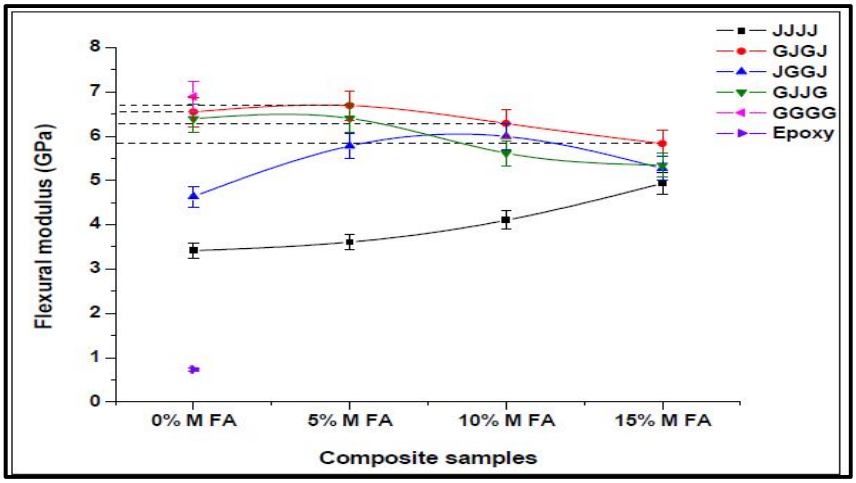

Figure 4.17 Effect of micro fly ash on flexural modulus of hybrid composites

4.4.4.2 Alumina micro filler

4.4.4.2.1 Effect of micro alumina on tensile strength

The effect of alumina micro filler on the tensile and flexural strength of the hybrid composite as well as jute composite has also been carried out as per the procedure followed for fly ash micro filler. Same weight percent (5, 10 and 15 wt.%) of alumina filler were added to the hybrid composite. Figure 4.18 shows the results of the tests. It is clearly observed from the plot that the strength of composites increases due to the filler addition in hybrid as well as pure jute composites. As the filler addition increases up to 10 wt. % the strength also increases and beyond which it decreases. This might have happened due to higher volume fraction of filler, which leads to debonding of fibers with the matrix. This also leads to non-adherence of filler with the matrix. This in turn decreases the load carrying capacity of the composite to which in turn shows lower strength of the composites with higher particle loading [203].

It is also found that even after hybridization and filler addition, none of the composites crosses the strength of the glass fibers. Among all the composite glass as outer layer (GJJG) composites with 10 wt.% alumina filler addition shows the best result which approaches the strength achieved by pure glass fiber i.e. (GGGG) composites.

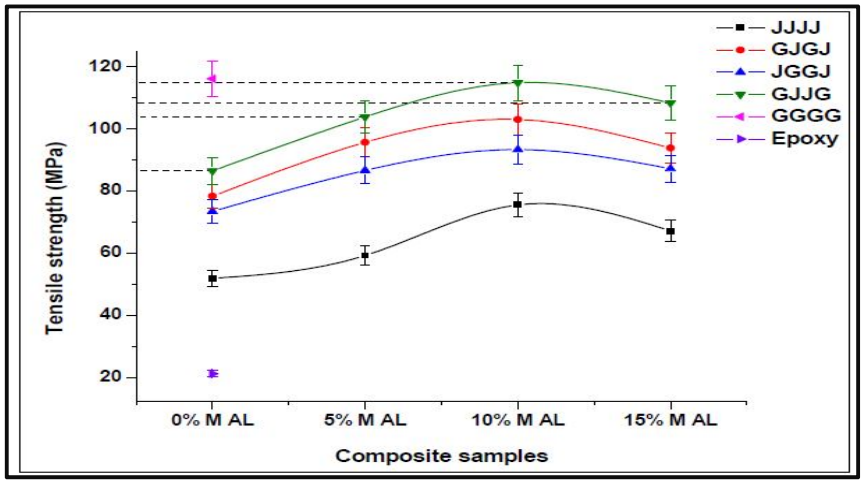

Figure 4.18 Effect of micro alumina on tensile strength of hybrid composites

4.4.4.2.2 Effect of micro alumina on flexural strength

Figure 4.19 shows that the effect of alumina micro fillers in hybrid composites and pure jute composites. Different weight percentages (5, 10 and 15 wt.%) are added to the hybrid composites and tested for the flexural properties as per ASTM standards. For a comparison a glass fiber, jute fiber and neat epoxy composites are also tested. From the figure, it is clearly observed that even after hybridization and filler addition, none of the composites crosses the strength of the glass fibers. It is also noticed that with the alumina filler addition the strength increases continuously in jute fiber composites this might be due to filler adhesion in this matrix. The role of the matrix and the fillers in a fiber reinforced composite is to transfer the load to the stiff fibers through shear stresses at the interface [201]. The filler addition here helps in transfer of load which in turn increases the strength. It is also found that in hybrid composite the strength increases up to 10 wt.% filler further increase in filler with the strength decreases. The same type of behavior was recorded for 15 wt.% of filler in tensile strength results. Among all the composites GJGJ composites with 10 wt.% alumina filler addition shows the better comparative result with the pure conventional (glass) fiber composites. It is interesting to note that for tensile strength GJJG i.e. glass fiber at the outer layers gives minimum strength, while (GJGJ) i.e. glass fiber at the outer layer on the application of loading side and jute fiber on the bottom side gives maximum strength. This happened because during flexural test resistance of glass fiber due to flexural load is more in comparison to jute fiber. Also for this composite third layer is glass fiber

hence the strength increase appreciable. Biswas et al. [198] reported the similar type of behavior in case of red mud and cooper slag filler addition in bamboo composites.

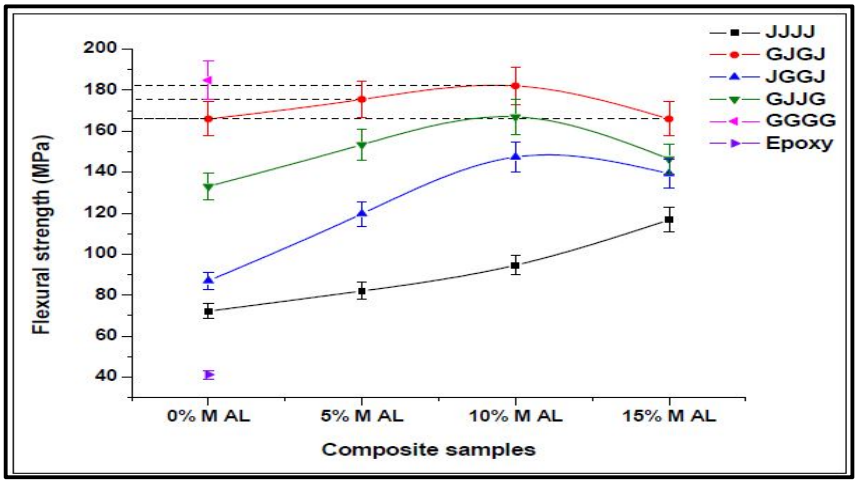

Figure 4.19 Effect of micro alumina on flexural strength of hybrid composites

4.4.4.2.3 Effect of micro alumina on tensile and flexural modulus

The tensile and flexural modulus for different laminate stacking sequences of jute and glass along with and without alumina filler addition are shown in Figure 4.20 and 4.21. Though the tensile modulus of all composites increases with addition of micro filler with respect to pure epoxy none of the composites except GJJG shows a comparative result with pure glass (GGGG) composite.

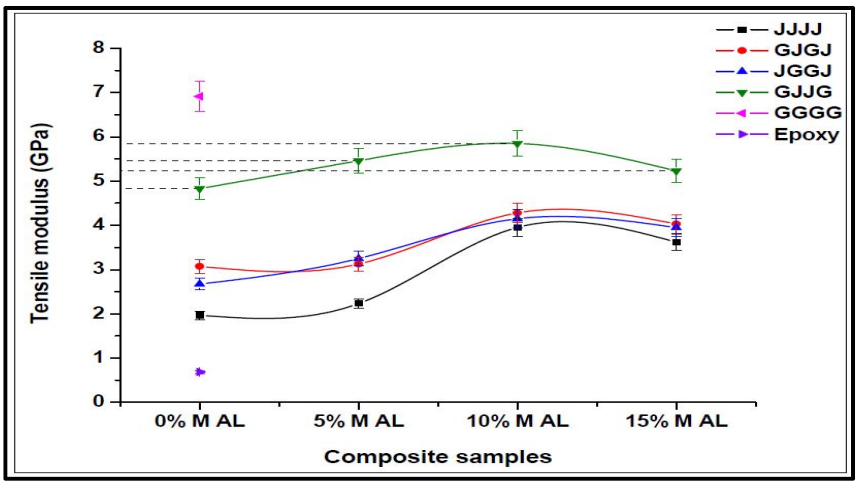

Figure 4.20 Effect of micro alumina on tensile modulus of hybrid composites

GJJG composite with 10 wt.% of filler (5.85 GPa) somehow approach the tensile modulus value of GGGG composite (6.92 GPa). In case of flexural modulus GJGJ composite (4.28 GPa) with 10 wt.% filler approach the value of GGGG composite (6.96 GPa).

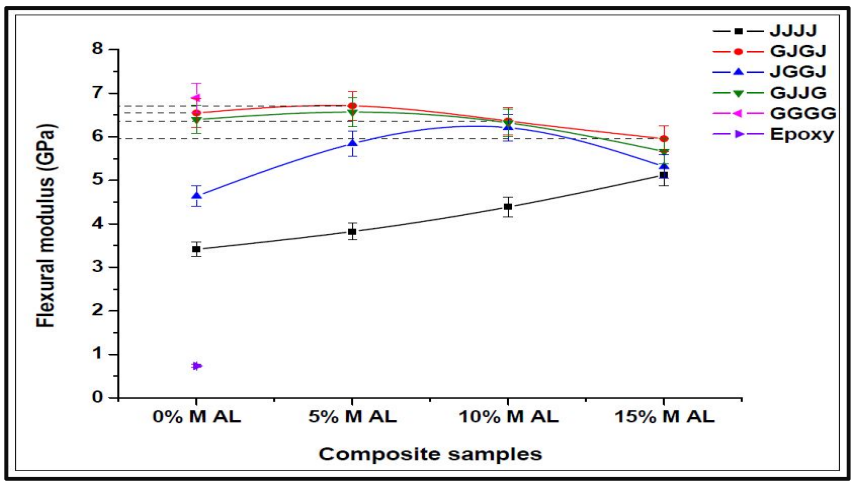

Figure 4.21 Effect of micro alumina on flexural modulus of hybrid composites

4.4.5 Nano Filler Hybrid Composites

4.4.5.1 Fly ash nano filler

4.4.5.1.1 Effect of nano fly ash on tensile strength

The effect of nano fly ash filler addition (2, 4 and 6 wt.%) on the tensile and flexural strength of the hybrid composite as well as jute composite has been carried out as per the procedure carried at micro filler addition. The experimental results for tensile strength as their modulus are presented in Table 4.7.

Figure 4.22 shows the effect of nano filler addition on tensile strength of hybrid and pure jute composite. All composite shows similar trend i.e. increase in the strength up to 4 wt.% of nano filler and there after it decreases. The interesting point here is 4 wt.% of nano filler reinforcement for GJJG composite strength almost reaches to equal strength of the glass fiber composite. Thus it can be conclude here that by incorporating two jute layers with 4 wt.% of filler reduces the use of synthetic fiber.

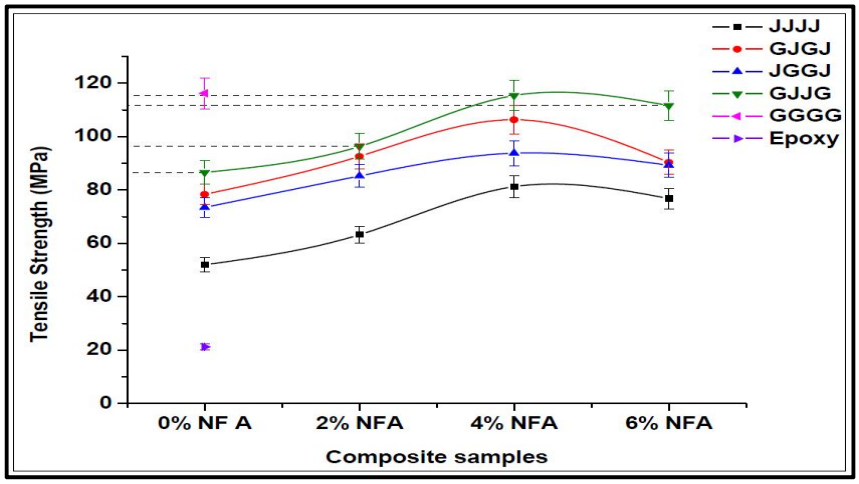

Figure 4.22 Effect of nano fly ash on tensile strength of hybrid composites

4.4.5.1.2 Effect of nano fly ash on flexural strength

The effect of nano filler addition (2, 4 and 6 wt. %) in hybrid and pure jute composites are shown in Figure 4.23. It is clearly observed that the nano fly ash filler addition increases up to 4 wt.%, the strength of the hybrid composites and jute composites increases. It is interesting to note here that flexural strength of GJGJ composites super past the strength of the GGGG composites with 4 wt.% of nano filler. This similar type of behavior has also been reported by Mohanty et al. [204] while they worked with Glass/Carbon fiber reinforced epoxy nano composites.

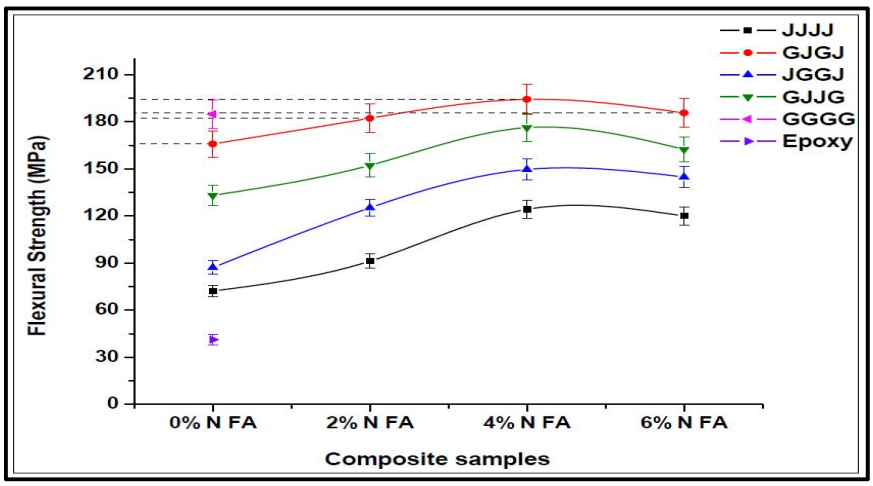

Figure 4.23 Effect of nano fly ash on flexural strength of hybrid composites

4.4.5.1.3 Effect of nano fly ash on tensile and flexural modulus

Figure 4.24 and 4.25 shows the plot of tensile and flexural modulus of all the composites along with pure glass and jute composites. Both the tensile and flexural modulus increases with addition of nano filler. From the figure it is clearly observed that tensile modulus of GJJG with 4 wt.% of nano filler increases the tensile modulus up to 90% of the strength of the glass fiber composite. However the flexural modulus of GJGJ with 4 wt.% of nano filler increases the modulus up to 5% than GGGG composite.

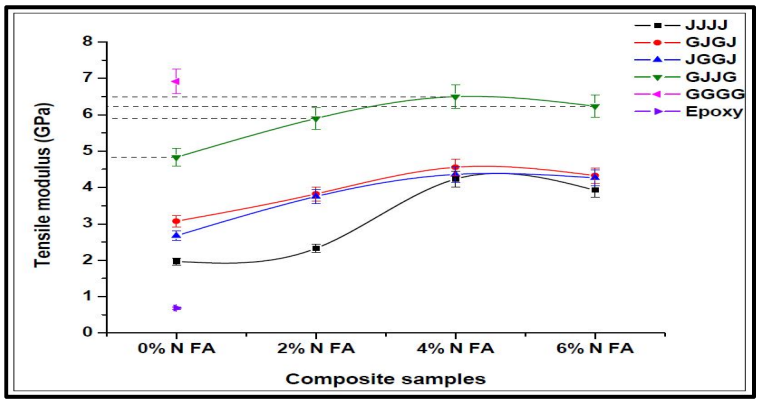

Figure 4.24 Effect of nano fly ash on tensile modulus of hybrid composites

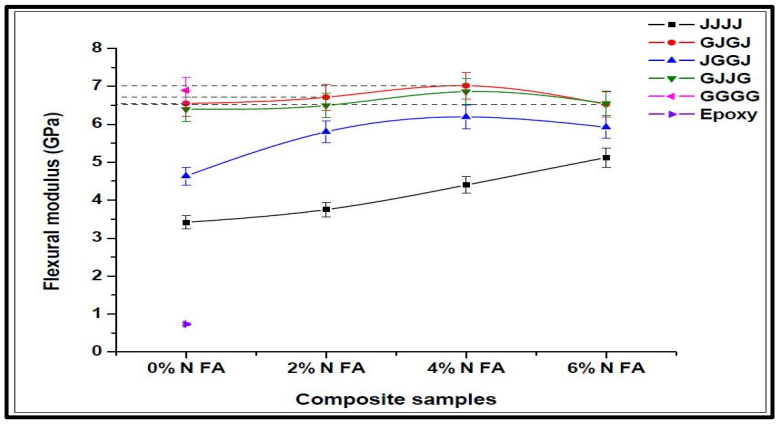

Figure 4.25 Effect of nano fly ash on flexural modulus of hybrid composites

4.4.4.5.2 Alumina Nano filler

4.4.5.2.1 Effect of Nano alumina on tensile and flexural strength

Effect of nano alumina filler on the tensile and flexural strength of the composites are shown in Figure 4.26 and 4.27. The results of nano alumina filler shows almost same trend for different composite for the strength values. The benefit of alumina nano filler in comparison to fly ash

nano filler indicates that both tensile and flexural strength values cross the strength of pure glass fiber composite. The increase in tensile strength is found to be 5% for GJJG with 4 wt.% nano alumina composite than GGGG composite. However GJGJ with 4 wt.% nano alumina gives higher flexural strength than pure GGGG composite. Since alumina is ceramic filler for which fracture toughness is higher [205], results higher strength of the composite with 4 wt.% of nano filler.

The reduction in the flexural strengths of the composites with an increase in filler content is probably caused by an incompatibility of the particulates with the matrix, leading to poor interface bonding. The lower values of flexural properties might also be attributed to fiber-to-fiber interaction, voids and dispersion problems [198]. This similar type of behavior is observed and reported by Jen et al. [206] in case of nano filler addition in AS-4/PEEK APC-2 nanocomposite laminates and Nathaniel Chisholm et al. [207] in case of carbon/Sic-epoxy nanocomposites.

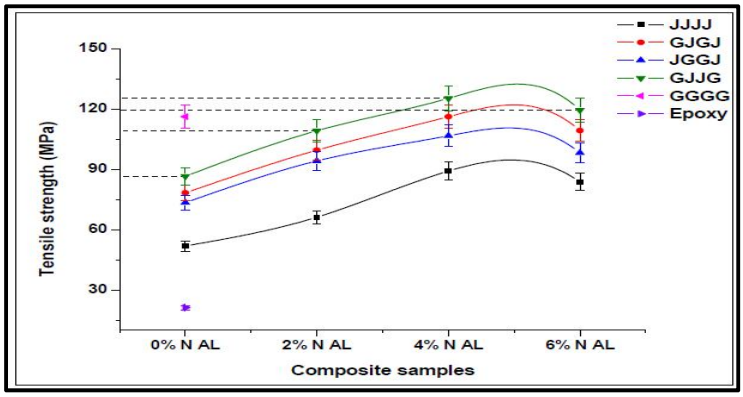

Figure 4.26 Effect of nano alumina on tensile strength of hybrid composite

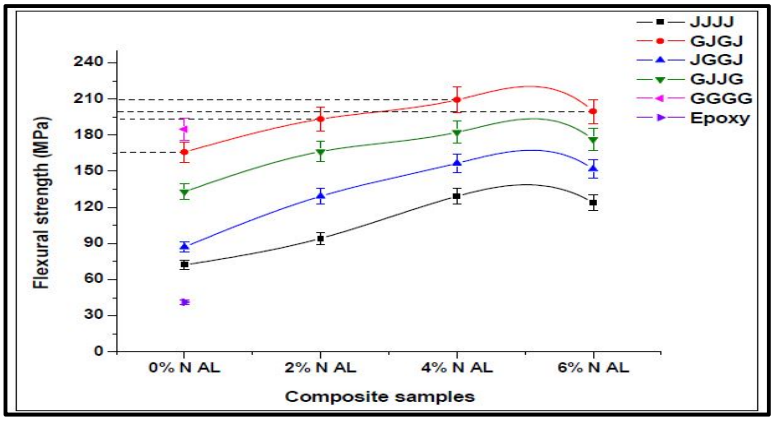

Figure 4.27 Effect of nano alumina on flexural strength of hybrid composites

4.4.5.2.2 Effect of nano alumina on tensile and flexural modulus

Tensile and flexural modulus of hybrid composites with nano alumina filler is also given the same trend as per fly ash nano filler. From the Figure 4.28 and 4.29 it is clearly observed that GJJG composite shows higher tensile modulus and GJGJ composite shows higher flexural modulus. Both the results show higher modulus than GGGG composite.

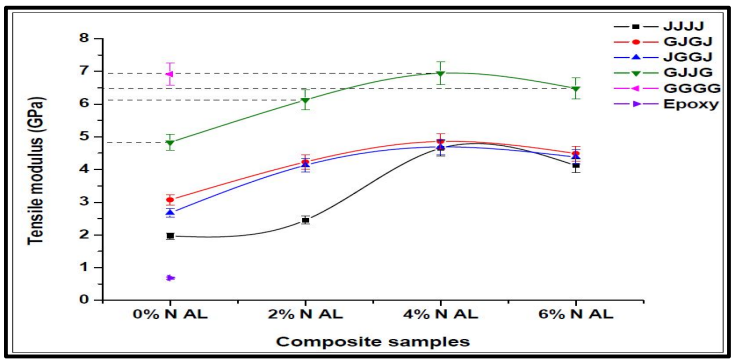

Figure 4.28 Effect of nano alumina on tensile modulus of hybrid composites

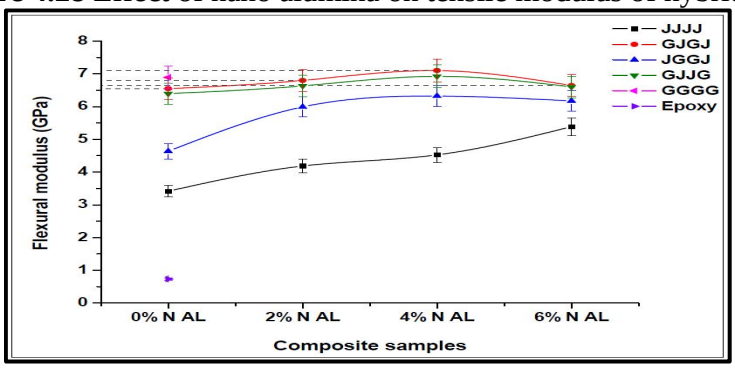

Figure 4.29 Effect of nano alumina on flexural modulus of hybrid composites

4.4.6 Comparison of flexural and tensile strength

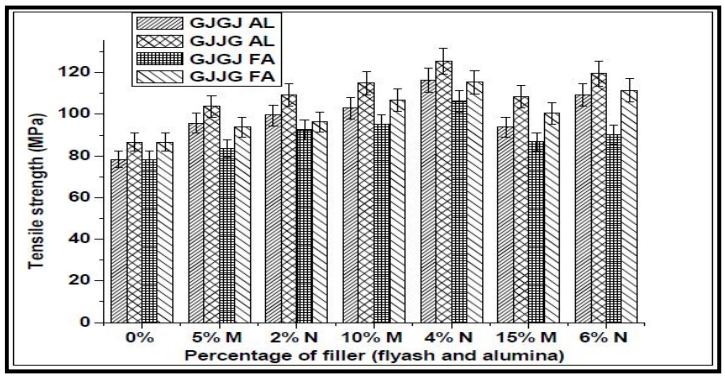

(a)

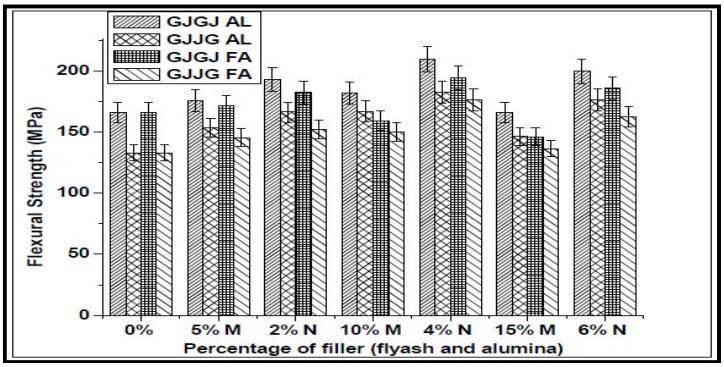

(b)

Figure 4.30 comparisons of filler effects on GJJG and GJGJ (a) Tensile strength (b) Flexural strength

Figure 4.30 (a and b) shows the comparison of the tensile and flexural of all the fillers of GJJG and GJGJ. Form the figures it is clearly observed that 4% nano filler reinforced GJJG and GJGJ epoxy composite giving better results in tensile and flexural strengths. The XRD analysis of both Fly ash and Alumina shown in Figure 3.9 and 3.8(a) in chapter 3 indicates that fly ash contains different materials like Quartz, Mullite, Hematite and Calcium oxide etc. whereas pure alumina contains only α-alumina. It is natural that α-alumina gives better result than fly ash. However our intension was to utilize fly ash in nano form. Here by utilizing nano fly ash it is observed that tensile and flexural strengths are 93% of GJJG+4% NFA and 92% of GJGJ+4%NFA which are comparable to pure alumina. Hence our objective is fulfilled.

4.4.7 Morphological Studies of tensile tested specimens

SEM micrographs of the tensile fracture surfaces of the pure jute, glass, hybrid with micro and nano filler composites are shown in Figure 4.31 (a-e) respectively.

From the SEM image 4.31(a) of raw jute fiber epoxy composites it is clearly observed that due to tensile load the fiber got little stretches and under gone breakage. This feature suggests weak interfacial bonding between the fiber and matrix.

When considered the glass fiber composite shown in figure 4.31(b) it is clearly observed that the fiber got stretched and finally got breakage after a long elongation. This validates the higher value of tensile strength of the glass fiber composites.

Figure 4.31 (a) SEM image of JJJJ fiber composite [208]

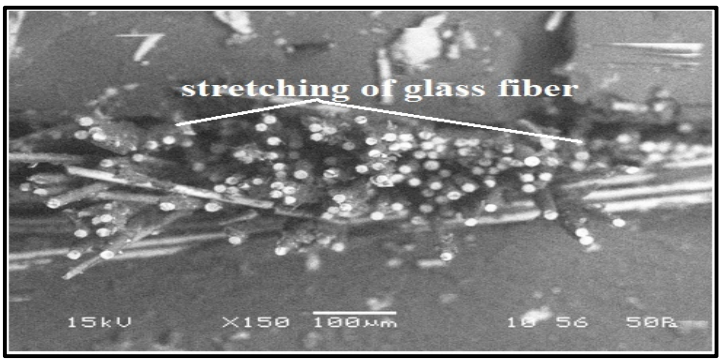

Figure 4.31 (b) SEM image of GGGG fiber composite [208]

When considering hybrid composites the tensile strength of the composites is less as compared to the pure glass fiber this is due to the early breakage of jute fibers and the morphology of the hybrid composite shown in the figure 4.31(c) supports the results.

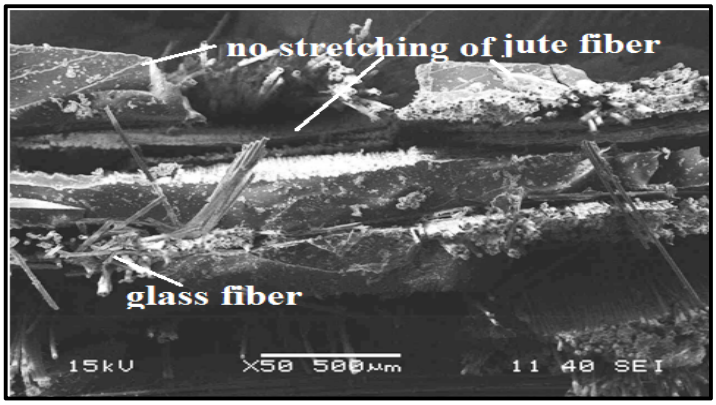

Figure 4.31 (c) SEM image of GJJG hybrid composite

From Figure 31(d) it is clearly observed that the crack propagation in epoxy composite is reduced with fly ash filler addition.

From Figure 31(e) it is clearly observed that the fiber twisting has been observed due to tensile load before it under gone breakage when compared to Figure 31(d) this effect is due to alumina filler addition in composites.

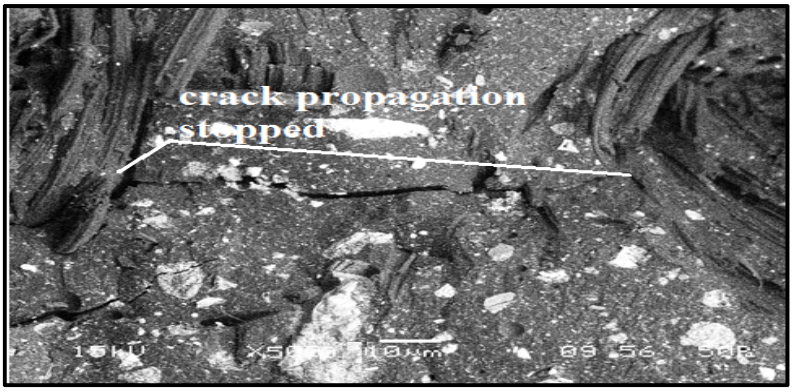

Figure 4.31 (d) SEM image of GJJG hybrid composite with nano fly ash filler

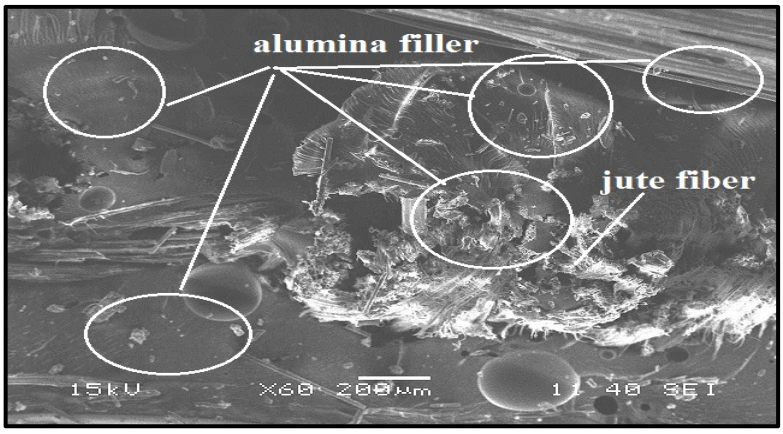

Figure 4.31 (e) SEM image of GJJG hybrid composite with nano alumina filler

4.4.8 Morphological studies of flexural tested specimens

Figure 4.32(a-f) shows the fracture surfaces of jute/glass fiber reinforced epoxy composite after the flexural test under different fiber loading.

A very small stretching and bending is observed in jute when compared to glass composites shown in Figure 4.32(a) it is also observed that a sharp cut of fiber at some places this define the brittle nature of the jute fiber. The figure indicates that the fiber fracture and pull out from the specimen and also the dislocation of fibers.

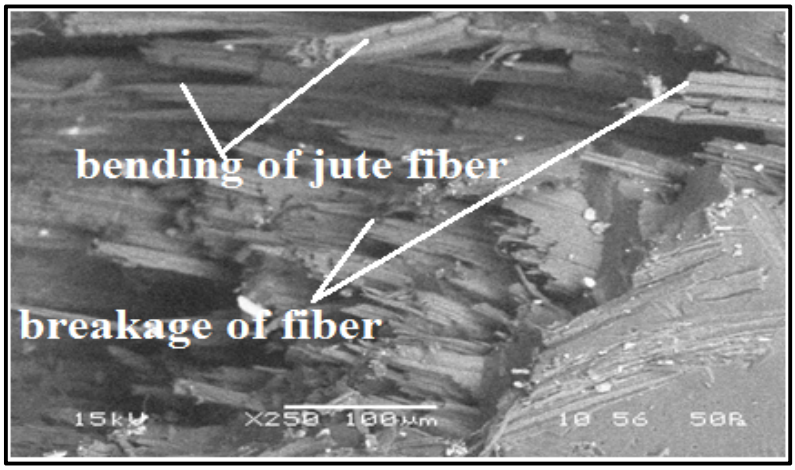

Figure 4.32(a) SEM image of JJJJ fiber composites [208]

The morphology of the glass fiber is shown in Figure 4.32(b). Bending of the glass fiber due to flexural load is observed in the glass fiber composites this validates the flexural strength results of glass fibers, which is the maximum among all the composites.

Figure 4.32(b) SEM image of GGGG fiber composites [208]

The reduction of bending strength of the glass fiber is observed in the Figure 4.32(c) this is due to addition of jute fiber. It is clearly observed from the figure that in half portion glass fiber got bended and stretched in the remaining half there is no stretching of jute fiber and also the fiber directly undergone breakage this figure validates the less strength result of hybrid composites.

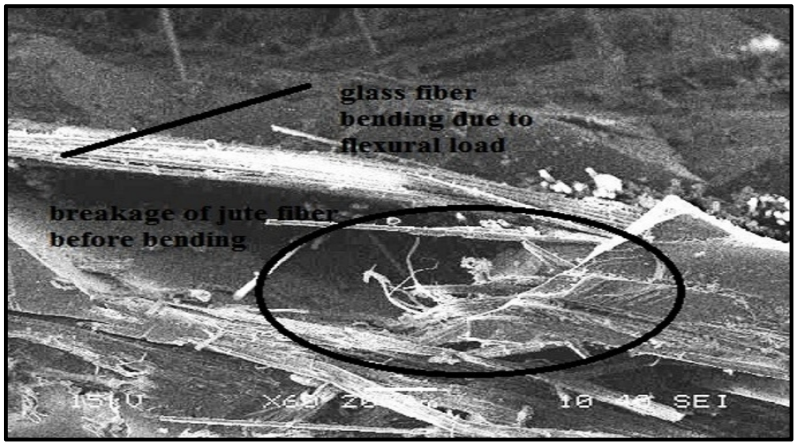

Figure 4.32(c) SEM image of GJGJ hybrid composites

Similar type of behavior is also observed in case of hybrid composites with micro fly ash filler which is shown in Figure 4.32(d).

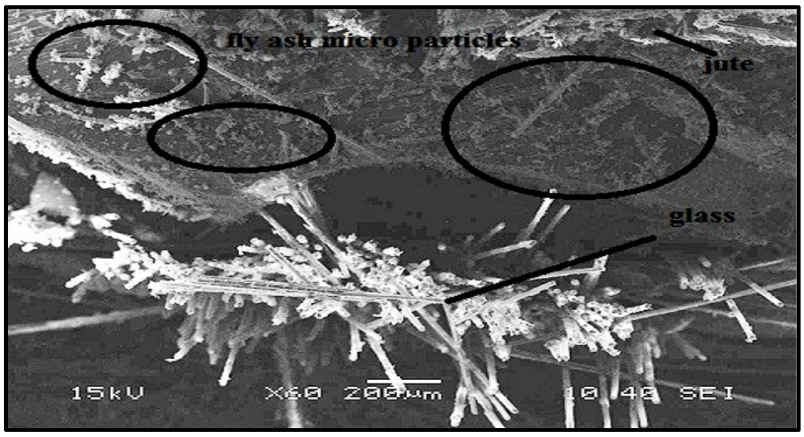

Figure 4.32(d) SEM image of GJGJ hybrid composites with micro fly ash filler

The effect of the nano filler in hybrid composites are shown in Figure 4.32(e). It is evident that due to lower flexural strength of glass fiber, it directly under gone breakage without any elongation. This indicates that due to addition of nano fly ash as filler in glass/jute fiber composites, the composite become brittle as well as strong.

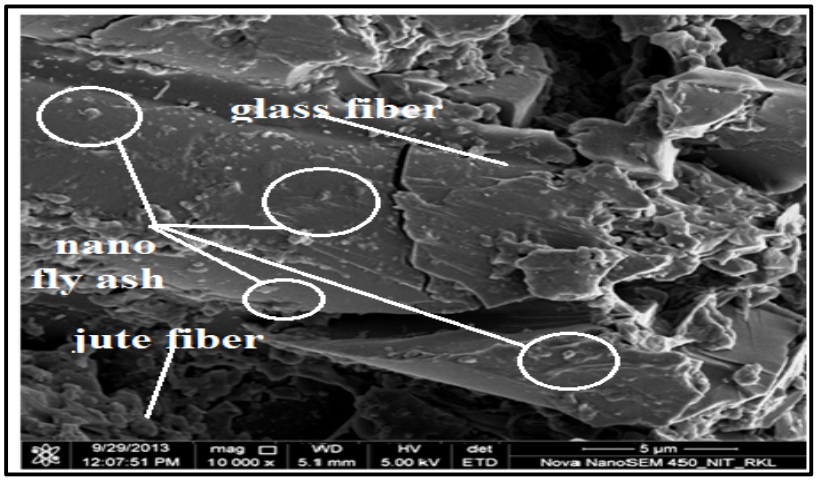

Figure 4.32(e) SEM image of GJGJ hybrid composites with nano fly ash filler

Similarly, for the case of hybrid composite with nano alumina filler is shown in Figure 4.32(f) the crack formation due to flexural load indicates the brittle nature of the hybrid based nano composites. It is also observed that due to flexural load the crack formation before breakage is less as compared to Figure 4.32(e). This indicates that due to nano alumina filler addition the strength of the composite increases.

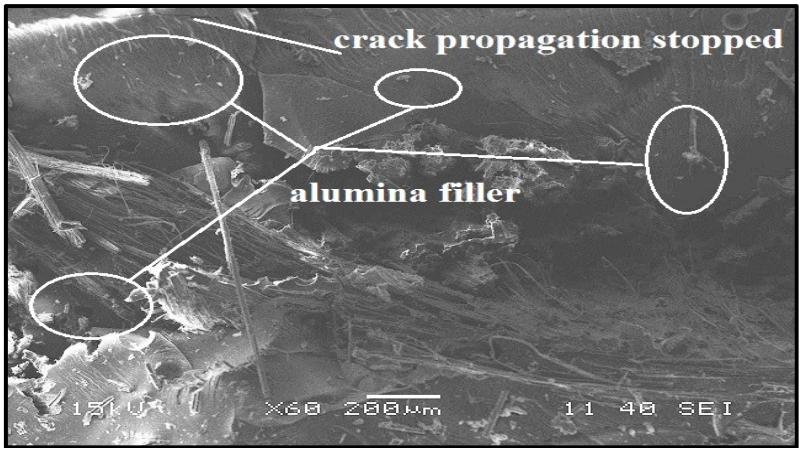

Figure 4.32(f) SEM image of GJGJ hybrid composites with nano alumina filler

4.5 Conclusion

1. Effect of alumina and fly ash micro/nano filler on tensile and flexural properties of jute/glass fabrics reinforced epoxy composites was studied with different layering sequence of fibre. It is clearly observed from the results that incorporation of nano filler enhanced the properties to an appreciable amount when compared with the micro filler.
2. The addition of 2 wt.% nano alumina reduces the void content in the composites. The void content in the composites found to increase with the microfiller addition.
3. Comparing the flexural strength of all composites filled with both micro and nano filler, it is found that 4wt.% of nano filler gives the best result. Comparing with all stacking sequences and the conventional composites with only jute and glass layer the GJGJ composites with alumina filler for all wt.% (2, 4 and 6) shows the best result.
4. The tensile strength of the composites is increased by 5% to 15% due to filler additions. The maximum tensile strength in all the composites is obtained for 4 wt.% nano filler addition. The best alternate for conventional composites, among the entire composite from tensile strength point of view with 4 wt.% and 6 wt.% alumina nano filler GJJG composite.
5. In the fly ash nano filler 4 wt.% nano filler GJJG hybrid composite is a better alternate than the glass fibre composites where tensile properties are the paramount importance. Whereas 4 wt.% nano fly ash GJGJ hybrid composites is a better alternate where the flexural properties are prominent.
6. The morphological study confirms that the strength of the hybrid and pure jute fibres, composites increases due to fillers additions.

Chapter 5

Solid Particle Erosion Studies of Jute-Glass Fibre Reinforced Epoxy Hybrid Composite

5.1 INTRODUCTION

Wear is probably the most important yet the least understood aspect of tribology. It is certainly the youngest of the tri of topics, friction, lubrication and wear, to attract scientific attention, although its practical significance has been recognizes throughout the ages. The findings of Guillaume Amontons in 1699 [209] establishing scientific studies of friction are almost of 300 years ago, while Petrov [210], Tower [211] and Reynolds [212] brought enlightenment to the subject of lubrication a century ago in the hectic 1880s. Substantial Studies of wear can be associated only with the five decades that have elapsed since R. Holm [213] explored the fundamental aspects of surface interactions encountered in electrical contacts.

One third of our global energy consumption has been devoured wastefully in friction. In addition to the primary saving of energy, very significant additional economics can be made by the reduction of the cost involved in the manufacture and replacement of prematurely worn out components. The dissipation of energy by wear impairs strongly to the national economy and the life style of most of the peoples. So, the effective decrease and control of wear of metals are always desired [214].

Wear causes an enormous annual expenditure by industry and consumers. Most of this is replacing or repairing equipment that has worn to the extent that it no longer performs a useful function. For many machine components, this occurs after a very small percentage of the total volume has been worn away. For some industries, such as agriculture, as many as 40% of the components replaced on equipment have failed by abrasive wear. Other major sources of expenditure are losses production consequential upon lower efficiency and plant shutdown, the need to invest more frequently in capital equipment and increased energy consumption as equipment wears. Estimates of direct cost of abrasive wear to industrial nations vary from 1 to 4 % of gross national product and Rigney [215] has estimated that about 10% of all energy generated by man is dissipated in various friction processes.

Wear is not an intrinsic material property but characteristics of the engineering system which depend on load, speed, temperature, hardness, presence of foreign material and the environmental condition [216]. Widely varied wearing conditions cause wear of materials. It

may be due to surface damage or removal of material from one or both of two solid surfaces in a sliding, rolling or impact motion relative to one another. In most cases wear occurs through surface interactions at asperities. During relative motion, material on contacting surface may be removed from a surface, may result in the transfer to the mating surface, or may break loose as a wear particle. The wear resistance of materials is related to its microstructure may take place during the wear process and hence, it seems that in wear research emphasis is placed on microstructure [217]. Wear of material depends on many variables, so wear research program must be planned systematically. Therefore researchers have normalized some of the data to make them more useful. The wear map proposed by Lim [218] is very much useful in this regard to understand the wear mechanism in different sliding conditions as well as the anticipated rates of wear.

5.2 RECENT TRENDS IN WEAR RESEARCH

Numerous wear researches have been carried out in the 1940's and 1950's by mechanical engineers and metallurgists to generate data for the construction of motor drive, trains, brakes, bearings, bushings and other types of moving mechanical assemblies [219].

It became apparent during the survey that wear of materials was a prominent topic in a large number of the responses regarding some future priorities for research in tribology. Some 22 experienced technologists in this field, who attended the 1983 'Wear of Materials Conference' in Reston, prepared a ranking list [220]. Their proposals with top priority were further investigations of the mechanism of wear and this no doubt reflects the judgments that particular effects of wear should be studied against a background of the basic physical and chemical processes involved in surface interactions. The list proposed is shown in Table- 5.1.

Peterson [214] reviewed the development and use of tribo-materials and concluded that metals and their alloys are the most common engineering materials used in wear applications. Grey cast iron for example has been used as early as 1388. Much of the wear research conducted over the past 50 years is in ceramics, polymers, composite materials and coatings [221].

Table 5.1 Priority in wears research [220]

Ranking	Topic
1.	Mechanism of Wear
2.	Surface Coatings and treatments
3.	Abrasive Wear
4.	Materials
5.	Ceramic Wear
6.	Metallic Wear
7.	Polymer Wear
8.	Wear with Lubrication
9.	Piston ring-cylinder liner Wear
10.	Corrosive Wear
11.	Wear in other Internal Combustion Machine component

Wear of materials encountered in industrial situations can be grouped into different categories as shown in Table-5.2. Though there are situations where one type changes to another or where two or more mechanism plays together.

Table 5.2 Type of wear in industry [219]

Type of wear in Industry	Approximate percentage involved
Abrasive	50
Adhesive	15
Erosion	8
Fretting	8
Chemical	5

5.3 THEORY OF WEAR

Wear occurs as a natural consequence when two surfaces with a relative motion interact with each other. Wear may be defined as the progressive loss of material from contacting surfaces in relative motion. Scientists have developed various wear theories in which the Physico-Mechanical characteristics of the materials and the physical conditions (e.g. the

resistance of the rubbing body and the stress state at the contact area) are taken in to consideration. In 1940 Holm [213] starting from the atomic mechanism of wear, calculated the volume of substance worn over unit sliding path.

Barwell and Strang [222] in 1952: Archard [223] in 1953 and Archard and Hirst [224] in 1956 developed the adhesion theory of wear and proposed a theoretical equation identical in structure with Holm's equation. In 1957, Kragelski [225] developed the fatigue theory of wear. This theory of wear has been widely accepted by scientists in different countries. Because of the Asperities in real bodies, their interactions in sliding is discrete, and contact occurs at individual locations, which, taken together, form the real contact area. Under normal force the asperities penetrate into each other or are flattened out and in the region of real contact points corresponding stress and strain rise. In sliding, affixed volume of material is subjected to the many times repeated action, which weakens the material and leads finally to rupture.In1973, Fleischer [226] formulated his energy theory of wear. The main concept of this theory is that the separation of wear particles requires that a certain volume of material accumulates a specific, critical store of internal energy. It is known that a large part of the work done in sliding is dissipated as heat, and that small proportion of it accumulates in the material as internal potential energy. When the energy attains a critical value, plastic flow of the material occurs in this volume or a crack is formed. Further theories of wear are found in [227]. Though all the theories are based on different mechanisms of wear, the basic consideration is the frictional work.

In past few decades, numerous research works have been carried out on abrasive wear performance of polymer and polymer based composite in view of their extensive application in the field industry and agricultural sectors where abrasive wear is a predominant mode of failure. Conveyor aids, vanes, gears, bushes, seals, bearings, chute liners etc. are some examples of their applications [228-231].Since abrasive wear is the most severe form of wear accounting for 50% of total wear, several researches has been devoted for exploring abrasive wear of polymer composites. Evans et al. [232] studied the abrasion wear behavior for 18 polymers and they noticed that low density polyethylene (LDPE) showed the lowest wear rate in abrasion against rough mild steel, but a higher wear rate in abrasion with coarse corundum paper. Unal et al. [233] studied abrasive wear behavior of polymeric materials. They concluded that the specific wear rate decreases with the decrease in abrasive surface roughness. They also concluded that,

the abrasive wear include micro-cracking, micro-cutting, and micro-ploughing mechanisms. Whereas in another investigation [234] they concluded that the sliding speed has stronger effect on the specific wear rate. Shipway and Ngao [235] investigated the abrasive behavior of polymeric materials in micro-scale level. They concluded that the wear behavior and wear rates of polymers depended critically on the polymer type. Harsha and Tewari [236] investigated the abrasive wear behavior of polyaryletherketone (PAEK) and its composites against SiC abrasive paper. They concluded that the sliding distance, load, abrasive grit size have a significant influence on abrasive wear performance. Further there are many references that illustrate the influence of fillers and fiber reinforcement on the abrasive wear resistance of polymeric composites. Cirino et al. [237, 238] investigated the sliding and abrasive wear behavior of polyetheretherketone (PEEK) with different continuous fiber types and reported that the wear rate decreases with increase in the fiber content. chand et al. [239] studied low stress abrasive wear behavior of short E-glass fiber reinforced polymer composites with and without fillers by using rubber wheel abrasion test apparatus. They reported that higher weight fraction of glass fibers (45%) in the composites improves the wear resistance as compared to the composite containing less glass fibers (40%). Bijwe et al. [240] tested polyamide6, polytetrafluoroethylene (PTFE) and their various composites in abrasive wear under dry and multi-pass conditions against silicon carbide (SiC) paper on pin-on-disc arrangement. They concluded that the polymers without fillers had better abrasive wear resistance than their composites. Liu et al. [241] investigated the abrasive wear behavior of ultrahigh molecular weight polyethylene (UHMWPE) polymer. They concluded that the applied load is the main parameter and the wear resistance improvement of filler reinforced UHMWPE was attributed to the combination of hard particles which prevent the formation of deep, wide and continuous furrows.

With regards to the usage of natural fiber as reinforcement for tribological application in polymeric composite, few works have been attempted. However, in recent years, some work has been done on natural fiber like jute [242], cotton [93, 243], oil palm [244], coir [245], kenaf [246], betel-nut [247], betel palm [248], wood flour [249] and bamboo powder [250] as reinforcement. In these works, the wear resistance of polymeric composites has been improved when natural fiber introduced as reinforcement.

5.4 TYPES OF WEAR

In most basic wear studies where the problems of wear have been a primary concern, the so-called dry friction has been investigated to avoid the influences of fluid lubricants. Dry friction is defined as friction under not intentionally lubricated conditions but it is well known that it is friction under lubrication by atmospheric gases, especially by oxygen [251].

A fundamental scheme to classify wear was first outlined by Burwell and Strang [252]. Later Burwell [253] modified the classification to include five distinct types of wear, namely (1) Abrasive (2) Adhesive (3) Erosive (4) Surface fatigue (5) Corrosive.

5.4.1 Abrasive wear

Abrasive wear can be defined as the wear that occurs when a hard surface slides against and cuts groove from a softer surface is shown in Figure 5.1. It can be account for most failures in practice. Hard particles or asperities that cut or groove one of the rubbing surfaces produce abrasive wear. This hard material may be originated from one of the two rubbing surfaces. In sliding mechanisms, abrasion can arise from the existing asperities on one surface (if it is harder than the other), from the generation of wear fragments which are repeatedly deformed and hence get work hardened for oxidized until they became harder than either or both of the sliding surfaces, or from the adventitious entry of hard particles, such as dirt from outside the system. Two body abrasive wear occurs when one surface (usually harder than the second) cuts material away from the second, although this mechanism very often changes to three body abrasion as the wear debris then acts as an abrasive between the two surfaces. Abrasives can act as in grinding where the abrasive is fixed relative to one surface or as in lapping where the abrasive tumbles producing a series of indentations as opposed to a scratch. According to the recent tribological survey, abrasive wear is responsible for the largest amount of material loss in industrial practice [227].

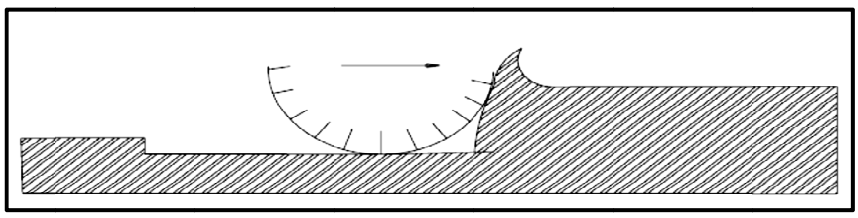

Figure 5.1 Schematic representations of the abrasion wear mechanism

5.4.2 Adhesive wear

Adhesive wear can be defined as the wear due to localized bonding between contacting solid surfaces leading to material transfer between the two surfaces or the loss from either surface. For adhesive wear to occur it is necessary for the surfaces to be in intimate contact with each other is shown in Figure 5.2. Surfaces, which are held apart by lubricating films, oxide films etc. reduce the tendency for adhesion to occur.

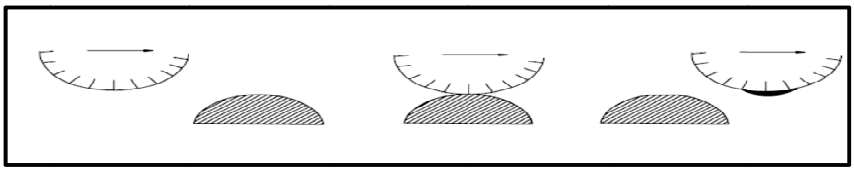

Figure 5.2 Schematic representations of the adhesive wear mechanism

5.4.3 Erosive wear

Erosive wear can be defined as the process of metal removal due to impingement of solid particles on surface is shown in Figure 5.3. Erosion is caused by a gas or a liquid, which may or may not carry, entrained solid particles, impinging on a surface. When the angle of impingement is small, the wear produced is closely analogous to abrasion. When the angle of impingement is normal to the surface, material is displaced by plastic flow or is dislodged by brittle failure.

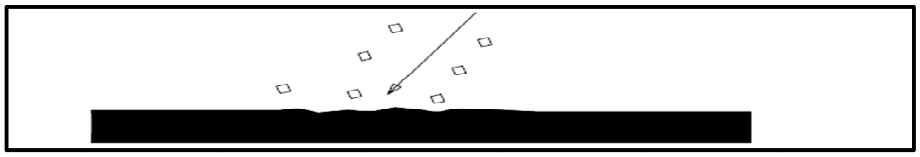

Figure 5.3 Schematic representations of the erosive wear mechanism

5.4.4 Surface fatigue wear

Wear of a solid surface is caused by fracture arising from material fatigue is shown in Figure 5.4. The term 'fatigue' is broadly applied to the failure phenomenon where a solid is subjected to cyclic loading involving tension and compression above a certain critical stress. Repeated loading causes the generation of micro cracks, usually below the surface, at the site of a pre-existing point of weakness. On subsequent loading and unloading, the micro crack propagates. Once the crack reaches the critical size, it changes its direction to emerge at the

surface, and thus flat sheet like particles is detached during wearing. The number of stress cycles required to cause such failure decreases as the corresponding magnitude of stress increases. Vibration is a common cause of fatigue wear.

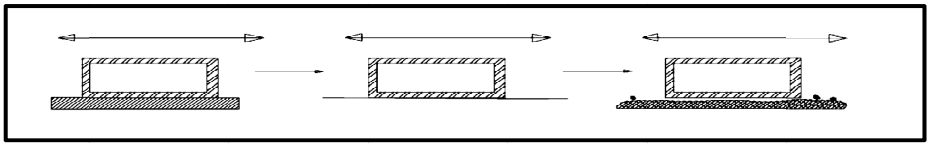

Figure 5.4 Schematic representations of the surface fatigue wear mechanism

5.4.5 Corrosive wear

Most metals are thermodynamically unstable in air and react with oxygen to form an oxide, which usually develop layer or scales on the surface of metal or alloys when their interfacial bonds are poor. Corrosion wear is the gradual eating away or deterioration of unprotected metal surfaces by the effects of the atmosphere, acids, gases, alkalis, etc. This type of wear creates pits and perforations and may eventually dissolve metal parts.

Wear process generally decides the choice of a particular tribological test. For the present case since we have design and fabricated layered composites the failure may occur depending on the application areas, either due to delamination or erosion. Hence in this work we have restricted our discussion to erosion tests only.

5.5 SYMPTOMS OF WEAR

A summary of the appearance and symptoms of different wear mechanism is indicated in Table-5.3 and the same is a systematic approach to diagnose the wear mechanisms.

Solid particle erosion manifests itself thinning of components, surface roughening, surface degradation, macroscopic scooping appearance and reduction in functional life of the structure. Hence, solid particle erosion has been considered as a serious problem as it is responsible for many failures in engineering applications. Hence several attempts to understand the basic mechanisms of the erosion were started in the last half of the 20^{th} century and have been continued to the present. In the year of 1995 an article on the past and the future of erosion was presented by Finnie [255]. In this article, the influencing parameters and dominating

mechanisms during solid particle erosion were reviewed on the erosion response of metals and ceramic materials. In the same year another article was published by Meng et al. [256] to provide information about the existing wear models and prediction equations.

Table 5.3 Symptoms and appearance of different types of wear [254]

Types of wear	**Symptoms**	**Appearance of the worn-out surface**
Abrasive	Presence of clean furrows cut out by abrasive particles.	Grooves
Adhesive	Metal transfer is the prime symptoms.	Seizure, catering rough and torn-out surfaces.
Erosion	Presence of abrasives in the fast moving fluid and short abrasion furrows.	Waves and troughs.
Corrosion	Presence of metal corrosion products.	Rough pits or depressions.
Fatigue	Presence of surface or subsurface cracks accompanied by pits and spalls.	Sharp and angular edges around pits.
Impacts	Surface fatigue, smallsub-micron particles or formation of spalls.	Fragmentation, peeling and pitting.
Delamination	Presence of subsurface cracks parallel to the surface with semi-dislodged or loose flakes.	Loose, long and thin sheet like particles
Fretting	Production of voluminous amount of loose debris.	Roughening, seizure and development of oxide ridges
Electric attack	Presence of micro craters or a track with evidence of smooth molten metal.	Smooth holes

According to Bitter [257], erosion is a material damage caused by the attack of particles entrained in a fluid system impacting the surface at high speed. Hutchings [258] defines it as an abrasive wear process in which the repeated impact of small particles entrained in a moving fluid against a surface result in the removal of material from the surface. Erosion due to the impact of solid particles can either be constructive (material removal desirable) or destructive (material

removal undesirable), and therefore, it can be desirable to either minimize or maximize erosion, depending on the application. The constructive applications include sand blasting, high-speed water-jet cutting, blast stripping of paint from aircraft and automobiles, blasting to remove the adhesive flash from bonded parts, erosive drilling of hard materials. Whereas the solid particle erosion is destructive in industrial applications such as erosion of machine parts, surface degradation of steam turbine blades, erosion of pipelines carrying slurries and particle erosion in fluidized bed combustion systems. In most erosion processes, target material removal typically occurs as the result of a large number of impacts of irregular angular particles, usually carried in pressurized fluid streams.

It is generally recognized that erosive wear is a characteristic of a system and is influenced by many parameters. Laboratory scale investigation if designed properly allows careful control of the tribo system whereby the effects of different variables on wear behavior of PMC scan be isolated and determined. The data generated through such investigation under controlled conditions may help in correct interpretation of the results.

5.6 SOLID PARTICLE EROSION OF POLYMER AND POLYMER NANO COMPOSITES

The subject of erosion wear of polymer composite has received substantial attention in the past decades. Interest in this area is commensurate with the increasing utilization of polymer based composites in aerospace, transportation and processes industries, where they can be subjected to multiple solid or liquid particle impact. Examples of such applications are pipe line carrying sand slurries in petroleum refining, helicopter rotor blades , pump impeller blades, high speed vehicles and aircraft operating in desert environments, radomes, surfing boats where the component encounter impact of lot of abrasives like dust, sand, splinters of materials, slurry of solid particle and consequently the material undergo erosive wear [259-261].

The most important factors influencing the erosion rate of the composite materials can be summarized under four categories; (i) The properties of the target materials (matrix material properties and morphology, reinforcement type, amount and orientation, interface properties between the matrices and reinforcements, etc.), (ii) Environment and testing conditions

(temperature, chemical interaction of erodent with the target), (iii) Operating parameters (angle of impingement, impinging velocity, particle flux–mass per unit time, etc.) and (iv) The properties of the erodent (size, shape, type, hardness, etc.) [262-264]. Thus it seems that the erosion resistance of the material can be evaluated after investigating the combination of above parameters. In general, erosive behavior of materials can be grouped into ductile and brittle when erosion rate is evaluated as a function of impact angle. The ductile behavior is characterized by maximum erosion at low impact angle in the range of 15°–30°. On the other hand, if maximum erosion occurs at 90°, then the behavior can be termed as brittle. Reinforced composites have also been some time found to exhibit an intermediate behavior known as semi-ductile with maximum erosion occurring at an angle in the range of 45°–60° [265].However, the above classification is not absolute as the erosion behavior of a material has a strong dependence on erosion conditions such as impact angle, impact velocity and erodent properties such as shape, hardness, size etc. In the literature, the erosion behavior of polymers and its composites has also been characterized by the value of the velocity exponent, '*n*' ($E \alpha v^n$)[261].

Many researchers have evaluated the resistance of various types of polymers like nylon, epoxy, polypropylene, bismileimide, etc. and their composites to solid particle erosion. Harsha et al. [265] has summarized the work done by some of the investigators on solid particle erosion of polymer composites. Roy et al. while working on erosive wear of polymer composite revealed that the composite materials present a rather poor erosion resistance as compared to metallic materials [266].

Bajpai [267] have developed a laminated composite using three plant fibers nettle, grew optiva and sisal) in to PLA polymer and wear and frictional characteristics of developing composite were investigated under dry contact condition at different operating parameters. The results indicate that incorporation of natural fiber mats into PLA matrix significantly improves the wear behavior of neat polymer.

Mishra and Acharya [268], Deo and Acharya [269] and Gupta et al. [270] have reported the tribo potential of sugarcane, lantana camaran and bamboo fiber reinforcement in thermoset polymers for enhancing erosive wear resistance. They have the opinion that fiber volume fraction has a significant influence on the erosion rate. Recently Mohanty et al. [271] and Ojha

et al. [272] studied the erosive wear behaviors of Date Palm Leaf fibers reinforced polyvinyl alcohol composites and wood apple shell fibers reinforced epoxy composites. It is reported that [273] if natural fiber is hybridized with a synthetic fiber in the same matrix the properties of natural fiber could be improved by taking the advantage of both the fibers. In this regards various attempt has been made by different researchers to combine varieties of natural fiber with synthetic fiber. Jose Almeida et al. [274] evaluated the enhancement in the properties of curaua polyester composites by incorporating chopped glass fibers with chopped caraus fibre. Patel et al. [275] reported that the erosive wear resistance of jute/epoxy composite can be improved significantly by hybridizing with synthetic fiber glass.

Barkoula and Karger-Kocsis [276] used glass fiber as reinforcement in thermoplastic polypropylene (PP) composite. They used modified sandblasting apparatus for erosion testing. The experimental parameters they used are impact angle (30, 60 and 90°), relative fibre-orientation (both parallel and perpendicular), fiber length (discontinuous, continuous) and fiber content (40–60 wt.%). They conclude that the fiber length did not affect the erosive wear behavior especially at high impact angles, due to inclusion of brittle Glass fiber led to higher erosive wear rates (ER) and as the glass fiber content increases erosion wear also increases.

As new developments are still under way to explore innovative fields for tribo-application of natural fiber base materials, in this chapter an attempt has been made to study the potential of using jute and glass fiber with different stacking sequences incorporating different fillers like fly ash and alumina in epoxy base for tribological applications. As an initial investigation in the present work the influence of impinging velocity, impingement angle and particulate loading on erosive wear has been carried out and results of these investigations are presented in the subsequent sections.

5.7 EXPERIMENT

5.7.1 Preparation for the test specimens

The preparation of the test specimens were carried out as per the procedure discussed in chapter-4, Art-4.2.2. Specimens of dimension 25 × 25 ×5 mm^3 were cut from the composite slabs. Adequate care has been taken to keep the thickness constant (5mm) for all the samples.

5.7.2 Micro-Hardness

Micro-hardness measurement is done using a Lecco Vickers Hardness (LV 700) tester. A diamond indenter, in the form of a right pyramid with a square base and an angle 136° between opposite faces, is forced into the material under a load F. The two diagonals X and Y of the indentation left on the surface of the material after removal of the load are measured and their arithmetic mean L is calculated. In the present study, the load (F) 10 N is considered and Vickers hardness number is calculated using the following equation:

$$H_v = \frac{0.1889\,F}{L^2} \text{ and } L = \frac{X + Y}{2} \tag{5.1}$$

Where 'F' is the applied load (N), 'L' is the diagonal of square impression (mm), 'X' is the horizontal length (mm) and 'Y' is the vertical length (mm)

5.7.3 Measurement of impact velocity of erodent particles: Double disc method

The most commonly used method for measuring impact velocity of the erodent particle is the double disc method. It consists of a pair of metal disc mounted on a common shaft and the stream of erodent particles is arranged to strike the upper disc, which has a thin radial slit cut in it. The exit particles from nozzle impinge on the upper disc with some of the particles passing through the slit, which eventually erode a mark on lower disc. Two erosion exposures are made, one with stationary disc and other with rotating disc at known rpm. These exposures give rise to erosion marks A and B on the lower disc (Figure5.5). Measurement of the angular displacement between these marks gives a measure of the flight time of the particles as they cross the space between the discs. The particle velocity can be found by using the following equation.

$$v = \frac{L}{t} = \frac{Lv360°}{\theta} \tag{5.2}$$

Where 'L' is separation of two discs, 't' is time in second, '$_v$' is rotation speed of disc per second and 'θ' is angular displacement between the marks. The above equation can also be expressed as

$$v = \frac{2\pi rvL}{S} \qquad (5.3)$$

Where 'r' is radius from the disc center and 'S' is linear separation of two marks. The details of impact velocity calibration at various pressures are given in Table 5.4.

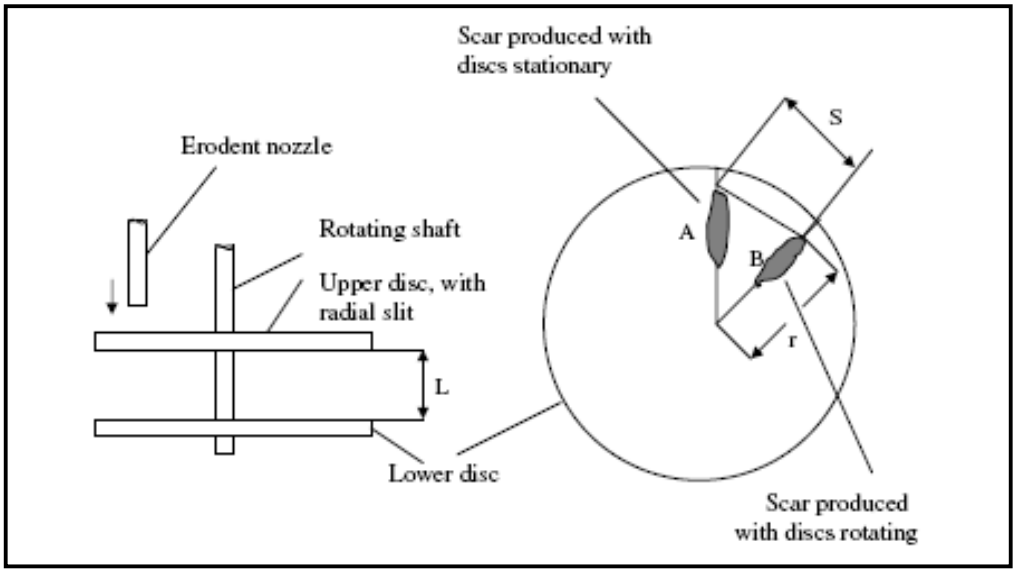

Figure 5.5 Schematic diagram of methodology used for velocity calibration

Table 5.4 Impact velocity calibration at various pressures

Pressure (bar)	Speed of rotating disc(rpm)	Angle θ (°)	Velocity(m/s)	Avg. impact velocity(m/s)
1 bar	2000	7.0	42.85	47.25
		6.5	46.15	
		6.0	50.00	
		6.0	50.00	
2 bar	2000	4.0	75.00	69.16
		4.5	66.67	
		4.0	75.00	
		5.0	60.00	
3 bar	2000	4.5	66.67	81.845
		4.0	75.00	
		3.5	85.71	
		3.0	100.00	

5.8 TEST APPARATUS & EXPERIMENT

The schematic Figure of the erosion test apparatus used for the present investigation designed as per ASTM-G76 standard is shown in Figure-5.6(a, b). The rig consists of an air compressor, a particle feeder, and an air particle mixing and accelerating chamber. The compressed dry air is mixed with the erodent particles, which are fed at a constant rate from a conveyor belt-type feeder in to the mixing chamber and then accelerated by passing the mixture through a tungsten carbide converging nozzle of 4 mm diameter. These accelerated particles impact the specimen, and the specimen could be held at various angles with respect to the impacting particles using an adjustable sample holder. The test apparatus has also been fitted with a rotating double disc to measure the velocity of the erodent particle. The impact velocities of the erodent particles has been evaluated experimentally using this rotating double disc method developed and as explained by Ives and Ruff [277].

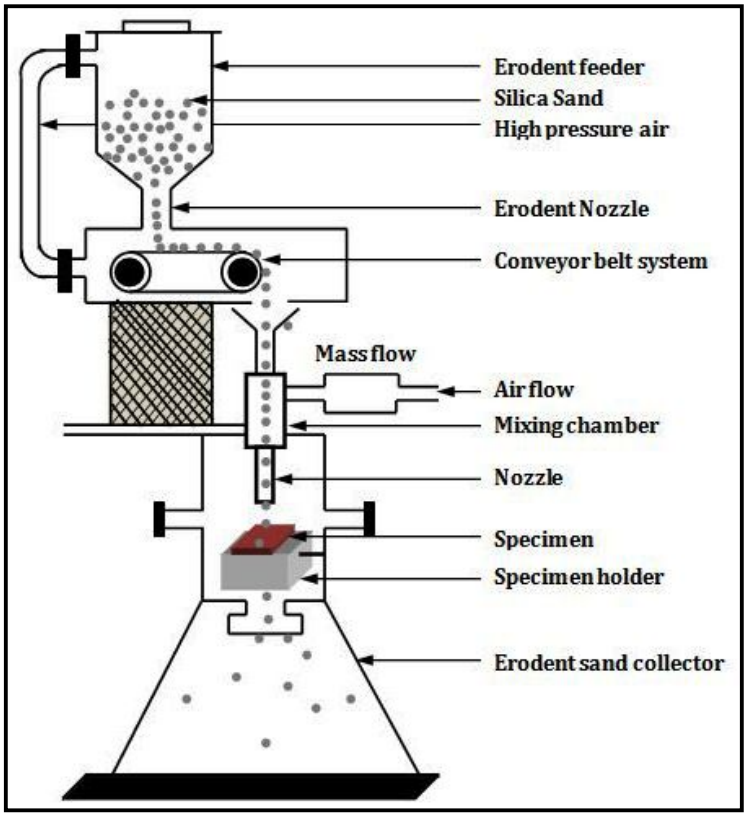

Figure 5.6 (a) Schematic diagram of erosion test rig

1 Sand hopper

2 Conveyor belt system for sand flow

3 Pressure transducer

4 Particle-air mixing chamber

5 Nozzle

6 X–Y and h axes assembly.

7 Sample holder

Figure5.6 (b) Photograph of the Solid Particle Erosion Test Set up

The conditions under which the erosion test has been carried out are given in Table 5.5. A standard test procedure is employed for each erosion test. Wear was measured by mass loss method. The samples were cleaned with a fine brush to remove any sand particles attached to the surface and then wiped with a fine brush to remove any sand particles attached to the surface and then wiped with a cotton plug dipped in acetone to avoid any entrapment of wear debris, prior and after each test then they were, dried and weighed to an accuracy of 1×10^{-3} gm using an electronic balance, prior and after each test.

The test samples after loading in the test rig were eroded for 10 min. at a given impingement angle and then weighed again to determine weight loss (Δw). The erosion rate 'E_r' is then calculated by using the following equation:

$$E_r = \frac{\Delta w}{w_e} \tag{5.4}$$

Where 'Δw' is the mass loss of test sample in gm and 'w_e'is the mass of eroding particles (i.e., testing time * particle feed rate). This procedure has been repeated until the erosion rate attains a constant steady-state value. In the present study the same procedure is repeated for 5 times.

The erosion efficiency (η) for the process was obtained by using the equation:

$$\eta = \frac{2E_r H}{\rho \times v^2} \tag{5.5}$$

where 'E_r' is erosion rate (kg/kg), 'H' is hardness of eroding material (Pas) and 'v' is velocity of impact (m/s), proposed by Sundararajan et al. [278]. Experimental results of the erosion test of jute/glass fiber reinforced epoxy composites for different stacking sequences with different impingement angle and velocities are tabulated and presented in Table 5.6-5.11.

5.9 RESULTS AND DISCUSSION

Figure5.7 to 5.9 (table 5.6 to 5.11) shows the variation of erosion rate of all the sequential layered composites along with pure jute, epoxy and glass composite as a function of impingement angle under different impact velocities (48m/s, 70m/s and 82m/s).It is observed that jute fiber/glass epoxy hybrid composite for all sequences shows peak erosion rate ($E_{r\,max}$) at 60° impact angle except jute and neat epoxy which shows ($E_{r\,max}$) at 90° impact angle. Minimum erosion rate (E_{rmin}) for all composite along with pure epoxy found at (30°) under all velocity of impact. Generally, it has been recognized that peak erosion exists at low impact angles(15°–30°) for ductile materials and at a high impact angle(90°) for brittle materials [279].However the maximum erosion occurring in the angular range 45°–60° indicates the semi-ductile behavior of the material [280]. From the experimental results it is clear that different layered composites respond to solid particle impact for the present case neither behaves in a purely ductile nor in a purely brittle manner. This behavior can be termed as semi-brittle in nature which may be attributed by the incorporation of jute and glass fibers within the epoxy body. The same type of behavior was also reported by Biswas et al. [281] while studying the erosive behavior of red mud filled Bamboo-epoxy composite. It is further noticed that irrespective of impact velocity and impact angle, the erosion rate is highest for neat epoxy and is lowest for jute fiber reinforced epoxy composite. It is also clear from the plot that jute fiber behavior which was showing purely ductile behavior to solid particle erosion changed to semi ductile nature due to incorporation of glass fiber. The erosion rate for different layered composite also found to be different and lies within neat epoxy and jute fiber composite.

The variation of steady-state erosion rate of all composite samples with impact velocity at different impact angles are shown in the form of a histogram in Figure5.10 to 5.13. It can be observed from these histograms that erosion rate of all composite samples increases with increase in the impact velocity. However, neat epoxy shows highest variation in the erosion rate with increase in the impact velocity at all impact angle. Also, it is clear from the plot that the best erosion resistance under all impact conditions is achieved for the composite made of jute fiber except at impact angle 90°.

Irrespective of impingement angle and impact velocity, there is a steady increase in erosion rate with different layered composite has also been observed. At higher velocities it is found that the erosion rate of composites is dominated by the hybrid composite. Similar type of observation was reported by Miyazaki et al. [282], while worked with glass and carbon fiber reinforced polyetheretherketon composites.

In the solid particle impact experiment the impact velocity of the erosive particles has a very strong effect on erosion rate. For any material, once the steady state condition have reached, the erosion rate *'E_r'* can be expressed as a simple power function of impact velocity (v) [283]:

$$E_r = kv^n \tag{5.6}$$

Where *k* is the constant of proportionality includes the effect of all the other variables. The value of '*n*' and '*k*' are found by least-square fitting of the data points in plots which represent the erosion rate dependence on impact velocity by using the power law. The value of *'n'*, the velocity exponent, is typically between 2 and 3, although much higher exponent is seen under some circumstances [284]. According to Pool et al. [285], for polymeric materials behaving in ductile manner, the velocity exponent *'n'* varies in the range 2-3 while polymer behaves in brittle when fashion exponent 'n' varies in the range 3-5.For the present investigation the least-squares fits to the data points were obtained by using the power law and the values of '*n*' and '*k*', are summarized in Table-5.13. The velocity exponent found for 30°, 45°, 60° and 90°impingement angles are in the range of 2.8-4.5, 2.22-4.7, 1.22-4.3 and 1.4-4.4 respectively. This velocity exponent at various impingement angles are in conformity with Harsha et al. [286].

It has been reported by Sundararajan et al. [287] that the erosion efficiency (η), can be used to characterize the nature and mechanism of erosion. They also showed that the ductile material possesses very low erosion efficiency i.e. is very $\eta<<<100\%$, whereas the brittle material exhibits an erosion efficiency even greater than 100%. The values of erosion efficiencies of composites under this study are calculated using equation-5.6 and are listed in Table-5.12 along with their hardness values and operating conditions. Since the steady-state erosion rate (R) of epoxy and its composites increases with increase in impact velocity 'v', which is proportional to 'v^2', hence, erosion efficiency is expected to increase with increasing 'v'.

The erosion efficiencies of jute E-glass epoxy and its composites vary from 1.40 to 6.52% for different impact velocities studied at angle 60° and it vary from 1.28 to 6.52% for 45^0 impact angles. The dependence of erosion rates of the jute E-glass epoxy and its composites with impact velocity is very strong at different impingement angles, as indicated by the velocity exponents (n) were in the range of 2.4–3.0. Thus, by observing erosion efficiency and velocity exponent (n) of GFRP and its composites erosion behavior can be broadly classified as semi-ductile. This also confirms to the result plotted in Fig 5.7 to 5.9

5.10 SEM ANALYSIS

SEM analysis has been carried out for the samples where optimum results have been obtained to know the material behaviour with the experimental parameters.

Figure 5.14(a) shows the micrographs of the jute sample eroded at 60° impingement angle. It is clearly visible the formation of crater and the damage caused to the composite due to this crater. It shows extensive damage of fibers (jute) but still fibers are not pullout from the matrix. No cracks are observed on the matrix.

Figure5.14 (b) shows the micro graph of the glass fiber composites. It is seen that fibres and the top layer matrix were chipped off from the base matrix due to continuous impingement of hard silica particles, which leads to the formation of grooves. This might have happened because particle impingement on the surface produces a rise in temperature which in turn leads to softening of the matrix material. On impact, the erodent particle kinetic energy is transferred to the composite body that leads to formation of grooves and subsequent material removal. At higher magnification it is clearly observed the poor bonding of glass and epoxy.Figure5.14(c)

shows the hybridize effect of natural fibre jute with the synthetic fibre glass. The removal of the jute fibre by particle impact on the surface is clearly visible. After removal of the outer layer the particles enters to the glass fibre layer. It is found that breaking of glass fibres took place but chipping of the fibres from the matrix is prevented by increasing no of layers of glass fiber.

5.11 CONCLUSION

Experiments were carried out to study the effect of jute and glass fiber stacking sequence on the erosion rate of jute E-glass epoxy and its composites at various impingement angles, impact velocities for different fiber volume fraction with silica sand as erodent. Based on the results the following conclusions are drawn.

1. The erosive wear of samples (JJJJ) with all jute layers gives the lowest value.
2. The influence of impingement angle on erosive wear of all composites except jute and neat epoxy under consideration exhibit semi ductile behavior with maximum wear rate at 60° impingement angle. Maximum erosion at 90° impingement angle for jute and neat epoxy indicates pure brittle nature of the composite.
3. Layering sequence and velocity of impact has a significant influence on the erosion rate of the composite.
4. The composites, erosion rate (E_r) displays power law behavior with particle velocity (V) as $E_r \alpha V^n$. The velocity exponents are in the range of 2.4-3.0 for various materials studied for different impingement angles (30°-90°) and impact velocities (48-72m/s).
5. It is clear from this study that erosive strength of natural fiber (jute) is higher in comparison to hybrid composite.
6. The morphologies of the eroded surfaces for the hybrid composite are observed by SEM. the results suggest that overall erosion damage of the composite is mainly due to breaking of fiber. Chipping out of fiber prevented due to good bonding between the fiber and the matrix.
7. Possible use of these composites in components such as pipes carrying coal dust, desert structure, low cost housing, boats/sporting equipment, partition boards, doors and window panels is recommended.

Table 5.5 Experiment conditions

Erodent	Silica sand
Erodent size (μm)	200 ± 50
Impingement angle (α^0)	30, 45, 60, 90
Impact velocity (m/s)	48, 70, 82
Erodent feed rate (g/min)	2+0.25
Test temperature	Room temperature
Nozzle to sample distance (mm)	10
Nozzle diameter	4
Time	10 min.

Table 5.6 Weight loss and erosion rate of epoxy composites with respect to impingement angle due to erosion for a period of 600 seconds

Velocity (m/s)	**Impact angle (°)**	**Epoxy**	
		Weight loss (g)	**Erosion rate×10^{-4} (g/g)**
48	30	0.0030	1.65
	45	0.0045	2.24
	60	0.0050	2.50
	90	0.0056	2.80
70	30	0.0048	2.40
	45	0.0059	2.94
	60	0.0064	3.20
	90	0.0072	3.60
82	30	0.0055	2.77
	45	0.0066	3.29
	60	0.0071	3.55
	90	0.0080	4.00

Table 5.7 Weight loss and erosion rate of GGGG composites with respect to impingement angle due to erosion for a period of 600 seconds

Velocity (m/s)	Impact angle (°)	GGGG	
		Weight loss (g)	Erosion rate×10^{-4}(g/g)
48	30	0.0024	1.20
	45	0.0030	1.50
	60	0.0040	2.00
	90	0.0030	1.50
70	30	0.0028	1.40
	45	0.0034	1.70
	60	0.0042	2.12
	90	0.0034	1.70
82	30	0.0032	1.60
	45	0.0035	1.80
	60	0.0044	2.22
	90	0.0037	1.84

Table 5.8 Weight loss and erosion rate of JJJJ composites with respect to impingement angle due to erosion for a period of 600 seconds

Velocity (m/s)	Impact angle (°)	JJJJ	
		Weight loss (g)	Erosion rate×10^{-4} (g/g)
48	30	0.0017	0.82
	45	0.0019	0.95
	60	0.0020	1.03
	90	0.0025	1.25
70	30	0.0020	1.00
	45	0.0022	1.10
	60	0.0024	1.20
	90	0.0026	1.32
82	30	0.0024	1.20
	45	0.0025	1.24
	60	0.0026	1.33
	90	0.0028	1.42

Table 5.9 Weight loss and erosion rate of GJJG composites with respect to impingement angle due to erosion for a period of 600 seconds

Velocity (m/s)	Impact angle (°)	GJJG	
		Weight loss (g)	Erosion rate $\times 10^{-4}$(g/g)
48	30	0.0024	1.22
	45	0.0026	1.29
	60	0.0040	2.02
	90	0.0026	1.30
70	30	0.0028	1.42
	45	0.0029	1.49
	60	0.0044	2.22
	90	0.0030	1.50
82	30	0.0034	1.72
	45	0.0034	1.68
	60	0.0047	2.34
	90	0.0034	1.70

Table 5.10 Weight loss and erosion rate of JGGJ composites with respect to impingement angle due to erosion for a period of 600 seconds

Velocity (m/s)	Impact angle (°)	JGGJ	
		Weight loss (g)	Erosion rate $\times 10^{-4}$(g/g)
48	30	0.0020	1.00
	45	0.0021	1.05
	60	0.0030	1.50
	90	0.0020	1.02
70	30	0.0022	1.10
	45	0.0024	1.21
	60	0.0032	1.60
	90	0.0023	1.14
82	30	0.0026	1.28
	45	0.0027	1.35
	60	0.0034	1.70
	90	0.0025	1.26

Table 5.11 Weight loss and erosion rate of GJGJ composites with respect to impingement angle due to erosion for a period of 600 seconds

Velocity (m/s)	Impact angle (°)	GJGJ	
		Weight loss (g)	Erosion rate×10^{-4}(g/g)
48	30	0.0022	1.10
	45	0.0024	1.22
	60	0.0034	1.70
	90	0.0039	1.09
70	30	0.0026	1.30
	45	0.0026	1.33
	60	0.0036	1.80
	90	0.0042	2.11
82	30	0.0030	1.50
	45	0.0031	1.51
	60	0.0038	1.90
	90	0.0045	2.24

Table-5.12 Erosion efficiency of Hybrid composite

Impact Velocity 'v' (m/s)	Impact angle (°)	Erosion efficiency (η)					
		Neat Epoxy	GGGG	JJJJ	GJJG	JGGJ	GJGJ
		Hv=193.0 Mpa	Hv=227.5 MPa	Hv=207.9 MPa	Hv=221.6 MPa	Hv=226.5 MPa	Hv=209.8 MPa
48	30	2.32	1.73	1.24	1.89	1.58	1.61
	45	3.15	2.16	1.44	2	1.66	1.79
	60	3.51	2.88	1.55	3.12	2.37	2.49
	90	3.93	2.16	1.89	2.01	1.61	2.85
70	30	1.58	0.95	0.71	1.03	0.82	0.89
	45	1.94	1.15	0.78	1.08	0.90	0.92
	60	2.11	1.44	0.85	1.61	1.19	1.24
	90	2.38	1.15	0.94	1.09	0.84	1.45
82	30	1.34	0.79	0.62	0.91	0.69	0.75
	45	1.58	0.89	0.64	0.89	0.73	0.75
	60	1.71	1.10	0.69	1.24	0.92	0.95
	90	1.92	0.91	0.73	0.90	0.69	1.12

Table 5.13 Parameters characterizing the velocity dependence of erosion rate of Epoxy and its composites

Samples	**Impingement angle (Degree)**	**K**	**N**	**R^2**
GGGG	30	0.1627	3.425	0.9641
	45	0.4037	2.226	0.9996
	60	0.965	1.250	0.9731
	90	0.3535	2.483	0.9895
JJJJ	30	0.0588	4.516	0.9576
	45	0.1484	3.185	0.9701
	60	0.1699	3.094	0.9857
	90	0.5277	1.474	0.9036
GJJG	30	0.1185	3.986	0.9133
	45	0.2051	3.153	0.9682
	60	0.7086	1.801	0.9952
	90	0.2019	3.192	0.9631
JGGJ	30	0.1916	2.821	0.8741
	45	0.1811	3.015	0.9753
	60	0.6315	1.482	0.9549
	90	0.2359	2.509	0.9599
GJGJ	30	0.1274	3.695	0.9653
	45	0.2907	2.449	0.8879
	60	0.7884	1.317	0.9541
	90	0.9027	1.681	0.9329

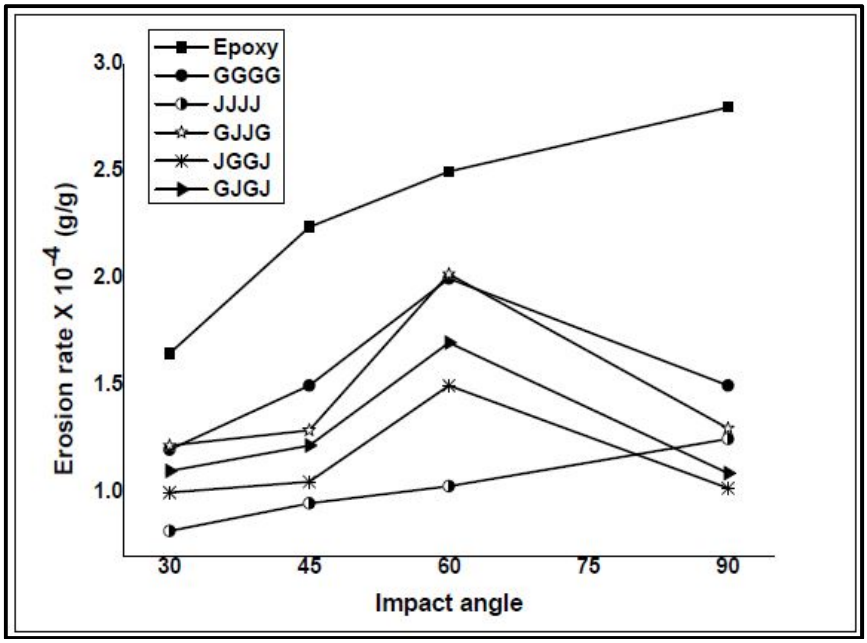

Figure 5.7 Variation of erosion rate with different impact angle at velocity 48 m/s

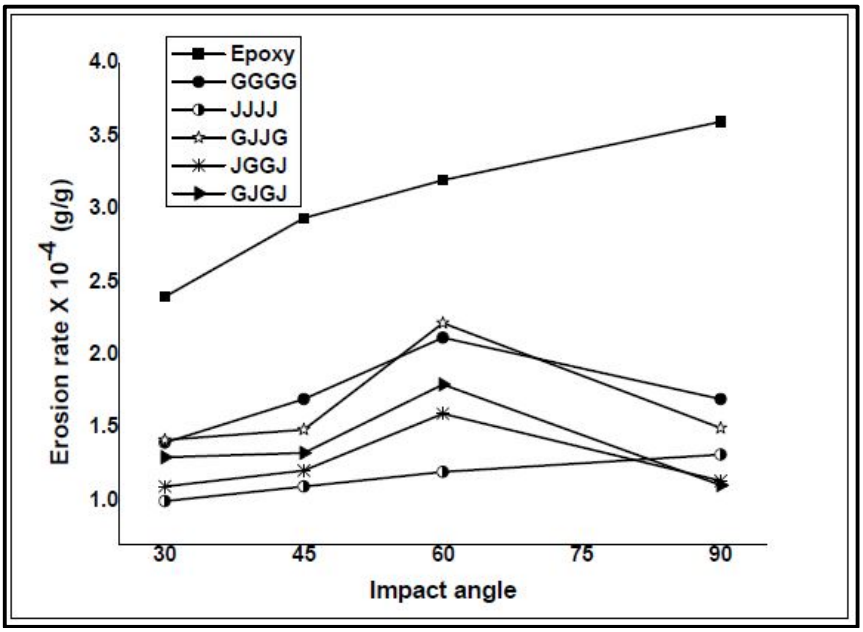

Figure 5.8 Variation of erosion rate with different impact angle at velocity 70 m/s

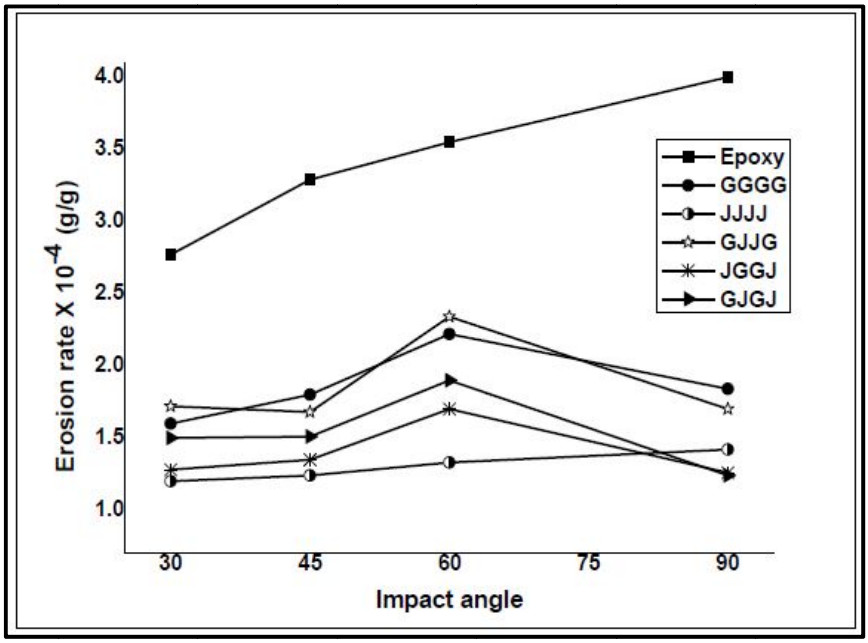

Figure 5.9 Variation of erosion rate with different impact angle at velocity 82 m/s

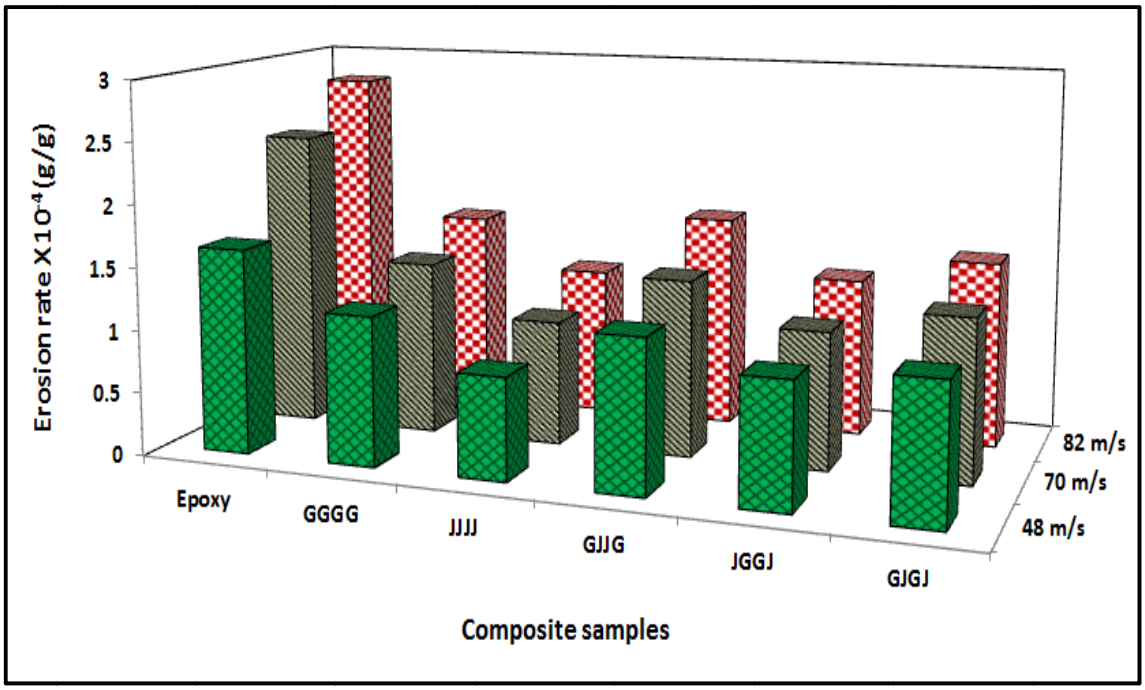

Figure 5.10 Histogram showing the steady state erosive wear rates of all the composites at different impact velocities (48, 70 and 82 m/s) for 30° impact angle

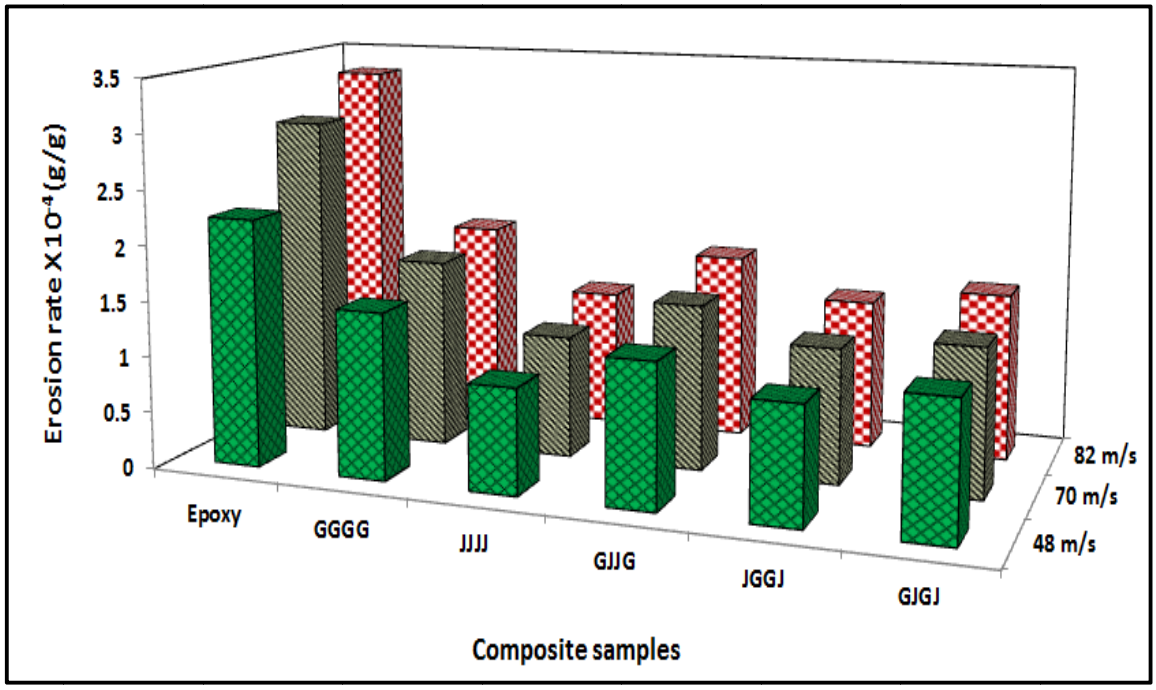

Figure 5.11 Histogram showing the steady state erosive wear rates of all the composites at different impact velocities (48, 70 and 82 m/s) for 45° impact angle

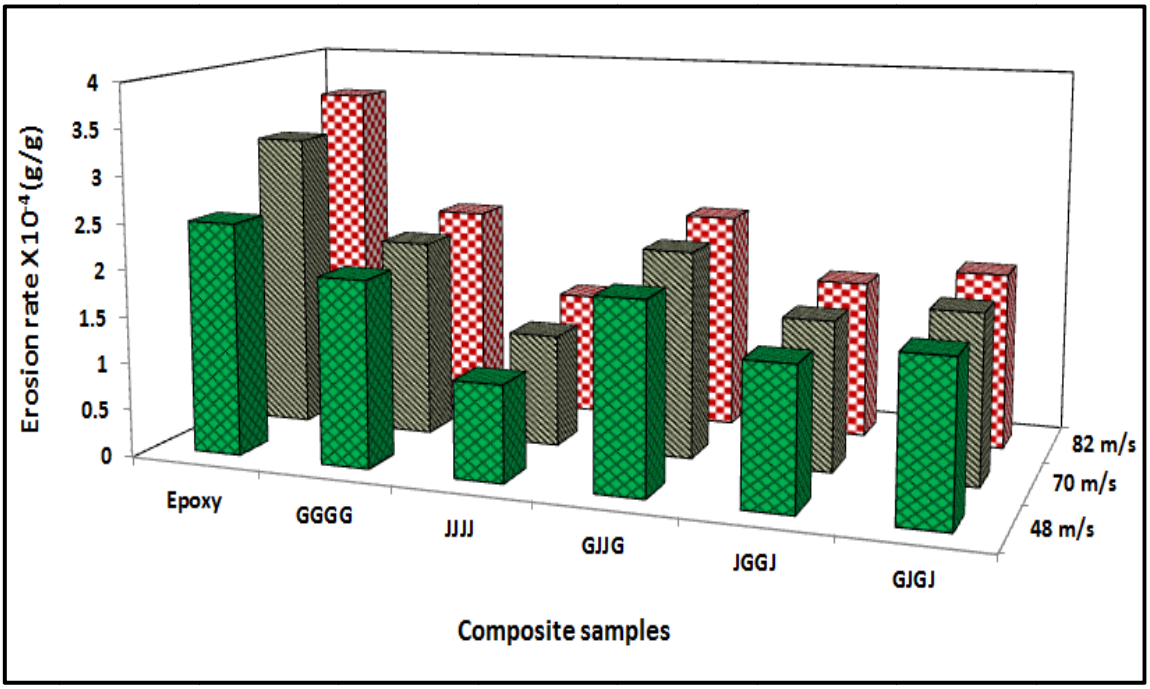

Figure 5.12 Histogram showing the steady state erosive wear rates of all the composites at different impact velocities (48, 70 and 82 m/s) for 60° impact angle

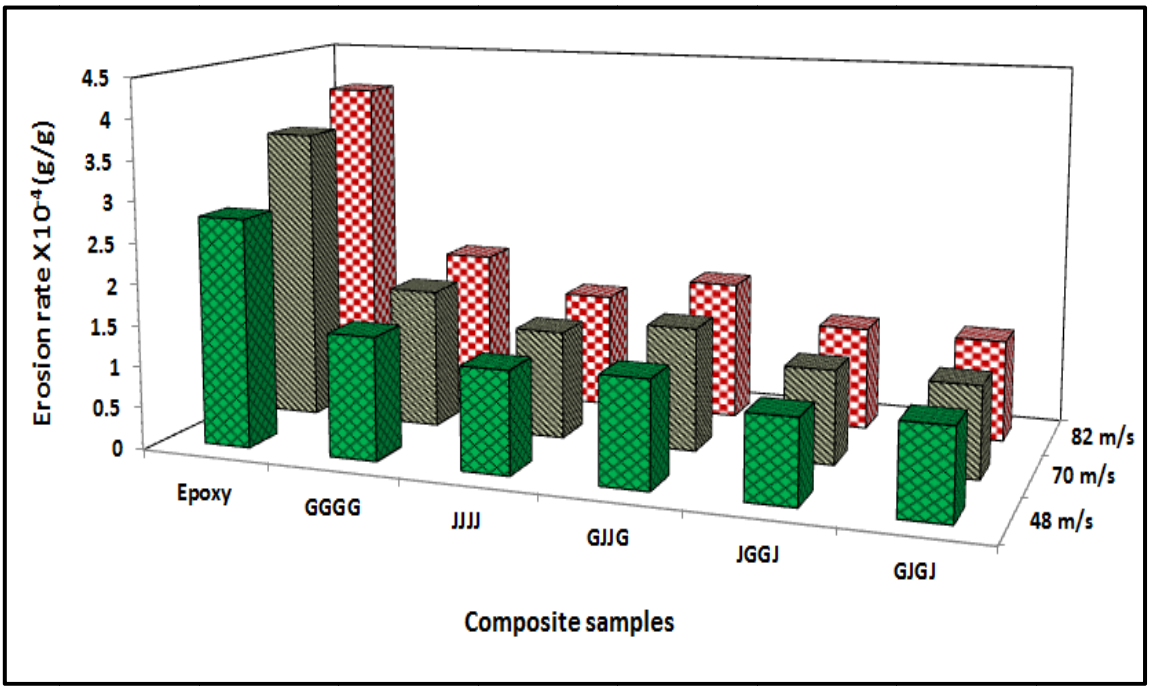

Figure 5.13 Histogram showing the steady state erosive wear rates of all the composites at different impact velocities (48, 70 and 82 m/s) for 90° impact angle

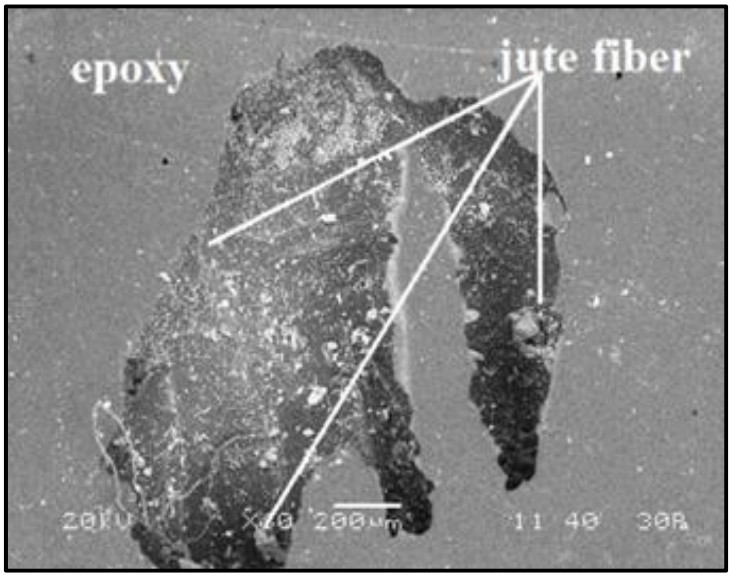

Figure 5.14 (a) Jute fiber composites at 60° impingement angle

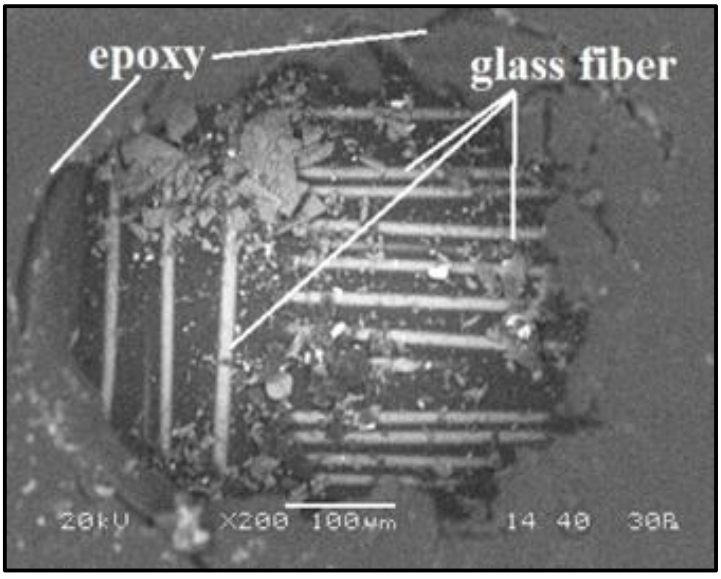

Figure 5.14(b) Glass fiber composite at 60° impingement angle

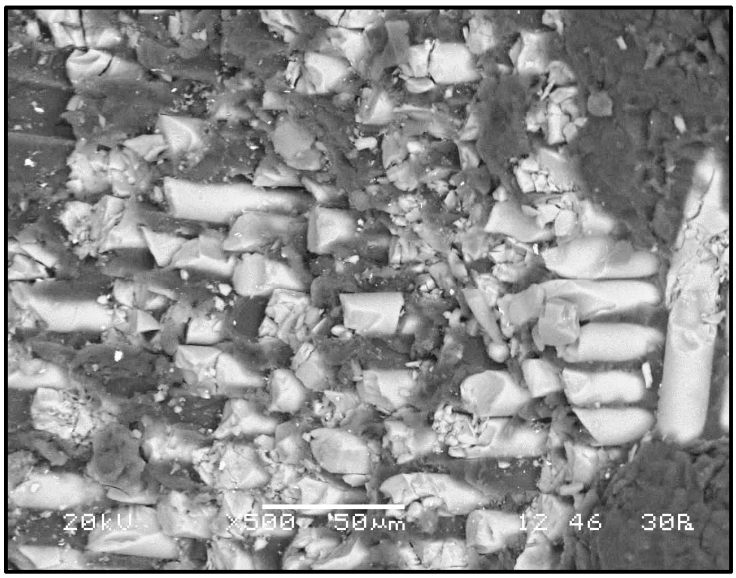

Figure 5.14(c) Hybrid fiber composite at 60° impingement angle

Chapter 6

Erosion Characterization of Jute-Glass Fibre Hybrid Composite with Micro and Nano Filler

6.1 INTRODUCTION

In the fibre reinforced plastics composites fillers may be added to the polymeric matrix for one are more of the following reasons (1) reduction of cost, (2) increase of modulus, (3) control of viscosity and (4) production of a smoother surface.

Nano-particles are presently considered as high-potential filler materials for the improvement of mechanical and physical properties of polymer composites [288]. As the nano scale fillers are usually free of defects, hence, their applications in the field of polymer composite area setup, new trends of prospect to overwhelm the restrictions of traditional/conventional micrometer scale. High matrix-filler interfacial area results because of uniform and homogeneous dispersion of nano particles are responsible for changing relaxation behavior, as well in ensuing the mechanical, molecular mobility, and thermal properties [289,290]. Generally, nano sized filler present in the minor zone whereas only few of the micro particles participate in the plastic zone deformation. This provides a way for the nano fillers to improve fracture and mechanical properties of the matrix having brittle property. Nano fillers, which possess greater aspect ratio (ratio of largest to smallest dimension) are of considerable interest, and, thus, show better reinforcement for the nanocomposites production [291]. Nanofillers are generally incorporated on a weight basis for the nanocomposite development [292]. The composite properties are greatly influenced by the specific surface area of nano fillers, which shows uninterrupted influence. Nano fillers could be belongs to organic and inorganic in nature. The particles like silica (SiO_2), titanium dioxide (TiO_2), calcium carbonate ($CaCO_3$), or polyhedral oligomeric silsesquioxane (POSS), *etc.*, are inorganic filler. However, the filler, such as coir nanofiller, carbon black and cellulosic nano filler and many others are derived organically and naturally represent organic nano Hybrid composite developed by various researchers, by combining natural fibers/natural fiber and natural fibers/synthetic fibers with epoxy, polyester, phenolic, poly vinyl ester, poly urethane resins, etc. are well established [293,294]. The environmental awareness attracted researchers to develop new composites with addition of more than one reinforcement from natural resources, such as natural fiber/natural fiber or natural fiber/nano filler from organic sources as an alternative to synthetic fibers [295].Hybridization involving the combination of nano filler and natural fiber in the matrix

results reduction of water absorption properties and increased in mechanical properties [296]. Several research works depicts all these facts. The mechanical and thermal properties of rice husk flour/high density polyethylene composites get improved by addition of small amount of nanoclay [297]. Mechanical and tribological performance of the date palm fiber/epoxy composites get enhanced by addition of graphite filler but high content of the graphite deteriorates the mechanical properties [298,290]. Natural fiber/nano filler-based hybrid composites can be utilized in building and construction sector, transportation (automobiles, railway coaches, aerospace) packaging, consumer products, etc., and also could be possible to produce acoustic insulator and extremely thermally stable materials.

In this work, experiments were carried out to study the effect of micro and nano (fly ash as well as alumina) filler, impingement angle and particle velocity on the solid particle erosion behavior of Jute/E-glass fibre reinforced hybrid composites,

6.2 MATERIALS AND METHOD

6.2.1 Raw Materials Used

Raw materials used in this experimental work are listed below:

1. Jute fiber
2. E glass fiber
3. Micro and nano filler (fly ash and alumina)
4. Epoxy resin and Hardener

6.2.1.1 Jute fiber

The details of the jute fiber, its chemical constituents used for the present investigation are explained in chapter 1 art 1.6.1.

6.2.1.2 E glass fiber

The details of the jute fiber, its chemical constituents used for the present investigation are explained in chapter 4 art 4.2.1.2.

6.2.1.3 Fly ash and alumina filler (both micro and nano)

The details of the fillers, their chemical constituents used for the present investigation are explained in chapter 3 art 3.4.1 and 3.4.2.

6.2.1.4 Epoxy resin and Hardener

The details of the epoxy resin and hardener used for the erosion test are same as explained in chapter4 art 4.2.1.3

6.3METHODS

6.3.1 Preparation of Composites:

Preparation of the hybrid composite with the filler addition is same as explained in chapter4 art.4.22. The preparation of the test samples are done as per the procedure explained in chapter 5art.5.7.1 Specimens of dimensions 30×30×5 mm^3 were used for the erosion test.

6.3.2 Test apparatus & Experiment

The erosion test apparatus for the present case is one which is used earlier. The details of the test apparatus, procedure and the conditions under which the test has been carried out is same for this investigation also and has been discussed in details in chapter-5, art-5.8.

The experimental results of the erosion test for micro and nano fillers addition with Jute/glass fiber reinforced epoxy composite for different stacking sequences with different impingement angle of velocities are tabulated in Table 6.1 to 6.48.

6.4 RESULTS AND DISCUSSION

Based on the tabulated results various graphs were plotted and presented in Figure-6.1 to 6.16 for micro and nano fillers addition with Jute/glass fiber reinforced epoxy composite.

Figure 6.1-6.12 (table 6.1 to 6.48) shows the erosion rate of the hybrid composite filled with 5, 10 and15 wt. % of micro fillers and 2, 4 and 6wt% of nano fillers of fly ash and alumina. The data presented in the Figures are for the three impact velocities 48, 70 and 82m/s. it is clearly observed from these plots that addition of 5wt.% of filler did not changes the behavior of the composite from semi brittle nature because maximum erosion occurs at 60º. Further addition of filler with 10 and 15 wt.% the behavior of the composites changes from semi brittle to brittle as maximum erosion occurs at 90º[280].

Figure 6.7 to 6.12 (table 6.13 to 6.24 and 6.37 to 6.48) shows the erosion rate of the composite with nano fillers both for fly ash and alumina. It is found from these plots that the behaviour of the composites with nano fillers is similar to micro fillers. However the erosion resistance achieved for nano filler is 20-30% higher compared to micro filler addition. This might have happened because the fly ash and alumina nano particles which were having higher surface area and lower particle sizes filled the gaps which are there in the jute fiber and creates a mechanical doping there by the jute fiber behaves like continuous fibers, creates a good interfacial adhesion between fibers and matrix and sustains micro damage caused by impacting particles. Dasari A et. al. reported similar type of observation in their work wear/scratch damage in polymer nanocomposites [299].

For comparing the steady state erosion rate of the jute fibre composite, hybrid composites with sequences GJJG and GJGJ filled with 10 wt.% of micro filler and 4 wt.% of nano filler (both fly ash and alumina) were taken into consideration.

The variation of the steady state erosion rate of the hybrid composite with 10 wt.% of fly ash and alumina micro filler and 4 wt.% of nano filler with different impact angle at a velocity of 48m/s is shown in the form of histogram in Figure 6.13 to 6.16. It is clearly observed that the peak erosion is observed at 90º impact angle in all the hybrid composites with filler addition. It is also observed that JJJJ layered composite with and without the filler addition shows the best wear resistance when compared to the hybrid composite with and without filler addition. This peculiar behavior of the jute fiber is due to the absorption and bonding behavior of the jute outer surface structure which indeed leads to great wetting and mixing ability of the jute with the epoxy when the epoxy got reacted with the hardener. This type of behavior is due to the presence of hydroxyl groups in jute and epoxy. A great amount of hydroxyl groups is present on the outer surface of the jute layer as discussed by Macmillan & Gupta [300] and Kolar and Svitilova [301] present in the epoxy this might be responsible for this type of behavior for the developed composites in the present investigation.

Figure 6.17 (a, b) shows the\microscopic image of glass and jute fiber obtained from fracture zone of tensile tested specimen to ascertain the bonding of epoxy with jute and glass fiber. These Figures clearly show the traces of epoxy in the jute fiber whereas no traces of epoxy

are found with the glass fiber after the test. This might be the cause of higher resistance to impact of jute fiber composites with micro and nano fillers.

The best mechanical properties are observed for the hybrid composite (GJGJ in flexural and GJJG in tensile) are confirmed by the studies conducted in the 4th chapter whereas the better tribological properties are observed for the natural fiber composites (JJJJ).

As discussed earlier the erosion efficiency (η) plays an important role to characterize the nature and mechanism of erosion. Here also for fly ash and alumina filled composite the erosion efficiency has been calculated as per equation 5.5and are listed in Table-6.49-6.60 along with their hardness values and operating conditions. The erosion efficiency of fly ash and alumina filled composite varies from 0.16% to 3.42% for different impact velocities studied. Similar observations are also reported by Srivastavaet al. [117] while they worked with glass fibre reinforced fly-ash filled epoxy composite. Basing on their work, they have identified the brittle and ductile response of various materials considering the erosion mechanism. They have the opinion that ideal micro ploughing involving just the displacement of material from the crater without any fracture (and hence no erosion) will have zero erosion efficiency. Alternately, in the case of ideal micro cutting, efficiency will be 100%. And if erosion occurs by the formation of a lip and its subsequent fracture, then erosion efficiency will be in the range 0–100%. In contrast, as happens with brittle material, if the erosion takes place by sapling and removal of large chunks of material by interlinking lateral or radial cracks, then the erosion efficiency is expected to be even greater than 100%. Thus it can be concluded that erosion efficiency is not exclusively a material property; but also depends on other operational variables such as impact velocity and impingement angle. This lower erosion efficiency of fly ash and alumina filled epoxy composite indicates a better erosion resistance in comparison to hybrid composite.

6.4.1 Surface morphology

Figure 6.18 (a-d) presents the SEM of the jute-glass-epoxy hybrid composite with alumina filler addition under the velocity of 48 m/sec for time duration of 10 min with a 2 gram flow rate at an impact angle 90º. Figure6.18 (a and b) SEM of jute alumina nano filler epoxy composites. The alumina filler increases the wear resistance of material to reduce the erosion

rate the formation of cracks due to sand impact supports the statement. At higher magnification from micrograph reveal that solid sand particles impact on the fibres and causes the fibres to break owing to the formation of cracks perpendicular to their length but the fibre chip out is resisted by the nano fillers.

Figure6.18(c and d) shows the SEM of hybrid composites with nano alumina filler epoxy composites. Fibre breakage and detaching of the fibre is observed at the places of glass fibre even after addition of the nano fillers.Form the micro graph it is clearly observed that due to filler addition the material removal is less and due to the jute hybridization the bonding between the fiber and matrix is also increased. When the damage enters the glass fiber layers it breaks the fibers but chipping up of fibers (Figure 6.18(c)) from the matrix is not visible. At higher magnification (Figure 6.18(d)) it is it is found that the groove formation is less because of higher surface area of nano particle. The hardness of the composite also plays an important role to increase the erosion resistance.

6.5Conclusions

1. Successful fabrication of new class of epoxy based hybrid composite with micro and nano fillers have been achieved.
2. The present investigation revealed that the erosion resistance of the hybrid composites increases with the addition of micro and nano filler.
3. The semi brittle behavior of the composite remains same even after addition of 5 wt.% micro filler. However the behavior changes from semi brittle to brittle with addition of 10 and 15 wt. % of micro filler.
4. The behavior of the composite remains same with addition of nano filler also. However the erosion resistance increases to about 20-30% higher in comparison to micro filler addition.
5. The fracture surface study indicates the removal of glass fiber with breakage even after addition of nano fillers for hybrid composite (GJJG). However hybridization with jute fiber and the nano filler addition has less chipping out of the fiber from matrix when compared to pure glass and hybrid composites.

Table 6.1 Weight loss and erosion rate of 5% MFA (GJJG) composites with respect to impact angle due to erosion for a period of 600 seconds

Velocity (m/s)	Impact angle (°)	5% MFA (GJJG)	
		Weight loss (g)	Erosion rate $\times 10^{-4}$ (g/g)
48	30	0.0020	1.01
	45	0.0024	1.21
	60	0.0038	1.88
	90	0.0024	1.20
70	30	0.0026	1.31
	45	0.0028	1.41
	60	0.0039	1.98
	90	0.0028	1.40
82	30	0.0029	1.49
	45	0.0032	1.59
	60	0.0040	2.20
	90	0.0036	1.80

Table 6.2 Weight loss and erosion rate of 5% MFA (JGGJ) composites with respect to impact angle due to erosion for a period of 600 seconds

Velocity (m/s)	Impact angle (°)	5% MFA (JGGJ)	
		Weight loss (g)	Erosion rate $\times 10^{-4}$ (g/g)
48	30	0.0018	0.90
	45	0.0019	0.99
	60	0.0025	1.25
	90	0.0030	1.50
70	30	0.0024	1.20
	45	0.0022	1.12
	60	0.0027	1.34
	90	0.0033	1.65
82	30	0.0028	1.40
	45	0.0025	1.23
	60	0.0030	1.50
	90	0.0037	1.85

Table 6.3 Weight loss and erosion rate of 5% MFA (JJJJ) composites with respect to impact angle due to erosion for a period of 600 seconds

Velocity (m/s)	Impact angle (°)	5% MFA (JJJJ)	
		Weight loss (g)	Erosion rate $\times 10^{-4}$(g/g)
48	30	0.0014	0.68
	45	0.0018	0.89
	60	0.0018	0.91
	90	0.0022	1.10
70	30	0.0016	0.80
	45	0.0020	1.00
	60	0.0019	0.98
	90	0.0024	1.20
82	30	0.0023	1.13
	45	0.0022	1.12
	60	0.0024	1.20
	90	0.0028	1.40

Table 6.4 Weight loss and erosion rate of 5% MFA (GJGJ) composites with respect to impact angle due to erosion for a period of 600 seconds

Velocity (m/s)	Impact angle (°)	5% MFA (GJGJ)	
		Weight loss (g)	Erosion rate $\times 10^{-4}$(g/g)
48	30	0.0020	1.02
	45	0.0020	1.00
	60	0.0030	1.50
	90	0.0030	1.50
70	30	0.0024	1.21
	45	0.0022	1.10
	60	0.0032	1.60
	90	0.0032	1.60
82	30	0.0027	1.38
	45	0.0028	1.40
	60	0.0034	1.70
	90	0.0038	1.90

Table 6.5 Weight loss and erosion rate of 10% MFA (GJJG) composites with respect to impact angle due to erosion for a period of 600 seconds

Velocity (m/s)	Impact angle (°)	10% MFA (GJJG)	
		Weight loss (g)	Erosion rate $\times 10^{-4}$ (g/g)
48	30	0.0018	0.90
	45	0.002	1.13
	60	0.0034	1.68
	90	0.0033	1.65
70	30	0.0024	1.20
	45	0.0027	1.34
	60	0.0038	1.88
	90	0.0037	1.85
82	30	0.0028	1.40
	45	0.0029	1.44
	60	0.0038	1.93
	90	0.0039	1.95

Table 6.6 Weight loss and erosion rate of 10% MFA (JGGJ) composites with respect to impact angle due to erosion for a period of 600 seconds

Velocity (m/s)	Impact angle (°)	10% MFA (JGGJ)	
		Weight loss (g)	Erosion rate $\times 10^{-4}$ (g/g)
48	30	0.0017	0.85
	45	0.0018	0.90
	60	0.0024	1.20
	90	0.0038	1.90
70	30	0.0020	1.00
	45	0.0022	1.10
	60	0.0030	1.50
	90	0.0042	2.10
82	30	0.0023	1.15
	45	0.0028	1.40
	60	0.0029	1.59
	90	0.0046	2.30

Table 6.7 Weight loss and erosion rate of 10% MFA (JJJJ) composites with respect to impact angle due to erosion for a period of 600 seconds

Velocity (m/s)	Impact angle (°)	10% MFA (JJJJ)	
		Weight loss (g)	Erosion rate $\times 10^{-4}$(g/g)
48	30	0.0012	0.59
	45	0.0017	0.85
	60	0.0018	0.90
	90	0.0021	1.05
70	30	0.0018	0.91
	45	0.0025	1.21
	60	0.0024	1.20
	90	0.0027	1.35
82	30	0.0022	1.10
	45	0.0026	1.29
	60	0.0027	1.35
	90	0.0030	1.50

Table 6.8 Weight loss and erosion rate of 10% MFA (GJGJ) composites with respect to impact angle due to erosion for a period of 600 seconds

Velocity (m/s)	Impact angle (°)	10% MFA (GJGJ)	
		Weight loss (g)	Erosion rate $\times 10^{-4}$(g/g)
48	30	0.0020	1.00
	45	0.0024	1.20
	60	0.0030	1.50
	90	0.0040	2.00
70	30	0.0024	1.22
	45	0.0032	1.61
	60	0.0034	1.70
	90	0.0044	2.20
82	30	0.0026	1.33
	45	0.0030	1.51
	60	0.0035	1.75
	90	0.0045	2.27

Table 6.9 Weight loss and erosion rate of 15% MFA (GJJG) composites with respect to impact angle due to erosion for a period of 600 seconds

Velocity (m/s)	Impact angle (°)	15% MFA (GJJG)	
		Weight loss (g)	Erosion rate $\times 10^{-4}$(g/g)
48	30	0.0092	1.46
	45	0.0031	1.56
	60	0.0044	2.20
	90	0.0040	2.00
70	30	0.0033	1.68
	45	0.0034	1.70
	60	0.0048	2.40
	90	0.0044	2.20
82	30	0.0035	1.78
	45	0.0036	1.80
	60	0.0050	2.52
	90	0.0047	2.37

Table 6.10 Weight loss and erosion rate of 15% MFA (JGGJ) composites with respect to impact angle due to erosion for a period of 600 seconds

Velocity (m/s)	Impact angle (°)	15% MFA (JGGJ)	
		Weight loss (g)	Erosion rate $\times 10^{-4}$(g/g)
48	30	0.0020	1.02
	45	0.0025	1.25
	60	0.0036	1.82
	90	0.0040	2.00
70	30	0.0024	1.21
	45	0.0027	1.35
	60	0.0038	1.92
	90	0.0042	2.10
82	30	0.0026	1.31
	45	0.0030	1.51
	60	0.0041	2.05
	90	0.0046	2.30

Table 6.11 Weight loss and erosion rate of 15% MFA (JJJJ) composites with respect to impact angle due to erosion for a period of 600 seconds

Velocity (m/s)	Impact angle (°)	15% MFA (JJJJ)	
		Weight loss (g)	Erosion rate $\times 10^{-4}$(g/g)
48	30	0.0018	0.92
	45	0.0021	1.05
	60	0.0026	1.30
	90	0.0036	1.80
70	30	0.0020	1.015
	45	0.0023	1.15
	60	0.0028	1.40
	90	0.0038	1.90
82	30	0.0023	1.13
	45	0.0027	1.36
	60	0.0030	1.50
	90	0.0042	2.10

Table 6.12 Weight loss and erosion rate of 15% MFA (GJGJ) composites with respect to impact angle due to erosion for a period of 600 seconds

Velocity (m/s)	Impact angle (°)	15% MFA (GJGJ)	
		Weight loss (g)	Erosion rate $\times 10^{-4}$(g/g)
48	30	0.0024	1.20
	45	0.0031	1.55
	60	0.0032	1.60
	90	0.0042	2.10
70	30	0.0027	1.37
	45	0.0032	1.62
	60	0.0034	1.70
	90	0.0046	2.30
82	30	0.0028	1.41
	45	0.0033	1.67
	60	0.0036	1.80
	90	0.0049	2.49

Table 6.13 Weight loss and erosion rate of 2% NFA (GJJG) nanocomposites with respect to impact angle due to erosion for a period of 600 seconds

Velocity (m/s)	Impact angle (°)	2% NFA (GJJG)	
		Weight loss (g)	Erosion rate $\times 10^{-4}$(g/g)
48	30	0.0016	0.81
	45	0.0018	0.91
	60	0.0021	1.07
	90	0.0023	1.15
70	30	0.0018	2.40
	45	0.0020	2.94
	60	0.0022	3.20
	90	0.0025	3.60
82	30	0.0021	1.04
	45	0.0023	1.14
	60	0.0024	1.19
	90	0.0027	1.33

Table 6.14 Weight loss and erosion rate of 2% NFA (JGGJ) nanocomposites with respect to impact angle due to erosion for a period of 600 seconds

Velocity (m/s)	Impact angle (°)	2% NFA (JGGJ)	
		Weight loss (g)	Erosion rate $\times 10^{-4}$(g/g)
48	30	0.0013	0.63
	45	0.0017	0.84
	60	0.0019	0.95
	90	0.0017	0.86
70	30	0.0014	0.70
	45	0.1887	0.94
	60	0.0021	1.05
	90	0.0019	0.98
82	30	0.0016	0.80
	45	0.0021	1.04
	60	0.0023	1.15
	90	0.0024	1.16

Table 6.15 Weight loss and erosion rate of 2% NFA (JJJJ) nanocomposites with respect to impact angle due to erosion for a period of 600 seconds

Velocity (m/s)	Impact angle (°)	2% NFA (JJJJ)	
		Weight loss (g)	Erosion rate $\times 10^{-4}$(g/g)
48	30	0.0009	0.48
	45	0.0013	0.65
	60	0.0015	0.79
	90	0.0018	0.92
70	30	0.0011	0.54
	45	0.0014	0.70
	60	0.0017	0.84
	90	0.0019	0.98
82	30	0.0012	0.61
	45	0.0015	0.75
	60	0.0018	0.89
	90	0.0021	1.09

Table 6.16 Weight loss and erosion rate of 2% NFA (GJGJ) nanocomposites with respect to impact angle due to erosion for a period of 600 seconds

Velocity (m/s)	Impact angle (°)	2% NFA (GJGJ)	
		Weight loss (g)	Erosion rate $\times 10^{-4}$(g/g)
48	30	0.0018	0.90
	45	0.0019	0.98
	60	0.0020	1.00
	90	0.0023	1.15
70	30	0.0200	1.00
	45	0.0021	1.07
	60	0.0022	1.10
	90	0.0025	1.25
82	30	0.0022	1.10
	45	0.0023	1.15
	60	0.0024	1.10
	90	0.0028	1.40

Table 6.17 Weight loss and erosion rate of 4% NFA (GJJG) nanocomposites with respect to impact angle due to erosion for a period of 600 seconds

Velocity (m/s)	Impact angle (°)	4% NFA (GJJG)	
		Weight loss (g)	Erosion rate $\times 10^{-4}$(g/g)
48	30	0.0012	0.59
	45	0.0012	0.61
	60	0.0014	0.73
	90	0.0019	0.98
70	30	0.0013	0.64
	45	0.0014	0.70
	60	0.0016	0.79
	90	0.0021	1.05
82	30	0.0015	0.73
	45	0.0016	0.82
	60	0.0017	0.87
	90	0.0024	1.20

Table 6.18 Weight loss and erosion rate of 4% NFA (JGGJ) nanocomposites with respect to impact angle due to erosion for a period of 600 seconds

Velocity (m/s)	Impact angle (°)	4% NFA (JGGJ)	
		Weight loss (g)	Erosion rate $\times 10^{-4}$(g/g)
48	30	0.0007	0.37
	45	0.0009	0.48
	60	0.0011	0.53
	90	0.0018	0.92
70	30	0.0009	0.44
	45	0.0010	0.54
	60	0.0012	0.61
	90	0.0022	1.09
82	30	0.0011	0.55
	45	0.0013	0.64
	60	0.0014	0.71
	90	0.0026	1.29

Table 6.19 Weight loss and erosion rate of 4% NFA (JJJJ) nanocomposites with respect to impact angle due to erosion for a period of 600 seconds

Velocity (m/s)	Impact angle (°)	4% NFA (JJJJ)	
		Weight loss (g)	Erosion rate $\times 10^{-4}$(g/g)
48	30	0.0005	0.28
	45	0.0006	0.31
	60	0.0008	0.42
	90	0.0010	0.53
70	30	0.0006	0.34
	45	0.0007	0.37
	60	0.0010	0.49
	90	0.0012	0.61
82	30	0.0008	0.42
	45	0.0009	0.44
	60	0.0011	0.55
	90	0.0014	0.71

Table 6.20 Weight loss and erosion rate of 4% NFA (GJGJ) nanocomposites with respect to impact angle due to erosion for a period of 600 seconds

Velocity (m/s)	Impact angle (°)	4% NFA (GJGJ)	
		Weight loss (g)	Erosion rate $\times 10^{-4}$(g/g)
48	30	0.0014	0.68
	45	0.0016	0.80
	60	0.0018	0.91
	90	0.0022	1.08
70	30	0.0016	0.78
	45	0.0018	0.88
	60	0.0020	1.00
	90	0.0024	1.18
82	30	0.0018	0.88
	45	0.0020	0.99
	60	0.0022	1.10
	90	0.0026	1.30

Table 6.21 Weight loss and erosion rate of 6% NFA (GJJG) nanocomposites with respect to impact angle due to erosion for a period of 600 seconds

Velocity (m/s)	Impact angle (°)	6% NFA (GJJG)	
		Weight loss (g)	Erosion rate $\times 10^{-4}$(g/g)
48	30	0.0013	0.63
	45	0.0014	0.71
	60	0.0016	0.82
	90	0.0022	1.12
70	30	0.0014	0.71
	45	0.0016	0.81
	60	0.0018	0.91
	90	0.0024	1.19
82	30	0.0016	0.83
	45	0.0019	0.96
	60	0.0021	1.04
	90	0.0026	1.29

Table 6.22 Weight loss and erosion rate of 6% NFA (JGGJ) nanocomposites with respect to impact angle due to erosion for a period of 600 seconds

Velocity (m/s)	Impact angle (°)	6% NFA (JGGJ)	
		Weight loss (g)	Erosion rate $\times 10^{-4}$(g/g)
48	30	0.0009	0.44
	45	0.0010	0.51
	60	0.0013	0.64
	90	0.0021	1.03
70	30	0.0010	0.51
	45	0.0012	0.59
	60	0.0014	0.70
	90	0.0024	1.21
82	30	0.0012	0.61
	45	0.0014	0.69
	60	0.0016	0.79
	90	0.0026	1.31

Table 6.23 Weight loss and erosion rate of 6% NFA (JJJJ) nanocomposites with respect to impact angle due to erosion for a period of 600 seconds

Velocity (m/s)	Impact angle (°)	6% NFA (JJJJ)	
		Weight loss (g)	Erosion rate $\times 10^{-4}$(g/g)
48	30	0.0007	0.34
	45	0.0008	0.37
	60	0.0010	0.51
	90	0.0015	0.74
70	30	0.0008	0.41
	45	0.0009	0.42
	60	0.0011	0.56
	90	0.0016	0.81
82	30	0.0010	0.52
	45	0.0010	0.51
	60	0.0013	0.63
	90	0.0019	0.89

Table 6.24 Weight loss and erosion rate of 6% NFA (GJGJ) nanocomposites with respect to impact angle due to erosion for a period of 600 seconds

Velocity (m/s)	Impact angle (°)	6% NFA (GJGJ)	
		Weight loss (g)	Erosion rate $\times 10^{-4}$(g/g)
48	30	0.0016	0.82
	45	0.0018	0.91
	60	0.0020	1.01
	90	0.0024	1.22
70	30	0.0018	0.91
	45	0.0020	1.00
	60	0.0023	1.13
	90	0.0026	1.32
82	30	0.0020	1.00
	45	0.0022	1.10
	60	0.0024	1.22
	90	0.0029	1.45

Table 6.25 Weight loss and erosion rate of 5% MAL (GJJG) composites with respect to impact angle due to erosion for a period of 600 seconds

Velocity (m/s)	Impact angle (°)	5% MAL (GJJG)	
		Weight loss (g)	Erosion rate $\times 10^{-4}$(g/g)
48	30	0.0016	0.80
	45	0.0020	0.01
	60	0.0032	1.58
	90	0.0200	1.00
70	30	0.0022	1.10
	45	0.0026	1.31
	60	0.0035	1.76
	90	0.0024	1.20
82	30	0.0027	1.35
	45	0.0028	1.41
	60	0.0039	1.96
	90	0.0028	1.40

Table 6.26 Weight loss and erosion rate of 5% MAL (JGGJ) composites with respect to impact angle due to erosion for a period of 600 seconds

Velocity (m/s)	Impact angle (°)	5% MAL (JGGJ)	
		Weight loss (g)	Erosion rate $\times 10^{-4}$(g/g)
48	30	0.0014	0.70
	45	0.0017	0.84
	60	0.0018	0.89
	90	0.0026	1.30
70	30	0.0020	1.00
	45	0.0022	1.08
	60	0.0025	1.24
	90	0.0029	1.45
82	30	0.0026	1.28
	45	0.0024	1.18
	60	0.0029	1.48
	90	0.0025	1.25

Table 6.27 Weight loss and erosion rate of 5% MAL (JJJJ) composites with respect to impact angle due to erosion for a period of 600 seconds

Velocity (m/s)	Impact angle (°)	5% MAL (JJJJ)	
		Weight loss (g)	Erosion rate $\times 10^{-4}$(g/g)
48	30	0.0008	0.42
	45	0.0017	0.62
	60	0.0014	0.71
	90	0.0017	0.85
70	30	0.0022	1.08
	45	0.0016	0.80
	60	0.0015	0.78
	90	0.0020	1.00
82	30	0.0021	1.09
	45	0.0022	1.10
	60	0.0019	0.98
	90	0.0024	1.20

Table 6.28 Weight loss and erosion rate of 5% MAL (GJGJ) composites with respect to impact angle due to erosion for a period of 600 seconds

Velocity (m/s)	Impact angle (°)	5% MAL (GJGJ)	
		Weight loss (g)	Erosion rate $\times 10^{-4}$(g/g)
48	30	0.0016	0.80
	45	0.0015	0.75
	60	0.0024	1.20
	90	0.0024	1.20
70	30	0.0019	0.98
	45	0.0017	0.87
	60	0.0028	1.40
	90	0.0030	1.50
82	30	0.0022	1.10
	45	0.0026	1.30
	60	0.0030	1.50
	90	0.0036	1.80

Table 6.29 Weight loss and erosion rate of 10% MAL (GJJG) composites with respect to impact angle due to erosion for a period of 600 seconds

Velocity (m/s)	Impact angle (°)	10% MAL (GJJG)	
		Weight loss (g)	Erosion rate $\times 10^{-4}$(g/g)
48	30	0.0016	0.80
	45	0.0020	1.01
	60	0.0028	1.38
	90	0.0027	1.35
70	30	0.0020	1.00
	45	0.0025	1.23
	60	0.0032	1.58
	90	0.0033	1.65
82	30	0.0026	1.30
	45	0.0028	1.39
	60	0.0038	1.88
	90	0.0037	1.85

Table 6.30 Weight loss and erosion rate of 10% MAL (JGGJ) composites with respect to impact angle due to erosion for a period of 600 seconds

Velocity (m/s)	Impact angle (°)	10% MAL (JGGJ)	
		Weight loss (g)	Erosion rate $\times 10^{-4}$(g/g)
48	30	0.0011	0.55
	45	0.0016	0.80
	60	0.0016	0.80
	90	0.0032	1.60
70	30	0.0014	0.70
	45	0.0019	0.96
	60	0.0022	1.10
	90	0.0034	1.70
82	30	0.0020	1.00
	45	0.0024	1.19
	60	0.0025	1.27
	90	0.0038	1.90

Table 6.31 Weight loss and erosion rate of 10% MAL (JJJJ) composites with respect to impact angle due to erosion for a period of 600 seconds

Velocity (m/s)	Impact angle (°)	10% MAL (JJJJ)	
		Weight loss (g)	Erosion rate $\times 10^{-4}$(g/g)
48	30	0.0012	0.62
	45	0.0014	0.71
	60	0.0018	0.90
	90	0.0021	1.05
70	30	0.0014	0.71
	45	0.0022	1.10
	60	0.0022	1.10
	90	0.0024	1.19
82	30	0.0016	0.81
	45	0.0025	1.23
	60	0.0024	1.20
	90	0.0026	1.30

Table 6.32 Weight loss and erosion rate of 10% MAL (GJGJ) composites with respect to impact angle due to erosion for a period of 600 seconds

Velocity (m/s)	Impact angle (°)	10% MAL (GJGJ)	
		Weight loss (g)	Erosion rate $\times 10^{-4}$(g/g)
48	30	0.0016	0.80
	45	0.0018	0.90
	60	0.0026	1.30
	90	0.0036	1.80
70	30	0.0019	0.96
	45	0.0026	1.30
	60	0.0032	1.60
	90	0.0040	2.00
82	30	0.0024	1.20
	45	0.0029	1.47
	60	0.0034	1.70
	90	0.0042	2.10

Table 6.33 Weight loss and erosion rate of 15% MAL (GJJG) composites with respect to impact angle due to erosion for a period of 600 seconds

Velocity (m/s)	Impact angle (°)	15% MAL (GJJG)	
		Weight loss (g)	Erosion rate $\times 10^{-4}$(g/g)
48	30	0.0025	1.26
	45	0.0027	1.38
	60	0.0040	2.00
	90	0.0032	1.60
70	30	0.0020	1.47
	45	0.0030	1.50
	60	0.0042	2.10
	90	0.0038	1.90
82	30	0.0033	1.63
	45	0.0034	1.70
	60	0.0046	2.30
	90	0.0042	2.10

Table 6.34 Weight loss and erosion rate of 15% MAL (JGGJ) composites with respect to impact angle due to erosion for a period of 600 seconds

Velocity (m/s)	Impact angle (°)	15% MAL (JGGJ)	
		Weight loss (g)	Erosion rate $\times 10^{-4}$(g/g)
48	30	0.0014	0.69
	45	0.0020	1.01
	60	0.0031	1.52
	90	0.0036	1.80
70	30	0.0020	1.00
	45	0.0024	1.22
	60	0.0035	1.725
	90	0.0040	2.00
82	30	0.0025	1.23
	45	0.0026	1.32
	60	0.0038	1.90
	90	0.0044	2.20

Table 6.35 Weight loss and erosion rate of 15% MAL (JJJJ) composites with respect to impact angle due to erosion for a period of 600 seconds

Velocity (m/s)	Impact angle (°)	15% MAL (JJJJ)	
		Weight loss (g)	Erosion rate $\times 10^{-4}$(g/g)
48	30	0.0015	0.75
	45	0.0014	0.70
	60	0.0022	1.10
	90	0.0030	1.50
70	30	0.0016	0.80
	45	0.0022	1.09
	60	0.0026	1.30
	90	0.0032	1.60
82	30	0.0020	1.00
	45	0.0025	1.24
	60	0.0028	1.40
	90	0.0038	1.90

Table 6.36 Weight loss and erosion rate of 15% MAL (GJGJ) composites with respect to impact angle due to erosion for a period of 600 seconds

Velocity (m/s)	Impact angle (°)	15% MAL (GJGJ)	
		Weight loss (g)	Erosion rate $\times 10^{-4}$(g/g)
48	30	0.0020	1.00
	45	0.0023	1.15
	60	0.0028	1.40
	90	0.0038	1.90
70	30	0.0023	1.17
	45	0.0028	1.42
	60	0.0030	1.50
	90	0.0042	2.12
82	30	0.0022	1.11
	45	0.0031	1.55
	60	0.0032	1.60
	90	0.0046	2.32

Table 6.37 Weight loss and erosion rate of 2% NAL (GJJG) nanocomposites with respect to impact angle due to erosion for a period of 600 seconds

Velocity (m/s)	Impact angle (°)	2% NAL (GJJG)	
		Weight loss (g)	Erosion rate $\times 10^{-4}$(g/g)
48	30	0.0012	0.61
	45	0.0014	0.71
	60	0.0019	0.97
	90	0.0020	1.00
70	30	0.0016	0.80
	45	0.0018	0.90
	60	0.0022	1.13
	90	0.0025	1.25
82	30	0.0018	0.91
	45	0.0020	1.00
	60	0.0020	1.00
	90	0.0026	1.30

Table 6.38 Weight loss and erosion rate of 2% NAL (JGGJ) nanocomposites with respect to impact angle due to erosion for a period of 600 seconds

Velocity (m/s)	Impact angle (°)	2% NAL (JGGJ)	
		Weight loss (g)	Erosion rate $\times 10^{-4}$(g/g)
48	30	0.0009	0.43
	45	0.0015	0.74
	60	0.0017	0.85
	90	0.0016	0.78
70	30	0.0013	0.60
	45	0.0017	0.84
	60	0.0015	0.75
	90	0.0014	0.68
82	30	0.0015	0.74
	45	0.0018	0.90
	60	0.0022	1.10
	90	0.0022	1.09

Table 6.39 Weight loss and erosion rate of 2% NAL (JJJJ) nanocomposites with respect to impact angle due to erosion for a period of 600 seconds

Velocity (m/s)	Impact angle (°)	2% NAL (JJJJ)	
		Weight loss (g)	Erosion rate $\times 10^{-4}$(g/g)
48	30	0.0007	0.34
	45	0.0009	0.49
	60	0.0013	0.69
	90	0.0014	0.72
70	30	0.0008	0.43
	45	0.0011	0.58
	60	0.0014	0.72
	90	0.0016	1.79
82	30	0.0011	0.53
	45	0.0013	0.63
	60	0.0016	0.80
	90	0.0018	0.90

Table 6.40 Weight loss and erosion rate of 2% NAL (GJGJ) nanocomposites with respect to impact angle due to erosion for a period of 600 seconds

Velocity (m/s)	Impact angle (°)	2% NAL (GJGJ)	
		Weight loss (g)	Erosion rate $\times 10^{-4}$(g/g)
48	30	0.0016	0.80
	45	0.0016	0.79
	60	0.0014	0.70
	90	0.0022	1.10
70	30	0.0018	0.90
	45	0.0014	0.70
	60	0.0020	1.00
	90	0.0022	1.10
82	30	0.0020	1.00
	45	0.0022	1.10
	60	0.0022	1.10
	90	0.0024	1.20

Table 6.41 Weight loss and erosion rate of 4% NAL (GJJG) nanocomposites with respect to impact angle due to erosion for a period of 600 seconds

Velocity (m/s)	Impact angle (°)	4% NAL (GJJG)	
		Weight loss (g)	Erosion rate $\times 10^{-4}$(g/g)
48	30	0.0008	0.43
	45	0.0008	0.42
	60	0.0010	0.53
	90	0.0015	0.78
70	30	0.0010	0.53
	45	0.0013	0.65
	60	0.0013	0.64
	90	0.0017	0.89
82	30	0.0012	0.64
	45	0.0014	0.74
	60	0.0014	0.73
	90	0.0020	1.00

Table 6.42 Weight loss and erosion rate of 4% NAL (JGGJ) nanocomposites with respect to impact angle due to erosion for a period of 600 seconds

Velocity (m/s)	Impact angle (°)	4% NAL (JGGJ)	
		Weight loss (g)	Erosion rate $\times 10^{-4}$(g/g)
48	30	0.0003	0.16
	45	0.0005	0.25
	60	0.0009	0.48
	90	0.0014	0.72
70	30	0.0006	0.33
	45	0.0007	0.34
	60	0.0010	0.52
	90	0.0016	0.82
82	30	0.0008	0.43
	45	0.0012	0.62
	60	0.0012	0.63
	90	0.0018	0.92

Table 6.43 Weight loss and erosion rate of 4% NAL (JJJJ) nanocomposites with respect to impact angle due to erosion for a period of 600 seconds

Velocity (m/s)	Impact angle (°)	4% NAL (JJJJ)	
		Weight loss (g)	Erosion rate $\times 10^{-4}$(g/g)
48	30	0.0004	0.18
	45	0.0003	0.16
	60	0.0006	0.32
	90	0.0009	0.48
70	30	0.0005	0.24
	45	0.0003	0.19
	60	0.0007	0.39
	90	0.0010	0.53
82	30	0.0006	0.30
	45	0.0008	0.39
	60	0.0010	0.50
	90	0.0013	0.65

Table 6.44 Weight loss and erosion rate of 4% NAL (GJGJ) nanocomposites with respect to impact angle due to erosion for a period of 600 seconds

Velocity (m/s)	Impact angle (°)	4% NAL (GJGJ)	
		Weight loss (g)	Erosion rate $\times 10^{-4}$(g/g)
48	30	0.0012	0.80
	45	0.0012	0.79
	60	0.0011	0.70
	90	0.0020	1.10
70	30	0.0013	0.66
	45	0.0014	0.71
	60	0.0018	0.90
	90	0.0022	1.10
82	30	0.0015	0.78
	45	0.0018	0.90
	60	0.0020	1.00
	90	0.0024	1.05

Table 6.45 Weight loss and erosion rate of 6% NAL (GJJG) nanocomposites with respect to impact angle due to erosion for a period of 600 seconds

Velocity (m/s)	Impact angle (°)	6% NAL (GJJG)	
		Weight loss (g)	Erosion rate $\times 10^{-4}$(g/g)
48	30	0.0010	0.51
	45	0.0012	0.59
	60	0.0013	0.63
	90	0.0022	1.11
70	30	0.0012	0.59
	45	0.0015	0.73
	60	0.0016	0.77
	90	0.0023	1.16
82	30	0.0001	0.78
	45	0.0018	0.92
	60	0.0018	0.9
	90	0.0023	1.16

Table 6.46 Weight loss and erosion rate of 6% NAL (JGGJ) nanocomposites with respect to impact angle due to erosion for a period of 600 seconds

Velocity (m/s)	Impact angle (°)	6% NAL (JGGJ)	
		Weight loss (g)	Erosion rate $\times 10^{-4}$(g/g)
48	30	0.0006	0.34
	45	0.0008	0.41
	60	0.0010	0.54
	90	0.0018	0.90
70	30	0.0008	0.44
	45	0.0009	0.48
	60	0.0012	0.64
	90	0.0020	1.00
82	30	0.0011	0.56
	45	0.0012	0.61
	60	0.0014	0.72
	90	0.0022	1.10

Table 6.47 Weight loss and erosion rate of 6% NAL (JJJJ) nanocomposites with respect to impact angle due to erosion for a period of 600 seconds

Velocity (m/s)	Impact angle (°)	6% NAL (JJJJ)	
		Weight loss (g)	Erosion rate $\times 10^{-4}$(g/g)
48	30	0.0004	0.22
	45	0.0005	0.25
	60	0.0008	0.43
	90	0.0013	0.65
70	30	0.0006	0.32
	45	0.0006	0.31
	60	0.0011	0.53
	90	0.0016	0.78
82	30	0.0008	0.40
	45	0.0009	0.46
	60	0.0012	0.60
	90	0.0017	0.86

Table 6.48 Weight loss and erosion rate of 6% NAL (GJGJ) nanocomposites with respect to impact angle due to erosion for a period of 600 seconds

Velocity (m/s)	Impact angle (°)	6% NAL (GJGJ)	
		Weight loss (g)	Erosion rate $\times 10^{-4}$(g/g)
48	30	0.0014	0.72
	45	0.0014	0.71
	60	0.0018	0.90
	90	0.0022	1.10
70	30	0.0016	0.80
	45	0.0018	0.88
	60	0.0021	1.09
	90	0.0024	1.20
82	30	0.0018	0.90
	45	0.0021	1.05
	60	0.0022	1.10
	90	0.0026	1.30

Table 6.49 Erosion efficiency of 5% MFA hybrid composite

Impact Velocity 'v' (m/s)	Impact angle (°)	Erosion efficiency (η)					
		Neat Epoxy	GGGG	GJJG+5 %MFA	JGGJ+5 %MFA	JJJJ+5 %MFA	GJGJ+5 %MFA
		Hv=193.0 MPa	Hv=227.5 MPa	Hv=235.3 MPa	Hv=236.3 MPa	Hv=218.6 MPa	Hv=215.7 MPa
48	30	2.32	1.73	1.67	1.50	1.10	1.55
	45	3.15	2.16	2.00	1.66	1.43	1.52
	60	3.51	2.88	3.12	2.08	1.46	2.28
	90	3.93	2.16	1.99	2.50	1.76	2.28
70	30	1.58	0.95	1.02	0.94	0.60	0.87
	45	1.94	1.15	1.10	0.88	0.75	0.79
	60	2.11	1.44	1.54	1.05	0.74	1.14
	90	2.38	1.15	1.09	1.29	0.90	1.14
82	30	1.34	0.79	2.47	2.33	1.81	2.10
	45	1.58	0.89	0.90	0.70	0.62	0.73
	60	1.71	1.10	1.25	0.86	0.66	0.89
	90	1.92	0.91	1.02	1.06	0.77	0.99

Table 6.50 Erosion efficiency of 10% MFA hybrid composite

Impact Velocity 'v' (m/s)	Impact angle (°)	Erosion efficiency (η)					
		Neat Epoxy	GGGG	GJJG+10 %MFA	JGGJ+10 %MFA	JJJJ+10 %MFA	GJGJ+10 %MFA
		Hv=193.0 MPa	Hv=227.5 MPa	Hv=239.2 MPa	Hv=237.3 MPa	Hv=225.5 MPa	Hv=218.6 MPa
48	30	2.32	1.73	1.53	1.45	1.01	1.55
	45	3.15	2.16	1.91	1.52	1.44	1.86
	60	3.51	2.88	2.85	2.03	1.53	2.32
	90	3.93	2.16	2.80	3.21	1.78	3.10
70	30	1.58	0.95	0.96	0.80	0.73	0.89
	45	1.94	1.15	1.07	0.87	0.97	1.17
	60	2.11	1.44	1.50	1.19	0.96	1.24
	90	2.38	1.15	1.48	1.67	1.08	1.60
82	30	1.34	0.79	2.38	1.95	1.87	2.06
	45	1.58	0.89	0.84	0.81	0.75	0.80
	60	1.71	1.10	1.12	0.86	0.79	0.93
	90	1.92	0.91	1.13	1.33	0.87	1.21

Table 6.51 Erosion efficiency of 15% MFA hybrid composite

Impact Velocity 'v' (m/s)	Impact angle (°)	Erosion efficiency (η)					
		Neat Epoxy	GGGG	GJJG+15 %MFA	JGGJ+15 %MFA	JJJJ+15 %MFA	GJGJ+15 %MFA
		Hv=193.0 MPa	Hv=227.5 MPa	Hv=236.3 MPa	Hv=234.3 MPa	Hv=224.5 MPa	Hv=227.5 Mpa
48	30	2.32	1.73	2.48	1.73	1.58	1.95
	45	3.15	2.16	2.65	2.13	1.80	2.52
	60	3.51	2.88	3.74	3.12	2.23	2.61
	90	3.93	2.16	3.40	3.41	3.08	3.42
70	30	1.58	0.95	1.34	0.97	0.82	1.05
	45	1.94	1.15	1.36	1.08	0.93	1.24
	60	2.11	1.44	1.92	1.54	1.13	1.30
	90	2.38	1.15	1.76	1.69	1.53	1.76
82	30	1.34	0.79	3.03	2.24	1.94	2.30
	45	1.58	0.89	1.05	0.88	0.80	0.93
	60	1.71	1.10	1.47	1.20	0.88	1.00
	90	1.92	0.91	1.38	1.35	1.23	1.39

Table 6.52 Erosion efficiency of 2% NFA hybrid nanocomposite

Impact Velocity 'v' (m/s)	Impact angle (°)	Erosion efficiency (η)					
		Neat Epoxy	GGGG	GJJG+2 % NFA	JGGJ+2 % NFA	JJJJ+2% NFA	GJGJ+2 % NFA
		Hv=193.0 MPa	Hv=227.5 MPa	Hv=240.2 MPa	Hv=245.1 MPa	Hv=221.6 MPa	Hv=221.6 MPa
48	30	2.32	1.73	1.35	1.08	0.77	1.39
	45	3.15	2.16	1.52	1.44	1.04	1.51
	60	3.51	2.88	1.78	1.63	1.27	1.54
	90	3.93	2.16	1.93	1.47	1.48	1.77
70	30	1.58	0.95	0.71	0.56	0.41	0.73
	45	1.94	1.15	0.80	0.76	0.53	0.78
	60	2.11	1.44	0.89	0.85	0.64	0.80
	90	2.38	1.15	0.99	0.79	0.75	0.91
82	30	1.34	0.79	0.60	0.47	0.34	0.58
	45	1.58	0.89	0.65	0.61	0.41	0.61
	60	1.71	1.10	0.68	0.67	0.49	0.63
	90	1.92	0.91	0.78	0.68	0.60	0.74

Table 6.53 Erosion efficiency of 4% NFA hybrid nanocomposite

Impact Velocity 'v' (m/s)	Impact angle (°)	Erosion efficiency (η)					
		Neat Epoxy	GGGG	GJJG+4 % NFA	JGGJ+4 % NFA	JJJJ+4% NFA	GJGJ+4 % NFA
		Hv=193.0 MPa	Hv=227.5 MPa	Hv=245.1 MPa	Hv=251.0 MPa	Hv=228.5 MPa	Hv=225.5 MPa
48	30	2.32	1.73	1.02	0.66	0.48	1.08
	45	3.15	2.16	1.05	0.86	0.52	1.27
	60	3.51	2.88	1.26	0.96	0.71	1.44
	90	3.93	2.16	1.69	1.64	0.89	1.71
70	30	1.58	0.95	0.52	0.38	0.27	0.58
	45	1.94	1.15	0.57	0.45	0.29	0.65
	60	2.11	1.44	0.64	0.52	0.39	0.74
	90	2.38	1.15	0.85	0.91	0.48	0.88
82	30	1.34	0.79	0.43	0.34	0.24	0.48
	45	1.58	0.89	0.48	0.39	0.25	0.54
	60	1.71	1.10	0.52	0.44	0.31	0.60
	90	1.92	0.91	0.71	0.79	0.41	0.70

Table 6.54 Erosion efficiency of 6% NFA hybrid nanocomposite

Impact Velocity 'v' (m/s)	Impact angle (°)	Erosion efficiency (η)					
		Neat Epoxy	GGGG	GJJG+6 % NFA	JGGJ+6 % NFA	JJJJ+6% NFA	GJGJ+6 % NFA
		Hv=193.0 MPa	Hv=227.5 MPa	Hv=244.1 MPa	Hv=246.1 MPa	Hv=234.3 MPa	Hv=230.4 MPa
48	30	2.32	1.73	1.10	0.78	0.60	1.35
	45	3.15	2.16	1.23	0.89	0.66	1.49
	60	3.51	2.88	1.43	1.13	0.89	1.66
	90	3.93	2.16	1.95	1.81	1.30	2.00
70	30	1.58	0.95	0.58	0.42	0.34	0.70
	45	1.94	1.15	0.66	0.49	0.35	0.77
	60	2.11	1.44	0.74	0.58	0.46	0.87
	90	2.38	1.15	0.97	1.00	0.67	1.02
82	30	1.34	0.79	0.50	0.37	0.31	0.56
	45	1.58	0.89	0.57	0.42	0.31	0.62
	60	1.71	1.10	0.62	0.48	0.38	0.69
	90	1.92	0.91	0.77	0.79	0.54	0.82

Table 6.55 Erosion efficiency of 5% MAL hybrid composite

Impact Velocity 'v' (m/s)	Impact angle (°)	Erosion efficiency (η)					
		Neat Epoxy	GGGG	GJJG+5 %MAL	JGGJ+5 %MAL	JJJJ+5 %MAL	GJGJ+5 %MAL
		Hv=193.0 MPa	Hv=227.5 MPa	Hv=234.3 MPa	Hv=240.2 MPa	Hv=223.5 MPa	Hv=209.8 MPa
48	30	2.32	1.73	1.28	1.15	0.66	1.15
	45	3.15	2.16	1.62	1.37	0.99	1.07
	60	3.51	2.88	2.53	1.46	1.13	1.72
	90	3.93	2.16	1.60	2.13	1.35	1.72
70	30	1.58	0.95	0.83	0.77	0.81	0.66
	45	1.94	1.15	0.99	0.83	0.60	0.59
	60	2.11	1.44	1.33	0.96	0.58	0.94
	90	2.38	1.15	0.90	1.12	0.75	1.01
82	30	1.34	0.79	0.74	0.72	0.59	0.54
	45	1.58	0.89	0.77	0.66	0.60	0.64
	60	1.71	1.10	1.08	0.83	0.53	0.74
	90	1.92	0.91	0.77	0.93	0.65	0.88

Table 6.56 Erosion efficiency of 10% MAL hybrid composite

Impact Velocity 'v' (m/s)	Impact angle (°)	Erosion efficiency (η)					
		Neat Epoxy	GGGG	GJJG+10 %MAL	JGGJ+10 %MAL	JJJJ+10 %MAL	GJGJ+10 %MAL
		Hv=193.0 MPa	Hv=227.5 MPa	Hv=243.2 MPa	Hv=236.3 MPa	Hv=229.4 MPa	Hv=218.6 MPa
48	30	2.32	1.73	1.30	0.88	1.00	1.17
	45	3.15	2.16	1.63	1.27	1.15	1.31
	60	3.51	2.88	2.24	1.27	1.46	1.90
	90	3.93	2.16	2.19	2.54	1.71	2.62
70	30	1.58	0.95	0.76	0.52	0.55	0.66
	45	1.94	1.15	0.94	0.72	0.84	0.89
	60	2.11	1.44	1.21	0.82	0.84	1.10
	90	2.38	1.15	1.26	1.27	0.91	1.37
82	30	1.34	0.79	0.72	0.54	0.45	0.60
	45	1.58	0.89	0.77	0.65	0.68	0.73
	60	1.71	1.10	1.05	0.69	0.67	0.85
	90	1.92	0.91	1.03	1.03	0.72	1.05

Table 6.57 Erosion efficiency of 15% MAL hybrid composite

Impact Velocity 'v' (m/s)	Impact angle (°)	Erosion efficiency (η)					
		Neat Epoxy	GGGG	GJJG+15 %MAL	JGGJ+15 %MAL	JJJJ+15 %MAL	GJGJ+15 %MAL
		Hv=193.0 MPa	Hv=227.5 MPa	Hv=237.3 MPa	Hv=235.3 MPa	Hv=226.5 MPa	Hv=229.4 MPa
48	30	2.32	1.73	1.96	1.08	1.19	1.50
	45	3.15	2.16	2.12	1.57	1.10	1.72
	60	3.51	2.88	3.12	2.37	1.73	2.09
	90	3.93	2.16	2.49	2.80	2.36	2.84
70	30	1.58	0.95	1.08	0.73	0.59	0.82
	45	1.94	1.15	1.10	0.89	0.81	1.00
	60	2.11	1.44	1.54	1.26	0.96	1.05
	90	2.38	1.15	1.39	1.46	1.18	1.49
82	30	1.34	0.79	0.87	0.66	0.54	0.57
	45	1.58	0.89	0.91	0.70	0.67	0.79
	60	1.71	1.10	1.23	1.01	0.75	0.82
	90	1.92	0.91	1.12	1.17	1.02	1.19

Table 6.58 Erosion efficiency of 2% NAL hybrid nanocomposite

Impact Velocity 'v' (m/s)	Impact angle (°)	Erosion efficiency (η)					
		Neat Epoxy	GGGG	GJJG+2 %NAL	JGGJ+2 %NAL	JJJJ+2 %NAL	GJGJ+2 %NAL
		Hv=193.0 MPa	Hv=227.5 MPa	Hv=245.1 MPa	Hv=249.0 MPa	Hv=225.5 MPa	Hv=226.5 MPa
48	30	2.32	1.73	1.02	0.74	0.55	1.24
	45	3.15	2.16	1.19	1.27	0.79	1.23
	60	3.51	2.88	1.63	1.46	1.11	1.09
	90	3.93	2.16	1.68	1.34	1.16	1.71
70	30	1.58	0.95	0.63	0.51	0.32	0.66
	45	1.94	1.15	0.71	0.68	0.44	0.51
	60	2.11	1.44	0.89	0.61	0.54	0.73
	90	2.38	1.15	0.99	0.55	0.60	0.80
82	30	1.34	0.79	0.52	0.43	0.29	0.53
	45	1.58	0.89	0.58	0.53	0.35	0.58
	60	1.71	1.10	0.58	0.64	0.44	0.58
	90	1.92	0.91	0.75	0.64	0.50	0.64

Table 6.59 Erosion efficiency of 4% NAL hybrid nanocomposite

Impact Velocity 'v' (m/s)	Impact angle (°)	Erosion efficiency (η)					
		Neat Epoxy	GGGG	GJJG+4 %NAL	JGGJ+4 %NAL	JJJJ+4 %NAL	GJGJ+4 %NAL
		Hv=193.0 MPa	Hv=227.5 MPa	Hv=250.0 MPa	Hv=254.0 MPa	Hv=234.3 MPa	Hv=233.4 Mpa
48	30	2.32	1.73	0.74	0.29	0.31	0.93
	45	3.15	2.16	0.70	0.44	0.28	0.96
	60	3.51	2.88	0.91	0.84	0.54	1.31
	90	3.93	2.16	1.34	1.25	0.81	1.59
70	30	1.58	0.95	0.43	0.27	0.19	0.49
	45	1.94	1.15	0.53	0.28	0.16	0.53
	60	2.11	1.44	0.52	0.42	0.31	0.67
	90	2.38	1.15	0.72	0.67	0.42	0.82
82	30	1.34	0.79	0.38	0.26	0.17	0.43
	45	1.58	0.89	0.43	0.35	0.22	0.49
	60	1.71	1.10	0.42	0.38	0.29	0.55
	90	1.92	0.91	0.59	0.55	0.37	0.66

Table 6.60 Erosion efficiency of 6% NAL hybrid nanocomposite

Impact Velocity 'v' (m/s)	Impact angle (°)	Erosion efficiency (η)					
		Neat Epoxy	GGGG	GJJG+6 %NAL	JGGJ+6 %NAL	JJJJ+6 %NAL	GJGJ+6 %NAL
		Hv=193.0 MPa	Hv=227.5 MPa	Hv=246.1 MPa	Hv=249.0 MPa	Hv=235.3 Mpa	Hv=234.3 MPa
48	30	2.32	1.73	0.86	0.59	0.37	1.14
	45	3.15	2.16	0.99	0.70	0.43	1.13
	60	3.51	2.88	1.06	0.93	0.74	1.43
	90	3.93	2.16	1.87	1.54	1.12	1.75
70	30	1.58	0.95	0.47	0.36	0.26	0.60
	45	1.94	1.15	0.58	0.39	0.25	0.66
	60	2.11	1.44	0.61	0.52	0.43	0.81
	90	2.38	1.15	0.92	0.81	0.62	0.90
82	30	1.34	0.79	0.45	0.33	0.23	0.49
	45	1.58	0.89	0.53	0.36	0.27	0.57
	60	1.71	1.10	0.52	0.42	0.35	0.60
	90	1.92	0.91	0.67	0.65	0.50	0.71

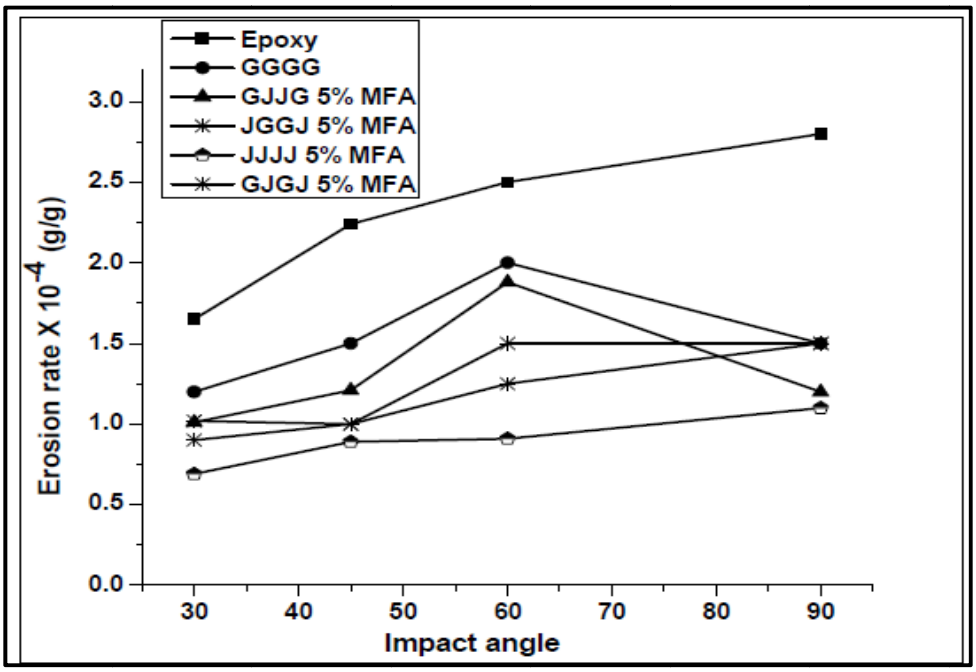

Figure 6.1 Erosion rate vs. impact angle of 5% MFA hybrid composite at velocity 48 m/sec

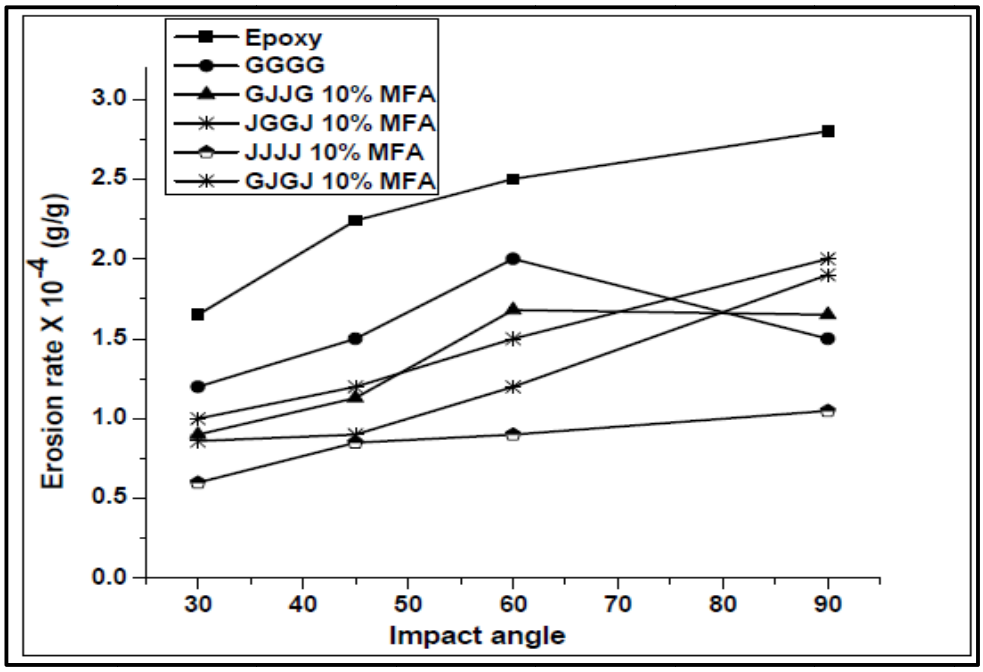

Figure 6.2 Erosion rate vs. impact angle of 10% MFA hybrid composite at velocity 48 m/sec

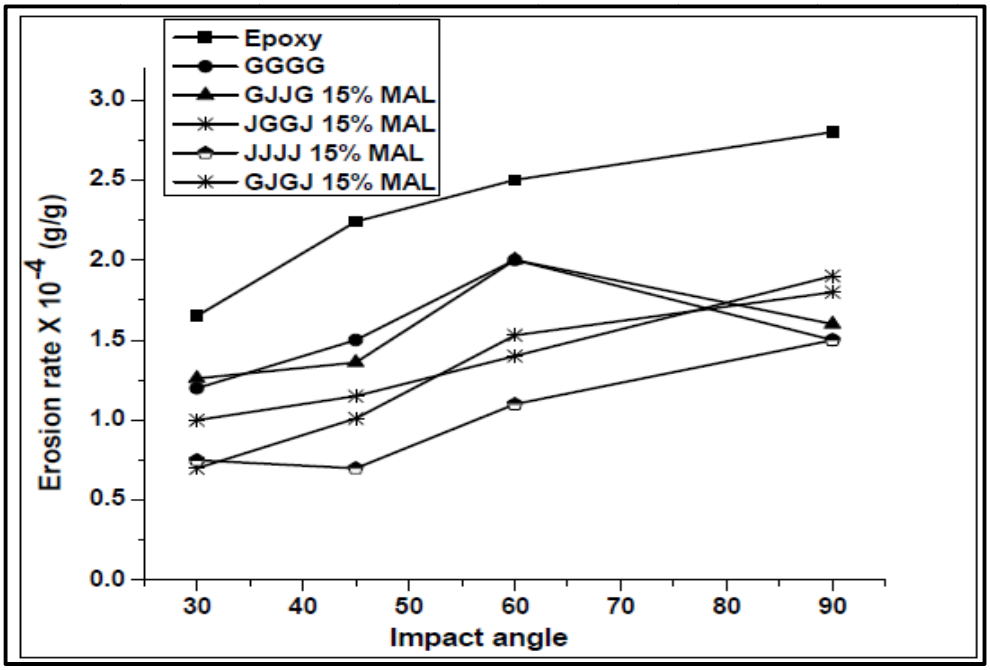

Figure 6.3 Erosion rate vs. impact angle of 15% MFA hybrid composite at velocity 48 m/sec

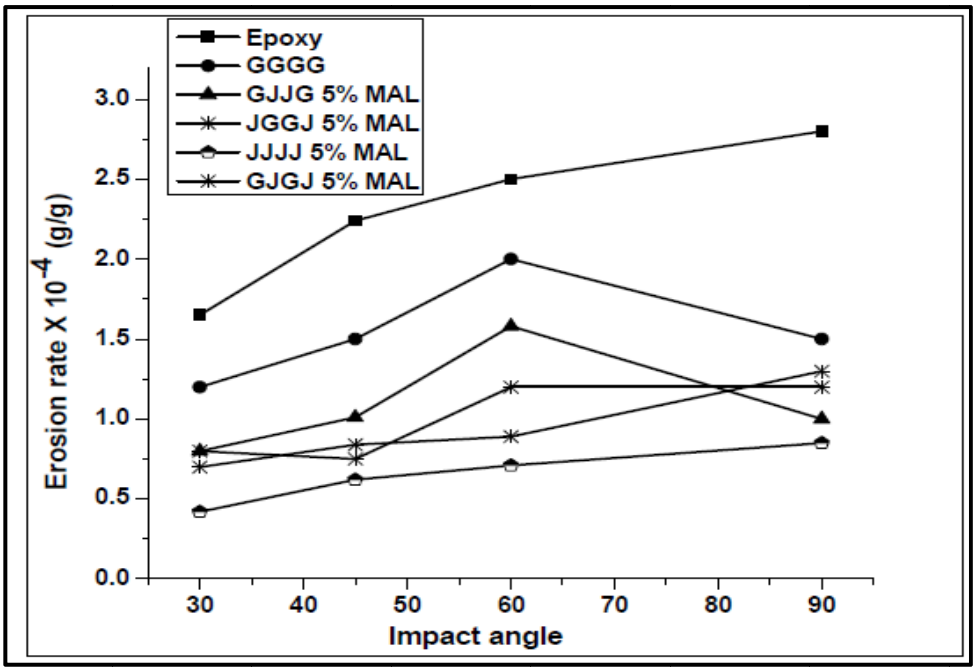

Figure 6.4 Erosion rate vs. impact angle of 5% MAL hybrid composite at velocity 48 m/sec

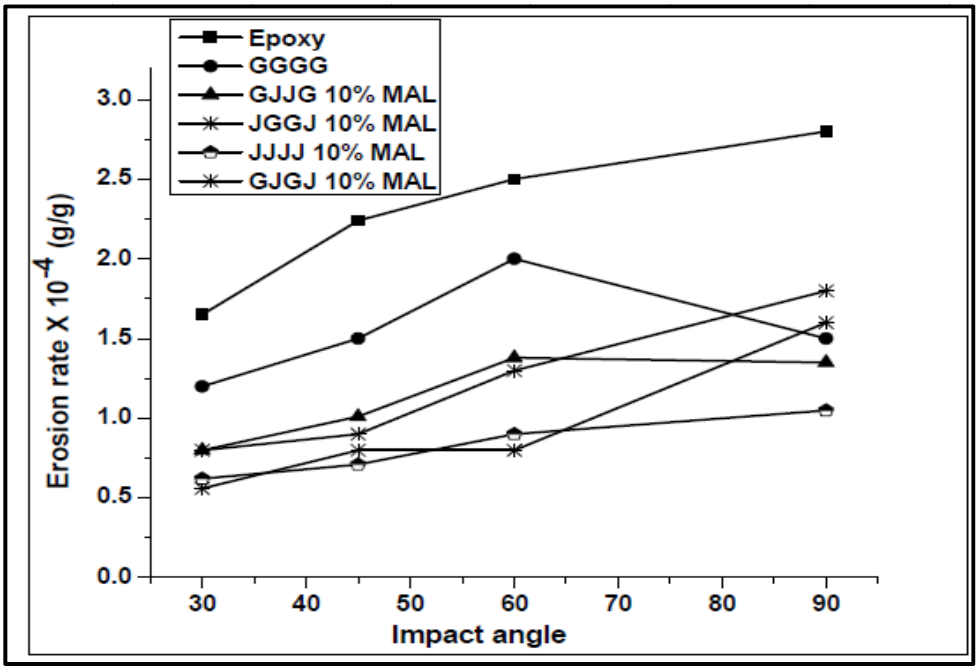

Figure 6.5 Erosion rate vs. impact angle of 10% MAL hybrid composite at velocity 48 m/sec

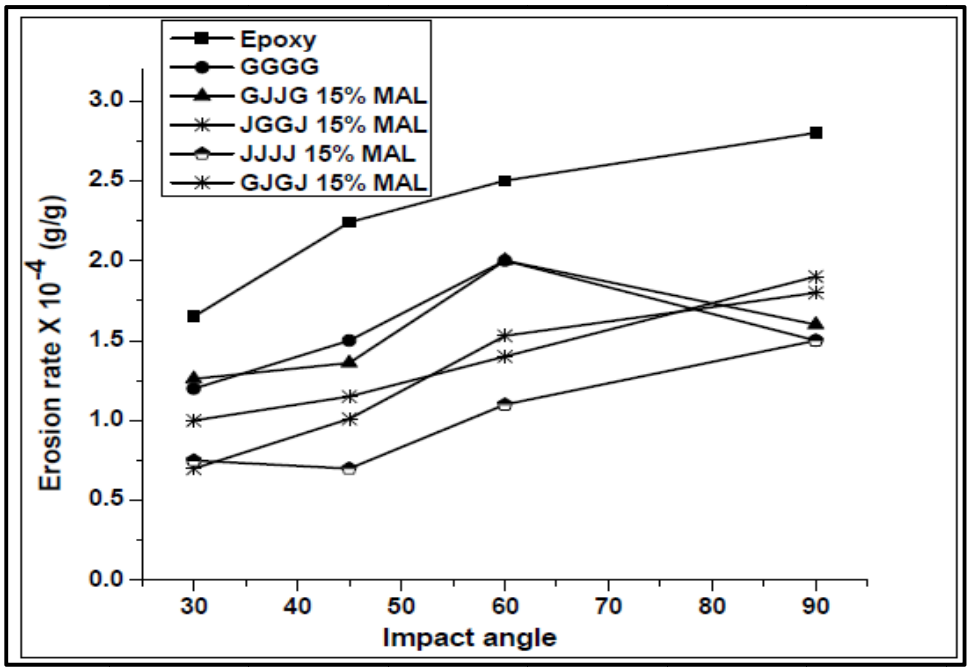

Figure 6.6 Erosion rate vs. impact angle of 15% MAL hybrid composite at velocity 48 m/sec

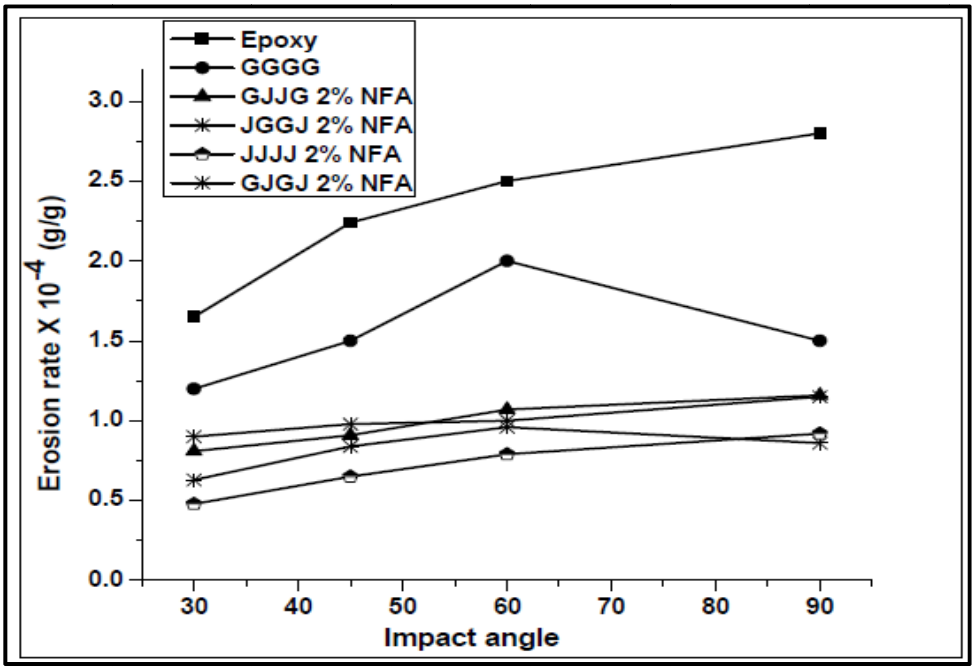

Figure 6.7 Erosion rate vs. impact angle of 2% NFA hybrid nanocomposite at velocity 48 m/sec

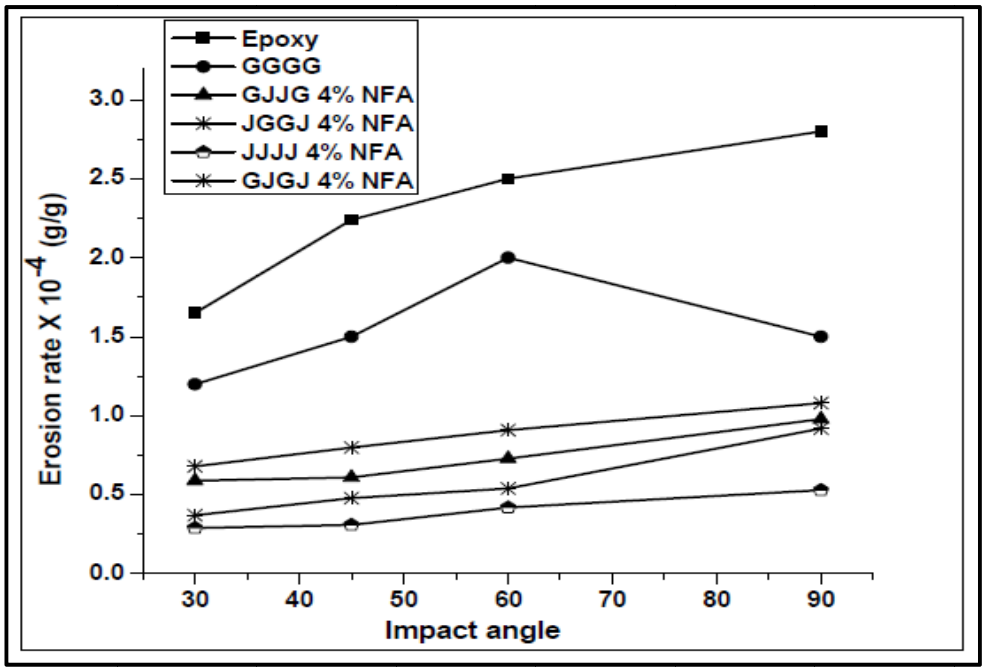

Figure 6.8 Erosion rate vs. impact angle of 4% NFA hybrid nanocomposite at velocity 48 m/sec

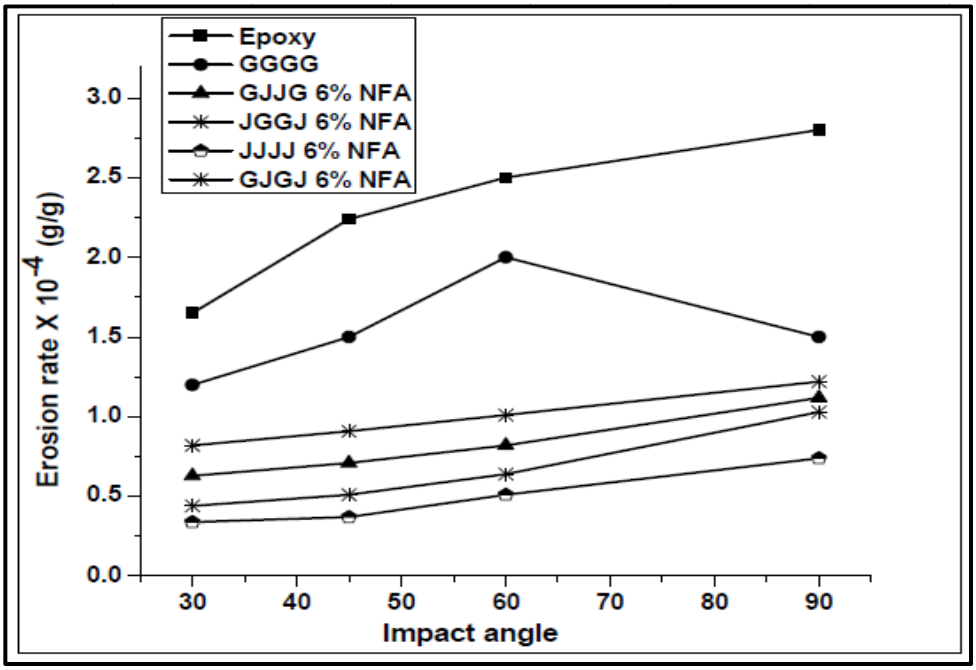

Figure 6.9 Erosion rate vs. impact angle of 6% NFA hybrid nanocomposite at velocity 48 m/sec

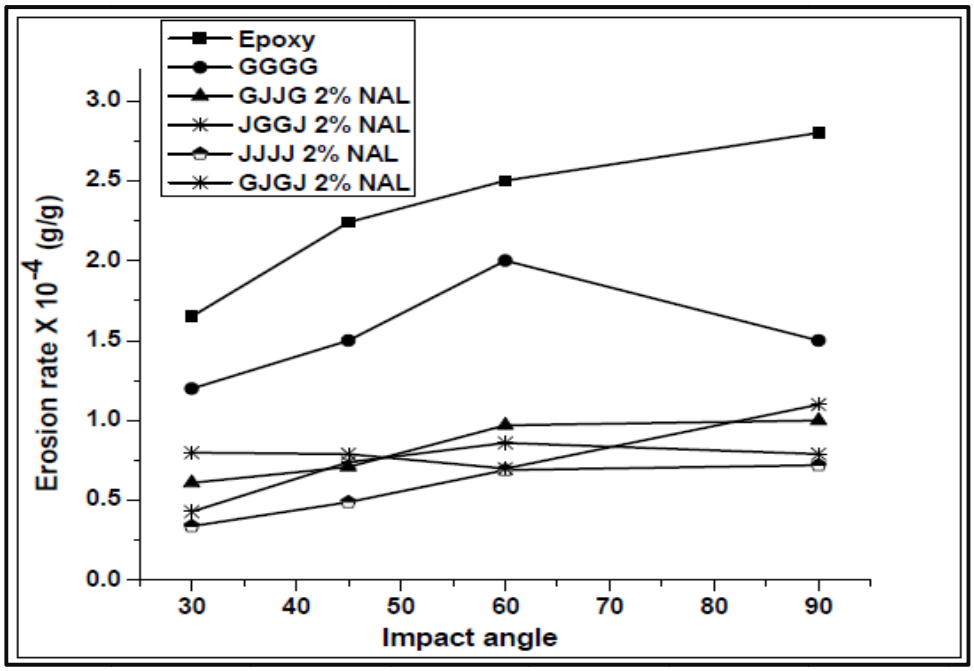

Figure 6.10 Erosion rate vs. impact angle of 2% NAL hybrid nanocomposite at velocity 48 m/sec

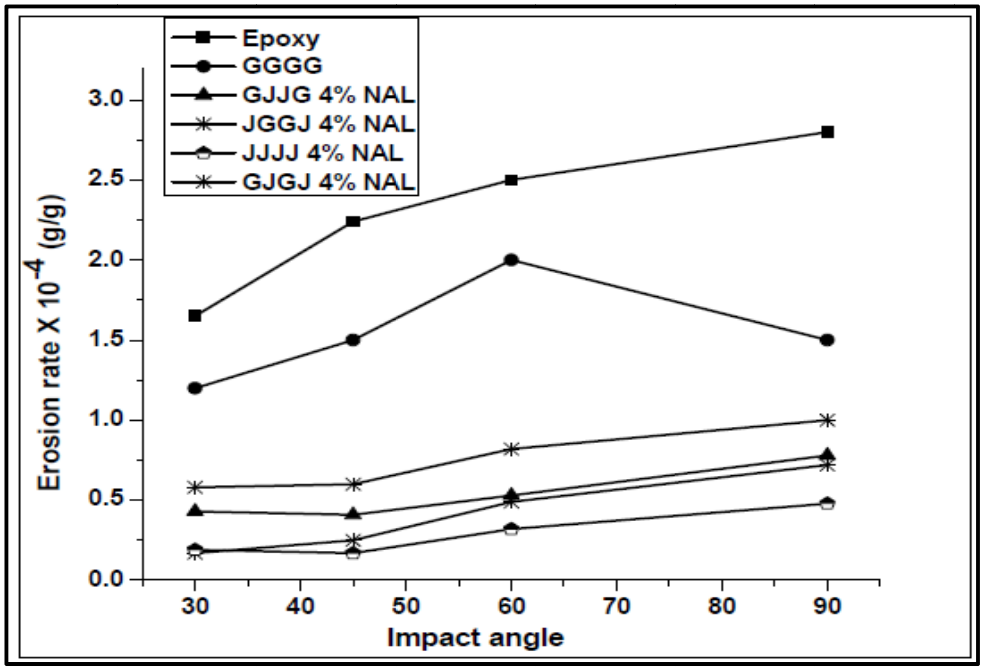

Figure 6.11 Erosion rate vs. impact angle of 4% NAL hybrid nanocomposite at velocity 48 m/sec

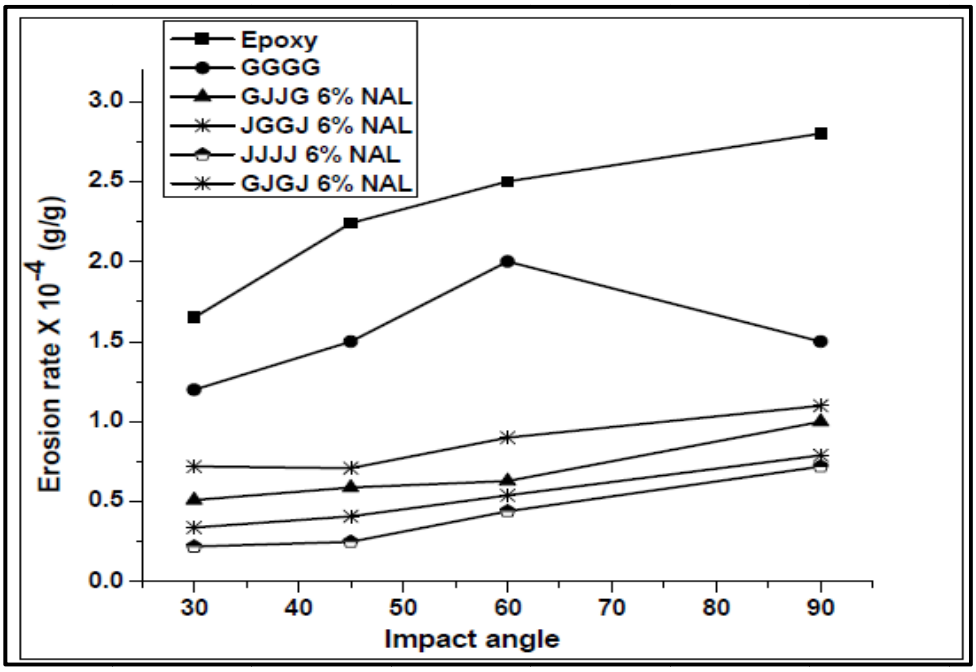

Figure 6.12 Erosion rate vs. impact angle of 6% NAL hybrid nanocomposite at velocity 48 m/sec

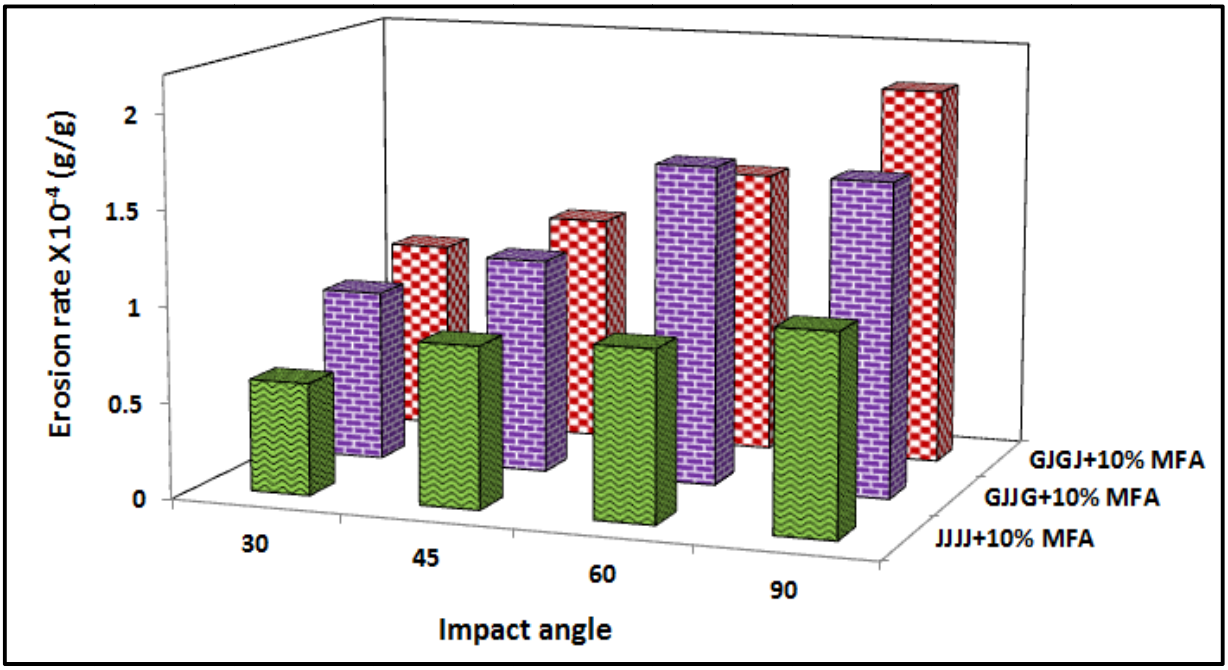

Figure 6.13 Histogram shows the Erosion rate vs. impact angle of 10% MFA hybrid nanocomposite at velocity 48 m/sec

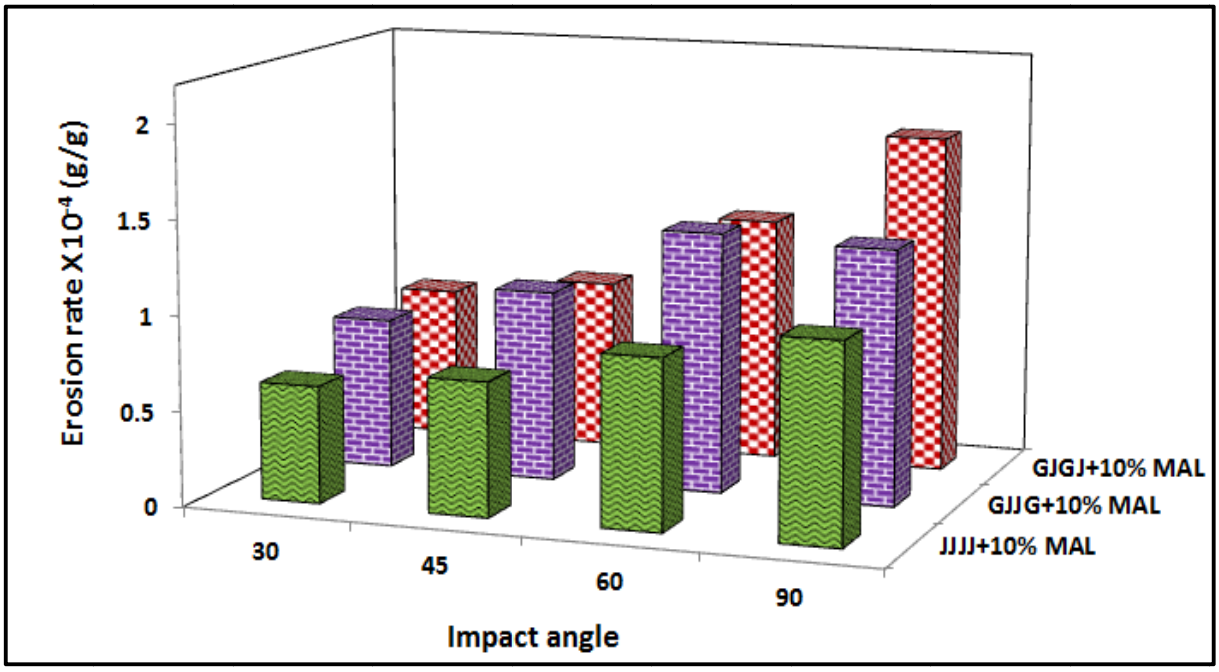

Figure 6.14 Histogram shows the Erosion rate vs. impact angle of 10% MAL hybrid nanocomposite at velocity 48 m/sec

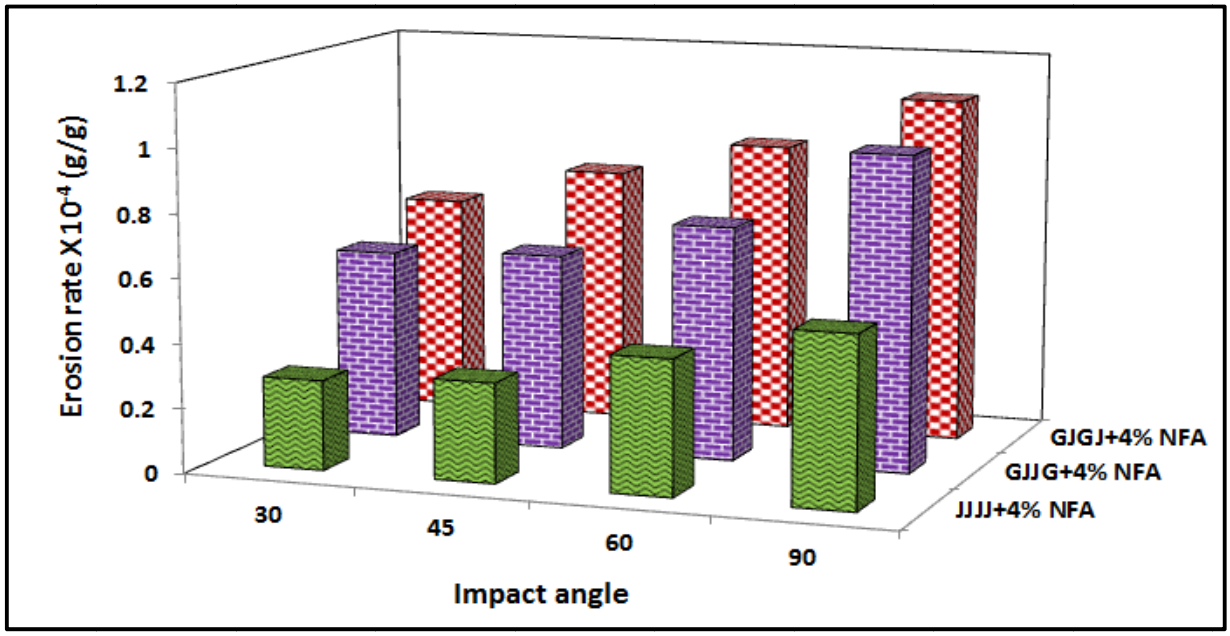

Figure 6.15 Histogram shows the Erosion rate vs. impact angle of 4% NFA hybrid nanocomposite at velocity 48 m/sec

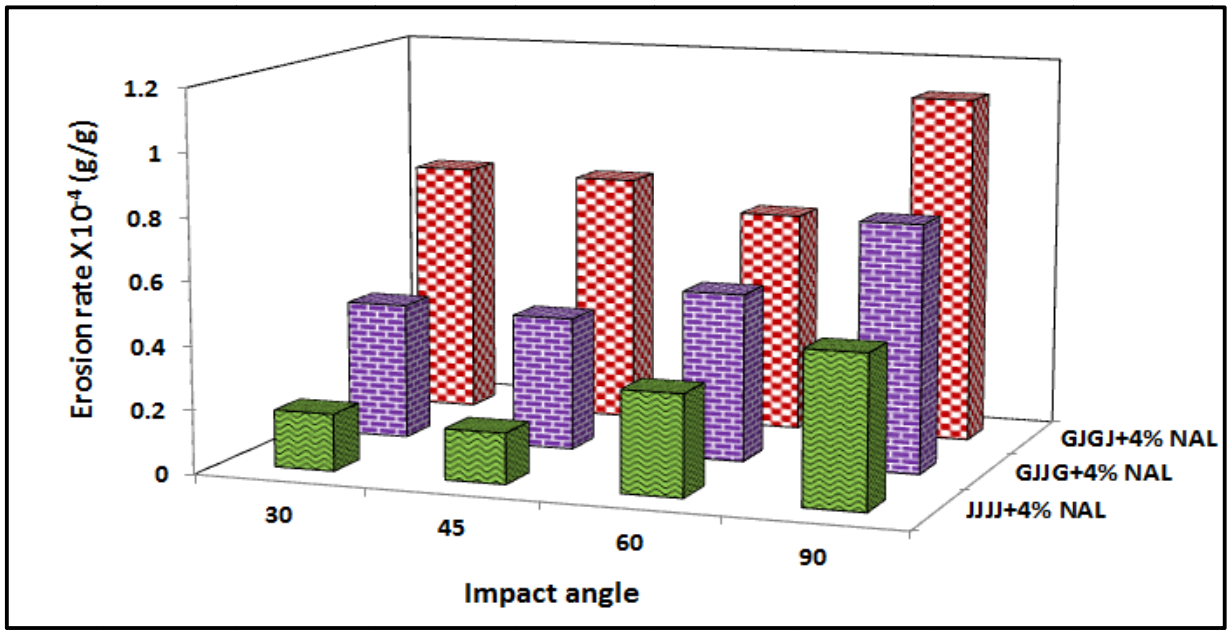

Figure 6.16 Histogram shows the Erosion rate vs. impact angle of 4% NAL hybrid nanocomposite at velocity 48 m/sec

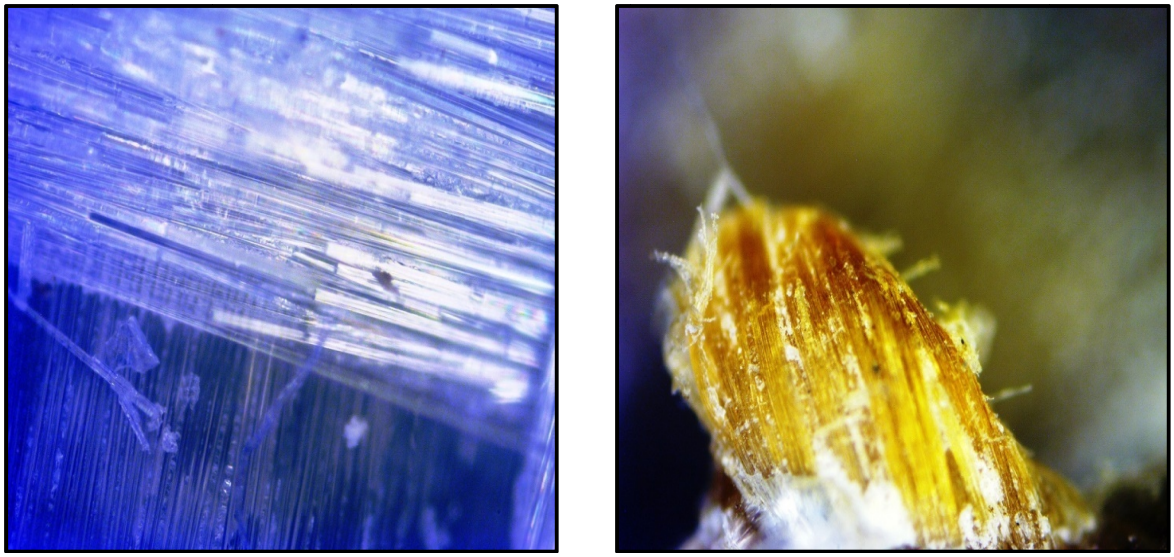

Figure 6.17(a) microscopic image of glass in epoxy (b) microscopic image of jute in epoxy

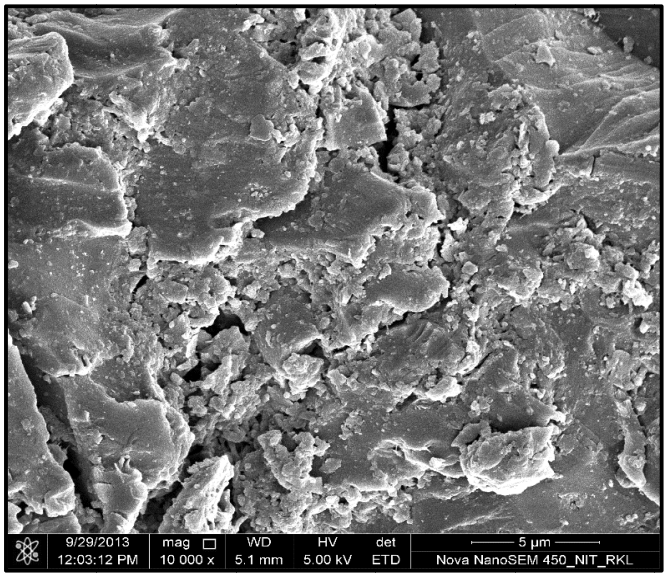

Figure 6.18(a) jute fiber composite with nano alumina filler at 90° impact angle

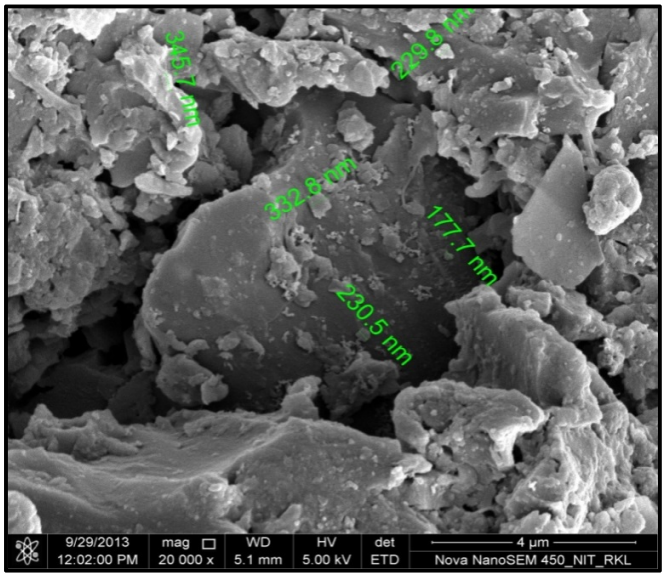

Figure 6.18(b) Jute fiber composite with nano alumina filler at 90° impact angle with higher magnification

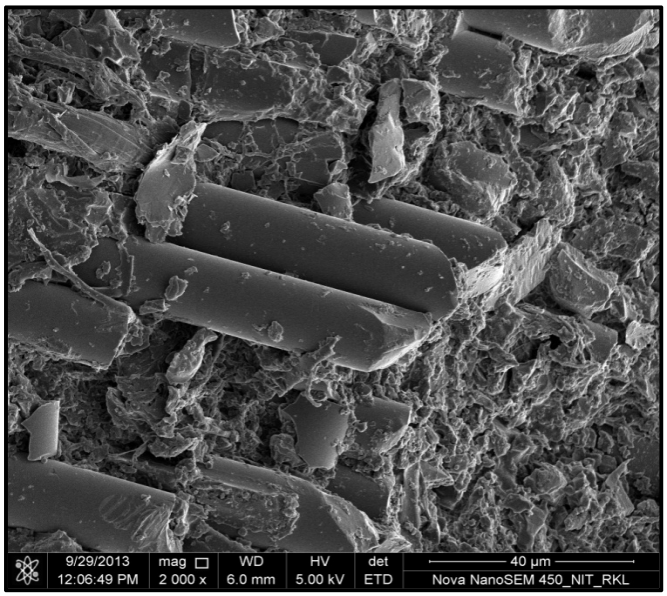

Figure 6.18(c) glass fiber hybrid composite with nano alumina filler at 90° impact angle

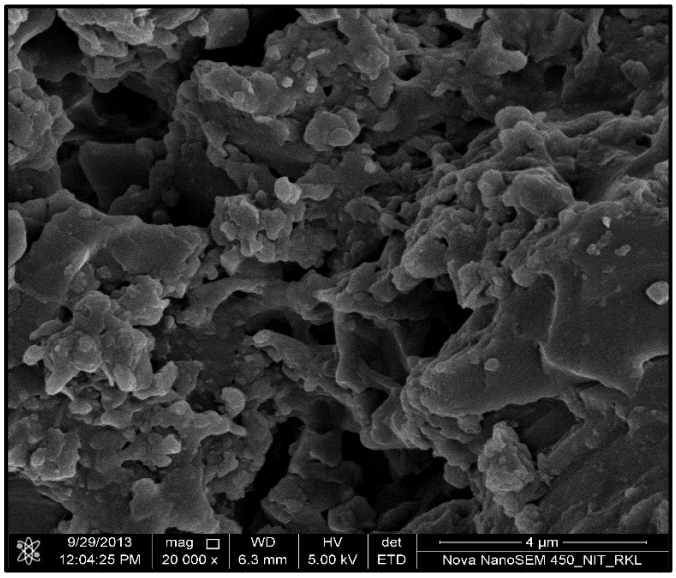

Figure 6.18(d) glass fiber hybrid composite with nano alumina filler at 90°impact angle with higher magnification

Chapter 7

Conclusions and Scope for Future Work

7.1 CONCLUSION

The conclusions drawn from the present investigations are as follows.

1. A new class of epoxy based composites reinforced with jute and glass fibres with micro and nano fillers have been fabricated successfully in the laboratory for the development of value added products.
2. Both nano alumina and nano fly ash were successfully fabricated in the laboratory by auto combustion and planetary ball milling process.
3. Effect of filler addition (both micro and nano) increases the tensile, flexural properties of the hybrid composite for different stacking sequences.
4. The erosion resistance of the composite with different stacking sequences increases with addition of both micro and nano filler. The best result was achieved for only jute fiber filled with fly ash as well as alumina nano particles.
5. The layered composites shows a semi ductile behavior to solid particle erosion since the erosion efficiency (η) is found in the range 1.40% to 6.52%.
6. The erosion efficiency of fly ash and alumina filled composite varies from 0.16% to 3.42% for different impact velocities. This lower erosion efficiency of fly ash and alumina filled epoxy composite indicates a better erosion resistance in comparison to hybrid composite.
7. The morphologies of the eroded surfaces for the hybrid composite without filler addition as observed by SEM suggest that overall erosion damage of the composite is mainly due to breaking of fiber. Chipping out of fiber prevented due to good bonding between the fiber and the matrix.
8. The fracture surface study with micro and nano filler addition indicates the breaking of glass fiber without detachment from the matrix, which in turn improves the erosion resistance of the composite.

7.2 RECOMMENDATION FOR FURTHER RESEARCH

1. In the present investigation we have used jute and glass fabric to prepare a hybrid composite. However there exists other natural fibers like bamboo, bagasses etc. which could be tried and a final conclusion can be drawn their after.
2. Hand-lay-up technique is used to fabricate the composite in the present work. However there exists other manufacturing process for polymer matrix composite. They could be tried and analyzed, so that a final conclusion can be drawn there from. However the results provided in this thesis can act as a base for the utilization of this fiber and fillers.
3. From this work it is found that fly ash and alumina micro/ nano fillers significantly improve the mechanical and tribological performance of the composite. Other ceramic or metal micro/nano fillers could be tried and a final conclusion can be drawn thereafter.
4. In the erosion test sand particle of 200±50 microns only have been used. This work can be further extended to other particle size and types of particle like glass bead etc, to study the effect of particle size and type of particles on wear behavior of the composite.

Chapter 8

Miscellaneous

REFERENCES

1) Roco, M. C. (1999). Nanoparticles and nanotechnology research. *Journal of Nanoparticle Research*, *1*(1), 1-6.
2) Rothon, R. N. (2002). *Particulate fillers for polymers*. Rapra Technology Limited.
3) Reynaud, E., Gauthier, C., & Perez, J. (1999). Nanophases in polymers. *Revue de Metallurgie, Cahiers d'Informations Techniques(France)*, *96*(2), 169-176.
4) Gyeong, M. K., Reinforcing mechanisms on the macro-, micro and nanoscale in heterogeneous polymer materials, Habilitation thesis, University of Halle.
5) Zhang, M. Q., Rong, M. Z., Zeng, H. M., Schmitt, S., Wetzel, B., & Friedrich, K. (2001). Atomic force microscopy study on structure and properties of irradiation grafted silica particles in polypropylene-based nanocomposites. *Journal of applied polymer science*, *80*(12), 2218-2227.
6) Chand N., Rohatgi P.K., (1994), Natural fibers and their composites, *Publishers, Periodical Experts*, Delhi.
7) Chand, N., & Dwivedi, U. K. (2006). Effect of coupling agent on high stress abrasive wear of chopped Jute/PP composites. *Journal of Wear*, *261*, 1057.
8) Tong, J., Ren, L., Li, J., & Chen, B. (1995). Abrasive wear behavior of bamboo. *Tribology International*, *28*(5), 323-327.
9) Jain, S., Kumar, R., & Jindal, U. C. (1992). Mechanical behavior of bamboo and bamboo composite. *Journal of Materials Science*, *27*(17), 4598-4604.
10) Mohanty, A. K., Khan, M. A., & Hinrichsen, G. (2000). Influence of chemical surface modification on the properties of biodegradable jute fabrics—polyester amide composites. *Composites Part A: Applied Science and Manufacturing*, *31*(2), 143-150.
11) Joseph, P. V., Joseph, K., & Thomas, S. (1999). Effect of processing variables on the mechanical properties of sisal-fiber-reinforced polypropylene composites. *Composites Science and Technology*, *59*(11), 1625-1640.
12) Mukherjee, P. S., & Satyanarayana, K. G. (1984). Structure and properties of some vegetable fibres. *Journal of Materials Science*, *19*(12), 3925-3934.
13) Nishino, T., Hirao, K., Kotera, M., Nakamae, K., & Inagaki, H. (2003). Kenaf reinforced biodegradable composite. *Composites Science and Technology*, *63*(9), 1281-1286.
14) Vazquez, A., Dominguez, V. A., & Kenny, J. M. (1999). Bagasse fiber-polypropylene based composites. *Journal of Thermoplastic Composite Materials*, *12*(6), 477-497.

15) Carus, M., Eder, A., Dammer, L., Korte, H., Scholz, L., Essel, R., & Breitmayer, E. (2012). Wood-plastic composites (WPC) and natural fibre composites (NFC): European and global markets 2012 and future trends. *Nova-Institut GmbH.*

16) El-Tayeb, N. S. M. (2008). A study on the potential of sugarcane fibers/polyester composite for tribological applications. *Wear*, *265*(1), 223-235.

17) Bledzki, A. K., & Gassan, J. (1999). Composites reinforced with cellulose based fibres. *Progress in polymer science*, *24*(2), 221-274.

18) Ahmaruzzaman, M. (2010). A review on the utilization of fly ash. *Progress in Energy and Combustion Science*, *36*(3), 327-363.

19) Kumar v., zakariak.a and Sharma p., (1999) Fly ash utilization: Indian scenario & case studies, in: proc. of Int. Conf. On fly ash disposal and utilization, New Delhi

20) Dhingra, A.K., (1986). Metal replacement by composite. JOM, 38(3), 17.

21) Mehrabian, R. G. R. R., Riek, R. G., & Flemings, M. (1974). Preparation and casting of metal-particulate non-metal composites. Metallurgical Transactions, 5(8), 1899-1905.

22) Eliasson, J., & Sandström, R. (1995). Applications of aluminium matrix composites. Key Engineering Materials, 104, 3-36.

23) Outwater Jr, J.O. (1956). The mechanics of plastics reinforcement in tension. Modern Plastics, 33(7), 156ff.

24) Robson, D.; Hague, J., & Newman, G., Jeronomidis, G., & Ansell, M., (1996). Survey of natural materials for use in structural composites as reinforcement and matrices. Woodland Publishing Ltd., Abingdon (UK).

25) Kohler, R., Wedler, R.M., (1994). Non-textile applications of flax fibers. TECHTEXTIL–Symposium 331. Vortrags-Nr, 1–8.

26) Joseph, K., Varghese, S., Kalaprasad, G., Thomas, S., Prasannakumari, L., Koshy, P., & Pavithran, C. (1996). Influence of interfacial adhesion on the mechanical properties and fracture behavior of short sisal fiber reinforced polymer composites. European Polymer Journal, 32(10), 1243-1250.

27) Patel, R.D., Patel, R.G., & Patel, V.S., (1988). J Therm Anal, 34, 1283.

28) Yu, L., Dean, K., & Li, L. (2006). Polymer blends and composites from renewable resources. Progress in polymer science, 31(6), 576-602.

29) Bax, B., & Müssig, J. (2008). Impact and tensile properties of PLA/Cordenka and PLA/flax composites. Composites Science and Technology, 68(7), 1601-1607.

30) Oksman, K., Skrifvars, M., & Selin, J. F. (2003). Natural fibers as reinforcement in polylactic acid (PLA) composites. Composites science and technology, 63(9), 1317-1324.

31) Meinander, K., Niemi, M., Hakola, J.S., & Selin, J.F. (1997). Polylactides-degradable polymers for fibres and films. In Macromolecular Symposia, 123(1), 147-153. Hüthig & Wepf Verlag.

32) Jiang, L., & Hinrichsen, G. (1999). Flax and cotton fiber reinforced biodegradable polyester amide composites, 2. Characterization of biodegradation. Die Angewandte Makromolekulare Chemie, 268(1), 18-21.

33) Riedel, U., & Nickel, J. (1999). Natural fiber-reinforced biopolymers as construction materials-new discoveries. Die Angewandte Makromolekulare Chemie, 272, 34–40.

34) Keller, A., Bruggmann, D., Neff, A., Müller, B., & Wintermantel, E. (2000). Degradation kinetics of biodegradable fiber composites. Journal of Polymers and the Environment, 8(2), 91-96.

35) Leaversuch, R.D. (2000). Wood-fiber Composites Build Promising Role in Extrusion. Modern Plastics, 77(12), 56–60.

36) Holbery, J., & Houston, D. (2006). Natural-fiber-reinforced polymer composites in automotive applications. Jom, 58(11), 80-86.

37) Burgueno, R., Quagliata, M. J., Mehta, G. M., Mohanty, A. K., Misra, M., & Drzal, L. T. (2005). Sustainable cellular biocomposites from natural fibers and unsaturated polyester resin for housing panel applications. Journal of Polymers and the Environment, 13(2), 139-149.

38) Rials, T. G., Wolcott, M. P., & Nassar, J. M. (2001). Interfacial contributions in lignocellulosic fiber-reinforced polyurethane composites. Journal of applied polymer science, 80(4), 546-555.

39) Mueller, D. H., & Krobjilowski, A. (2003). New discovery in the properties of composites reinforced with natural fibers. Journal of Industrial Textiles, 33(2), 111-130.

40) Eichhorn, S. J., Baillie, C. A., Zafeiropoulos, N., Mwaikambo, L. Y., Ansell, M. P., Dufresne, A., ... & Wild, P. M. (2001). Review: current international research into cellulosic fibers and composites. Journal of materials Science, 36(9), 2107-2131.

41) Brouwer, W. D. (2000, December). Natural fibre composites in structural components: Alternative applications for sisal. In Seminar, Commond Fund for Commodities-Alternative Applications for Sisal and Henecuen.

42) Bodros, E., Pillin, I., Montrelay, N., & Baley, C. (2007). Could biopolymers reinforced by randomly scattered flax fibre be used in structural applications?. Composites Science and Technology, 67(3), 462-470.

43) Pal, P.K. (1984). Jute reinforced plastics: a low cost composite material. Plastics Rubber Process Appl, 4, 215–219.

44) Mohanty, A. K., Misra, M., & Drzal, L. T. (2002). Sustainable bio-composites from renewable resources: opportunities and challenges in the green materials world. Journal of Polymers and the Environment, 10(1-2), 19-26.

45) Joseph, S., Sreekala, M. S., Oommen, Z., Koshy, P., & Thomas, S. (2002). A comparison of the mechanical properties of phenol formaldehyde composites reinforced with banana fibres and glass fibres. Composites Science and Technology, 62(14), 1857-1868.

46) Roe, P. J., & Ansell, M. P. (1985). Jute-reinforced polyester composites. Journal of Materials Science, 20(11), 4015-4020.

47) Lu, X., Zhang, M. Q., Rong, M. Z., Shi, G., & Yang, G.C. (2003). Self-reinforced melt processable composites of sisal. Composites science and technology, 63(2), 177-186.

48) Baiardo, M., Zini, E., & Scandola, M. (2004). Flax fibre–polyester composites. Composites Part A: Applied Science and Manufacturing, 35(6), 703-710.

49) George, J., Sreekala, M. S., & Thomas, S. (2001). A review on interface modification and characterization of natural fiber reinforced plastic composites. Polymer Engineering & Science, 41(9), 1471-1485.

50) Valadez-Gonzales, A., Cetvantes-Uc, J.M., Olayo, R., Herrera Franco, P.J. (1999). Effect of fibre surface treatment on the fibre-matrix bond strength of natural fibre reinforced composites. Composites, Part B, 30 (3), 309–320.

51) Rana, A.K., Mitra, B.C., & Banerjee, A.N. (1999). Short jute fibre reinforced polypropylene composites: dynamic mechanical study. J. Applied Polymer Science, 71, 531-539.

52) Nair, K.C., Diwan, S. M., & Thomas, S. (1996). Tensile properties of short sisal fiber reinforced polystyrene composites. Journal of Applied Polymer Science, 60(9), 1483-1497.

53) Mariatti, M., Jannah, M., Bakar, A. A., & Khalil, H. A. (2008). Properties of banana and pandanus woven fabric reinforced unsaturated polyester composites. Journal of composite materials, 42(9), 931-941.

54) El-Tayeb, N.S.M. (2009). Development and characterization of low-cost polymeric composite materials. Materials & Design, 30(4), 1151-1160.

55) Jacob, M., Thomas, S., & Varughese, K. T. (2004). Mechanical properties of sisal/oil palm hybrid fiber reinforced natural rubber composites. Composites Science and Technology, 64(7), 955-965.

56) Pothan, L. A., Oommen, Z., & Thomas, S. (2003). Dynamic mechanical analysis of banana fiber reinforced polyester composites. Composites Science and Technology, 63(2), 283-293.

57) Yousif, B. F., & El-Tayeb, N. S. M. (2006). Mechanical and tribological characteristics of OPRP and CGRP composites. The Proceedings ICOMAST, GKH Press, Melaka, Malaysia, 384-387.

58) Tong, J., Arnell, R. D., & Ren, L. Q. (1998). Dry sliding wear behavior of bamboo. Wear, 221(1), 37-46.

59) Tong, J., Ma, Y., Chen, D., Sun, J., & Ren, L. (2005). Effects of vascular fiber content on abrasive wear of bamboo. Wear, 259(1), 78-83.

60) Hornsby, P. R., Hinrichsen, E., & Tarverdi, K. (1997). Preparation and properties of polypropylene composites reinforced with wheat and flax straw fibres: part I fibre characterization. Journal of Materials Science, 32(2), 443-449.

61) Pothan, L. A., Thomas, S., & Neelakantan, N. R. (1997). Short banana fiber reinforced polyester composites: mechanical, failure and aging characteristics. Journal of Reinforced Plastics and Composites, 16(8), 744-765.

62) Gassan, J. (2002). A study of fibre and interface parameters affecting the fatigue behavior of natural fibre composites. *Composites Part A: Applied Science and Manufacturing*, *33*(3), 369-374.

63) Hepworth, D. G., Hobson, R. N., Bruce, D. M., & Farrent, J. W. (2000). The use of unretted hemp fibre in composite manufacture. Composites Part A: Applied Science and Manufacturing, 31(11), 1279-1283.

64) Joseph, P. V., Joseph, K., & Thomas, S. (2002). Short sisal fiber reinforced polypropylene composites: the role of interface modification on ultimate properties. Composite Interfaces, 9(2), 171-205.

65) El-Sayed, A. A., El-Sherbiny, M. G., Abo-El-Ezz, A. S., & Aggag, G. A. (1995). Friction and wear properties of polymeric composite materials for bearing applications. *Wear*, *184*(1), 45-53.

66) Ranganathan, S.R., & Pal, P.K. (1986). Jute plastics composites for the building industry popular plast, 31, 22-24.

67) Ghose, P., & Gangoli, P.K.(1993). Plast rubber composite proc. 171.

68) Shah, A. N., & Lakkad, S. C. (1981). Mechanical properties of jute-reinforced plastics. Fibre Science and Technology, 15(1), 41-46.

69) Karmakar , A.C. (1991): Polym.Plast.Technology Engg, 30, 609.

70) Rana, A.K., & Jayachandran, K. (2000). Molecular Crystals and Liquid Crystals science and Technology, section A: Molecular Crystals, 353, 35-45.

71) Shima, K., Okubo, K., Fujii, T., (2003). Computer methods and Experimental Measurement for surface treatment Effects. Computational and Experimental Methods, 7, 261-268.

72) Ray, D., Sarkar, B. K., Rana, A. K., & Bose, N. R. (2001). The mechanical properties of vinylester resin matrix composites reinforced with alkali-treated jute fibres. Composites Part A: applied science and manufacturing, 32(1), 119-127.

73) Dash, B. N., Mishra, H. K., & Tripathy, S. S. (1999). Processing, mechanical properties, and SEM analysis. Jute-Polymer composite, part 1, 20(1), 132-139.

74) Giridhar & Rao. (1986). Moisture absorption characteristics of natural fiber composites", J-Reinforced plastics composites. 5(2), 141-150.

75) Ray, D., Sarkar, B. K., & Rana, A. K. (2002). Fracture behavior of vinylester resin matrix composites reinforced with alkali-treated jute fibers. *Journal of applied polymer science*, *85*(12), 2588-2593.

76) Mitra, B. C., Basak, R. K., & Sarkar, M. (1998). Studies on jute-reinforced composites, its limitations, and some solutions through chemical modifications of fibers. Journal of Applied Polymer Science, 67(6), 1093-1100.

77) Rahman, M. R., Huque, M. M., Islam, M. N., & Hasan, M. (2008). Improvement of physico-mechanical properties of jute fiber reinforced polypropylene composites by post-treatment. Composites Part A: Applied Science and Manufacturing, 39(11), 1739-1747.

78) Ahmed, K. S., & Vijayarangan, S. (2008). Tensile, flexural and interlaminar shear properties of woven jute and jute-glass fabric reinforced polyester composites. Journal of materials processing technology, 207(1), 330-335.

79) Santulli, C., & Caruso, A. P. (2009). A comparative study on falling weight impact properties of jute/epoxy and hemp/epoxy laminates. *Malaysian Polymer Journal*, *4*(1), 19-29.

80) Kanakasabai, P., Deshpande, A. P., & Malhotra, S. K. Effect of fabric treatment and filler content on jute polyester composites. Composite Technology Center, IIT, Chennai

81) Acharya, S. K., Mishra, P., & Mishra, S. C. (2008). Effect of environment on the mechanical properties of fly ash-jute-polymer composite. *Indian J Eng Mater Sci*, *15*, 483-488.

82) Doan, T. T. L., Brodowsky, H., & Mäder, E. (2012). Jute fibre/epoxy composites: surface properties and interfacial adhesion. *Composites Science and Technology*, *72*(10), 1160-1166.

83) Freidrich, K., Haupert, F.,& Chang, L. (2008). Polymer composites in tribology" iCAT016 pp.97-99.

84) Zhao, L. X., Zheng, L. Y., & Zhao, S. G. (2006). Tribological performance of nano-Al_2O_3 reinforced polyamide 6 composites. *Materials Letters*, *60*(21), 2590-2593.

85) Wang, Y., Lim, S., Luo, J. L., & Xu, Z. H. (2006). Tribological and corrosion behaviors of Al_2O_3/polymer nanocomposite coatings. *Wear*, *260*(9), 976-983.

86) Chang, L., Zhang, Z., Breidt, C., & Friedrich, K. (2005).Tribological Properties of Epoxy Nanocomposites: I. Enhancement of the Wear Resistance by Nano-TiO_2 Particles. Wear, 258(1-4), 141-148.

87) Lin, J. C., Chang, L. C., Nien, M. H., & Ho, H. L. (2006). Mechanical behavior of various nanoparticle filled composites at low-velocity impact. *Composite Structures*, *74*(1), 30-36.

88) Kumar, S., Rath, T., Mahaling, R. N., Reddy, C. S., Das, C. K., Pandey, K. N., ... & Yadaw, S. B. (2007). Study on mechanical, morphological and electrical properties of carbon nanofiber/polyetherimide composites. *Materials Science and Engineering: B*, *141*(1), 61-70.

89) Kolluri, D. K., Satapathy, B. K., Bijwe, J., & Ghosh, A. K. (2007). Analysis of load and temperature dependence of tribo-performance of graphite filled phenolic composites. *Materials Science and Engineering: A*, *456*(1), 162-169.

90) Jiang, Z., Gyurova, L. A., Schlarb, A. K., Friedrich, K., & Zhang, Z. (2008). Study on friction and wear behavior of polyphenylene sulfide composites reinforced by short carbon fibers and sub-micro TiO_2particles. *Composites Science and Technology*, *68*(3), 734-742.

91) Zhang, G., Schlarb, A. K., Tria, S., & Elkedim, O. (2008). Tensile and tribological behaviors of PEEK/nano-SiO_2composites compounded using a ball milling technique. *Composites Science and Technology*, *68*(15), 3073-3080.

92) Su, F. H., Zhang, Z. Z., & Liu, W. M. (2008). Friction and wear behavior of hybrid glass/PTFE fabric composite reinforced with surface modified nanometer ZnO. *Wear*, *265*(3), 311-318.

93) Zhang, H. J., Zhang, Z. Z., Guo, F., Jiang, W., & Liu, W. M. (2009). Study on the tribological behavior of hybrid PTFE/cotton fabric composites filled with Sb_2O_3 and melamine cyanurate. *Tribology International*, *42*(7), 1061-1066.

94) Li, W., Zheng, S., Cao, B., & Ma, S. (2011). Friction and wear properties of ZrO2/SiO2 composite nanoparticles. *Journal of Nanoparticle Research*, *13*(5), 2129-2137.

95) Song, H. J., Zhang, Z. Z., Men, X. H., & Luo, Z. Z. (2010). A study of the tribological behavior of nano-ZnO-filled polyurethane composite coatings. *Wear*, *269*(1), 79-85.

96) Mirmohseni, A., & Zavareh, S. (2010). Preparation and characterization of an epoxy nanocomposite toughened by a combination of thermoplastic, layered and particulate nano-fillers. *Materials & Design*, *31*(6), 2699-2706.

97) Yan, Y., Jia, Z., & Yang, Y. (2011). Preparation and Mechanical Properties of PTFE/nano-EG Composites Reinforced with Nanoparticles. *Procedia Environmental Sciences*, *10*, 929-935.

98) Sharma, M., & Bijwe, J. (2011). Influence of fiber–matrix adhesion and operating parameters on sliding wear performance of carbon fabric polyethersulphone composites. *Wear*, *271*(11), 2919-2927.

99) Shi, Y., Mu, L., Feng, X., & Lu, X. (2011). The tribological behavior of nanometer and micrometer TiO_2 particle-filled polytetrafluoroethylene/polyimide. *Materials & Design*, *32*(2), 964-970.

100) Kurahatti, R. V., Surendranathan, A. O., Srivastava, S., Singh, N., Ramesh Kumar, A. V., & Suresha, B. (2011). Role of zirconia filler on friction and dry sliding wear behavior of bismaleimide nanocomposites. *Materials & Design*, *32*(5), 2644-2649.

101) Lin, G. M., Xie, G. Y., Sui, G. X., & Yang, R. (2012). Hybrid effect of nanoparticles with carbon fibers on the mechanical and wear properties of polymer composites. *Composites Part B: Engineering*, *43*(1), 44-49.

102) Ben Difallah, B., Kharrat, M., Dammak, M., & Monteil, G. (2012). Mechanical and tribological response of ABS polymer matrix filled with graphite powder. *Materials & Design*, *34*, 782-787.

103) Chang, B. P., Md Akil, H., &Bt Md Nasir, R. (2013). Comparative study of micro-and nano-ZnO reinforced UHMWPE composites under dry sliding wear. *Wear*, *297*(1), 1120-1127.

104) Chauhan, S. R., & Thakur, S. (2013). Effects of particle size, particle loading and sliding distance on the friction and wear properties of cenosphere particulate filled vinylester composites. *Materials & Design*, *51*, 398-408.

105) Wang, Z. Z., Gu, P., Wu, X. P., Zhang, H., Zhang, Z., & Chiang, M. Y. (2013). Micro/nano-wear studies on epoxy/silica nanocomposites. *Composites Science and Technology*, *79*, 49-57.

106) Antunes, P. V., Ramalho, A., & Carrilho, E. V. P. (2014). Mechanical and wear behaviors of nano and microfilled polymeric composite: Effect of filler fraction and size. *Materials & Design*, *61*, 50-60.

107) Dai, H., Gong, J., Kim, H., & Lee, D. (2002). A novel method for preparing ultra-fine alumina-borate oxide fibres via an electrospinning technique. Nanotechnology, 13(5), 674.

108) Shashikala, V., Siva Kumar, V., Padmasri, A. H., David Raju, B., Venkata Mohan, S., Nageswara Sarma, P., & Rama Rao, K. S. (2007). Advantages of nano-silver-carbon covered alumina catalyst prepared by electro-chemical method for drinking water purification. Journal of Molecular Catalysis A: Chemical, 268(1), 95-100.

109) Padmaja, P., Pillai, P. K., Warrier, K. G. K., & Padmanabhan, M. (2004). Adsorption isotherm and pore characteristics of nano alumina derived from sol-gel boehmite. Journal of Porous Materials, 11(3), 147-155.

110) Gojny, F. H., Wichmann, M. H., Fiedler, B., Bauhofer, W., & Schulte, K. (2005). Influence of nano-modification on the mechanical and electrical properties of conventional fibre-reinforced composites. Composites Part A: Applied Science and Manufacturing, 36(11), 1525-1535.

111) Zhao, H., & Li, R. K. (2008). Effect of water absorption on the mechanical and dielectric properties of nano-alumina filled epoxy nanocomposites. Composites Part A: Applied Science and Manufacturing, 39(4), 602-611.

112) F. Mirjalili, M. Hasmaliza, and L. C. Abdullah, “Size-controlled synthesis of nano α-alumina particles through the solgelmethod,” Ceramics International, vol. 36, no. 4, pp. 1253–1257, 2010.

113) R. Kavitha and V. Jayaram, “Deposition and characterization of alumina films produced by combustion flame pyrolysis,” Surface and Coatings Technology, vol. 201, no. 6, pp. 2491–2499, 2006.]

114) Singla, M., & Chawla, V. (2010). Mechanical Properties of Epoxy Resin–Fly Ash Composite. Journal of Minerals and Materials Characterization and Engineering, 9, 199.

115) Chaowasakoo, T., & Sombatsompop, N. (2007). Mechanical and morphological properties of fly ash/epoxy composites using conventional thermal and microwave curing methods. composites science and technology, 67(11), 2282-2291.

116) Gupta, N., Brar, B. S., & Woldesenbet, E. (2001). Effect of filler addition on the compressive and impact properties of glass fibre reinforced epoxy. Bulletin of Materials Science, 24(2), 219-223.

117) Srivastava, V. K., & Pawar, A. G. (2006). Solid particle erosion of glass fibre reinforced fly ash filled epoxy resin composites. Composites Science and Technology, 66(15), 3021-3028.

118) Ray, D., & Gnanamoorthy, R. (2007). Friction and wear behavior of vinylester resin matrix composites filled with fly ash particles. Journal of reinforced plastics and composites, 26(1), 5-13.

119) Amar, P., Satapathy, A., Mahapatra, S. S., & Dash, R. R. (2008). Modeling and prediction of erosion response of glass reinforced polyester-fly ash composites. Journal of Reinforced Plastics and Composites.

120) Raghavendra, G., Ojha, S., Acharya, S. K., & Pal, S. K. (2013, November). Mechanical and Tribological Behavior of Alumina Nano Filler Reinforced Epoxy Hybrid Composites. In ASME 2013 International Mechanical Engineering Congress and Exposition (pp. V02BT02A053-V02BT02A053). American Society of Mechanical Engineers.

121) Raghavendra, G., Ojha, S., Acharya, S. K., & Pal, S. K. Preparation of Alumina (Al_2O_3) Nano Powder by Auto Combustion Process, International Journal of Systems, Algorithms & Applications, 2(11):74-76, 2012;

122) Raghavendra, G., Ojha, S., Acharya, S. K., & Pal, S. K. Influence of micro/nanofiller alumina on the mechanical behavior of novel hybrid epoxy nanocomposites, High Performance Polymers, DOI: 10.1177/0954008314550889

123) Raghavendra, G., Ojha, S., Acharya, S. K., & Pal, S. K. Fabrication and characterization of nano Fly ash by planetary ball Milling,International Journal of Material Science Innovations (IJMSI) 2(3): 59-68, 2014

124) Akbari, B., Tavandashti, M. P., &Zandrahimi, M. (2011). Particle Size Characterization of Nanoparticles–A Practicalapproach. Iranian Journal of Materials Science and Engineering, 8(2), 48-56.

125) Bowen, P. (2002). Particle size distribution measurement from millimeters to nanometers and from rods to platelets. Journal of dispersion science and technology, 23(5), 631-662.

126) Agarwal BD, Broutman LJ. Analysis and performance of fiber composites: Second Edition. John Wiley and Sons, Inc., 1990.

127) Paul, K. Thomas, et al. "Preparation and characterization of nano structured materials from fly ash: A waste from thermal power stations, by high energy ball milling." Nanoscale Research Letters 2.8 (2007): 397-404..

128) Ishikawa A, Okano T and Sugiyama J. Fine structure and tensile properties of ramies in the crystalline form of cellulose I, II, IIII and IVI. Polymers 1997; 38(2):463–8.

129) Helbert W, Sugiyma J, Ishihara M, et al. Characterization of native crystalline cellulose in the cell walls of Oomycota. J Biotechnol 1997; 57(1–3): 29–37.

130) D'Almeida JRM, Aquino RCMP and Monteiro SN. Tensile mechanical properties, morphological aspects and chemical characterization of piassava (Attalafunifera) fibers. Composites A 2006; 37(9): 1473–9.

131) Akerholm M, Hinterstoisser B and Salmen L. Characterization of the crystalline structures of cellulose using static and dynamic FT-IR spectroscopy. Carbohydr Res 2004; 339(3): 569–78.

132) Elenga RG, Dirras GF, Maniongui JG, et al. On the microstructure and physical properties of untreated raffia textilisfiber. Composites: Part A 2009; 40:418–422.

133) Mwaikambo LY and Ansell MP. Chemical modification of hemp, sisal, jute, and kapok fibers by alkalisation. J ApplPolymSci 2002; 84(12): 2222–34.

134) Subramanian K, Kumar PS, Jeyapal P, et al. Characterization of lignocellulosic seed fiber from Wrightiatinctoria plants for textile applications an exploratory investigation. EurPolym J 2005; 41(4): 853–61.

135) Kumar A, Yoon M and Purtell C. Optimizing the use of cellulose enzymes in finishing cellulosic fabrics. TexChem Col 1997; 29: 37 42.

136) Anuradha S, Jabasingh and ValliNachiyarC. Process Optimization for the Biopolishing of Jute Fibers with Cellulases from AspergillusNidulansAJ SU04, International Journal of Bioscience, Biochemistry and Bioinformatics January 2012; 2(1).

137) Senthilkumaar S, Krishna SK, Kalaamani P, et al. Adsorption of Organo phosphorous Pesticide from Aqueous Solution Using "Waste" Jute Fiber Carbon. Modern Applied Science 2010; 4: 67-83.

138) Raghavendra, G., Ojha, S., Acharya, S. K., & Pal, S. K. A Comparative Analysis of Woven Jute/Glass Hybrid Polymer Composite With and Without Reinforcing of Fly Ash Particles, POLYMER COMPOSITES—2014, DOI 10.1002/pc.23222

139) Ganan P, Zulunga R, Restrepo A, et al. Plantain fibre bundles isolated from Colombian agro-industrial residues. Bioresource Technology 2008; 99: 486–491.

140) Sugiyama J, Person J and Chanzy H. Combined infrared and electron diffraction study of the polymorphism of celluloses. Macromolecules 1991; 24(9): 2461–6.

141) Nunn TR, Howard JB and Longwel JP. Product compositions and kinetics in the rapid pyrolysis of sweet gum hardwood. Ind. Eng. Chem. Process 1985; 24: 836–844.

142) Zeriouh A and Belbirl L. Thermal decomposition of a Moroccan wood under a nitrogen atmosphere. Thermochim. Acta 1995; 258: 243–248.

143) Zhang XJ, Yi XS and Xu YZ. Cure-induced phase separation of epoxy/DDS/PEK-C composites and its temperature dependency. J ApplPolymSci 2008; 109(4): 2195–206.

144) Li G, Li P, Zhang C, et al. Inhomogeneous toughening of carbon fiber/epoxy composite using electrospunpolysulfonenanofibrous membranes by in situ phase separation. Compos SciTechnol 2008; 68(3–4): 987–94.

145) Allan, G.G., Carroll, P., Negri, A.R., Raghurarnan, M., Ritzenthaler, P., & Yabiaoui, A. (1992). The micro porosity of pnlp; the precipitation of inorganic fillers within the micropores of the cell wall. Tappi Journal, 75(1), 175-178.

146) Lee, S.Y. (2002). Transcrystallization behavior and interfacial strength of a semicrystalline polymer combined with thermomechanical pulp (TMP) fiber (Doctoral dissertation, University of Idaho).

147) Ma, C.G., Rong, M. Z., Zhang, M.Q., & Friedrich, K. (2005). Irradiation-induced surface graft polymerization onto calcium carbonate nanoparticles and its toughening effects on polypropylene composites. Polymer Engineering & Science, 45(4), 529-538.

148) Lee, S.Y., Shupe, T.F., Groom, L.R., & Hse, C.Y. (2006). Heterogeneous nucleation of a semicrystalline polymer on fiber surfaces. In: Recent developments in the particleboard, fiberboard, and molded wood products industry. Shupe, T.F. ed. Forest Products Society. Madison, WI. 99-105.

149) Mullin, J.W., (1993). Crystallization, 3rd Ed. Butterworth-heinemann Ltd. Oxford, England. 527.

150) Gasser, U., Weeks, E.R., Schofield, A., Pusey, P.N., & Weitz1, D.A. (2001). Real-space imaging of nucleation and growth in colloidal crystallization. Science. 292, 258-262.

151) Sawyer, W. G., Freudenberg, K. D., Bhimaraj, P., & Schadler, L. S. (2003). A study on the friction and wear behavior of PTFE filled with alumina nanoparticles. Wear, 254(5), 573-580.

152) Kim, J. I., Kang, P. H., & Nho, Y. C. (2004). Positive temperature coefficient behavior of polymer composites having a high melting temperature. Journal of Applied Polymer Science, 92(1), 394-401.

153) Nikkeshi, S., Kudo, M., & Masuko, T. (1998). Dynamic viscoelastic properties and thermal properties of Ni powder–epoxy resin composites. Journal of Applied Polymer Science, 69(13), 2593-2598.

154) Zhu, K., & Schmauder, S. (2003). Prediction of the failure properties of short fiber reinforced composites with metal and polymer matrix. Computational Materials Science, 28(3), 743-748.

155) Rusu, M., Sofian, N., & Rusu, D. (2001). Mechanical and thermal properties of zinc powder filled high density polyethylene composites. Polymer Testing, 20(4), 409-417.

156) Tavman, I.H., (1997). Thermal and mechanical properties of copper powder filled poly (ethylene) composites. Powder Technology, 91(1), 63-67.

157) Rothon, R.N., (1997). Mineral fillers in thermoplastics: filler manufacture. Journal Adhesion, 64(1), 87-109.

158) Rothon, R.N., (1999). Effects of Particulate Fillers on Flame Retardant Properties of Composites. Advanced Polymer Science. 139, 67–107.

159) Nielsen, L.E., Landel, R.F., (1994). Mechanical properties of polymers and composites. 2nded. New York: Marcel Deckker, 377–459.

160) Peters ST. Handbook of composites. 2nd ed. London: Chapman and Hall; 1998, 242–243.

161) Young, R. J., & Beaumont, P. W. R. (1977). Failure of brittle polymers by slow crack growth. Journal of Materials Science, 12(4), 684-692.

162) Kinloch, A. J., Maxwell, D. L., & Young, R. J. (1985). The fracture of hybrid-particulate composites. Journal of materials science, 20(11), 4169-4184.

163) Young, R. J., Maxwell, D. L., & Kinloch, A. J. (1986). The deformation of hybrid-particulate composites. Journal of materials science, 21(2), 380-388.

164) Koh, S. W., Kim, J. K., & Mai, Y. W. (1993). Fracture toughness and failure mechanisms in silica-filled epoxy resin composites: effects of temperature and loading rate. Polymer, 34(16), 3446-3455.

165) Cantwell, W.J., & Moloney, A.C., (1994). Fractography and failure mechanisms of polymers and composites. Amsterdam: Elesvier; 233.

166) Imanaka, M., Takeuchi, Y., Nakamura, Y., Nishimura, A., & Iida, T. (2001). Fracture toughness of spherical silica-filled epoxy adhesives. International journal of adhesion and adhesives, 21(5), 389-396.

167) Wang, H., Bai, Y., Liu, S., Wu, J., & Wong, C. P. (2002). Combined effects of silica filler and its interface in epoxy resin. Acta Materialia, 50(17), 4369-4377.

168) Yamamoto, I., Higashihara, T., & Kobayashi, T. (2003). Effect of Silica-Particle Characteristics on Impact/Usual Fatigue Properties and Evaluation of Mechanical Characteristics of Silica-Particle Epoxy Resins. JSME International Journal Series A, 46(2), 145-153.

169) Nakamura, Y., Yamaguchi, M., Kitayama, A., Okubo, M., & Matsumoto, T. (1991). Effect of particle size on fracture toughness of epoxy resin filled with angular-shaped silica. Polymer, 32(12), 2221-2229.

170) Nakamura, Y., Yamaguchi, M., Okubo, M., & Matsumoto, T. (1991). Effect of particle size on impact properties of epoxy resin filled with angular shaped silica particles. Polymer, 32(16), 2976-2979.

171) Nakamura, Y., Yamaguchi, M., Okubo, M., & Matsumoto, T. (1992). Effects of particle size on mechanical and impact properties of epoxy resin filled with spherical silica. Journal of applied polymer science, 45(7), 1281-1289.

172) Satyanarayana, K.G., Sukumaran, K., Mukherjee, P.S., Pavithran, C., & Pillai, S.G.K. (1990). Natural Fiber–Polymer Composites, J Cement and Concrete Composites, 12(2), 117–136.

173) Satyanarayana, K.G., Sukumaran, K., Kulkarni, A.G., Pillai, S.G.K., & Rohatgi, P.K. (1986). Fabrication and Properties of Natural Fiber-Reinforced Polyester Composites", J. Composites, 17(4)), 329–333.

174) Mansur, M. A., & Aziz, M. A. (1983). Study of bamboo-mesh reinforced cement composites. International Journal of Cement composites and lightweight concrete, 5(3), 165-171.

175) Munikenche Gowda, T., Naidu, A. C. B., & Chhaya, R. (1999). Some mechanical properties of untreated jute fabric-reinforced polyester composites. Composites Part A: applied science and manufacturing, 30(3), 277-284.

176) Lundquist, L., Marque, B., Hagstrand, P. O., Leterrier, Y., & Månson, J. A. (2003). Novel pulp fibre reinforced thermoplastic composites. Composites Science and Technology, 63(1), 137-152.

177) Corbiere-Nicollier, T., Gfeller Laban, B., Lundquist, L., Leterrier, Y., Månson, J. A., & Jolliet, O. (2001). Life cycle assessment of biofibres replacing glass fibres as reinforcement in plastics. Resources, Conservation and Recycling, 33(4), 267-287.

178) Luo, S., & Netravali, A. N. (1999). Mechanical and thermal properties of environment-friendly "green" composites made from pineapple leaf fibers and poly (hydroxybutyrate-co-valerate) resin. Polymer Composites, 20(3), 367-378.

179) Belmares, H., Barrera, A., & Monjaras, M. (1983). New composite materials from natural hard fibers. 2. Fatigue studies and a novel fatigue degradation model. Industrial & engineering chemistry product research and development, 22(4), 643-652.

180) Cazaurang-Martinez, M. N., Herrera-Franco, P. J., Gonzalez-Chi, P. I., & Aguilar-Vega, M. (1991). Physical and mechanical properties of henequen fibers. Journal of applied polymer science, 43(4), 749-756.

181) Ahmed, E. M., Sahari, B., & Pedersen, P. (1999, July). Non-linear behavior of unidirectional filament wound COTFRP, CFRP, and GFRP composites. In Proceedings of World Engineering Congress, WEC (Vol. 99, pp. 537-43).

182) Khalid, A. A., Sahari, B., & Khalid, Y. A. (1998, August). Environmental effects on the progressive crushing of cotton and glass fibre/epoxy composite cones. In Proceedings of the Fourth International Conference on Advances in Materials and Processing Technologies (Vol. 98, pp. 680-89).

183) Fuad, M. Y. A., Rahmad, S., & Azlan, M. R. N. (1998, August). Filler content determination of bio-based thermoplastics composites by thermogravimetric analysis. In Proceedings of the Fourth International Conference on Advances in Materials and Processing Technologies, Kuala Lumpur (pp. 24-28).

184) Schneider JP, Karmaker AC. J Mater Sc 1996; 15:201.

185) Sreekala, M. S., Kumaran, M. G., Joseph, S., Jacob, M., & Thomas, S. (2000). Oil palm fibre reinforced phenol formaldehyde composites: influence of fibre surface modifications on the mechanical performance. Applied Composite Materials, 7(5-6), 295-329.

186) Mishra, S., M. Misra, S.S., Tripathy, S.K., Nayak, & Mohanty, A.K. (2002). The influence of chemical surface modification on the performance of sisal polyester biocomposites. Polymer Composites 23(2):164-170.

187) Ichazo, M.N., Albano, C., Gonza ´lez, J., Perera, R., & Candal, M.V. (2001). Polypropylene/wood¯our composites: treatments and properties. Compos. Struct. 54, 207-214.

188) K. Joseph and S. Thomas, Polymer., 37, 5139 (1996).

189) Berenbrok, P.A., & Liles, B.E., (1997). Effect of WF fillers on polyethylene", In:Proceedings of the annual technical conference of the society of plastic engineers (ANTEC), Totonto, April, 2931-2934.

190) Zaini, M. J., Fuad, M. A., Ismail, Z., Mansor, M. S., & Mustafah, J. (1996). The effect of filler content and size on the mechanical properties of polypropylene/oil palm wood flour composites. Polymer International, 40(1), 51-55.

191) Pavithran, C., Mukherjee, P. S., & Brahmakumar, M. (1991). Coir-glass intermingled fibre hybrid composites. Journal of Reinforced Plastics and Composites, 10(1), 91-101.

192) Mohan, R., Shridhar, M. K., & Rao, R. M. V. G. K. (1983). Compressive strength of jute-glass hybrid fibre composites. Journal of Materials Science Letters, 2(3), 99-102.

193) Pavithran, C., Mukherjee, P. S., Brahmakumar, M., & Damodaran, A.D. (1991). Impact properties of sisal-glass hybrid laminates. Journal of materials science, 26(2), 455-459.

194) Mishra, S., Mohanty, A.K., Drzal, L.T., Misra, M., Parija, S., Nayak, S.K., & Tripathy, S.S. (2003). Studies on mechanical performance of biofiber/glass reinforced polyester hybrid composites. Compos. Sci. Technol. 63, 1377–1385.

195) John, K., & Venkata Naidu, S. (2004). Sisal fibre/glass fibre hybrid composites: impact and compressive properties. Journal of Reinforced Plastic Composite. 23 (12), 1253–1258.

196) John, K., & Venkata Naidu, S. (2004). Effect of fibre content and fibre treatment of flexural properties of sisal fibre/glass fibre hybrid composites. Journal of Reinforced Plastic Composite. 23 (15), 1601–1605.

197) John, K., & Venkata Naidu, S. (2004). Tensile properties of unsaturated polyester based sisal fibre-glass fibre hybrid composites. Journal of Reinforced Plastic Composite. 23 (17), 1815–1819.

198) Biswas, S., Patnaik, A., & Kaundal, R. (2012). Effect of Red Mud and Copper Slag Particles on Physical and Mechanical Properties of Bamboo-Fiber-Reinforced Epoxy Composites. Advances in Mechanical Engineering, 2012.

199) Hamidi, Y. K., Aktas, L., & Altan, M. C. (2008). Effect of nanoclay content on void morphology in resin transfer molded composites. Journal of Thermoplastic Composite Materials, 21(2), 141-163.

200) Kong, D., Su, Y., Du, X., Yang, Y., Wei, S., & Shah, S. P. (2013). Influence of nano-silica agglomeration on fresh properties of cement pastes. *Construction and Building Materials*, *43*, 557-562.

201) Wambua, P., Ivens, J., & Verpoest, I. (2003). Natural fibres: can they replace glass in fibre reinforced plastics?.composites science and technology, 63(9), 1259-1264.

202) Munikenche Gowda, T., Naidu, A. C. B., & Chhaya, R. (1999). Some mechanical properties of untreated jute fabric-reinforced polyester composites. Composites Part A: applied science and manufacturing, 30(3), 277-284.

203) Fu, S. Y., Feng, X. Q., Lauke, B., & Mai, Y. W. (2008). Effects of particle size, particle/matrix interface adhesion and particle loading on mechanical properties of particulate–polymer composites. Composites Part B: Engineering, 39(6), 933-961.

204) Mohanty, A., Srivastava, V. K., & Sastry, P. U. (2014). Investigation of mechanical properties of alumina nanoparticle-loaded hybrid glass/carbon-fiber-reinforced epoxy composites. Journal of Applied Polymer Science, 131(1).

205) Camargo, P. H. C., Satyanarayana, K. G., & Wypych, F. (2009). Nanocomposites: synthesis, structure, properties and new application opportunities. Materials Research, 12(1), 1-39.

206) Jen, M. H. R., Tseng, Y. C., & Wu, C. H. (2005). Manufacturing and mechanical response of nanocomposite laminates. Composites science and technology, 65(5), 775-779.

207) Chisholm, N., Mahfuz, H., Rangari, V. K., Ashfaq, A., & Jeelani, S. (2005). Fabrication and mechanical characterization of carbon/SiC-epoxy nanocomposites. Composite structures, 67(1), 115-124.

208) Gujjala, R., Ojha, S., Acharya, S. K., & Pal, S. K. (2013). Mechanical properties of woven jute–glass hybrid-reinforced epoxy composite. Journal of Composite Materials, 0021998313501924.

209) Amontons, G. (1999). De la Resistance Cause'e dans les Machines (1). *Journal-Japanese Society Of Tribologists*, *44*, 229-235.

210) Petrov, N. P. (1883). Friction in Machines and the Effect of the Lubricant. *Inzherernii Zhurnal*, *1*, 71-140.

211) Tower, B. (1884). First report on friction experiments. *Proceedings of the Institution of Mechanical Engineers*, *35*(1), 29-35.

212) Reynolds, O. (1886). On the Theory of Lubrication and Its Application to Mr. Beauchamp Tower's Experiments, Including an Experimental Determination of the Viscosity of Olive Oil. *Proceedings of the Royal Society of London*, *40*(242-245), 191-203.

213) Holm, R. (1938). The friction force over the real area of contact. *Wiss. Veroeff. Siemens-Werken*, *17*(4), 38-42.

214) Peterson, M. B., (1990) "Advanced in tribo-materials-I Achievements in Tribology", Amer, Soc, Mech. Eng., Vol.1, New York; pp.91-109.

215) Rigney, D. A. (1981). *Fundamentals of friction and wear of materials: papers presented at the 1980 ASM Materials Science Seminar, 4-5 October 1980, Pittsburgh, Pennsylvania*. American Society for Metals.

216) Ashby, M. F., & Lim, S. C. (1990). Wear-mechanism maps. *Scripta Metallurgica et Materialia*, *24*(5), 805-810.

217) Wang, Y., Lei, T. C., &Gao, C. Q. (1990). Influence of isothermal hardening on the sliding wear behavior of 52100 bearing steel. *Tribology International*, *23*(1), 47-53.

218) Lim, S. C. (1998). Recent developments in wear-mechanism maps. *Tribology International*, *31*(1), 87-97.

219) Eyre, T. S. (1976). Wear characteristics of metals. *Tribology International*, *9*(5), 203-212.

220) Dowson, D. (1985). Wear oh where? *Wear*, *103*(3), 189-203.

221) Blau, P. J. (1997). Fifty years of research on the wear of metals. *Tribology International*, *30*(5), 321-331.

222) Barwell, F. T. and Strang, C. D. (1952) Metallic Wear, *Proc. Roy. Soc. London*, A, 212 (III): pp. 470-477

223) Archard, J. (1953). Contact and rubbing of flat surfaces. *Journal of applied physics*, *24*(8), 981-988.

224) Archard, J. F., & Hirst, W. (1956). The wear of metals under unlubricated conditions. *Proceedings of the Royal Society of London. Series A. Mathematical and Physical Sciences*, *236*(1206), 397-410.

225) Igor'V, K., Dobyčin, M. N., & Kombalov, V. S. (1982). *Grundlagen der Berechnung von Reibung und Verschleiß*. Verlag Technik.

226) Fleischer, G. (1973). Energetische methode der bestimmung des verschleißes. *Schmierungstechnik*, *4*(9), 269-274.

227) Zum Gahr, K. H. (1987). *Microstructure and wear of materials* (Vol. 10). Elsevier.

228) Batchelor, A. W., & Stachowiak, G. W. (1995). Tribology in materials processing. *Journal of materials processing technology*, *48*(1), 503-515.

229) Friedrich, K. (Ed.). (1986). *Friction and wear of polymer composites*. Elsevier.

230) Thorp, J. M. (1982). Abrasive wear of some commercial polymers. *Tribology international*, *15*(2), 59-68.

231) Budinski, K. G. (1997). Resistance to particle abrasion of selected plastics. *Wear*, *203*, 302-309.

232) EVANS, C. (1979). The wear of polymers. *Treatise Mater. Sci. Technol.*, *13*, 85.

233) Unal, H., Sen, U., & Mimaroglu, A. (2005). Abrasive wear behavior of polymeric materials. *Materials & design*, *26*(8), 705-710.

234) Unal, H., Sen, U., & Mimaroglu, A. (2004). Dry sliding wear characteristics of some industrial polymers against steel counterface. *Tribology International*, *37*(9), 727-732.

235) Shipway, P. H., & Ngao, N. K. (2003). Microscale abrasive wear of polymeric materials. *Wear*, *255*(1), 742-750.

236) Harsha, A. P., & Tewari, U. S. (2003). Two-body and three-body abrasive wear behavior of polyaryletherketone composites. *Polymer testing*, *22*(4), 403-418.

237) Cirino, M., Pipes, R. B., & Friedrich, K. (1987). The abrasive wear behavior of continuous fibre polymer composites. *Journal of Materials Science*, *22*(7), 2481-2492.

238) Cirino, M., Friedrich, K., & Pipes, R. B. (1988). Evaluation of polymer composites for sliding and abrasive wear applications. *Composites*, *19*(5), 383-392.

239) Chand, N., Naik, A., & Neogi, S. (2000). Three-body abrasive wear of short glass fibre polyester composite. *Wear*, *242*(1), 38-46.

240) Bijwe, J., Logani, C. M., & Tewari, U. S. (1990). Influence of fillers and fibre reinforcement on abrasive wear resistance of some polymeric composites. *Wear*, *138*(1), 77-92.

241) Liu, C., Ren, L., Arnell, R. D., & Tong, J. (1999). Abrasive wear behavior of particle reinforced ultrahigh molecular weight polyethylene composites. *Wear*, *225*, 199-204.

242) Chand, N., & Dwivedi, U. K. (2006). Effect of coupling agent on abrasive wear behavior of chopped jute fibre-reinforced polypropylene composites. *Wear*, *261*(10), 1057-1063.

243) Hashmi, S. A. R., Dwivedi, U. K., & Chand, N. (2007). Graphite modified cotton fibre reinforced polyester composites under sliding wear conditions. *Wear*, *262*(11), 1426-1432.

244) Yousif, B. F., & El-Tayeb, N. S. M. (2007). The effect of oil palm fibers as reinforcement on tribological performance of polyester composite. *Surface Review and Letters*, *14*(06), 1095-1102.

245) Yousif, B. F. (2009). Frictional and wear performance of polyester composites based on coir fibres. *Proceedings of the Institution of Mechanical Engineers, Part J: Journal of Engineering Tribology*, *223*(1), 51-59

246) Chin, C. W., & Yousif, B. F. (2009). Potential of kenaf fibres as reinforcement for tribological applications. *Wear*, *267*(9), 1550-1557.

247) Yousif, B. F., Lau, S. T., & McWilliam, S. (2010). Polyester composite based on betelnut fibre for tribological applications. *Tribology international*, *43*(1), 503-511.

248) Lai, W. L., & Mariatti, M. (2008). The properties of woven betel palm (areca catechu) reinforced polyester composites. *Journal of Reinforced Plastics and Composites*.

249) Dwivedi, U. K., & Chand, N. (2008). Influence of wood flour loading on tribological behavior of epoxy composites. *Polymer Composites*, *29*(11), 1189-1192.

250) Dwivedi, U. K., Ghosh, A., & Chand, N. (2007). Abrasive Wear Behavior of Bamboo (Dendrocalamus Strictus) Powder Filled Polyester Composites. *BioResources*, *2*(4), 693-698.

251) Soda, N., Kimura, Y., & Tanaka, A. (1975). Wear of some fcc metals during unlubricated sliding part I. Effects of load, velocity and atmospheric pressure on wear. *Wear*, *33*(1), 1-16.

252) Burwell, J. T., & Strang, C. D. (1952). Metallic wear. *Proceedings of the Royal Society of London. Series A, Mathematical and Physical Sciences*, 470-477.

253) Burwell Jr, J. T. (1957). Survey of possible wear mechanisms. *Wear*, *1*(2), 119-141.

254) Ko, P. L. (1987). Metallic wear—a review with special references to vibration-induced wear in power plant components. *Tribology International*, *20*(2), 66-78.

255) Finnie, I. (1995). Some reflections on the past and future of erosion. *Wear*, *186*, 1-10.

256) Meng, H. C., & Ludema, K. C. (1995). Wear models and predictive equations: their form and content. *Wear*, *181*, 443-457.

257) Bitter, J. G. A. (1963). A study of erosion phenomena: Part II. *Wear*, *6*(3), 169-190.

258) Hutchings, I. M., Winter, R. E., & Field, J. E. (1976). Solid particle erosion of metals: the removal of surface material by spherical projectiles. *Proceedings of the Royal Society of London. Series A, Mathematical and Physical Sciences*, 379-392.

259) Pool, K. V., Dharan, C. K. H., & Finnie, I. (1986). Erosive wear of composite materials. *Wear*, *107*(1), 1-12.

260) Kulkarni, S. M. (2001). Influence of matrix modification on the solid particle erosion of glass/epoxy composites. *Polymers & polymer composites*, *9*(1), 25-30.

261) Rajesh, J. J., Bijwe, J., Tewari, U. S., & Venkataraman, B. (2001). Erosive wear behavior of various polyamides. *Wear*, *249*(8), 702-714.

262) Barkoula, N. M., & Karger-Kocsis, J. (2002). Solid particle erosion of unidirectional GF reinforced EP composites with different fiber/matrix adhesion. *Journal of reinforced plastics and composites*, *21*(15), 1377-1388.

263) Tewari, U. S., Harsha, A. P., Häger, A. M., & Friedrich, K. (2003). Solid particle erosion of carbon fibre–and glass fibre–epoxy composites. *Composites Science and Technology*, *63*(3), 549-557.

264) Bhushan, B. (2013). *Principles and applications of tribology*. John Wiley & Sons.

265) Harsha, A. P., Tewari, U. S., & Venkatraman, B. (2003). Solid particle erosion behavior of various polyaryletherketone composites. *Wear*, *254*(7), 693-712.

266) Roy, M., Vishwanathan, B., & Sundararajan, G. (1994). The solid particle erosion of polymer matrix composites. *Wear*, *171*(1), 149-161.

267) Bajpai, P. K., Singh, I., & Madaan, J. (2013). Tribological behavior of natural fiber reinforced PLA composites. *Wear*, *297*(1), 829-840.

268) Mishra, P., & Acharya, S. K. (2010). Anisotropy abrasive wear behavior of bagasse fiber reinforced polymer composite. *International Journal of Engineering, Science and Technology*, *2*(11).

269) Deo, C., & Acharya, S. K. (2009). Solid particle erosion of lantana camara fiber-reinforced polymer matrix composite. *Polymer-Plastics Technology and Engineering*, *48*(10), 1084-1087.

270) Gupta, A., Kumar, A., Patnaik, A., & Biswas, S. (2011). Effect of different parameters on mechanical and erosion wear behavior of bamboo fiber reinforced epoxy composites. *International Journal of Polymer Science*, *2011*.

271) Mohanty, J. R., Das, S. N., Das, H. C., Mahanta, T. K., & Ghadei, S. B. (2014). Solid Particle Erosion of Date Palm Leaf Fiber Reinforced Polyvinyl Alcohol Composites. *Advances in Tribology*, *2014*.

272) Shakuntala, O., Raghavendra, G., & Samir Kumar, A. (2014). Effect of Filler Loading on Mechanical and Tribological Properties of Wood Apple Shell Reinforced Epoxy Composite. *Advances in Materials Science and Engineering*, *2014*.

273) Jawaid, M. H. P. S., & Abdul Khalil, H. P. S. (2011). Cellulosic/synthetic fibre reinforced polymer hybrid composites: A review. *Carbohydrate Polymers*, *86*(1), 1-18.

274) Almeida Jr, J. H. S., Amico, S. C., Botelho, E. C., & Amado, F. D. R. (2013). Hybridization effect on the mechanical properties of curaua/glass fiber composites. *Composites Part B: Engineering*, *55*, 492-497.

275) Patel, B. C., Acharya, S. K., & Mishra, D. (2011). Effect of stacking sequence on the erosive wear behavior of jute and juteglass fabric reinforced epoxy composite. *International Journal of Engineering, Science and Technology*, *3*(1).

276) Barkoula, N. M., & Karger-Kocsis, J. (2002). Review processes and influencing parameters of the solid particle erosion of polymers and their composites. *Journal of materials science*, *37*(18), 3807-3820.

277) Ruff, A. W., & Ives, L. K. (1975). Measurement of solid particle velocity in erosive wear. *Wear*, *35*(1), 195-199

278) Sundararajan, G., Roy, M., & Venkataraman, B. (1990). Erosion efficiency-a new parameter to characterize the dominant erosion micromechanism. *Wear*, *140*(2), 369-381.

279) Arjula, S., & Harsha, A. P. (2006). Study of erosion efficiency of polymers and polymer composites. *Polymer testing*, *25*(2), 188-196

280) Barkoula, N. M., & Karger-Kocsis, J. (2002). Effects of fibre content and relative fibre-orientation on the solid particle erosion of GF/PP composites. *Wear*, *252*(1), 80-87

281) Biswas, S., & Satapathy, A. (2010). A comparative study on erosion characteristics of red mud filled bamboo–epoxy and glass–epoxy composites. *Materials & Design*, *31*(4), 1752-1767.

282) Miyazaki, N., & Hamao, T. (1994). Solid particle erosion of thermoplastic resins reinforced by short fibers. *Journal of composite materials*, *28*(9), 871-883.

283) Moore, D. F. (1975). *Principles and applications of tribology* (Vol. 1). Oxford: Pergamon Press.

284) Roy, M., Vishwanathan, B., & Sundararajan, G. (1994). The solid particle erosion of polymer matrix composites. *Wear*, *171*(1), 149-161.

285) Pool, K. V., Dharan, C. K. H., & Finnie, I. (1986). Erosive wear of composite materials. *Wear*, *107*(1), 1-12.

286) Harsha, A. P., Tewari, U. S., & Venkatraman, B. (2003). Solid particle erosion behavior of various polyaryletherketone composites. *Wear*, *254*(7), 693-712.

287) Sundararajan, G., Roy, M., & Venkataraman, B. (1990). Erosion efficiency-a new parameter to characterize the dominant erosion micromechanism. *Wear*, *140*(2), 369-381.

288) Njuguna, J., Pielichowski, K., & Desai, S. (2008). Nanofiller-reinforced polymer nanocomposites. Polymers for Advanced Technologies, 19(8), 947-959.

289) Azeredo, H. (2009). Nanocomposites for food packaging applications. *Food Research International*, *42*(9), 1240-1253.

290) Saba, N., Tahir, P. M., & Jawaid, M. (2014). A review on potentiality of nano filler/natural fiber filled polymer hybrid composites. *Polymers*, *6*(8), 2247-2273.

291) Schadler, L. S., Brinson, L. C., & Sawyer, W. G. (2007). Polymer nanocomposites: a small part of the story. *Jom*, *59*(3), 53-60.

292) Hari, J., & Pukanszky, B. (2011). Nanocomposites: preparation, structure, properties. *Applied Plastics Engineering Handbook. Amsterdam: Elsevier*, 109-142

293) Jawaid, M. H. P. S., & Abdul Khalil, H. P. S. (2011). Cellulosic/synthetic fibre reinforced polymer hybrid composites: A review. *Carbohydrate Polymers*, *86*(1), 1-18.

294) Sathishkumar, T. P., Naveen, J., & Satheeshkumar, S. (2014). Hybrid fiber reinforced polymer composites–a review. *Journal of Reinforced Plastics and Composites*, *33*(5), 454-471.

295) Sathishkumar, T. P., Navaneethakrishnan, P., Shankar, S., & Rajasekar, R. (2013). Characterization of new cellulose sansevieria ehrenbergii fibers for polymer composites. *Composite Interfaces*, *20*(8), 575-593.

296) Borba, P. M., Tedesco, A., & Lenz, D. M. (2014). Effect of reinforcement nanoparticles addition on mechanical properties of SBS/curauá fiber composites. *Materials Research*, *17*(2), 412-419.

297) Kord, B. (2011). Nanofiller reinforcement effects on the thermal, dynamic mechanical, and morphological behavior of HDPE/rice husk flour composites. *BioResources*, *6*(2), 1351-1358.

298) Shalwan, A., & Yousif, B. F. (2014). Influence of date palm fibre and graphite filler on mechanical and wear characteristics of epoxy composites. *Materials & Design*, *59*, 264-273.

299) Dasari, A., Yu, Z. Z., & Mai, Y. W. (2009). Fundamental aspects and recent progress on wear/scratch damage in polymer nanocomposites. *Materials Science and Engineering: R: Reports*, 63(2), 31-80.

300) Macmillan, W. G., Sen Gupta, A. B., & Majumdar, S. K. (1954). 45—A Study of the Action of Alkalis on Jute. *Journal of the Textile Institute Transactions*, *45*(9), T703-T715.

301) Kolar, F., & Svitilova, J. (2007). Kinetics and mechanism of curing epoxy/anhydride systems. *Acta Geodyn. Geomater*, *4*, 85-92.

PUBLICATIONS

International Journal:

1) Gujjala, R., Ojha, S., Acharya, S. K., & Pal, S. K. (2014). **Mechanical properties of woven jute–glass hybrid-reinforced epoxy composite.** Journal of Composite Materials, 48(28), 3445-3455. (Impact factor: 1.257).

2) Raghavendra, G., Ojha, S., Acharya, S. K., & Pal, S. K. (2014). **Jute fiber reinforced epoxy composites and comparison with the glass and neat epoxy composites**. Journal of Composite Materials, 48(20), 2537-2547. (Impact factor: 1.257).

3) Raghavendra, G., Ojha, S., Acharya, S. K., & Pal, S. K. (2014). **A comparative analysis of woven jute/glass hybrid polymer composite with and without reinforcing of fly ash particles. Polymer Composites**. DOI 10.1002/pc.23222 (Impact factor: 1.632).

4) Raghavendra, G., Ojha, S., Acharya, S. K., & Pal, S. K. (2015). **Influence of micro/nanofiller alumina on the mechanical behavior of novel hybrid epoxy nanocomposites.** High Performance Polymers, 27(3), 342-351. (Impact factor: 1.286).

5) Raghavendra, G., Ojha, S., Acharya, S. K., Pal, S. K., & Ramu, I. (2014). **Evaluation of mechanical behaviour of nanometer and micrometer fly ash particle-filled woven bidirectional jute/glass hybrid nanocomposites.** Journal of Industrial Textiles, DOI: 10.1177/0954008314550889 (Impact factor: 1.2).

6) Raghavendra, G., Ojha, S., Acharya, S. K., & Deo, C. R. (2012). **Studying the Parameters of the Solid Particle Erosion and Test Procedure.** Caspian Journal of Applied Sciences Research, 1(13). pp. 176-181.

7) Raghavendra, G., Ojha, S., Acharya, S. K., & Pal, S. K. (2014). **Fabrication and characterization of nano Fly ash by planetary ball Milling.** International Journal of Material Science Innovations, (2), 59-68.

8) Raghavendra, G., Ojha, S., Acharya, S. K., & Pal, S. K. (2013, November). **Mechanical and Tribological Behavior of Alumina Nano Filler Reinforced Epoxy Hybrid Composites.** In ASME 2013 International Mechanical Engineering Congress and Exposition (pp. V02BT02A053-V02BT02A053). American Society of Mechanical Engineers. DOI: 10.1115/IMECE2013-64159.

9) Gujjala Raghavendra, S.K.Acharya, S.K.Pal. **Preparation of Alumina (Al_2O_3) Nano Powder by Auto Combustion Process.** International Journal of Systems, Algorithms & Applications (IJSAA), Volume 2, 2012, pp 74-76.

10) Gujjala Raghavendra, S.K.Pal, S.K.Acharya, Shakuntala Ojha. **Erosive Wear Behavior of Jute-Glass Woven Reinforced Epoxy Composite using Taguchi Approach.** International Journal of Systems, Algorithms & Applications (IJSAA), Volume 2, 2012, pp 72-75.

International/ National Conferences:

1) Gujjala Raghavendra, S.K.Acharya, S.K.Pal .**Preparation of Nano structured Materials from Fly Ash: By planetary ball Milling, filtration process**. ICMIE, 8-April, 12 pp 74, Goa, 2012, India.

2) Gujjala Raghavendra, S.K.Acharya, S.K.Pal. **Preparation of Alumina (Al_2O_3) Nano Powder by Auto Combustion Process.** International conference on Applied science and Engineering (ICASE-2012.July 30th, Taj Deccan, Hyderabad, India, (**Best paper award**).

3) Gujjala Raghavendra, S.K.Pal, S.K.Acharya, Shakuntala Ojha. **Erosive Wear Behavior of Jute-Glass Woven Reinforced Epoxy Composite using Taguchi Approach.** ICRASE-2012. November 30th, Taj Deccan, Hyderabad, India. (best paper award)

4) Dr S.K.Acharya, Gujjala Raghavendra , "**Mechanical and Tribological Behavior of Nano Fly Ash Reinforced Hybrid Composites**", International Conference on

Utilization of Fly Ash - Exploring New Frontiers (ICUFA-2013), January 10-11, 2013, Kolkata, West Bengal, India.

5) G.Raghavendra, S.K.Acharyar, S.K.Pal, S.Ojha, **Mechanical Properties Of Fly ash Filler In Natural Fiber- Hybrid epoxy Composites,** 7th International Symposium on Feedstock Recycling of Polymeric Materials (7th ISFR), New Delhi, 23-26th October 2013.

6) G.Raghavendra, S.K.Acharyar, S.K.Pal, S.Ojha, **Mechanical and Tribological Behavior Of Alumina Nano Filler Reinforced Epoxy Hybrid Composites, ASME congress & Exposition 2013**, Sandiego, 15-21st November 2013.

7) G.Raghavendra, S.K.Acharyar, S.K.Pal, S.Ojha, **Mechanical Properties of Nano Fly Ash Filled Nano Composites,** International Conference on Smart Technologies for Mechanical Engineering (STME) New Delhi Oct 25-26th**2013**,

8) G.Raghavendra, S.K.Acharyar, S.K.Pal, S.Ojha, **Investigation on Mechanical and Tribological Behavior of Novel Hybrid fly ash nano polymer Composite Materials,** ASIATRIB Jaypee Palace Hotel and Convention Centre Agra, India Feb17-20th**2014**,

9) G.Raghavendra, S.K.Acharyar, S.K.Pal, S.Ojha, **A Comparative Study of Mechanical and Tribological Properties of Jute-Glass Epoxy Hybrid Composites Filled By Micro-Nano Alumina Fillers,** ASIATRIB Jaypee Palace Hotel and Convention Centre Agra, India Feb17-20th2014,

10) Gujjala Raghavendra, S.K.Acharya, S.K.Pal. **Fabrication of nano fly ash by planetary ball milling.** ENMEA-2013. January 19th -20th, VSSUT, Burla, Odisha, India. pp 52.

11) Gujjala Raghavendra, Shakuntala ojha, S.K.Acharya, S.K. Pal "**Fabrication and characterization of Alumina (Al2O3) Nano particles**". Journal of Institution of engineers, India, 2013, pp 93-99 (Ganesh Mishra Memorial Award and Gold medal).

12) Gujjala Raghavendra, Shakuntala ojha, S.K.Acharya, "**Investigation in to Mechanical Properties of Hybrid Reinforced Epoxy Composite**". Journal of Institution of engineers, India 2013, pp 257-266.

BIBLIOGRAPHY

Mr. GUJJALA RAGHAVENDRA is a faculty member in the Department of Mechanical Engineering, National Institute of Technology Warangal (NITW), Warangal, Telengana, India-506004. He has 5 years of research and two year of teaching experience in his field. He had more than 30 international journal and more than 40 international conference journals. He did M.E. in Mechanical Engineering from NIT Rourkela. This dissertation is being submitted for the fulfillment the Ph.D. degree. The contact address is:

Address:-

Gujjala Raghavendra (Asst. Prof.)
Department of Mechanical Engineering
National Institute of Technology Warangal (NITW),
Warangal, Telengana,
India-506004
E mail: raghavendra.gujjala@gmail.com, raghavendra.gujjala@nitw.ac.in
Phone: 09985803317(M)

Residence-

Door no. 8/888/8
Jayanagar colony,
Kalyandurg-515761, Anantapur(D)
Andhra Pradesh.